Journal of Life Sciences

Volume 5, Number 12, December 2011 (Serial Number 44)

David Publishing Company
www.davidpublishing.org

Publication Information
Journal of Life Sciences is published monthly in hard copy (ISSN 1934-7391) and online (ISSN 1934-7405) by David Publishing Company located at 9460 TELSTAR AVE SUITE 5, EL MONTE, CA 91731, USA.

Aims and Scope
Journal of Life Sciences, a monthly professional academic journal, covers all sorts of researches on molecular biology, microbiology, botany, zoology, genetics, bioengineering, ecology, cytology, biochemistry, and biophysics, as well as other issues related to life sciences.

Manuscripts and correspondence are invited for publication. You can submit your papers via Web Submission, or E-mail to life-sciences@davidpublishing.org or life-sciences@hotmail.com. Submission guidelines and Web Submission system are available at http://www.davidpublishing.org.

Editorial Office
9460 TELSTAR AVE SUITE 5, EL MONTE, CA 91731, USA
Tel: 1-323-9847526, 1-302-5977046; Fax: 1-323-9847374
E-mail: life-sciences@davidpublishing.org, life-sciences@hotmail.com

Abstracted / Indexed in
Database of EBSCO, Massachusetts, USA
Chemical Abstracts Service (CAS), USA
Cambridge Scientific Abstracts (CSA), USA
Chinese Database of CEPS, American Federal Computer Library center (OCLC), USA
Ulrich's Periodicals Directory, USA
Chinese Scientific Journals Database, VIP Corporation, Chongqing, China

Subscription Information
Price (per year): Print $420, Online $300, Print and Online $560.

David Publishing Company
9460 TELSTAR AVE SUITE 5, EL MONTE, CA 91731, USA
Tel: 1-323-9847526, 1-302-5977046; Fax: 1-323-9847374
E-mail: order@davidpublishing.org

JLS

Journal of Life Sciences

Volume 5, Number 12, December 2011 (Serial Number 44)

Contents

Research Papers

Reviews

Journal of Life Sciences 5 (2011) 981-985

Construction and Expression of Sugarcane UGPase cDNA Prokaryotic Expression Vector

Ling Lian[1, 2], Jianfu Zhang[1], Bingying Ye[2, 3], Youqiang Chen[2, 3] and Rukai Chen[3]

1. Key Laboratory of Hybrid Rice Germplasm Innovation and Molecular Breeding of South China, Ministry of Agriculture, P.R.China/Fuzhou Branch, National Rice Improvement Center of China/Fujian Engineering Laboratory of Crop Molecular Breeding/Fujian Key Laboratory of Rice Molecular Breeding/Rice Research Institute, Fujian Academy of Agricultural Sciences, Fuzhou 350003, China

2. College of Life Sciences, Fujian Normal University, Fuzhou 350108, China

3. Key Laboratory of Sugarcane Genetics and Breeding, Ministry of Agriculture, Fuzhou 350108, China

Received: July 05, 2011 / Accepted: September 20, 2011 / Published: December 30, 2011.

Abstract: UGPase (UDP-glucose pyrophosphorylase), one of the primary enzymes concerned with carbohydrate metabolism, catalyzes the formation of UDPG. By inserting the UGPase cDNA fragment cloned from *Saccharum officinarum* into PQE-30, the prokaryotic expression vector of PQE-UGP was successfully constructed. Then the vector plasmid of PQE-UGP was transformed into host bacteria M15 and the expression of target gene was induced by Isopropyl β-D-1-Thiogalactopyranoside (IPTG). The research laid foundation for study on the prokaryotic expression of UGPase.

Key words: UGPase, construction of prokaryotic expression vector, induced expression.

1. Introduction

UGPase (UDP-glucose pyrophosphorylase) plays an important role during the growth and development of plant, participating in the glycometabolism of plant, mainly catalyzing the reaction of Glc-1-P + UTP $\rightleftharpoons$ UDPG + PPi. UDPG (uridine diphosphate glucose), the main form of activated glucose in the plant, is concerned with the synthesis of saccharose, cellulose, hemicellulose, trehalose, pectin, callose, uridine diphosphate galactose and uridine diphosphate glucose acid etc by serving as the donor of glucosyl [1-3]. Likewise, it is just because of such special effect of UDPG that it can also play an important role *in vitro* and determine some glycosyltransferase activity by serving as the substrate. For instance, the determination of Sucrose phosphate synthase (SPS) catalytic activity requires the participation of UDPG. There are two ways of the synthesis of UDPG: chemical synthesis and enzymatic synthesis. The synthetic UDPG of chemical synthesis can't be utilized because of erroneous configuration, while the enzymatic synthesis is feasible and the synthetic UDPG can be utilized [4]. Obviously, enzymatic synthesis possesses its advantages, one of the enzymes participated in the enzymatic synthesis is just UGPase. If the UGPase is extracted from plant, it will consume a mass of material and the efficiency is low. Whereas, if a great deal of activated UGPase can be obtained by using prokaryotic expression, the previous problem will be well solved. Moreover, according to previous studies, monomer is the activated form of UGPase [5], which provides possibility for the prokaryotic expression of UGPase.

In this study, the prokaryotic expression vector of sugarcane UGPase was constructed and transformed into host bacteria M15, simultaneously, the expression

Author: Ling Lian, research intern, research fields: plant physiology and plant molecular biology. E-mail: lianling51@163.com.

Corresponding author: Youqiang Chen, Ph.D., professor, research fields: plant physiology and plant molecular biology. E-mail: yqchen@fjnu.edu.cn.

of target gene was induced by IPTG. The object is to obtain activated UGPase through prokaryotic expression and use it for the synthesis of UDPG. Meanwhile, this makes preparations for the further study on protein antibody.

2. Materials and Methods

2.1 Materials

Vector pQE-30, DH5α and M15 are preserved by our lab.

T4 DNA Ligase, PrimeSTAR^{TM} HS DNA Polymerase, *Bam*H I and *Sac* I restriction enzymes are bought from TaKaRa. Am and Km are bought from bioengineering corporation of Shanghai.

2.2 Methods

2.2.1 Amplification of Sugarcane UGPase cDNA

Using cloned sugarcane UGPase sequence (cloned by our team, NCBI GenBank accession number is FJ536261) as template, the PCR amplification primer is as follows:

UP1

5'-CGGGATCCATGGCCGCCGCTGCTGC-3'

*Bam*H I

UP2

5'-CCGGAGCTCTTAAAGATCCTCAGGGCCATTGACAT-3'

Sac I

For the convenience of vector construction afterward, *Bam*H I and *Sac* I restriction enzyme cutting sites were introduced into the upstream primer and downstream primer separately.

Using PGM-UGP recombinant plasmid as template, amplified by PCR, the optimized PCR reaction system was as follows: 6 μL 5 × PrimeSTAR^{TM} HS DNA Polymerase Buffer, 2.4 μL dNTP (2.5 mmol/L each), 3 μL primer UP1 and UP2 (4 μmol/L each), 0.6 μL plasmid template, 1.5 μL PrimeSTAR^{TM} HS DNA Polymerase (2.5 U/μL), then adding ddH_2O to total volume 30 μL. The optimum PCR program was as follows: pre-denaturing under 94°C for 5 min, then denaturing under 94°C for 30 s, annealing under 60°C for 30 s and extending under 72°C for 1.5 min. After 30 cycles, the sample was extended under 72°C for 7 min.

PCR production was recycled and purified according to the instructions come with SV Gel and PCR Clean-Up System from Promega.

2.2.2 Vector Construction

The target band amplified by PCR was double-digested after purification, the enzymatic system was as follows: 15 μL PCR production, 2.5 μL 0.5 × K Buffer, *Bam*H I and *Sac* I (5 μL each), then adding ddH_2O to volume 50 μL. Digested overnight at 37°C.

The pQE-30 vector was double-digested, and the enzymatic system was as follows: 20 μL pQE-30 plasmid, 2.5 μL 0.5 × K Buffer, *Bam*H I and *Sac* I (5 μL each), then adding ddH_2O to volume 50 μL, digesting overnight under 37°C. The digested products were recycled and purified according to instructions come with SV Gel and PCR Clean-Up System from Promega.

The target fragment and vector were linked together in a ratio of 3:1 with T_4 DNA ligase, then incubated overnight at 16°C.

2.2.3 Transformation of Ligation Product

Using calcium chloride method, the ligation product was transformed into *E. coli* DH5α competent cells. Screening was performed on the LB medium which contained 60 μg/mL Am (the PQE-30 vector contains an ampicillin selection marker) by using smearing plate culture method.

2.2.4 Extraction and Identification of Recombinant Plasmid

Selected a resistant single colony and carried out a shake flask culture, then performed an identification of bacteria liquid by PCR and a plasmid DNA extraction using Alkaline Lysis method. After identification of plasmid by PCR, a digestion with *Sac* I and a double digestion with *Bam*H I /*Sac* I were performed to identify the recombinant plasmid, and named it as pQE-UGP.

The positive identified colony was sequenced in TaKaRa and the accuracy of open reading frame (ORF) was validated.

2.2.5 Transformation of Recombinant Plasmid into M15 and the Induced Expression

Using calcium chloride method, the recombinant plasmid was transformed into host bacteria M15 competent cells. Screening was performed on the LB medium which contained 100 μg/mL Am and 25 μg/mL Ka (the host bacteria M15 contains a kanamycin selection marker which exists in another plasmid of pREP4) by using smearing plate culture method. Selected a resistant single colony and carried out a shake flask culture, then performed an identification of bacteria liquid by PCR.

Selected a positive clone, incubated it in a constant temperature shaker at 37°C overnight. Inoculated the overnight culture into culture medium in a ratio of 1:20, waited until OD = 0.6 by using shaking culture, took 1 mL sample as the control without induction. Added IPTG into the rest bacteria liquid until the final concentration reached 1 mM so that the expression of target gene could be well induced, then took 1 mL bacteria liquid after induction for 0.5 h, 1 h, 2 h, 3 h, 4 h, 5 h, 6 h, respectively. The control sample and induced samples were as following: resuspending bacteria in 50 μL 5 × SDS-PAGE loading buffer and in 100 μL 5 × SDS-PAGE loading buffer separately. Placed samples in a boiling water bath for 5 min, centrifuged at 10,000 rpm for 2 min, aspirated the supernatant fluid for use, then ran a SDS-PAGE gel electrophoresis.

The protein profiles was analyzed by Quantity One (a software package for imaging and analyzing 1-D electrophoresis gels, dot blots, arrays, and colonies), and then relative data was processed by SPSS (Statistical Product and Service Solutions).

3. Results and Analysis

3.1 Construction of Prokaryotic Expression Vector

The UGPase with *Bam*H I and *Sac* I restriction enzyme cutting sites on two ends was cloned into pQE-30 vector (Fig. 1), then the recombinant pQE-UGP was identified by *Sac* I digestion and *Bam*H I /*Sac* I double digestion (Fig. 2). After *Bam*H I /*Sac* I double digestion, two bands appeared in the gel electrophoresis, one band located at 1,500 bp and was in accordance with the size of UGPase-L, the other band corresponded with the size of pQE-30 vector. Sequence analysis of the positive clones, the result was in accordance with the sequencing of cloning. This illustrated that the target fragment had been cloned into pQE-30 vector successfully and the expression vector had been constructed correctly.

3.2 Induced Expression

The ORF of sugarcane UGPase was 1,431 bp and it encoded 476 amino acids, the molecular weight of this protein was 52.292 Kda by prediction (//cn.expasy.org/tools). As seen in Fig. 3, lane 1-7 represented the total proteins of bacteria induced with IPTG for 0.5 h, 1 h, 2 h, 3 h, 4 h, 5 h, 6 h respectively, the band corresponding with the size of target protein

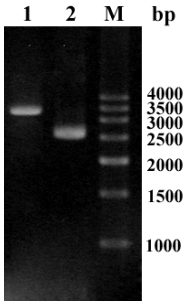

Fig. 1 Restriction enzyme digestion of plasmid pQE-30.
1: *Bam*H I /*Sac* I digestion; 2: Plasmid; M: marker, 4,000 bp.

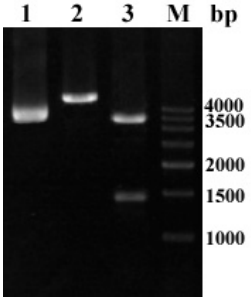

Fig. 2 Restriction enzyme digestion of recombinant plasmid pQE-UGP.
1: Plasmid; 2: *Sac* I digestion; 3: *Bam*H I /*Sac* I digestion; M: marker, 4,000 bp.

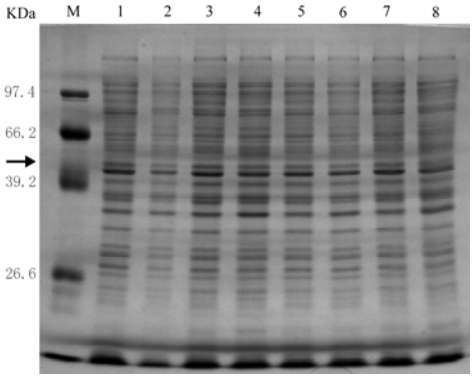

Fig. 3 Time course of expression induced with IPTG.
M: marker; 1-7: total proteins of bacteria induced with IPTG for 0.5 h, 1 h, 2 h, 3 h, 4 h, 5 h, 6h respectively; 8: total proteins of bacteria without induction.

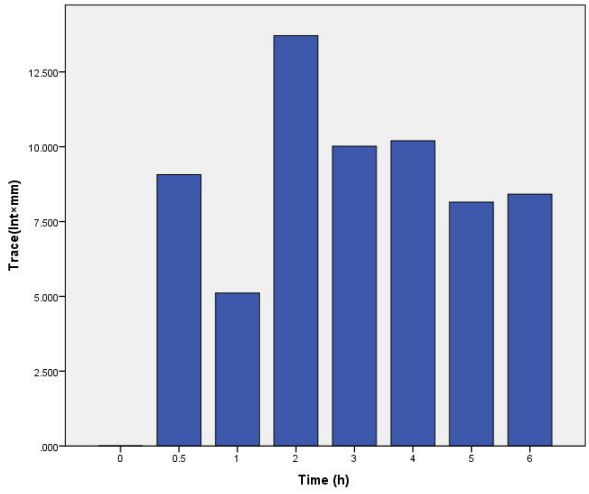

Fig. 4 Trace of soluble target protein in the protein profiles.

was more distinct. The amount of the soluble target protein was the maximum after induced with IPTG for 2 h (Fig. 4).

4. Discussions

As the substrate, UDPG can be used to determine the transferase activity of some carbohydrates. Meanwhile, the ^{13}C labeled UDPG possesses wider application prospect, such as discovering new UDPG-dependent glycosyl transferase and detecting new glycosyl compound by means of nuclear magnetism, determining the connection mode between glycosyls, labeling oligosaccharide and polysaccharide by means of isotopes.

The synthesis of UDPG has two ways: chemical synthesis and enzymatic synthesis. The chemical synthesis of UDPG begins with glucose. This process involves the synthesis and purification of intermediate product such as glucose derivatives, and the protection and de-protection of active groups. Therefore, the total yield of chemical synthesis was low because of complicated procedures. Furthermore, high price of 4-^{13}C labeled glucose causes high cost. In addition, the UDPG obtained from chemical synthesis is mixed α-β type, while the glucosyl of the natural bioactive UDPG is α-type, only the α-type of UDPG can be utilized by enzyme. The process of enzymatic synthesis is simple,

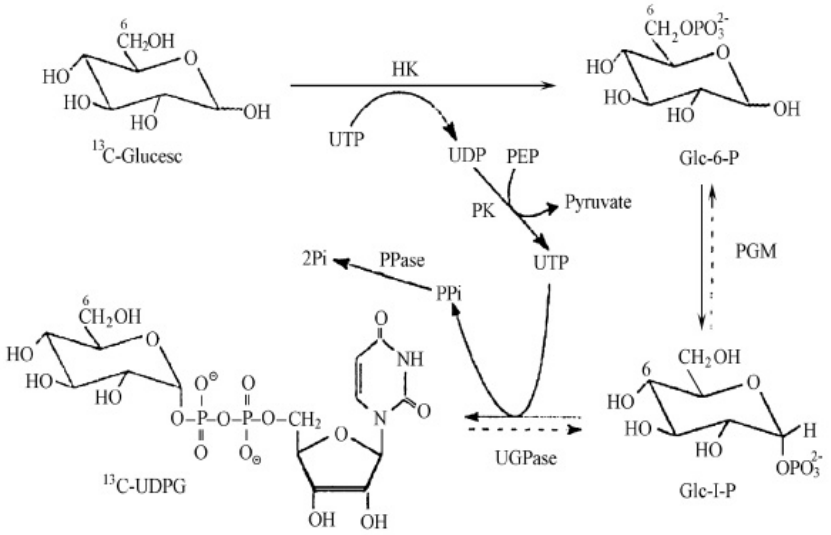

Fig. 5 Enzymatic synthesis of UDPG.

from which the UDPG is obtained has native configuration and can be used for further application. Q.I. Chao [6] improved the enzymatic synthesis of UDPG, established an economical, feasible and simple method of enzymatic synthesis which could synthesize a great deal of isotope labeling UDPG (Fig. 5). The phosphorylation of glucose with HK (hexokinase) generates Glc-6-P, which can be transformed into Glc-1-P with the catalysis of PGM (phosphoglucomutase). Finally, the Glc-1-P and UTP are transformed into UDPG with the catalysis of UDPase. This process includes a regeneration system of UTP: with the catalysis of PK (pyruvate kinase) and the phosphate group provided by PEP (phosphoenolpyruvate), the UTP can regenerate. The UTP not only serves as the donor of phosphate group during the first step, but also participates with the synthesis of UDPG during the last step. Furthermore, adding equimolar glucose and UTP during the reaction will make the reaction proceed toward the direction of synthesis of UDPG [6].

The enzymatic synthesis is simple, but if large volume of reaction system is performed, plenty of enzymes will be consumed. Furthermore, some of the enzymes, such as UGPase, are expensive; this is quite infeasible for the enzymatic synthesis. Therefore, the enzymatic source is the problem to be solved urgently.

Acknowledgments

This research was supported by The National Natural Science Foundation Projects (30871575), Ministry of Agriculture, industry, modern agricultural technology system special fund (No. CARS-20-4-4).

References

[1] L.A. Kleczkowski, Glucose activation and metabolism through UDP-glucose pyrophosphorylase in plants, Phytochemistry 37 (1994) 1507-1515.

[2] L.A. Kleczkowski, M. Geisler, I. Ciereszko, H. Johansson, UDP-Glucose Pyrophosphorylase, An old protein with new tricks, Plant Physiology 134 (2004) 912-918.

[3] Q.I. Chao, Purification and characterization of UGPase from apocynaceae cell, Journal of the Graduate School of the Chinese Academy of Sciences 21 (2004) 345-351.

[4] Q.I. Chao, Research development on uridine diphosphate glucose, Chemical Research 15 (2004) 73-75.

[5] F. Martz, M. Wilczynska, L.A. Kleczkowski, Oligomerization status, with the monomer as active species, defines catalytic efficiency of UDP-glucose pyrophosphorylase, Biochemical Society 367 (2002) 295-300.

[6] Q.I. Chao, Characterization of 13C-labeled uridine diphosphoglucose of enzymatic synthesis by NMR, Journal of the Graduate School of the Chinese Academy of Sciences 21 (2004) 487-492.

Journal of Life Sciences 5 (2011) 986-995

Oncologic Trogocytosis Protects Tumour Stromal Cells from γδ Cell Cytotoxicity

Emilie Decaup[1, 2], Pejman Mirshahi[3], Arash Rafii[4], Massoud Mirshahi[3], Jean-Jacques Fournié[1, 2] and Mary Poupot[1, 2]

1. INSERM UMR1037-Cancer Research Center of Toulouse, CNRS ERL, CHU Purpan, Toulouse 31024, France

2. University of Toulouse 3, Toulouse 31000, France

3. UMRS 872 INSERM, University of Pierre et Marie Curie-Paris 6 and University of Paris Descartes, Team 18, CRC, 15 Rue de l'Ecole de Médecine, Paris Cedex 06 75270, France

4. Department of Genetic Medecine and Obstetrics and Gynecology, WCMC-Qatar, Doha, Qatar

Received: June 27, 2011 / Accepted: July 25, 2011 / Published: December 30, 2011.

Abstract: Tumours progressively develop chemoresistance and immunoescape abilities thanks to support from their stromal microenvironment. In ovarian carcinomas, for instance, tumour-associated mesenchymal stem cells (TAMC) can transfer multi-drug-resistant proteins to develop metastases. However, since the microenvironment of such carcinomas is frequently infiltrated by both TAMC and γδ T lymphocytes, the consequences of interactions between these cell types were unclear. Here, we report that whilst γδ T lymphocytes were not activated when co-incubated *in vitro* with TAMC, their cell membranes were trogocytosed by the TAMC. Since TAMC constitutively express a low level of HLA class I, which is increased by trogocytosis of γδ cell-derived HLA class I, the interaction increased the expression of HLA class-I molecules on TAMC. In addition, γδ T lymphocytes are HLA-unrestricted cytolytic cells and their activity is regulated by inhibitory receptors (KIR) for self-HLA class I. Hence, although the lytic activity of γδ T lymphocytes for unrelated target cells was unaffected by trogocytosis, it spared the TAMC. Therefore, interactions between TAMC and cytolytic γδ T cells avoided the killing of these stromal cells due to an active transfer of their protective HLA class-I molecules. These results suggest that trogocytosis contributes to the maintenance of cancer-associated stromal cells.

Key words: Membrane transfer, tumour microenvironment, stromal cells, HLA-class I molecules.

1. Introduction

Despite the presence of tumour-infiltrating T cells, ovarian cancer is the most lethal gynaecological malignancy due to frequent peritoneal metastasis and ascitis [1, 2], a tolerant tumourous microenvironment encompassing immunoregulatory cells and immunosuppressive mediators [3-5]. The tumour stroma generally plays an essential role in tumour cell survival and growth via the production of cytokines, growth factors or metalloproteinases [6, 7]. It can also promote metastatic invasion through mesenchymal stem cell (MSC)-derived chemokine CCL5 [8] or through N-cadherin, released from cancer cells interacting with tumour-associated mesenchymal stem cells (TAMC) [9]. Stromal fibroblasts and TAMC also promote tumour growth and angiogenesis [10, 11]. Direct interactions between stromal and cancer cells prevent their apoptosis via the up-regulation of anti-apoptotic proteins [12] or CXCL12 [13]. Moreover, TAMC from ovarian carcinomas can confer chemoresistance through oncologic trogocytosis, mediating the transfer of multi-drug resistant proteins [14].

Beside its direct tumour-promoting activities, the tumour microenvironment also favours tumour immunoescape. MSC and tumour-associated fibroblasts can inhibit natural killer (NK) cell

Corresponding author: Mary Poupot, Ph.D., research fields: immunology and oncology. E-mail: mary.poupot@inserm.fr.

proliferation, cytotoxicity and cytokine production through indoleamine 2,3-dioxygenase and prostaglandin E2 [15, 16]. MSC also inhibit αβ T cell proliferation, either by soluble TGF_{β}, NO and PGE2 or by cell contact-mediated PD1 signalling [17-19], whereas MSC (and ovarian cancer TAM) inhibit γδ T cell proliferation and cytokine production [20, 21]. In addition, MSC can also impair the maturation and function of dendritic cells [22, 23]. Hence the tumour stroma protects against immunological attacks via various means.

However, the activity of immune cells on stromal cells is still poorly documented. In the tumour microenvironment, IFNγ induces MSC to secrete immunosuppressive molecules [24, 25]. In response to MSC, however, NK cells remain capable of killing targets through NKG2D or NKp30 signalling combined with a low level of inhibitory ligands on the targets [26]. We previously showed that T CD4, T CD8 and γδ T lymphocyte proliferation and cytokine production are immunosuppressed by TAMC from ovarian carcinoma patients [20]. Moreover, ovarian and mammary carcinoma tissue microarrays evidenced a correlation of chemoresistance with the presence of TAMC [14]. Independent tissue microarray studies revealed the presence of tumour-infiltrating γδ T lymphocytes in ovarian carcinomas [2]. Considering these observations, we questioned the molecular consequences of direct interactions between TAMC and γδ T lymphocytes. Here, we report that upon direct contact, the TAMC selectively acquire HLA class-I molecules from the γδ T lymphocytes through oncologic trogocytosis. Although they were spared from γδ T cell cytotoxicity by acquiring their protective HLA class-I molecules, the TAMC did not impair the γδ T cell cytotoxicity of cancer cell targets. Thus, oncologic trogocytosis could represent a new mechanism of immunological protection of the tumour stroma, and thereby contribute to the development of tumours.

2. Materials and Methods

2.1 Antibodies and Flow Cytometry

Fluorochrome-conjugated monoclonal antibodies (mAbs): anti-HLA-ABC-PE-Cy5, anti-CD107a-PE-Cy5, anti-TCR Vγ9-PE, anti-NKAT2-PE and anti-NKB1-PE were purchased from BD Biosciences (San Jose, CA); anti-CD3-PB and anti-TCR Vγ9-FITC were purchased from Biolegend (San Diego, CA); anti-CD166-PE, anti-CD25-PE-Cy5, anti-NKG2D-PE-Cy5, anti-NKG2A-PE and anti-CD94-PE were purchased from Beckman Coulter (Fullerton, CA); anti-CD166-AlexaFluor 647 was purchased from Serotec (Oxford, UK); and 1-7F9-APC was purchased from Innate Pharma (Marseille, France).

The lipophilic fluorochrome PKH67 was purchased from Sigma-Aldrich (St. Louis, MO), and the cytoplasmic Cell Tracker CMTMR (5-(and 6)-(((4-chloromethyl) benzoyl) amino) tetramethylrhodamine) was obtained from Molecular Probes (Eugene, OR).

Flow cytometry was performed with LSR-II and FACSDiva (BD Biosciences) and FlowJo 7.5.5 (Tree Star, Ashland, OR) software.

2.2 Reagents

rhIL-2 was provided by Sanofi-Aventis (Labège, France) and the synthetic phosphoantigen bromohydrin pyrophosphate (BrHPP) was provided by Innate Pharma (Marseille, France).

Cells were cultured in complete medium containing RPMI 1640 (Invitrogen, Cergy Pontoise, France) supplemented with 2 mM L-glutamine, 100 μg/mL streptomycin, 100 IU/mL penicillin and 1 mM sodium pyruvate (Cambrex Biosciences, Rockland, ME).

2.3 Culture of TAMC

The TAMC were isolated from the ascitis fluids of untreated ovarian cancer patients (stage III) undergoing ascitis evacuation [14].

Immunohistochemical characterization of the

TAMC involved staining for cytokeratin, vimentin, CD45, CD20, CD68, CD34, Protein S100, myeloperoxidase, CD166, CD146, CD10 and CD3, as previously described Ref. [14]. Briefly, primary cultures of TAMC isolated from five different ovarian carcinoma patients were infected by the SV40 large T antigen-expressing retroviral vector. The LT-expressing TAMC were selected in a medium containing neomycin (experiment performed by the Laboratoire de Therapie Genique, CHU Nantes, France). The immortalized TAMC cell line M16 was cultured at 37°C in 5% CO_2 and complete RPMI medium supplemented with 10% FCS.

2.4 Vγ9Vδ2 T Cells Samples and Culture

Fresh blood samples were collected from different healthy donors and the peripheral blood mononuclear cells (PBMCs) were prepared on a Ficoll-Hypaque density gradient (Amersham Biosciences AB, Upssala, Sweden) by centrifugation (800 g for 30 min at room temperature). Primary γδ T cell lines were obtained from PBMCs by *in vitro* PBMC culture for 14 days in complete medium supplemented with 10% Fetal Clone I (HyClone/Thermo Fisher Scientific, Brebières, France), BrHPP (3 μM) and rhIL-2 (300 IU/mL) on day 0 followed by supplementation of rhIL-2 (300 IU/mL) every three days. The TCR phenotype of all of the γδ T cells lines comprised > 90% TCRVγ9$^+$ cells.

2.5 Cytotoxicity Assays

The Daudi Burkitt's lymphoma cell line, the ovarian carcinoma cell line called OVCAR and the TAMC used as target cells were cultured at 37°C in complete medium and 10% FCS. Specific lysis by γδ T cells was measured by the standard 4 h [^{51}Cr] release assay. The percentage of specific lysis was obtained by ((experimental release-spontaneous release) / (maximum release-spontaneous release)) × 100. Maximum release was determined by adding 0.1% Triton X-100. Data are presented as the mean of triplicate samples.

2.6 Expression of CD107a

After a 4 h co-incubation at 37°C in medium with PE-Cy5-conjugated anti-CD107a or the isotopic control antibody of the γδ T cells and Daudi cells in the presence or absence of the TAMC line at different ratios, the cells were labelled for the TCR Vγ9 and the CD166. The expression of CD107a was then analysed by flow cytometry on the gated γδ T cells specifically.

2.7 Trogocytosis

The cells were stained with the lipophilic dyes PKH67 (green) or with cytoplasmic CMTMR (red) according to the manufacturer's instructions; 2×10^5 PKH67-labelled cells were co-cultured for 3 h at 37°C with 10^5 CMTMR-labelled cells in 96-well U-bottom tissue culture plates. The cells were then washed twice with PBS containing 2 mM EDTA and green fluorescence was analysed by flow cytometry and confocal microscopy.

2.8 Transfer of the Membrane Proteins

We applied two settings for assessing the transfer of membrane proteins. The first method was the co-culture of TAMC and γδ T cells for 3 h, separation of the cells with PBS containing 2 mM EDTA and then labelling of the cells with PE-Cy5-conjugated anti-HLA-ABC, PE-Cy5-conjugated antibody directed to NKG2D or PE-Cy5-conjugated antibody directed to CD25. The HLA-ABC expression by the CD166$^+$ TAMC and by TCR Vγ9$^+$ γδ T cells was then analysed by flow cytometry.

The second method was labelling the γδ T cells with PE-Cy5-conjugated anti-HLA-ABC for 10 min at 4°C, washing twice with PBS and co-incubating these cells for 3 h with the TAMC (at TAMC/γδ T cell ratio of 1/2). After 3 h, all cells were labelled for TCR Vγ9 and CD166 prior to analysing HLA-ABC expression by flow cytometry.

2.9 Confocal Microscopy of Trogocytosis

The PKH67 and CMTMR orange

(CMTMR)-stained cells were processed for confocal microscopy as follows. After 3 min or 3 h of co-culture, the cells were gently suspended and plated on poly-L-lysine (Sigma-Aldrich)-coated slides for 5 min at 37°C. After fixation with PBS containing 4% p-formaldehyde, the cells were washed and directly mounted in PBS containing 90% glycerol and 2% 1-4-diazabicyclo (2.2.2) octane (DABCO; Sigma-Aldrich). The samples were examined using a Carl Zeiss LSM 510 confocal microscope (Jena, Germany).

2.10 Statistical Analysis

Data are means and SD from independent experiments performed with γδ T cells from different healthy donors. The normality and equal variance of each sample series were evaluated prior to statistical analysis by the specified tests. A one-tailed, paired Student's *t*-test was used whenever appropriate or a one-way Mann-Whitney rank-sum test was used otherwise, with $\alpha = 5\%$ for statistical significance. All statistical analyses were performed using the SigmaStat 3.0 software (SPSS, Chicago, IL).

3. Results

3.1 Strong γδ T Cell Trogocytosis by TAMC

Since direct cell contact with lymphocytes usually favours molecular transfers onto the lymphocyte cell membrane, a process called trogocytosis, we first asked whether or not the direct cell contact of γδ lymphocytes with TAMC led to trogocytosis. Therefore, TAMC stained with PKH67 were co-incubated with γδ T cells for 3 min and 3 h, and the PKH67 green fluorescence on the γδ T lymphocytes (gated) was compared at these two time points. For microscopy, the γδ T lymphocytes were stained before co-culture with the CMTMR red cytoplasmic fluorochrome. Both flow cytometry (Fig. 1, top) and confocal microscopy analysis (Fig. 1, bottom) indicated that γδ T cells acquired a minute amount of PKH67 upon cell contact with TAMC, indicating that the level of trogocytosis of TAMC by γδ lymphocytes was very low (Fig. 1A).

In contrast, strikingly different results were obtained when analysing trogocytosis in the opposite direction. The γδ T cells stained with PKH67 were co-incubated with TAMC for 3 min and 3 h, and the PKH67 green fluorescence on the TAMC (gated) was compared as above. For microscopy, the TAMC were stained before co-culture with the CMTMR red cytoplasmic fluorochrome. We found that upon direct cell contact, the TAMC acquired a high amount of green fluorescence from the γδ T cells (Fig. 1B). Since this fluorochrome is stably inserted into cell membranes, its appearance on the TAMC meant that these cells had

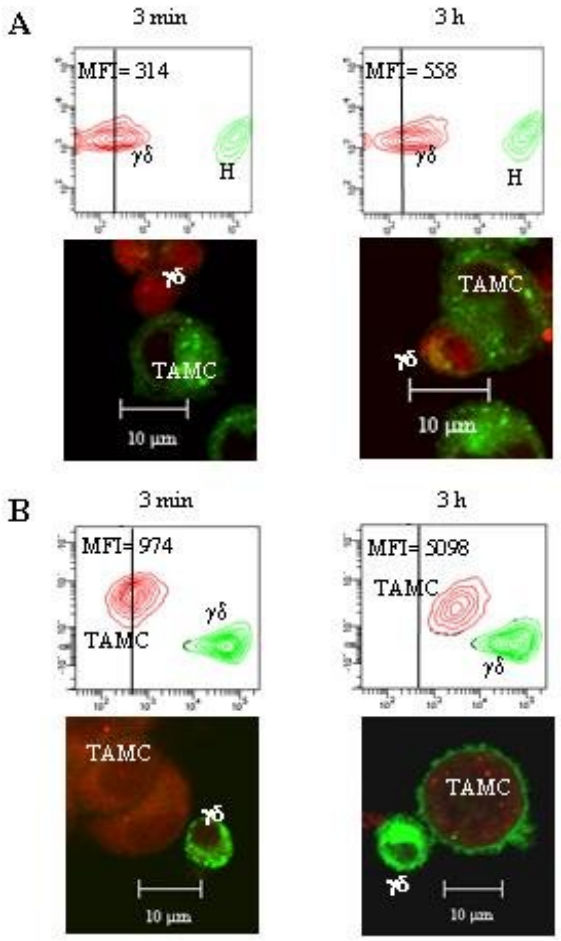

Fig. 1 Trogocytosis of γδ T cells by TAMC.
A: MFI of PKH67 on gated $CMTMR^+$ γδ T cells after 3 min or 3 h of contact with $PKH67^+$ TAMC measured by flow cytometry (top) and by confocal microscopy (bottom); **B:** MFI of PKH67 on gated $CMTMR^+$ TAMC after 3 min or 3 h of contact with $PKH67^+$ γδ T cells measured by flow cytometry (top) and by confocal microscopy (bottom).

mediated a strong trogocytosis of the γδ T lymphocytes upon cell contact.

Together, these results indicated that direct contact between γδ lymphocytes and TAMC leads to an almost unidirectional trogocytosis of γδ cells by the TAMC.

3.2 TAMC Acquired γδ T Cell-Derived HLA Class-I Molecules by Trogocytosis

We thus questioned whether the trogocytosis of γδ T cells led to the acquisition of γδ T cell-derived membrane proteins by the TAMC. Using the same experimental conditions as above, we then labelled all cells in the co-cultures with antibodies directed against different γδ T cell membrane proteins. Before the co-culture, the TAMC weakly expressed HLA class-I molecules and did not express any of the γδ T cell markers Vγ9Vδ2 TCR, NKG2D and IL2-receptor α chain CD25. After 3 h of contact with γδ T cells, however, although the TAMC still lacked expression of Vγ9Vδ2 TCR, NKG2D, CD25 and CD69 (data not shown), their HLA class-I expression was increased (Fig. 2A). On average, from four independent experiments, the mean fluorescence intensity of HLA-A,B,C at the cell surface of TAMC co-cultured with the γδ T cells became three times higher than that of the TAMC alone (Fig. 2B).

However, the increased HLA class-I expression by the TAMC in contact with the γδ T cells could have been due to the up-regulation of endogenous HLA class-I. In order to assess this, the γδ T cells were labelled with PE-Cy5-conjugated anti-HLA-A,B,C prior to contact with the TAMC. Both HLA-labelled γδ T cells and TAMC were then co-cultured for 3 h, separated with EDTA solution and analysed by flow cytometry. Under these conditions, the TAMC co-incubated with labelled γδ T cells were positive for HLA-A,B,C-PE-Cy5 whereas those co-incubated for only 3 min were not (Fig. 2C).

These data indicated that trogocytosis of the γδ T cells by the TAMC increased the level of HLA class-I molecules at their cell surface most significantly through the selective acquisition of γδ T cell-derived molecules.

3.3 TAMC Are Weakly Killed by γδ T Cells

The primary γδ T cell lines expressed the inhibitory

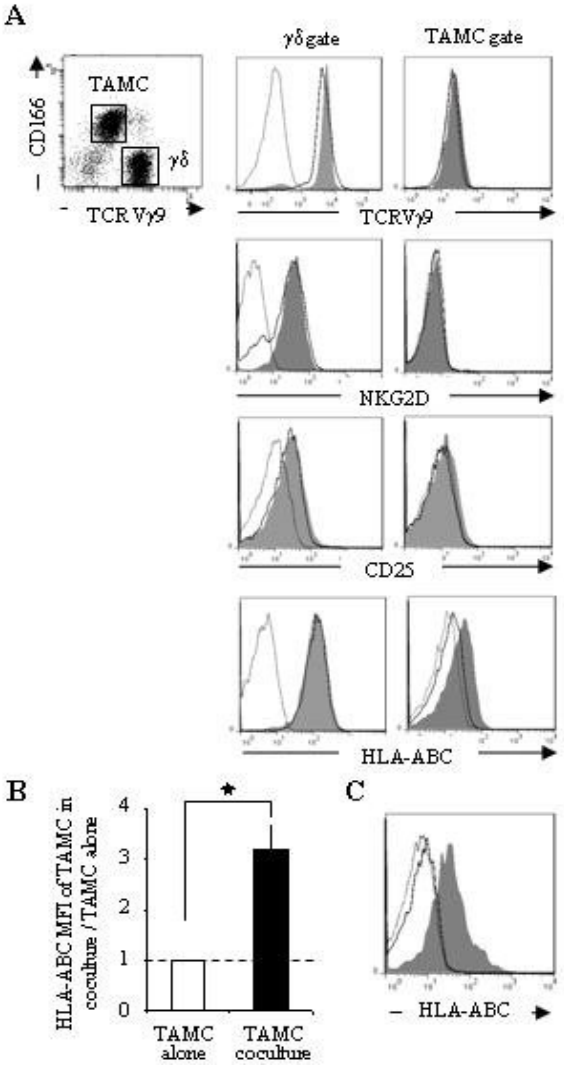

Fig. 2 Trogocytosis of γδ T cell-derived HLA class-I molecules by TAMC.

A: Expression of TCRVγ9, NKG2D, CD25 and HLA-A,B,C by the TAMC (H gate) and by the γδ T cells (γδ gate) after 3 h of contact (shaded histogram) and 3 min of contact (black line) compared to the isotypic control (dotted line); **B:** Mean of the ratio of the MFI of the HLA-A,B,C for the TAMC alone (white bar) or after a 3 h co-culture with the γδ T cells (black bar) from four independent experiments; **C:** Expression of HLA-A,B,C by the TAMC after 3 h (shaded histogram) or 3 min (black line) of contact with the γδ T cells labelled with the anti-HLA-A,B,C compared to the isotype control (dotted line).

receptors CD94/NKG2A, KIR2DL1, KIR2DL2, KIR2DL3, KIR2DS1 and KIR2DS2 (Fig. 3A). Since self-HLA class-I molecules are ligands for the KIR inhibitory receptors expressed by the γδ T cells, their presence at the cell surface of TAMC might protect against cytolysis by γδ T lymphocytes. We thus tested whether or not the 4 h of cell contact with TAMC induced the γδ T cells to secrete their lytic granules and kill these target cells. Lytic granule secretion by γδ T cells, as monitored by cell surface expression of the CD107a marker, was not significant when co-incubated with TAMC (Fig. 3B). Accordingly, the TAMC were weakly killed by the γδ T cells under these conditions (Fig. 3C). These results indicated that 4 h of contact between TAMC and γδ T cells spared the stromal cells from cytolytic attacks. In order to refute the possibility that it is merely reflected incubation with inactivated γδ T cells, the same experiment was performed in the presence of the strong agonist BrHPP, known to trigger γδ T cell responses within seconds [27]. Again, the TAMC were spared from cytolysis mediated by BrHPP-activated γδ T lymphocytes (Fig. 3C).

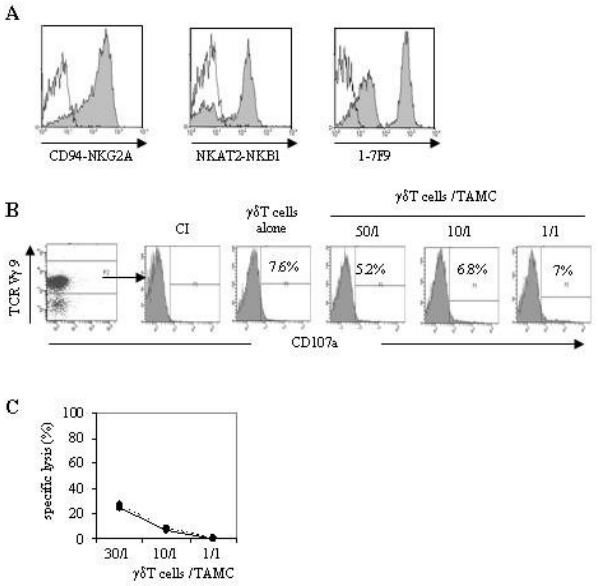

Fig. 3 Weak lysis of the TAMC by the γδ T cells.
A: Expression of KIR inhibitory receptors by the γδ T cells (shaded histogram) compared to the isotypic control (black line), the NKAT2 antibody recognized KIR2DL2, KIR2DL3 and KIR2DS2; the NKB1 antibody recognized KIR2DL1, and the 1-7F9 antibody recognized KIR2DL1, KIR2DL2, KIR2DL3, KIR2DS1 and KIR2DS2; **B:** Expression (%) of the CD107a by the γδ T cells alone or after 3 h of contact with the TAMC compared to the isotopic control (CI); **C:** Percentage of specific lysis of the TAMC by the γδ T cells reactivated (dotted line) or not (black line) by the BrHPP.

3.4 TAMC Do Not Inhibit the Allogenic Lysis Function of the γδ T Cells

The above result suggested that cell contact with TAMC might have abrogated any lytic activity from the activated γδ T cells. To address this, we asked whether or not co-incubation of TAMC and γδ T cells inhibited the strong killing of Daudi cells, a well-known γδ T cell target cell line of HLA class-I-deficient Burkitt's lymphoma [28]. When in the presence of Daudi target cells alone, 50% of the γδ T cells were induced to secrete cytolytic granules. When tested in the presence of Daudi cells plus increasing numbers of TAMC or culture supernatant, however, the same rate of secreting γδ T cells were recorded, suggesting that the presence of TAMC had not abrogated any lytic activity from the activated γδ T cells (Fig. 4A). Accordingly, the specific lysis of Daudi cells was not affected by the presence of TAMC in the co-culture (Fig. 4B). Along the same line, the low level of lysis of the ovarian carcinoma cell line OVCAR was not affected by TAMC initially derived from the ascitis of ovarian carcinoma patients (Fig. 4C). Again, a similar conclusion was reached when this type of experiment was performed in presence of BrHPP. The strong γδ T cell stimulus triggered a higher specific lysis of OVCAR, but this was not impaired by the presence of TAMC (Fig. 4D).

Altogether, these results indicated that co-incubation with TAMC had not broadly abrogated all cytolytic activity by γδ T lymphocytes, but only that directed against the TAMC.

4. Discussion

In this study, we showed that direct contact between γδ T lymphocytes and TAMC induces the trogocytosis

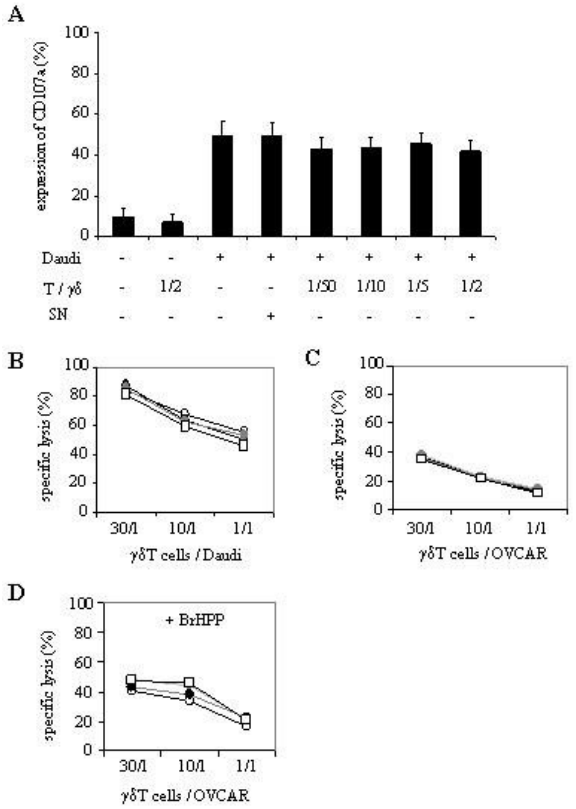

Fig. 4 TAMC did not inhibit the allogenic lysis function of the γδ T cells.

A: Expression of CD107a by the γδ T cells activated or not by the Daudi cell line and in the presence or absence of the TAMC or of their culture supernatant (SN); **B:** Specific lysis of Daudi cells by γδ T cells without TAMC (white circle), with TAMC (1/2 ratio: black circle, 1/50 ratio: grey circle), and with the supernatant of the TAMC culture (white square); **C:** Specific lysis of OVCAR cells by the γδ T cells without TAMC (white circle), with TAMC (1/2 ratio: black circle, 1/50 ratio: grey circle), and with the supernatant of the TAMC culture (white square); **D:** Specific lysis of OVCAR cells by the γδ T cells without TAMC (white circle), with TAMC (1/2 ratio: black circle, 1/50 ratio: grey circle), with the supernatant of the TAMC culture (white square) with reactivation of the γδ T cells by BrHPP.

of γδ cells, leading to a selective acquisition of their HLA class-I molecules at the cell surface of TAMC. This did not impair the anti-tumour cytolytic activity of γδ T lymphocytes, although their lytic activity spared these stromal cells.

Usually, γδ T cells are considered as immune cytotoxic effectors that engage immunological synapses, recognize target cells and kill them [29-31]. The conjugation of a cytolytic CD8 T lymphocyte to its target cell involves a fusion of both plasma membranes at the immunological synapse [32], a structure prone to yielding to trogocytosis. The immunological synapses of cytolytic γδ T lymphocytes and their target cells also permit the acquisition of cell membrane molecules through trogocytosis [27]. In addition, both trogocytosis and the release of cytolytic granules occur simultaneously in these immunological synapses [28]. Although trogocytosis between non-immune cells was depicted previously [14, 33-35], few reports have documented the reciprocal acquisition of immune cell-derived markers such as NK cell receptors [36] or $CD4^+$ T cell proteins [37] by non-immune cells. Here, we showed for the first time the transfer of γδ T cell-derived membrane molecules onto the membrane of stromal cells and particularly HLA-class I molecules. Some studies showed the transfer of HLA molecules such as HLA-G1 but from the target (APC) onto CD4 or CD8 T cells and not from the effector cells on the target [38]. Moreover, the selectivity of the molecular acquisition by TAMC, i.e. of γδ T cell-derived HLA class-I molecules but not of CD25, CD69, Vγ9Vδ2 TCR or NKG2D, is puzzling, but not unprecedented. The T cells efficiently acquire CD9 and moderately acquire CXCR4 (but not MeCP2) from the surface of HEK cells by trogocytosis [39]. Whatever the molecular mechanism underlying this molecular specificity, however, TAMC constitutively express a very low amount of HLA class-I molecules, so conceivably, their trogocytically-increased level of cell surface HLA class-I molecules could protect against lytic attack by the γδ T lymphocytes. The level of KIR on the γδ cells supports the view that their cytolytic activity might be dampened by self-HLA class-I ligands. This model is supported by the weak lysis of TAMC that we report here.

5. Conclusion

Here, we showed for the first time the specific transfer of γδ T cell-derived membrane HLA-class I

molecules onto the membrane of tumor-associated stromal cells.

The microenvironment of ovarian carcinomas contains γδ T [2], NK [40] and TAMC [14] tumour-infiltrating cells. Therefore, physiologically, the TAMC could acquire a higher level of self-HLA class-I molecules through immunological synapses with γδ T cells and thus be spared from cytolytic attack. However, NK cells are able to kill foetal and adult stromal cells such as MSC by NKG2D or TRAIL-mediated pathways, and this killing can be inhibited by the up-regulation of HLA class-I molecules upon exposure to IFNγ [26, 41]. Moreover, cancer-associated stromal cells might differ from healthy stromal cells and represent better targets for cytolytic lymphocytes. For instance, MSC from AML patients show abnormal morphology and impaired differentiation [42]. MSC from patients with multiple myeloma also display distinct genomic and phenotypic profiles compared to MSC from healthy individuals [43, 44]. Due to these distinctive characteristics, cancer-associated stromal cells could therefore be targeted by cytolytic effector cells. Their ability to acquire protective molecules like HLA-class I upon trogocytosis could be a salvage mechanism for their maintenance in the microenvironment. In fact, stromal cells have dual facets of bioactivity. At the same time they can be immunosuppressive for T or NK cell functions [15, 18, 20, 21, 45-47] and they can also support tumour development by conferring chemoresistance [14], promoting metastases [13, 48] and favouring tumour progression [49-51].

Trogocytosis has been proposed as a mechanism leading to the modulation of immune responses, mediating the acquisition of multidrug resistance in tumour cells, favouring fusion of the oocyte with spermatozoa and facilitating the antiviral role of T cells [33, 34, 52, 53].

Thus, we propose that by contributing to the maintenance of cancer-associated stromal cells, trogocytosis might also participate in tumour progression. Future studies at our laboratory will determine whether or not the targeting of cancer-associated stromal cells and their cell interactions might have a therapeutic activity for cancer.

Acknowledgments

This work was supported by institutional grants from l'Institut National de la Santé et de la Recherche Médicale and by the Innate Pharma, Marseille. The authors would like to thank the “Plateau Technique d'Imagerie Cellulaire de Toulouse Purpan” for the confocal microscopy.

References

[1] J. Pfisterer, J.A. Ledermann, Management of platinum-sensitive recurrent ovarian cancer, Semin. Oncol. 33 (2 Suppl. 6) (2006) 12-16.

[2] M.R. Raspollini, F. Castiglione, D. Rossi Degl'innocenti, G. Amunni, A. Villanucci, F. Garbini, et al., Tumour-infiltrating gamma/delta T-lymphocytes are correlated with a brief disease-free interval in advanced ovarian serous carcinoma, Ann. Oncol. 16 (4) (2005) 590-596.

[3] W. Zou, V. Machelon, A. Coulomb-L'Hermin, J. Borvak, F. Nome, T. Isaeva, et al., Stromal-derived factor-1 in human tumors recruits and alters the function of plasmacytoid precursor dendritic cells, Nat. Med. 7 (12) (2001) 1339-1346.

[4] R. Yigit, L.F. Massuger, C.G. Figdor, R. Torensma, Ovarian cancer creates a suppressive microenvironment to escape immune elimination, Gynecol. Oncol. 117 (2) (2010) 366-372.

[5] U.K. Scarlett, J.R. Cubillos-Ruiz, Y.C. Nesbeth, D.G. Martinez, X. Engle, A.T. Gewirtz, et al., *In situ* stimulation of CD40 and Toll-like receptor 3 transforms ovarian cancer-infiltrating dendritic cells from immunosuppressive to immunostimulatory cells, Cancer Res. 69 (18) (2009) 7329-7337.

[6] L.A. Liotta, E.C. Kohn, The microenvironment of the tumour-host interface, Nature 411 (6835) (2001) 375-379.

[7] L.M. Coussens, C.L. Tinkle, D. Hanahan, Z. Werb, MMP-9 supplied by bone marrow-derived cells contributes to skin carcinogenesis, Cell 103 (3) (2000) 481-490.

[8] A.E. Karnoub, A.B. Dash, A.P. Vo, A. Sullivan, M.W. Brooks, G.W. Bell, et al., Mesenchymal stem cells within tumour stroma promote breast cancer metastasis, Nature

449 (7162) (2007) 557-563.

[9] R. Lis, J. Capdet, P. Mirshahi, M. Lacroix-Triki, F. Dagonnet, C. Klein, et al., Oncologic trogocytosis with Hospicells induces the expression of N-cadherin by breast cancer cells, Int. J. Oncol. 37 (6) (2010) 1453-1461.

[10] A. Orimo, P.B. Gupta, D.C. Sgroi, F. Arenzana-Seisdedos, T. Delaunay, R. Naeem, et al., Stromal fibroblasts present in invasive human breast carcinomas promote tumor growth and angiogenesis through elevated SDF-1/CXCL12 secretion, Cell 121 (3) (2005) 335-348.

[11] M. Pasquet, M. Golzio, E. Mery, A. Rafii, N. Benabbou, P. Mirshahi, et al., Hospicells (ascites-derived stromal cells) promote tumorigenicity and angiogenesis, Int. J. Cancer 126 (9) (2010) 2090-2101.

[12] M. Konopleva, S. Konoplev, W. Hu, A.Y. Zaritskey, B.V. Afanasiev, M. Andreeff, Stromal cells prevent apoptosis of AML cells by up-regulation of anti-apoptotic proteins, Leukemia 16 (9) (2002) 1713-1724.

[13] R. Lis, C. Touboul, P. Mirshahi, F. Ali, S. Mathew, D.J. Nolan, et al., Tumor associated mesenchymal stem cells protects ovarian cancer cells from hyperthermia through CXCL12, Int. J. Cancer 128 (3) (2011) 715-725.

[14] A. Rafii, P. Mirshahi, M. Poupot, A.M. Faussat, A. Simon, E. Ducros, et al., Oncologic trogocytosis of an original stromal cells induces chemoresistance of ovarian tumours, PLoS. One 3 (12) (2008) 3894.

[15] G.M. Spaggiari, A. Capobianco, H. Abdelrazik, F. Becchetti, M.C. Mingari, L. Moretta, Mesenchymal stem cells inhibit natural killer-cell proliferation, cytotoxicity, and cytokine production: Role of indoleamine 2,3-dioxygenase and prostaglandin E2, Blood 111 (3) (2008) 1327-1333.

[16] M. Balsamo, F. Scordamaglia, G. Pietra, C. Manzini, C. Cantoni, M. Boitano, et al., Melanoma-associated fibroblasts modulate NK cell phenotype and antitumor cytotoxicity, Proc. Natl. Acad. Sci. USA 106 (49) (2009) 20847-20852.

[17] K. Sato, K. Ozaki, I. Oh, A. Meguro, K. Hatanaka, T. Nagai, et al., Nitric oxide plays a critical role in suppression of T-cell proliferation by mesenchymal stem cells, Blood 109 (1) (2007) 228-234.

[18] L. Martinet, S. Fleury-Cappellesso, M. Gadelorge, G. Dietrich, P. Bourin, J.J. Fournie, et al., A regulatory cross-talk between Vγ9Vδ2 T lymphocytes and mesenchymal stem cells, Eur. J. Immunol. 39 (3) (2009) 752-762.

[19] A. Augello, R. Tasso, S.M. Negrini, A. Amateis, F. Indiveri, R. Cancedda, et al., Bone marrow mesenchymal progenitor cells inhibit lymphocyte proliferation by activation of the programmed death 1 pathway, Eur. J. Immunol. 35 (5) (2005) 1482-1490.

[20] L. Martinet, R. Poupot, P. Mirshahi, A. Rafii, J.J. Fournie, M. Mirshahi, et al., Hospicells derived from ovarian cancer stroma inhibit T cell immune responses, Int. J. Cancer. 126 (9) (2010) 2143-2152.

[21] I. Petrini, S. Pacini, M. Petrini, R. Fazzi, L. Trombi, S. Galimberti, Mesenchymal cells inhibit expansion but not cytotoxicity exerted by gamma-delta T cells, Eur. J. Clin. Invest. 39 (9) (2009) 813-818.

[22] X.X. Jiang, Y. Zhang, B. Liu, S.X. Zhang, Y. Wu, X.D. Yu, et al., Human mesenchymal stem cells inhibit differentiation and function of monocyte-derived dendritic cells, Blood 105 (10) (2005) 4120-4126.

[23] S. Beyth, Z. Borovsky, D. Mevorach, M. Liebergall, Z. Gazit, H. Aslan, et al., Human mesenchymal stem cells alter antigen-presenting cell maturation and induce T-cell unresponsiveness, Blood 105 (5) (2005) 2214-2219.

[24] M. Krampera, L. Cosmi, R. Angeli, A. Pasini, F. Liotta, A. Andreini, et al., Role for interferon-gamma in the immunomodulatory activity of human bone marrow mesenchymal stem cells, Stem Cells 24 (2) (2006) 386-398.

[25] H. Maby-El Hajjami, P. Ame-Thomas, C. Pangault, O. Tribut, J. DeVos, R. Jean, et al., Functional alteration of the lymphoma stromal cell niche by the cytokine context: Role of indoleamine-2,3 dioxygenase, Cancer Res. 69 (7) (2009) 3228-3237.

[26] G.M. Spaggiari, A. Capobianco, S. Becchetti, M.C. Mingari, L. Moretta, Mesenchymal stem cell-natural killer cell interactions: Evidence that activated NK cells are capable of killing MSCs, whereas MSCs can inhibit IL-2-induced NK-cell proliferation, Blood 107 (4) (2006) 1484-1890.

[27] E. Espinosa, J. Tabiasco, D. Hudrisier, J.J. Fournie, Synaptic transfer by human gamma delta T cells stimulated with soluble or cellular antigens, J. Immunol. 168 (12) (2002) 6336-6343.

[28] J. Gertner, A. Wiedemann, M. Poupot, J.J. Fournie, Human gammadelta T lymphocytes strip and kill tumor cells simultaneously, Immunol. Lett. 110 (1) (2007) 42-53.

[29] P. Fisch, E. Meuer, D. Pende, S. Rothenfusser, O. Viale, S. Kock, et al., Control of B cell lymphoma recognition via natural killer inhibitory receptors implies a role for human Vgamma9/Vdelta2 T cells in tumor immunity, Eur. J. Immunol. 27 (12) (1997) 3368-3379.

[30] M. Todaro, M. D'Asaro, N. Caccamo, F. Iovino, M.G. Francipane, S. Meraviglia, et al., Efficient killing of human colon cancer stem cells by γδ T lymphocytes, J. Immunol. 182 (11) (2009) 7287-7296.

[31] B. Favier, E. Espinosa, J. Tabiasco, C. Dos Santos, M. Bonneville, S. Valitutti, et al., Uncoupling between immunological synapse formation and functional outcome in human gamma delta T lymphocytes, J. Immunol. 171 (10) (2003) 5027-5033.

[32] J.C. Stinchcombe, G. Bossi, S. Booth, G.M. Griffiths, The immunological synapse of CTL contains a secretory domain and membrane bridges, Immunity 15 (5) (2001) 751-761.

[33] V. Barraud-Lange, N. Naud-Barriant, M. Bomsel, J.P. Wolf, A. Ziyyat, Transfer of oocyte membrane fragments to fertilizing spermatozoa, FASEB J. 21 (13) (2007) 3446-3449.

[34] A. Levchenko, B.M. Mehta, X. Niu, G. Kang, L. Villafania, D. Way, et al., Intercellular transfer of P-glycoprotein mediates acquired multidrug resistance in tumor cells, Proc. Natl. Acad. Sci. USA 102 (6) (2005) 1933-1938.

[35] M. Poupot, J.J. Fournie, Spontaneous membrane transfer through homotypic synapses between lymphoma cells, J. Immunol. 171 (5) (2003) 2517-2523.

[36] B. Vanherberghen, K. Andersson, L.M. Carlin, E.N. Nolte-'t Hoen, G.S. Williams, P. Hoglund, et al., Human and murine inhibitory natural killer cell receptors transfer from natural killer cells to target cells, Proc. Natl. Acad. Sci. USA 101 (48) (2004) 16873-16878.

[37] T. He, C. Tang, Y. Liu, Z. Ye, X. Wu, Y. Wei, et al., Bidirectional membrane molecule transfer between dendritic and T cells, Biochem. Biophys. Res. Commun. 359 (2) (2007) 202-208.

[38] J. LeMaoult, J. Caumartin, M. Daouya, B. Favier, S. Le Rond, A. Gonzalez, et al., Immune regulation by pretenders: cell-to-cell transfers of HLA-G make effector T cells act as regulatory cells, Blood 109 (5) (2007) 2040-2048.

[39] S. Daubeuf, A. Aucher, C. Bordier, A. Salles, L. Serre, G. Gaibelet, et al., Preferential transfer of certain plasma membrane proteins onto T and B cells by trogocytosis, PLoS One 5 (1) (2010) e8716. doi: 10.1371/journal.pone.0008716.

[40] H.P. Dong, M.B. Elstrand, A. Holth, I. Silins, A. Berner, C.G. Trope, et al., NK-and B-cell infiltration correlates with worse outcome in metastatic ovarian carcinoma, Am. J. Clin. Pathol. 125 (3) (2006) 451-458.

[41] Y. Terui, Y. Mishima, N. Sugimura, K. Kojima, T. Sakurai, R. Kuniyoshi, et al., Identification of CD20 C-terminal deletion mutations associated with loss of CD20 expression in non-Hodgkin's lymphoma, Clin. Cancer Res. 15 (7) (2009) 2523-2530.

[42] Z.G. Zhao, Y. Liang, K. Li, W.M. Li, Q.B. Li, Z.C. Chen, et al., Phenotypic and functional comparison of mesenchymal stem cells derived from the bone marrow of normal adults and patients with hematologic malignant diseases, Stem. Cells Dev. 16 (4) (2007) 637-648.

[43] M. Garayoa, J.L. Garcia, C. Santamaria, A. Garcia-Gomez, J.F. Blanco, A. Pandiella, et al., Mesenchymal stem cells from multiple myeloma patients display distinct genomic profile as compared with those from normal donors, Leukemia 23 (8) (2009) 1515-1527.

[44] L. Garderet, C. Mazurier, A. Chapel, I. Ernou, L. Boutin, X. Holy, et al., Mesenchymal stem cell abnormalities in patients with multiple myeloma, Leuk Lymphoma 48 (10) (2007) 2032-2041.

[45] R. Ramasamy, C.K. Tong, H.F. Seow, S. Vidyadaran, F. Dazzi, The immunosuppressive effects of human bone marrow-derived mesenchymal stem cells target T cell proliferation but not its effector function, Cell Immunol. 251 (2) (2008) 131-136.

[46] F. Gieseke, J. Bohringer, R. Bussolari, M. Dominici, R. Handgretinger, I. Muller, Human multipotent mesenchymal stromal cells employ galectin-1 to inhibit immune effector cells, Blood 116 (19) (2010) 3770-3779.

[47] M. Najar, G. Raicevic, H.I. Boufker, H. Fayyad Kazan, C. De Bruyn, N. Meuleman, et al., Mesenchymal stromal cells use PGE2 to modulate activation and proliferation of lymphocyte subsets: Combined comparison of adipose tissue, Wharton's Jelly and bone marrow sources, Cell Immunol. 264 (2) (2010) 171-179.

[48] F.T. Martin, R.M. Dwyer, J. Kelly, S. Khan, J.M. Murphy, C. Curran, et al., Potential role of mesenchymal stem cells (MSCs) in the breast tumour microenvironment: Stimulation of epithelial to mesenchymal transition (EMT), Breast Cancer Res. Treat. 124 (2) (2010) 317-326.

[49] L. Kucerova, M. Matuskova, K. Hlubinova, V. Altanerova, C. Altaner, Tumor cell behaviour modulation by mesenchymal stromal cells, Mol. Cancer 9 (1) (2010) 129. doi: 10.1186/1476-4598-9-129.

[50] S.A. Patel, J.R. Meyer, S.J. Greco, K.E. Corcoran, M. Bryan, P. Rameshwar, Mesenchymal stem cells protect breast cancer cells through regulatory T cells: role of mesenchymal stem cell-derived TGF-beta, J. Immunol. 184 (10) (2010) 5885-5894.

[51] V.R. Placencio, X. Li, T.P. Sherrill, G. Fritz, N.A. Bhowmick, Bone marrow derived mesenchymal stem cells incorporate into the prostate during regrowth, PLoS one 5 (9) (2010) e12920. DOI: 10.1371/journal.pone.0012920.

[52] K.A. Ahmed, M.A. Munegowda, Y. Xie, J. Xiang, Intercellular trogocytosis plays an important role in modulation of immune responses, Cell Mol. Immunol. 5 (4) (2008) 261-269.

[53] G. Chaudhri, B.J. Quah, Y. Wang, A.H. Tan, J. Zhou, G. Karupiah, et al., T cell receptor sharing by cytotoxic T lymphocytes facilitates efficient virus control, Proc. Natl. Acad. Sci. USA 106 (35) (2009) 14984-14989.

Journal of Life Sciences 5 (2011) 996-1002

Process Capability Analysis of Delivering Neonatal Care with Normal Weight (Case Study of Neonatal Weight Data at a Maternity Clinic in Banjarmasin)

Dewi Anggraini

Department of Mathematics, Faculty of Mathematics and Natural Sciences, University of Lambung Mangkurat, Banjarmasin, South Kalimantan 70714, Indonesia

Received: January 13, 2011 / Accepted: May 26, 2011 / Published: December 30, 2011.

Abstract: Statistical Quality Control (SQC) is used to analyze and monitor quality characteristic measurements of normal neonatal weight in a maternity clinic in Banjarmasin in this paper. The objective of this study is to assist medical practitioners in observing pregnant women to deliver their babies with normal weight. It is also assumed that pregnant women who delivered their babies in the clinic have been monitored during their nine-month pregnancy. Thus, they can manage their own pregnancy to deliver normal weight babies. The use of Statistical Process Control (SPC) tools, such as frequency histogram, probability plot, and the implementation of Shewhart, R, and S control charts as primary techniques, are presented to display the monitoring aspects of the process. In addition, Process Capability Analysis (PCA) is performed to ensure that the process outcomes are capable of meeting certain requirements or specifications. The Process Capability Ratio (PCR) for the process is also presented. This analysis is an essential part of an overall quality improvement program.

Key words: Process capability analysis, Shewhart control chart, R-chart, normal neonatal weight.

1. Introduction

Statistical Process Control (SPC) is a collection of visual statistical problem-solving tools used for systematically monitoring a production process/service to achieve stability, and quality improvement in the process by reducing variability. This method has been adopted since 1940s in the industrial area. The use of this method has a significant improvement towards the quality characteristic of manufactured products in industrialized countries, such as Japan and United States. The idea of this method is to thoroughly control production process of products/services such that fit the customer satisfaction. The manufactured products should have fitness values for use, such as well-performed, reliable, durable, easy to repair, good visual appearance, outstanding function, good reputation, and satisfy the expected requirements.

The implementation of SPC has also been widely used in the medical area. This method can assist medical practitioners to improve the quality characteristic and healthcare process/service. Goldenberg et al. [1] described an early statistical detection of anthrax outbreaks by tracking Over-the-counter (OTC) medication sales. They used a statistical framework for monitoring grocery data to detect a large-scale but localized bioterrorism attack and an early detection statistical system designed for bio surveillance to improve clinical preparedness for bioterrorism. Stevens [2] has studied SPC with its core tool, the control chart, considerably potential to facilitate medical practitioners in managing the change of healthcare systems and improving patients' health. He also explained that SPC helped patients with

Corresponding author: Dewi Anggraini, S.Si., M.App.Sci., lecturer, research fields: statistics and operations research. E-mail: de28383wi@yahoo.com.

chronic conditions, such as asthma and diabetes, to manage their own health and therefore, improve therapeutic qualities.

Anshari [3] reported that neonatal mortality rate in 2003 is approximately 40%-60% or about 18 over 1,000 live birth caused by premature neonatal. Indonesia, as a developing country, still has the above problems. According to Dr. Effek Alamsyah, SpA, MPH (The Chairman of PP Perinatologi Indonesia), premature neonatal is caused by two major factors: minimum period of pregnancy, and fetal disturbance growth in the abdomen [3].

This study aims to evaluate the service characterization of a maternity clinic in monitoring pregnant women to deliver their babies with normal weight. This quality of service can be investigated first using histogram, probability plot, and the implementations of Shewhart, R, and S control charts as a primary technique to summarize the performance of the process. In addition, this study will display the potential capability of the clinical process. We will use Process Capability Ratio (PCR) to show how capable the clinic is in helping pregnant women to have normal neonatal weight.

This study uses a secondary data of 84 neonatal weight samples from Feb. 2007 to Sept. 2010. We use samples size 5. All babies are born in the maternity clinic in Banjarmasin.

2. Materials and Methods

2.1 Statistical Quality Control (SQC)

Statistical Quality Control (SQC) is a statistical method that requires a quality characteristic measurement of manufacturing data in order to analyze and maintain the quality of manufactured product [4]. The objectives of statistical methodology in quality control and improvement are to show that descriptive statistics is a simple tool to describe quantitatively variation in a quality characteristic when a sample of data is drawn from its related population and to introduce the use of probability distributions as a tool for modeling or describing the quality characteristic of a process [5].

2.2 Normal Distribution

Normal (Gaussian) distribution is probably the most important distribution in both the theory and application of statistics. It has the probability density function as:

$$f(x)=\frac{1}{\sqrt{2\pi}\sigma}e^{-\frac{1}{2}\left(\frac{x-\mu}{\sigma}\right)^2},\ -\infty<x<\infty$$

where μ ($-\infty<\mu<\infty$) and σ ($\sigma^2>0$) are the mean and the variance of the normal distribution, respectively.

If X is a random variable that is normally distributed with mean μ and standard deviation σ, then it can be written as: $X \sim N(\mu, \sigma^2)$.

In a normal distribution, there is a simple interpretation of σ. This standard deviation measures the distance on the horizontal scale associated with the limits defined by $\mu \pm \sigma$ (68.26% of the population values fall between the limits), $\mu \pm 2\sigma$ (95.46% of the population values fall between the limits), and $\mu \pm 3\sigma$ (99.73% of the population values fall between the limits) [4].

2.3 Statistical Process Control (SPC)

Statistical Process Control (SPC) is one of techniques used to monitor manufacturing processes and provide immediate feedback control. The feedback control is used to maintain and improve the capability of the process that result in product conformance to meet customer satisfaction.

Some techniques associated with SPC include histograms, and control charts. A histogram is a visual display of frequency distribution to show shape, location, and spread of data. While, a control chart is a statistical tool used to monitor the variation and trends occurring in a process and ensure that the process is in a state of control. A control chart has its limits: Upper Control Limit (UCL), Central Limit (CL), and Lower Control Limit (LCL) measured from the dispersion

happened in the process. These limits can be set as $\mu \pm \sigma$, $\mu \pm 2\sigma$, or $\mu \pm 3\sigma$, where μ is the process mean and σ is the process standard deviation [4].

A manufacturing process or service is well-controlled if the quality characteristic measurements of the process lie between the control limits. Generally, the statistical limits used in SPC are $\mu \pm 3\sigma$ and as well-known as "three sigma control limits". In a normal distribution, these limits imply that 99.73% of the values measured lie in the interval of width 6σ. Note that σ here refers to the standard deviation of the statistics plotted on the chart (i.e. $\sigma_{\bar{x}}$) not the standard deviation of the quality characteristic [5].

2.4 Process Capability Analysis (PCA)

Process capability analysis is a branch of statistical methods to ensure that the outcomes of a process are capable to fulfill certain requirements or specifications. Application of process capability analysis is an essential part of an overall quality improvement program in any industry today. It provides guidance to how to produce products that meet required specification limits.

Process capability analysis can produce a valid and accurate report if the observed process is in-control. The concept of process capability was introduced by Juran et al. [6-11]. The two most popular indices used in manufacturing industry are C_p and C_{pk} defined as follows:

$$C_p = \frac{USL - LSL}{6\sigma} \quad (1)$$

$$C_{pk} = min\left(\frac{\mu - LSL}{3\sigma}, \frac{USL - \mu}{3\sigma}\right) \quad (2)$$

$$C_{pk} = min\left(C_{pl}, C_{pu}\right) \quad (3)$$

C_p and C_{pk} are process capability indices which assess the ability of process products in meeting their respective specification limits. In the analysis of these measures, there are mainly two characteristics of importance, the process location in relation to its target value and the process spread. The closer the process output is to the target value or the smaller that the process spread is, the more capable is the process. The process capability indices combine the above characteristics of a capable process and transform them into a single number that reflects the capability of the process. The larger the value of a process capability index, the more capable the process is [4].

LSL and *USL* are the lower and upper specification limits, μ and σ are the process mean and standard deviation, respectively. Since the process mean μ and process variance σ^2 are unknown, they are often estimated using collected quality characteristics data [5].

Both of the above mentioned capability indices were designed to be used with the normally distributed data. However, these basic assumptions of normality are not usually fulfilled in practice. Most of the processes in the real world produce non-normal quality characteristics data and the quality practitioners need to consider the basic assumptions before deploying any conventional process capability technique [11].

2.5 Neonatal Mortality Rate (NMR)

Neonatal Mortality Rate (NMR) can be defined as the number of deaths happened in newborn babies' age from 0 to 28 days. In Indonesia, most of infant mortality occurs during the neonatal period. The delivery at home is usually without assistance of health provider, and too late in receiving a certain quality of care [12].

Indonesian Health and Household Survey 2001 reported that NMR in Indonesia has been reduced slowly from 28.2/1000-20/1000 live birth in 2001 [12, 13]. WHO reported that NMR in Indonesia is 18/1000 live birth or 40%-60% caused by premature newborn babies [12-14]. In addition, Indonesian Health and Demographic Survey 2007 reported that Indonesia has NMR = 19/1000 live birth with the 86.000 deaths per year, 236 deaths per day, and 10 deaths per hour. This value is still high compared to other Asian countries [13, 14].

The main cause of neonatal deaths is due to premature newborn babies approximately 48%,

followed by asphyxia 37% and sepsis 36.5% [14]. Indonesian Health and Household Survey 2001 also reported that the most significant factor influenced NMR is low birth weight (< 2,500 g) reported as 29 % and asphyxia (27%) [15]. Prof. Dr. M. Jufri explained that the main cause of neonatal deaths is extreme prematurity [16].

According to Kosim the normal weight of neonatal is between 2,500 and 4,000 g [17]. This also has been justified by Indonesian Health Department that normal newborns are babies delivered between 37 and 42 weeks with weight birth from 2,500 to 4,000 g. Therefore, the specification limits of normal neonatal weight can be ranged from 2,500 to 4,000 g [17].

In order to help reducing neonatal mortality prevalence in Indonesia, this study will first try to assess the capability of the process of delivering babies with normal weight in a maternity clinic in Banjarmasin. It is assumed that if pregnant women have monitored their nine-month pregnancy regularly in the clinic, it will probably improve the quality of their delivered babies; in this case babies may have normal weight.

3. Results and Discussion

This study has used 84 samples, each of size five, taken from a maternity clinic in Banjarmasin between Feb. 2007 and Sept. 2010. $\bar{x}$, R, and S have been designed based on all samples to monitor the process average or mean quality level, variability, and standard deviation, respectively.

In constructing control charts, it is suggested to plot R, and S chart first because the control limits on $\bar{x}$ chart depend on the process variability and standard deviation which are:

$$UCL = \bar{\bar{x}} + A_2\bar{R}, \quad UCL = \bar{\bar{x}} + A_3\bar{S}$$
$$CL = \bar{\bar{x}} \text{ and } CL = \bar{\bar{x}}$$
$$LCL = \bar{\bar{x}} - A_2\bar{R}, \quad LCL = \bar{\bar{x}} - A_3\bar{S}$$

where $\bar{\bar{x}}$ is the average of the samples averages (the grand average), $\bar{R}$ is the average range, and A_2 and A_3 are constants defined by:

$$A_2 = \frac{3}{d_2.\sqrt{n}} \text{ and } A_3 = \frac{3}{c_4.\sqrt{n}}.$$

Even though Figs. 1a, 1b, and 1e show that the process average ($\bar{x}$) is in control and normally distributed, R Chart (Fig. 1c) describes that there are 4 out of control observations: 34, 51, 55, and 82. The out of control signals are also showed in Fig. 1d, S chart where 3 observations: 34, 51, and 74 which are out of the control. These out of control signals are caused due to some low birth weight of neonatal. The normal practice is to look for assignable causes and rectify them. Assuming these causes are rectified then we have removed the out of control observations and recalculated the corresponding control limits from *R* and *S* charts. The new charts are presented below. The new charts after removing samples 34, 51, 55, and 82 (produced out of control signals in *R*-chart) are:

After removing samples 34, 51, 55, and 82, R Chart in Fig. 2c is now in control but S chart in Fig. 2d is still showing 3 out of control signals: 49, 71, and 75. These samples are out of control due to the influence of low birth weight of neonatal. Thus, observation 49, 71, and 75 are excluded from the calculation of control limits in all three charts. The new charts are:

Excluding the 49, 71 and 75 samples from the control limits, calculation have produced a process where $\bar{x}$, R and S charts are all in control (see Figs. 3c, 3d, and 3e). As mentioned earlier one can assess the capability of the process only when process is in control. Using the statistical package Minitab we have provided the result of the capability analysis in Fig. 4 below.

It can be seen from Fig. 4 that the value of C_p is 1.70 and C_{pk} is 1.24. The value of C_p (1.70) indicates that the potential capability of the delivering normal neonatal weight in the clinic is very good. According to our analysis, the chance of having neonatal with low birth weight is approximately 0.34 babies per million (ppm) live births. While, the value of C_{pk} (1.24) describes that the actual capability of the delivering normal neonatal weight in the clinic is also very high.

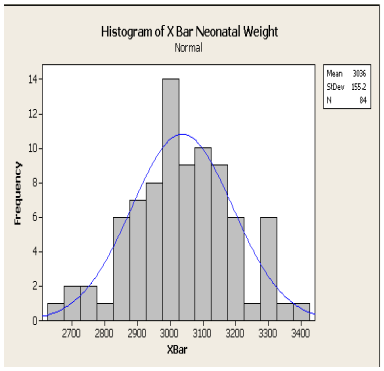

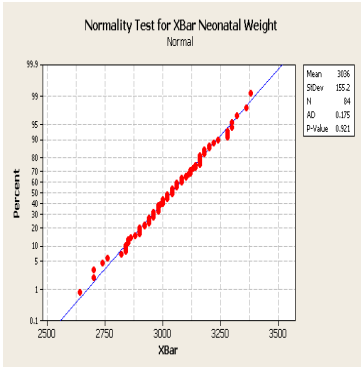

a. Histogram of $\overline{X}$ chart for normal neonatal weight. **b. Probability normal plot of $\overline{X}$ chart for normal neonatal weight.**

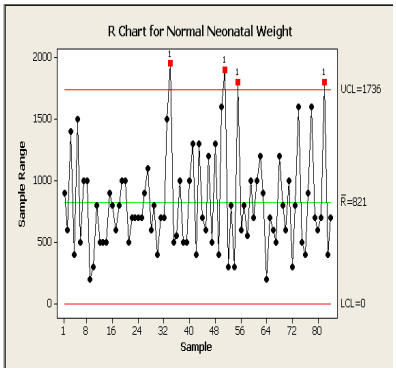

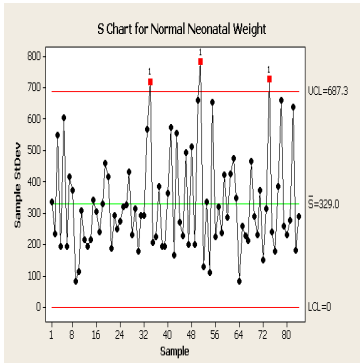

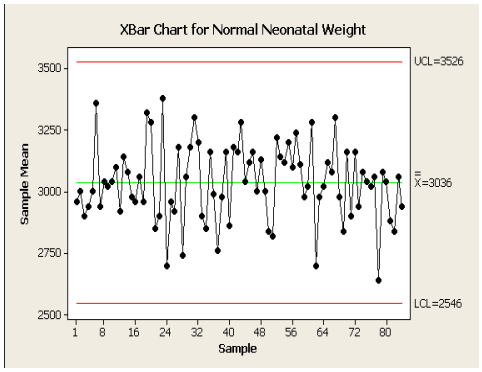

c. *R* chart for normal neonatal weight. **d. *S* chart for normal neonatal weight.** **e. $\overline{X}$ chart for normal neonatal weight.**

Fig. 1 Normal neonatal weight data plot.

a: Histogram of $\overline{X}$ chart; b: Probability normal plot of $\overline{X}$ chart; c: R chart; d: S chart; e: $\overline{X}$ chart.

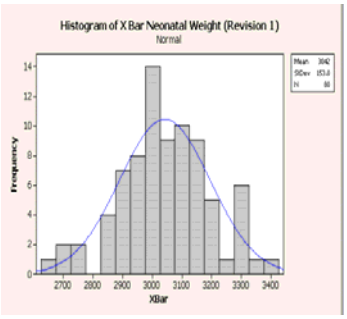

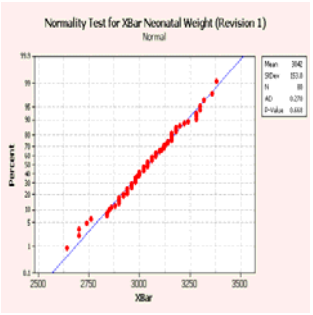

a. Histogram of $\overline{X}$ chart for normal neonatal weight (revision 1). **b. Probability normal plot of $\overline{X}$ chart for normal neonatal weight (revision 1).**

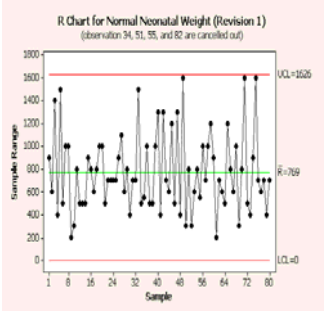

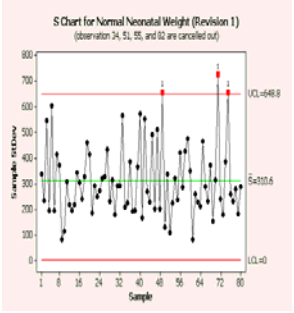

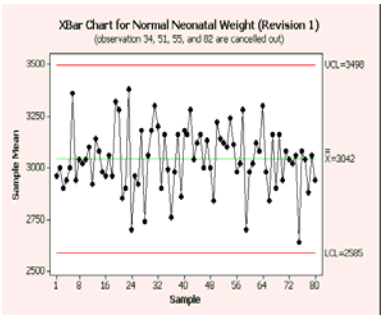

c. *R* chart for normal neonatal weight (revision 1). **d. *S* chart for normal neonatal weight (revision 1).** **e. $\overline{X}$ chart for normal neonatal weight (revision 1).**

Fig. 2 Normal neonatal weight data plot (revision 1).

a: Histogram of $\overline{X}$ chart; b: probability normal plot of $\overline{X}$ chart; c: *R* chart; d: *S* chart; e: $\overline{X}$ chart.

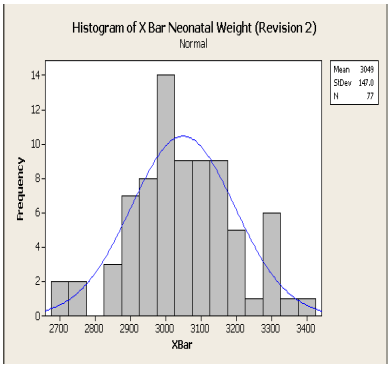

a. Histogram of $\bar{X}$ chart for normal neonatal weight (Revision 2).

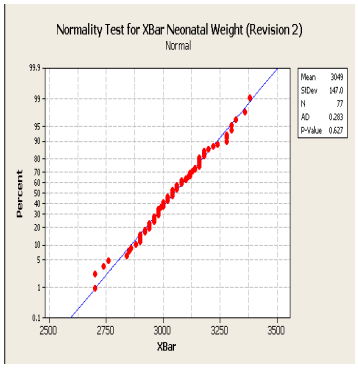

b. Probability normal Plot of $\bar{X}$ chart for normal neonatal weight (Revision 2).

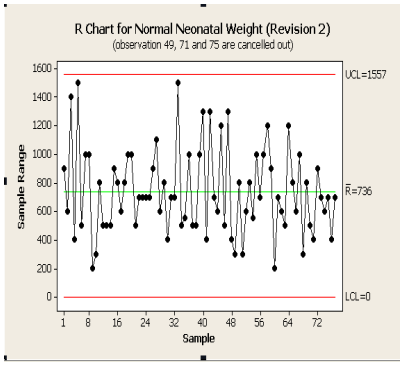

c. *R* chart for normal neonatal weight (Revision 2).

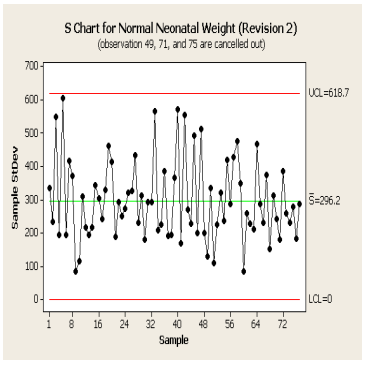

d. *S* chart for normal neonatal weight (Revision 2).

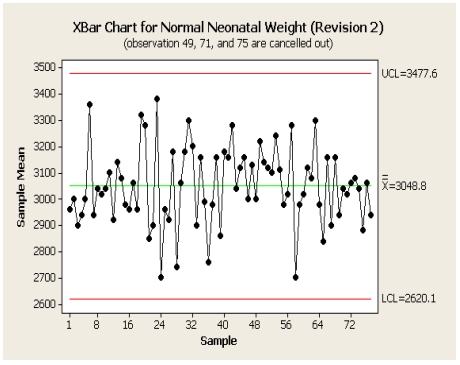

e. $\bar{X}$ chart for normal neonatal weight (Revision 2).

Fig. 3 Normal neonatal weight data plot (Revision 2).

a: Histogram of $\bar{X}$ chart; b: Probability normal plot of $\bar{X}$ chart; c: R chart; d: S chart; e: $\bar{X}$ chart.

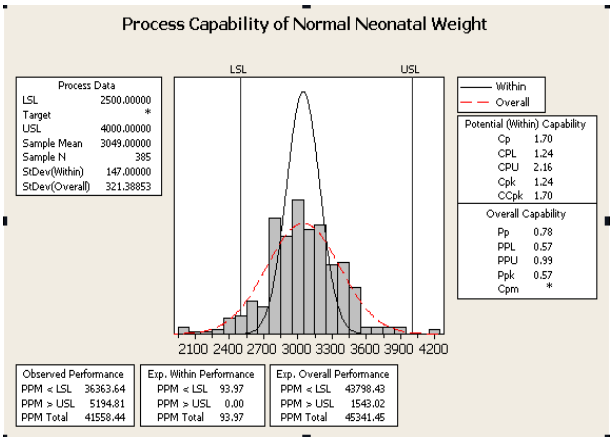

Fig. 4 Process capability analysis of normal neonatal weight data.

However, the fact that C_p is not equal C_{pk} means that the actual mean of birth weight delivery is different to the nominal mean of birth weight delivery. The nominal mean is the average of the upper and lower specifications.

4. Conclusions

In this paper, the author has shown that Statistical Quality Control (SQC) and Process Capability Analysis (PCA) can be applied effectively in health care service. Using real data based on the weight of the delivered babies in a maternity clinic in Banjarmasin, we have first monitored the weight using control charts. This is then followed by capability analysis to estimate the proportion of under weight babies. The significant assumption used in this study is the fact that the pregnant women who have delivered their babies in the clinic have been monitored during their nine month pregnancy.

The study was based on 84 samples of size 5. The data was normally distributed with mean $\mu = 3,036$ g, and standard deviation $\sigma_{\bar{X}} = 155.2$ g. After removing the out of control samples, the final analysis was based

on 77 samples with the average weight of delivered babies in the clinic μ = 3,049 g, and standard deviation $\sigma_{\bar{X}} = 147$ g. The results indicated that women who have been monitored in the clinic through out their pregnancy are certainly capable of delivering a healthy baby in the clinic at the maturity of their pregnancy period.

In conclusion, one can say that the service of an observed maternity clinic in Banjarmasin is a very effective process that can reduce the mortality rate in Indonesia and should be implemented nation wide in the country. During this study, it was also observed that the medical practitioners who run the clinic are highly qualified and provide an excellent service of care and monitoring for the pregnant women who attend the clinic.

Acknowledgments

The author would like to thank Dr. Mali Abdollahian (Senior Lecturer, Program Leader of Master and Graduate Diploma of Statistics and Operations Research, and Program Leader of Master and Graduate Diploma of Business Statistics of RMIT University, Melbourne, Australia) for her useful advice, discussion, and proof reading that were significantly contributed to the completion of this paper.

The author also would like to thank Supri Nuryani, SKM, SST, MKes, the owner of maternity clinic, for providing the neonatal weight data.

References

[1] A. Goldenberg, G. Shmueli, R.A. Carvana, S.E. Fienberg, Early statistical detection of anthrax outbreaks by tracking over-the-counter medication sales, in: Proceedings of the National Academy of Sciences (PMNAS), USA, Apr. 16, 2002, Vol. 99, No. 8, pp. 5237-5240.

[2] D.P. Stevens, Quality lines, in: Quality and Safe in Health Care, USA, Oct. 2007, Vol. 16, No. 5, p. 322.

[3] D. Anshari, Perawatan bayi yang "*cost-effective*" (Cost effective infant care), Sept. 2009, available online at http://bayikangguru.wordpress.com/2009/05/02/hello-world/ (accessed on Oct. 2010). (in Bahasa Indonesia)

[4] S.M. Hanna, Application of Statistical Process Control (SPC) in the manufacturing of medical accelerators, in: Proceedings of the 2003 Particle Accelerator Conference, Siemens Medical Solutions USA, Inc., Concord, CA, USA, May 12-16, 2003, Vol. 2, No. 8, pp. 1077-1079.

[5] D.C. Montgomery, Introduction to Statistical Quality Control, 4th ed., John Wiley and Sons Inc., USA, 2001.

[6] J. Juran, Juran's Quality Control Handbook, 3rd ed., McGraw-Hill, New York, 1974.

[7] S.M. Ali, M.A. Sarwar, A. Sultana, Finding characteristics of process capability index, C_{pk} with different distributions and sample sizes, Journal of Quality and Technology Management 4 (2) (2008) 5-11.

[8] M. Albing, Contributions to process capability indices and plots, Doctoral Thesis, Department of Mathematics, Lulea University of Technology, SE-97187, Lulea, Sweden, ISSN: 1402-1544/ISRN: LTU-DT—08/63-SE, 2008.

[9] M. Mottonen, P. Belt, J. Harkonen, H. Haapasalo, P. Kess, Manufacturing process capability and specification limits, Department of Industrial Engineering and Management, University of Oulu, Findland, The Open Industrial and Manufacturing Engineering Journal 1 (2008) 29-36.

[10] C.H. Hsu, C.M. Yang, Applying process capability analysis chart (PCAC) in measuring sewing machine quality, Department of Business Administration, Asia University, Taichung, Taiwan, R.O.C., African Journal of Business Management 4 (2) (2010) 2296-2301.

[11] S. Ahmad, M. Abdollahian, P. Zeephongsekul, Non-normal process capability evaluation, The 2007 International Conference on Information and Knowledge Engineering (IKE'07), Las Vegas, USA, June 25-28, 2007, pp. 321-326.

[12] S. Djaja, T. Afifah, A. Sukroni, Peran faktor sosio ekonomi dan biologi terhadap kematian neonatal di Indonesia (The role of socio-economic and biology factors towards neonatal mortality in Indonesia), Majalah Kedokteran (Indonesia Indonesian Medical Journal) 59 (8) (2009) 370-377. (in Bahasa Indonesia)

[13] C.R. Titaley, M.J. Dibley, K. Agho, C.L. Roberts, J. Hall, Determinants of neonatal mortality in Indonesia, BioMed Central Public Health Journal 8 (2008) 418. doi: 10.1186/1471-2458-8-418.

[14] A.M. Wijaya, Condition of Neonatal Mortality Rate (NMR), Infant Mortality Rate (IMR), Under-Five Mortality Rate (UFMR), Maternal Mortality Rate (MMR), and the causes in Indonesia, 2007, available online at http://www.scribd.com/doc/49660295/SDKI-2007, (accessed on Oct. 2010). (in Bahasa Indonesia)

[15] S.M.A Fernandez, Asuhan bayi baru lahir dan inisiasi menyusui dini, Suara Nusa Tenggara Timur-Spirit NTT/Pos Kupang. Com (Newborn care and early initiation of breastfeeding, Spirit NTT/Pos Kupang. com), No. 174/IV, Aug. 31-Sept. 6, 2009. (in Bahasa Indonesia)

[16] Tiga puluh persen kematian bayi karena premature (Thrity percent of infant mortality due to premature), KRyogya.com, Yogyakarta, June 21, 2010. Available online at http://www.krjogja.com/news/detail/37873/Tiga.Puluh.Persen.Kematian.Bayi.Karena.Prematur.html (accessed on Oct. 2010). (in Bahasa Indonesia)

[17] Bayi Baru Lahir (BBL) normal (Normal newborn weight), January 20, 2010, available online at http://ummukautsar.wordpress.com/2010/01/20/bayi-baru-lahir-bbl-normal/ (accessed on Oct. 2010). (in Bahasa Indonesia)

Journal of Life Sciences 5 (2011) 1003-1012

Biosynthesis of Polyhydroxyalkanoate (PHA) by *Hydrogenophaga* sp. Isolated from Soil Environment during Batch Fermentation

Varavut Tanamool[1], Tsuyoshi Imai[2], Paiboon Danvirutai[3] and Pakawadee Kaewkannetra[4]

1. Department of Biotechnology, Graduate School of Khon Kaen University, Khon Kaen 40002, Thailand

2. Division of Environmental Science and Engineering, Graduate School of Science and Engineering, Yamaguchi University Tokiwadai, Ube, Yamaguchi 755-8611, Japan

3. Fermentation Research Center for Value Added Agricultural Products (FerVAAP), Faculty of Technology, Khon Kaen University, Khon Kaen 40002, Thailand

4. Department of Biotechnology, Faculty of Technology, Khon Kaen University, Khon Kaen 40002, Thailand

Received: May 25, 2011 / Accepted: July 08, 2011 / Published: December 30, 2011.

Abstract: In this work, sucrose utilizing microbes from soil were screened to evaluate their ability for accumulation of biopolymer of polyhydroxyalkanoate (PHA). Among 72 isolates were transferred to mineral salt medium (MSM), 33 strains can be grown on sucrose agar medium. However, only one strain showed a strong black color for Sudan Black and gave positive result for Nile blue A. Identification by 16S rDNA nucleotide sequence homology of the isolate showed very closely to *Hydrogenophaga* sp. (99% identify). To consider PHA production, the isolate was grown in the medium containing sucrose as a sole carbon under controlled conditions of 35 °C and at pH 7. Maximum dry cell weight (DCW) and PHA production were obtained at 3.61 g/L and 2.41 g/L after 36 and 42 h batch fermentation. Sucrose uptake measured in term of total organic carbon (TOC) showed at 14.73 g within 48 h. The highest PHA was 68.15% (g_{PHA}/g_{DCW}) giving maximum PHA yield ($Y_{P/S}$) of 0.17 ($g_{PHA}/g_{Sucrose}$) and a productivity of 0.057 $g_{PHA}/L{\cdot}h$. This highlights the potential of microbial resources in soil environment and may be an exploitable application for the industrial production of PHA.

Key words: Polyhydroxyalkanoate (PHA), sucrose, screening, *Hydrogenophaga* sp..

1. Introduction

Synthesized plastic from petroleum industry has been widely used in daily. Because of non-degradable and accumulating for long time in environment, it causes the problems of air pollution, solid waste disposal and even global warming when it is destroyed by burning and the increasing demands of polymeric materials for our use. In addition, reserves of petroleum stock are limited and running out. The price of petroleum products are also increasing. Due to these results, many researchers have paid attention to investigating other materials to replace for synthesized plastic.

Polyhydroxyalkanoate (PHA), a main kinds of biodegradable plastic and classified as polyester, was the first biomaterial discovered in *Bacillus megaterium* and characterized in 1925 by the French microbiologist [1]. The polyester may contain proportions of 3-hydroxyacids [2]. The general formulae of the monomer unit is -[O-CH(R)-CH_2-CO]-. According to the size of the alkyl substituent (R) mechanical properties of PHA differ [3]. Typically, PHAs can be divided into three groups by number of carbon atoms in their side chain-Short chain length (*scl*) PHAs are

Corresponding author: Pakawadee Kaewkannetra, Ph.D., assistant professor, research fields: biomass and bioenergy technology, biopolymer production and chemical engineering. E-mail: paknar@kku.ac.th.

composed of 3-5 carbon atoms, while medium chain length (*mcl*) PHAs consisted 6-15 carbon atoms and long chain length (*lcl*) comprised 15 and above carbon atoms [4-6] . The structure of PHAs depends on carbon sources supplying and microbial types. The majority of biosynthesis of PHAs is performed using various microorganisms mostly bacteria. They can be produced PHAs from a number of substrates and accumulated in their cell as carbon source and energy reserve [5]. In addition, depending on PHAs accumulation behavior, microorganism can be categorized into two groups. The first group requires the limitation of some nutrient such as nitrogen or phosphate. The member of this group belong *Cupiavidus necator* (formerly from *Ralstronia eutropha*) and *Pseudomonas oleovorans* etc. Secondly, they do not depend on nutritional limitation and they also can be accumulated PHAs during their growth such as *Alcaligenes latus* [7], *Azotobacter vinelandii*, *P. putida*, *P. aeruginosa* [8], *Bacillus mycoides* [9] and recombinant *Escherichia coli*. However, Wang and Lee in 1998 [10] reported that PHAs in term of poly-3-hydroxybutyrate (PHB) can be produced with high productivity and high polymer content by *A. latus* via fed-batch fermentation.

Although, PHAs are interested and wildly studied by many researcher for a long time but the PHAs production are limited by their production cost. A major problem to the commercialization of PHAs is their much higher production cost compared with petrochemical-based synthetic plastic materials or other biodegradable polymers [11]. Much attempt has been devoted to reduce the cost of PHA by the isolation of better bacterial strains to produce PHAs from a cheap carbon source such as sweet sorghum [12]. These bacteria can be isolated from various sources such as water and soil environments using a simple method that can monitor the accumulation of PHAs. For example the conditions for bacterial PHB production can be met in soil, due to its heterogeneous nature. Nitrogen availability in soil varies with microsites. It may become a limiting factor for bacterial growth, especially in some nitrogen-poor (carbon-rich) sites [13]. According to these results, some PHA-producing strains such as *Bacillus*, *Arthrobacter*, *Aureobacterium*, *Corynebacterium*, *Curtobacterium*, *Pseudomonas*, *Micrococcus*, and *Acinetobacter* can be isolated from soil environments.

There are various simple methods for detecting intracellular PHA granules which are applied to the screening of PHA producers such as Sudan Black staining and Nile blue A staining [14] and etc. The positive result showed as a black color or fluorescent granules under microscope. Although they are feasible and easy methods, however they would take a rather time-consuming and labor intensive work to screen a large numbers of environmental isolates. Alternative staining methods have recently been developed for directly staining colonies or growing bacteria on plates containing Nile blue A or Nile red [15]. The dye can be directly diffused to microbial cytoplasm and resulting in fluorescent colonies that can be observed by UV illumination without the step of microscopic observation. Therefore, it would be stated that the colony-staining is a suitable method for screening large numbers of microbial strains.

Thailand is an agro-industry country, fruitful with very cheap sugar and starch based agricultural raw materials and it locates in the tropical area, thus there are accepted that, this area has appropriate environments and temperature for expansion of microorganisms. This study aims to isolate sucrose utilizing bacteria from agricultural crop plantation soil for production of PHAs via batch fermentation.

2. Material and Methods

2.1 Collection, Cultivation and Isolation of Soil Microbes

Soil samples were collected from sugarcane plantation area in the North-eastern of Thailand. The samples then were preserved at 4°C prior to use. Primary isolation of soil microbes was investigated by ten-fold serial dilution technique. A gram of soil

sample was transferred to sterile nutrient broth (NB) and incubated at 30°C for 24 h. Then, the culture was diluted in 0.9% normal saline with different dilutions (10^{-4}, 10^{-5}, 10^{-6} and 10^{-7}) and spread on sterile nutrient agar (NA). The plates were incubated at 30°C for 24 h. Finally, the several single colonies of soil bacteria were picked and transferred to mineral salt agar. Screening for the soil bacteria PHA producers were carried out in mineral salt agar containing with 10 g/L sucrose as a sole carbon source. The culture flasks were incubated at 30°C for 48 h. The PHAs producing capabilities of the microbes were confirmed using 0.3% Sudan Black B (w/v) in 70% alcohol (v/v) and Nile blue staining methods as described by Wang et al. [12, 13]. The viable colonies were directly observed under ultraviolet light (312 nm) and exposing fluorescence to detect the accumulation of lipid compounds including PHAs [15].

2.2 Identification of PHA-Producing Microbes

Pure isolates containing lipophilic inclusions were observed by microscopic technique. Their morphology and biochemical characters of the microbe were observed. The PHA-producing strains were identified by sequencing partial sequences of their 16S rDNA. The chromosomal DNA of the pure isolates was isolated by routine methods as previously described by Slater et al. [16] and Chien et al [17], and used for further identification. The partial sequencing of their 16S rDNA was amplified with bacterial universal primers PA (5'-AGAGTTTGATCCTGGCTCAG-3') and PH (5'-AAGGAG GTGATCCAG CCGCA-3') [18] and generated the product length of 1,519 bps. The PCR product was then subjected to ABI PRISM310 (PE Biosystems) according to manufacturer's instruction. The nucleotide sequences of partial 16S rDNA were compared with the 16S rDNA sequences available in the public nucleotide databases at the National Center for Biotechnology Information (NCBI), USA, by using their World Wide Web site (http://www.ncbi.nlm.nih.gov), and the BLAST (Basic Local Alignment Search Tool) algorithm program and then deposited in the database under accession numbers AB3000163.

2.3 Batch Fermentation of PHA in Shake Flasks

The selected strain was maintained in nutrient broth and incubated in orbital shaking at 200 rpm, 35°C for 24 h prior use. Then, the 5% (v/v) inoculums of the pre-culture was used to inoculate in 250 mL Erlenmeyer flask containing 50 mL sterilized mineral salt medium consist of (g/L); 20 g Sucrose, 1.5 g KH_2PO_4, 3.57 g Na_2HPO_4, 0.2 g $MgSO_4$ 7 H_2O, 1 g $(NH_4)_2SO_4$, 1 g and 1 mL trace element solution prepared following the method described by Grothe et al. [19]. The results obtained after fermentation were reported in terms of percentage on dry cell weight: DCW (% w/w), PHA productivity (g/L·h), PHA yield ($Y_{p/s}$) and biomass yield ($Y_{x/s}$).

2.4 Sucrose Uptake

Sucrose uptake informs sucrose in culture medium was monitored in terms of Total organic carbon (TOC) using TOC analyzer (TOC-5000, Shimadzu Corporation, Japan, with ASI-5000 auto injector).

2.5 Biomass Measurement

Biomass concentration was measured off-line by optical density (OD) at 660 nm (1 OD 660 nm = 0.308 g of dry cell weight, DCW) on a Shimadzu UV-Visible spectrophotometer. Calculation has been made by plotting a calibration curve between the DCW and OD values.

2.6 Biomass Recovery, Extraction and Determination of PHA

After fermentation, biomass was collected by centrifugation (×8,000, 10 min). Then, supernatant was discarded; the pellet was washed for twice with distilled water and dried in hot air oven at 60°C until constant weight. Intracellular PHA in biomass was measured using a modified method [4]. In brief, a

commercial bleach of sodium hypochlorite (NaClO, contained 6% active chlorine) was added to the wet biomass pellet and was mixed vigorously using vortex mixer. Then, the mixture was incubated at 37°C for 1 h until non-PHA biomass dissolved and white flocculants lipid was precipitated. Hereafter, the PHA recovery was conducted. The mixture was re-centrifuged and washed with distilled water twice to remove the bleach solution which was contained of dissolved cell debris. The cells were washed with acetone for twice to remove a low-molecular-weight lipid [5]. The white cell pellet was re-suspended with ethanol solution and then was re-centrifuged. The obtained white pellet was dried in hot air oven at 60°C until reached a constant weight. All measurements were weighed in triplication. It should be noted that in a large proportion of PHAs was extracted in Soxlhet apparatus and extraction with an excess of chloroform at 100°C for 3 h. The mixture was filtered to remove cell debris and precipitates in cold methanol or casted onto cleaning glass Petri disk. The PHA product was dried in hot air oven at 60°C over night. The PHA was characterized by nuclear magnetic resonance (NMR) analysis to confirm the structure of PHA meanwhile thermal properties were measured by differential scanning calorimetry (DSC) and thermal degradation of PHA using thermal gravimetric analysis (TGA).

2.7 Thermal Properties of Extracted PHA

The extracted PHA was analyzed in both differential scanning calorimetry (DSC) and thermal gravimetric analysis (TGA*)* compared to the standard of biopolymer in term of poly-β-hydroxybutyrate (PHB) (Sigma-Aldrich, USA). It was also remarked that the PHB is mostly found in PHAs. The DSC was performed using 10 mg samples under N_2 atmosphere, using the following temperature program: heating temp (-20 to 200°C) (10°C/min), cooling temp (200 to 20°C) (10°C/min) and a second heating (-20 to 200°C) (10°C/min) [20]. The phase transition temperatures were reported as glass transition temperature (Tg) and melting temperature (Tm). Thermal gravimetric analysis (TGA*)* was performed using a TGA instrument (Mettler-Toledo, TGA/SDTA 851, USA) calibrated with indium. The temperature was ramped at a heating rate of 10°C/min under nitrogen, to a temperature well above the degradation temperature of the polymers [21].

3. Results and Discussion

3.1 Isolation of Soil Microbes and PHAs Observation

Accumulation of PHA granules in the microbial cells was preliminary analyzed by Sudan black method. Among 72 isolates, 33 isolates can be grown on sucrose agar medium and were further observed PHA accumulated in their cells under microscopic technique. In this case the pure bacterial strain of *Alcaligenes eutrophus* TISTR 1095 has been used as a reference positive strain for PHAs accumulation. In Fig. 1, the results revealed that, only 3 isolated strains coded as the strains V22, V29 and V33 showed positive results after staining by Sudan black B and small black color represented PHAs granules in microbial cell. The Isolate strain V33 clearly showed in strong black color than others. Hence, only the strain V33 was further used. Then, the PHAs producing microbes was confirmed by staining method using Nile blue A. The results are shown in Fig. 2, when the 0.5 µg/ mL Nile blue A was directly added into mineral salt medium and incubated for 3 day. The culture plate contained of the isolated V33 and two reference strains (PHA-positive strain of *A. eutrophus* TISTR 1095 and PHA-negative strain of *E. coli*) were observed PHA intact in bacterial colony under UV light at 312 nm. Colonies from the portion plate of *A. eutrophus* TISTR 1095 and the isolate V33 clearly exhibited a very strong fluorescence caused by the presence of the PHAs in their cell which can be blinded by Nile blue A. In addition, the isolate V33 was defined as Gram negative bacteria having rod-shaped cell and yellow pigment (see Fig. 2 right). This observation is on agreement with previous studies; Ostle and Holt, 1982 [14] reported that Nile blue A could diffuse to only PHA

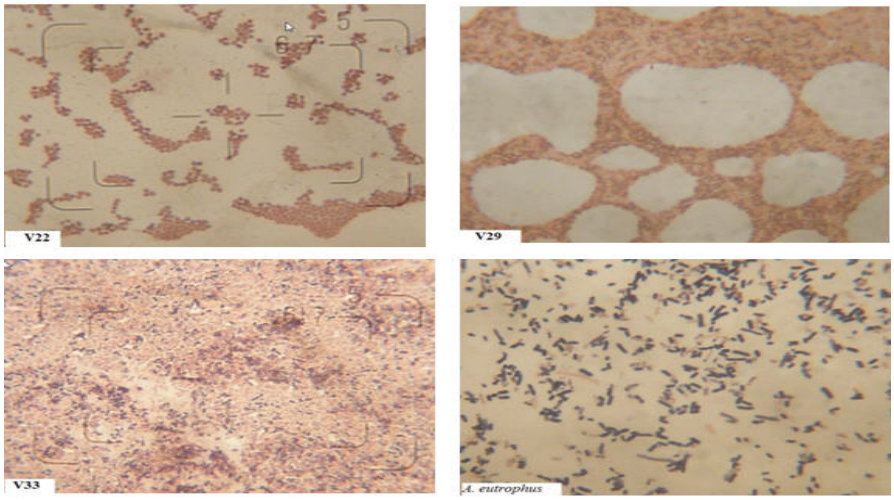

Fig. 1 Micrographs of bacteria containing PHA inclusions.

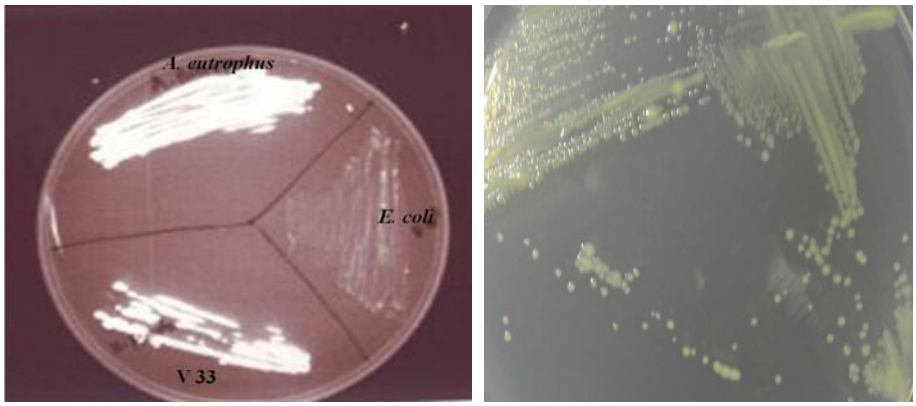

Fig. 2 (Left) *A. eutrophus*, the strain V33 33 and *E. coli*; (right) a yellow bright colony of the isolate V33.

granules while other inclusion bodies (such as glycogen and polyphosphate) do not stained with this dye. However, under the same agar plate, *E. coli* showed in a weak for fluorescence light because this microorganism, which originally had no PHA accumulation capability [22].

3.2 Identification of the Isolated Strain

The isolated V33 was identified using the sequences of partial 16S rDNA technique and compared to those available in the public databases. It was found that it was closely related to those bacterial strain of *Hydrogenophaga* sp. (99% identify). The phylogeny based on these partial 16S rDNA sequences and related *Hydrogenophaga* sp. is shown in Fig. 3. Previous studies have reported that *Hydrogenophaga* sp. was isolated from soil, mud, and water by enrichment for hydrogen bacteria. The strain was gram-negative, rod-shaped cell and yellow pigmented H_2-oxidizing bacteria [23]. They can grow and produce PHAs from various substrates such as glucose, galactose, xylose, arabinose [24] whey lactose [25], fructose [26] and recently in sucrose.

3.3 Batch Fermentation of Sucrose Medium

The *Hydrogenophaga* sp. was cultured in sucrose medium and its growth was monitored. In Fig. 4, it was found that the exponential phase appeared after 6 h until 36 h then the cell reached to stationary phase. The PHA were produced and accumulated in its granules after 30 h and maximum PHA production was obtained at 2.41 g/L within 42 h of batch fermentation. However, PHA concentration was decreased after 48 h because this strain had an intracellular depolymerase enzyme

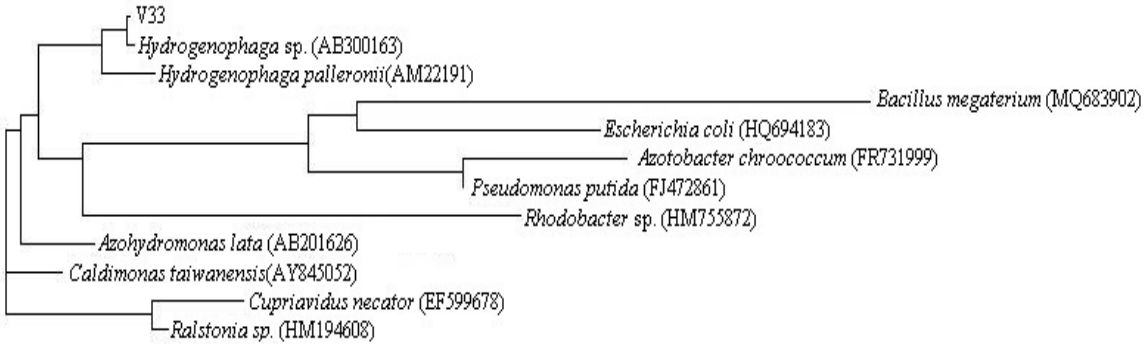

Fig. 3 Phylogenetic analysis of 16S rDNA sequence the isolate V33.

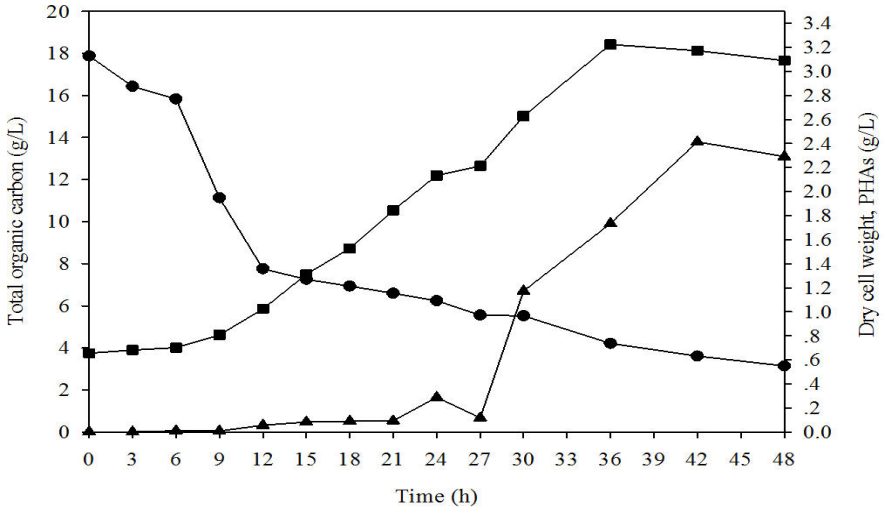

Fig. 4 Profiles of TOC, DCW and PHAs as functions of time during batch fermentation.

(-●-Total organic carbon (TOC),-■-Dry cell weight (DCW)-▲-PHAs).

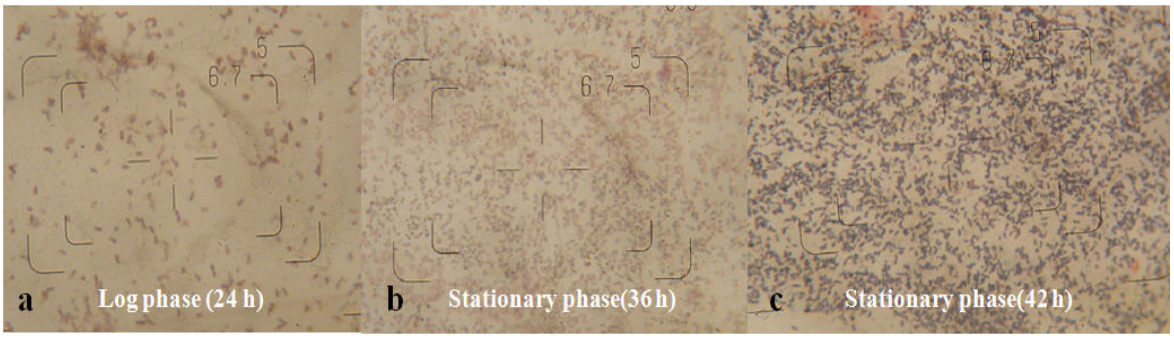

Fig. 5 PHA inclusions in *Hydrogenophaga* sp. cell after staining with Sudan black B under different culture times.

a: Log phase, 24 h; b: Stationary phase, 36 h; c: Stationary phase, 42 h.

and can be utilized PHA for its growth [27]. According to the results obtained, we could observe PHA accumulated by the *Hydrogenophaga* sp. by using Sudan black B staining during different fermentation times (see Fig. 5). The results indicated that, PHA was accumulated during mid-log phase (30 h) to stationary phase (48 h) due to carbon and nitrogen appeared to imbalance condition in fermentation media. However, microbial cell containing PHA showed a strong black color at 42 h of fermentation. In case of the sucrose uptake in culture medium showed at 14.73 g within 48 h. The highest PHA inclusions in microbial cell was

68.15% (g_{PHA}/g_{DCW}) giving a maximum PHA yield ($Y_{P/S}$) of 0.17 ($g_{PHA}/g_{Sucrose}$) and a volumetric productivity for PHA amounted to 0.057 g_{PHA}/ L·h.

3.4 Characterization of PHA

One gram of PHA produced from *Hydrogenophaga* sp. was extracted by hot chloroform and then was casted on clean Petri disk and oven-dried in circulating air at 50°C for 2 h [28] and finally a thin PHA film was obtained and illustrated in Fig. 6. The PHA film was further characterized using ^{1}H-NMR and ^{13}C-NMR techniques. The spectrum of ^{1}H-NMR obtained was as shown in Fig. 7a. Three groups of signals peak at 1.25, 2.52 and 5.23 ppm were found and corresponding to CH_3, CH_2 and CH, respectively. Meanwhile, the ^{13}C-NMR of PHA showed the chemical shifts of 19.72 (CH_3), 40.75 (CH_2), 67.58 (CH), and 169.10 (CO), respectively (see Fig. 7b). The results obtained in both techniques are in good agreement with previous works [27-29] and identified the PHA extracted from *Hydrogenophaga* sp. as polyhydroxybutyrate (PHB) or polyhydroxybutyric acid.

For the DSC and TGA results of the Tm (173.31°C) and the enthalpy of PHA fusion (87.73 J/g) are shown in Fig. 8. They showed in similarly matched with the data obtained both from standard PHB (176.29°C and 86.49 J/g) and from other works [7, 28]. All data were summarized in Table 1. However, it seems that the Tm of PHA was slightly lower than the value from the standard PHB. It may improve a widen PHA processing window and make the process become easier. In case of the Tg values, they were closely matched between the standard PHB and the PHA. High melting enthalpy was obtained from both cases. This can be explained that because of a high crystalline structure calculated to be 59.24% and 60.09% found in the standard PHB and PHA. Properties of a high Tm and a high crystalline nature indicate in a high degree of

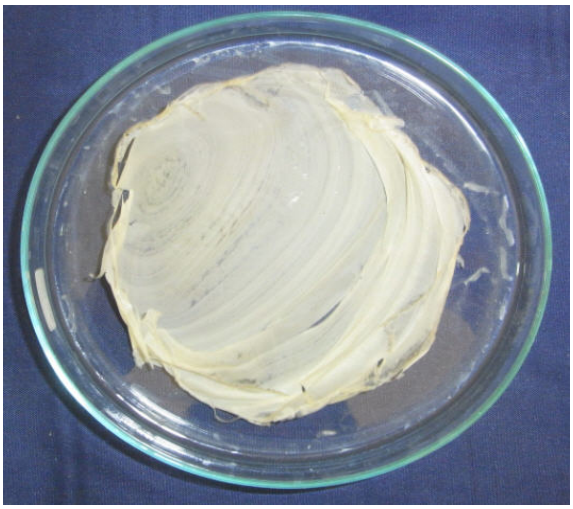

Fig. 6 A casted-film PHA obtained from *Hydrogenophaga* sp..

Table 1 Summarized data from differential scanning calorimeter (DSC) analysis of PHA samples.

Samples	Tg, °C	Tm, °C	ΔH, J/g	Crystallinity, %
Standard PHB	2.81	176.29	86.49	59.24
PHA*	2.32	173.31	87.73	60.09

*: PHA from *Hydrogenophaga* sp..

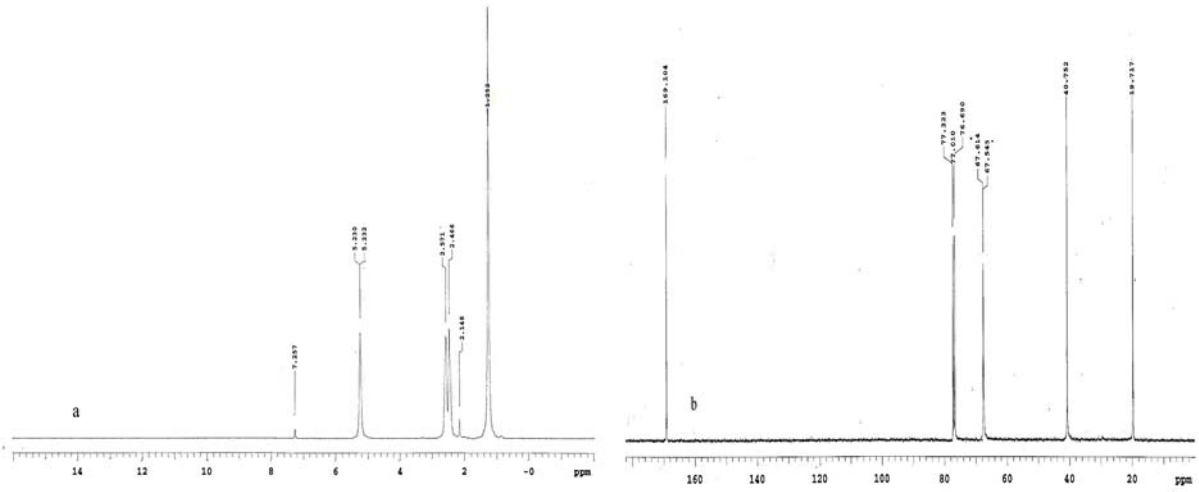

Fig. 7 a: ^{1}H-NMR spectrum; b: ^{13}C-NMR spectrum of the extracted PHA.

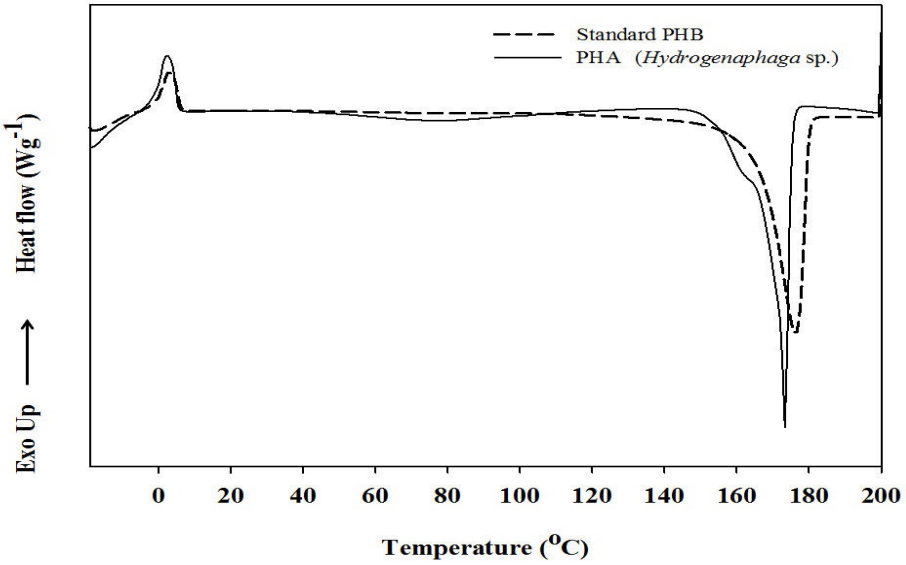

Fig. 8 The DSC thermogram of the standard PHB and PHA from *Hydrogenophaga* sp..

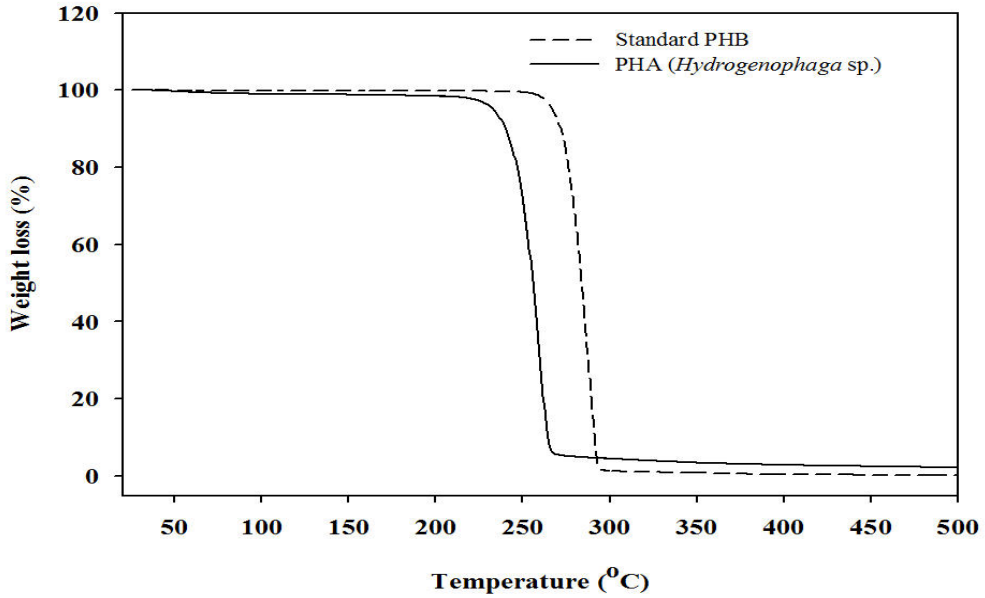

Fig. 9 Thermogravimetric analysis of the standard PHB and PHA from *Hydrogenophaga* sp..

polymerization. Hence, the PHB could be suitable for commercial utilization [11, 29-30]. For thermogravimetric analyses of the PHA produced by *Hydrogenophaga* sp. compared to the standard PHB are shown in Fig. 9. The PHA gave a rapid thermal degradation between 210 and 280°C while the standard PHB represented at between 255 and 293°C. It is indicated that biopolymeric material obtained can possibly be further used in a large scale processing of bioplastic [11].

4. Conclusions

An isolated soil bacteria and then identified as *Hydrogenophaga* sp showed successfully for utilizing several refined sugars especially sucrose. It has proven in its potential to produce PHAs in a high content (68.15% w/w) when sucrose medium was used as a sole carbon source and giving maximum PHA yield ($Y_{P/S}$) of 0.17 ($g_{PHA}/g_{Sucrose}$) and a productivity of 0.057 $g_{PHAs}/L{\cdot}h$. Further study will be fulfilled on the possibility

of *Hydrogenophaga* sp. to use directly mixed sugars obtained from agricultural crops such as sugar cane and sweet sorghum as sole carbon sources for production of PHAs by using media optimization technique via other fermentations of fed-batch, repeated batch, and repeated fed batch processes.

Acknowledgments

The authors would like to gratefully acknowledge Khon Kaen University and Thailand Research Fund (TRF) for matching fund (Contract no. DBG5380013 for P. Kaewkannetra) and JSPS-NRCT under Asian Core Program (ACP) for scientist exchange and collaborative research. In addition, V. Tanamool also would like to thanks, National Research Council of Thailand (NRCT), Fermentation Research Center for Value Added Agricultural Products (FerVAAP), Faculty of Technology, Khon Kaen University and Graduate School of Khon Kaen University, Thailand, for the innovation potential research for high social impact scholarship, facilities and travel bursary.

References

[1] M. Lemoigne, Products of dehydration and polymerization of the acid-oxybutyric, Bulletin Society Chemistry Biology 8 (1926).

[2] G. Braunegg, G. Lefebvre, K.L. Genser, Polyhydroxyalkanoates, biopolyesters from renewable resources: Physiological and engineering aspects, Journal Biotechnology 65 (1998) 127-161.

[3] I. Vroman, L. Tighzert, Review: Biodegradation polymer, Materials 2 (2) (2009) 307-344.

[4] K.M. Lee, D.F. Gilmore, Formulation and process modeling of biopolymer (polyhydroxyalkanoates: PHAs) production from industrial wastes by novel crossed experimental design, Process Biochemistry 40 (2005) 226-249.

[5] A.J. Anderson, E.A. Dawes, Occurrence, metabolism, metabolic role, and industrial uses of bacterial polyhydroxyalkanoates, Microbiology Research 54 (1990) 450-472.

[6] A. Steinbuchel, H.E. Valentin, Diversity of bacterial polyhydroxyalkanoic acids, FEMS Microbiology Letter 128 (1995) 219-228.

[7] A. Yezza, A. Halasz, W. Levadoux, J. Hawari, Production of poly-β-hydroxybutyrate (PHB) by *Alcaligenes latus* from maple sap, Apply Microbiology Biotechnology 77 (2007) 269-274.

[8] D. Fernandez, E. Rodriguez, M. Bassas, M. Vinas, Agro-industrial oily wastes as substrates for PHA production by the new strain *Pseudomonas aeruginosa* NCIB 40045: Effect of culture conditions, Biochemistry Engineering Journal 26 (2005) 159-167.

[9] P. Thakur, B. Borah, S. Baruah, J. Nigam, Growth -associated production of poly-3 hydroxybutyrate by *Bacillus mycoides*, Folia Microbiology 46 (2001) 488-494

[10] F. Wang, S.Y. Lee, Poly (3-hydroxybutyrate) production with high productivity and high polymer content by a fed-batch culture of *Alcaligenes latus* under nitrogen limitation, Apply Environment Microbiology 63 (1997) 3703-3706.

[11] J.M. Luengo, B. Garcia, A. Sandoval, G. Naharro, E.R. Olivera, Bioplastics from microorganisms, Current Opinion Microbiology 6 (2003) 251-260.

[12] P. Kaewkannetra, P. Tanonkeo, V. Tanamool, T. Imai, Biorefinery of squeeze sweet sorghum juice into value added product of biopolymer, Journal of Biotechnology 136 (2008) S412.

[13] J.G. Wang, L.R. Bakken, Screening of soil bacteria for poly-β-hydroxybutyric acid production and its role in the survival of starvation, Microbiology Ecology 35 (1998) 94-101.

[14] A. Ostle, J.G. Holt, Nile blue A as a fluorescent stain for poly-b-hydroxybutyrate, Apply Environment Microbiology 44 (1982) 238-241.

[15] P. Spiekermann, B.H. Rehm, R. Kalscheuer, D. Baumeister, A. Steinbuchel, A sensitive, viable-colony staining method using Nile red for direct screening of bacteria that accumulate polyhydroxyalkanoic acids and other lipid storage compounds, Archeology Microbiology 171 (1999) 73-80.

[16] S.C. Slater, W.H. Voige, D.E. Dennis, Cloning and expression in *Escherichia coli* of the *Alcaligenes eutrophus* H16 poly-3-hydroxybutyrate biosynthetic pathway, Bacteriology 170 (1988) 4431-4436.

[17] C.C. Chien, C.C. Chen, M.H. Choi, S.S. Kung, Y.H. Wei, Production of poly-β-hydroxybutyrate (PHB) by *Vibrio* spp. isolated from marine environment, Journal Biotechnology 132 (2007) 259-263.

[18] U. Edwards, T. Rogall, H. Bocker, M. Emde, E. Bottger, Isolation and direct complete nucleotide determination of entire genes: Characterization of a gene coding for 16S ribosomal DNA, Nucleic Acids Research 17 (1989) 7843-7853

[19] E. Grothe, M. Moo-Young, Y. Chisti, Fermentation optimization for the production of (poly-β-hydroxybutyric acid) microbial thermoplastic, Enzyme Microbiology Technology 25 (1999) 132-141.

[20] S. Xu, R. Luo, L. Wu, K. Xu, G.O. Chen, Blending and characterizations of microbial poly (3-hydroxybutyrate) with dendrimers, Journal Apply Polymer Science 102 (2006) 3782-3790.

[21] S. Modi, K. Koelling, Y. Vodovotz, Assessment of PHB with varying hydroxyvalerate content for potential packaging applications, European Polymer Journal 47 (2011) 179-186.

[22] M. Miyake, C. Miyamoto, J. Schnackenberg, R. Kurane, Y. Asada, Phosphotransacetylase as a key factor in biological production of polyhydroxybutyrate, Applied Biochemistry and Biotechnology, 84–86 (2000), 1039–1044.

[23] A. Willem, J. Busse, M. Goor, B. Pot, E. Falsen, E. Janzent, et al., *Hydrogenophaga*, a new genus of hydrogen-oxidizing bacteria that includes *Hydrogenophaga flava* comb. nov. (formerly *Pseudomonas flava*), *Hydrogenophaga palleronii* (formerly *Pseudomonas palleronii*), *Hydrogenophaga pseudoflava* (formerly *Pseudomonas pseudoflava* and *Pseudomonas carboxydoflava*), and *Hydrogenophaga taeniospiralis* (formerly *Pseudomonas taeniospiralis*), System Bacteriology 39 (1989) 319-333.

[24] M.H. Choi, J.J. Song, S.C. Yoon, Biosynthesis of copolyesters by *Hydrogenophaga pseudoflava* from various lactones, Canadian Journal Microbiology 41 (1995) 60-67.

[25] M. Koller, R. Bona, E. Chiellini, E.G. Fernandes, P. Horvat, C. Kutschera, et al., Polyhydroxyalkanoate production from whey by *Pseudomonas hydrogenovora*, Bioresource Technology 99 (2008) 4854-4863.

[26] M. Mahmoudi, M. Sharifzadeh-Baei, G.D. Najafpour, F. Tabandeh, H. Eisazadeh, Kinetic model for polyhydroxy butyrate (PHB) production by *Hydrogenophaga pseudoflava* and verification of growth conditions, African Journal Biotechnology 9 (2010) 3151-3157.

[27] S.C. Yoon, M.H. Choi, Local sequence dependence of polyhydroxyalkanoic acid degradation in *Hydrogenophaga pseudoflava*, Biology Chemistry 274 (1999) 37800-37808.

[28] W.M. Pachekoski, J.A.M. Agnelli, L.P. Belem, Thermal, mechanical and morphological properties of poly (hydroxybutyrate) and polypropylene blends after processing, Material Research 12 (2009) 159-164.

[29] S. Jan, C. Roblot, J. Courtois, B. Courtois, ^{1}H NMR spectroscopic determination of poly-3-hydroxybutyrate extracted from microbial biomass, Enzyme Microbiology Technology 18 (1996) 195-201.

[30] G. Redzwan, S.N. Gan, I.K.P. Tan, Isolation of polyhydroxyalkanoate-producing bacteria from an integrated-farming pond and palm-oil mill effluent ponds, World Journal Microbiology Biotechnology 13 (1997) 707-709.

Journal of Life Sciences 5 (2011) 1013-1021

Impact of Nitrogen Fertilization on the Oil, Protein, Starch, and Ethanol Yield of Corn (*Zea mays* L.) Grown for Biofuel Production

Roland Ahouelete Yaovi Holou[1, 2] and Valentin Kindomihou[3]

1. University of Missouri, Delta Research Center, P.O. Box 160, Portageville, MO 63873, USA

2. Monsanto Company, 800 N. Lindbergh Blvd., Mail Zone Q4B/Q420E-A, St. Louis, MO 63167, USA

3. Laboratory of Applied Ecology, Fac. of Agronomic Sci., University of Abomey-Calavi, Cotonou 01 BP 526, Benin

Received: May 31, 2011 / Accepted: July 22, 2011 / Published: December 30, 2011.

Abstract: Nitrogen fertilization is one of the greatest challenges associated with the production of biofuel from corn grain. The objective of this research was to determine the effect of N fertilization on the content and yield of oil, protein, and starch in corn grain. The project was done in Southeast Missouri (USA), from 2007 to 2009 in a silt loam soil. Corn grain contains 3.8-4.2% oil, 6.7%-8.9% protein, 68.0%-70.4% extractable starch, and 76.0%-77.7% total starch. The total starch yield ranged from 2.8 to 7.8 mg·ha^{-1} whereas the extractable starch varied between 2.5 to 7.1 mg·ha^{-1}. As the N rate went up, the oil and starch content of the grain decreased, whereas the protein content and the protein, starch, and oil yields increased, reaching their maximum at the N rate corresponding to 179.0 kg N·ha^{-1}. The potential ethanol yield varied between 616.2 and 7,035.1 L·ha^{-1} depending on the method of conversion of the starch into ethanol, the year and the N rate ($P < 0.0001$). The negative correlation between N fertilization rate and starch content suggested that when farmers add too much N to their soil to increase grain yield, they reduce the starch content in those grains, and consequently the conversion into bioethanol. Therefore, for biofuel production to be beneficial for both farmers and the power plant owners, an agreement needs to be made with regard to the use of fertilizers.

Key words: Starch, oil, protein, corn kernel, biofuel, ethanol, nitrogen.

1. Introduction

While Brazil focuses on sugarcane for biofuel production [1, 2], corn is currently the main feedstock used in USA [3]. In 2005, the US surpassed Brazil in the production of bioethanol [2]. Also in 2005, 10% of the corn grain produced in USA was converted into ethanol [3]; in 2007, that rate went to 20% [4]. From 2001 to 2007, bioethanol production in USA increased from 7.19 billion L to 27.5 billion L [5]. By 2015, the bioethanol production in USA is expected to reach 56.8 billion L [6]. As bioethanol production grows in popularity, a clearer understanding of how it is generated and ways to maximize production levels become important areas of study.

Ethanol from corn can be produced using the grain and/or the stover residues [4, 7]. When corn grain is used to produce bioethanol, starch is the main macromolecule of interest.

Starch generally accounts for 58% to 72% of corn grain weight [3, 8] and is often hydrolyzed into free and simple sugars before being fermented into ethanol by yeast [3, 9]. Starch can be processed into bioethanol by two main methods: the wet milling process and the dry milling process. Usually, the extractable starch is

Corresponding author: Roland Ahouelete Yaovi Holou, Ph.D., research scientist at Monsanto, international chair of the Sweet Sorghum Ethanol Association, research fields: biotechnology, plant biology and genetics, nutrient translocation and management, bioenergy, seed technology, drought, climate change and Africa's development. E-mail: rayholou@yahoo.fr.

accessible during wet milling. In contrast, total starch is considered for dry milling. The kind of starch (total or extractable starch) used to determine the ethanol yield, has to differ depending on the type of milling process. The grain starch and the ethanol yield are highly correlated [10]. Some improvements have been made in the conversion of corn grain into ethanol, and it is now possible to get 0.42 L ethanol per kg corn grain [3, 11]. With the demand for bioethanol and cleaner, reliable fuel sources increasing, more improvements must be made.

One possible area for improvement is in N fertilization. It is known that without N, the corn kernel cannot develop well [12] and that N fertilization improved protein accumulation in rice [13]. As the protein content of corn grain increases, the starch content decreases [10, 14]. Additionally, the protein content and the grain yield increased as the N uptake by corn grain went higher [15]. These results suggested that in an attempt to increase corn grain yield with the application of N, the composition of the kernel can significantly change. Commonly, when studying corn for biofuel production, the N fertilization rate assumed in most papers varied between 138 and 152 kg $N \cdot ha^{-1}$ [16-21]. Since the sources of the variation in N removal by corn is not well understood, Heckman et al. [22] recommended that further work is needed to design an accurate program to adequately fertilize the soil. A comparison of the impact of the N rate on the potential ethanol yields obtained by dry milling, wet milling or using the conventional conversion factor found in the literature (0.42 L ethanol per kg corn grain) is necessary. The results can help scientists choose the right methods to calculate ethanol yield from corn and further their understanding about how N rate affects ethanol production from plants. However, to our knowledge, an original study on the impact of N on the composition of corn grain is still lacking, particularly in the context of biofuel production. The understanding of the impact of N fertilization on the composition of the corn kernel is crucial to design a better production system that can maximize the starch yield and consequently the ethanol yield from that crop. In other words, the understanding of the relationship between starch, oil, and protein in the contest of N fertilization can help determine the variables that can be manipulated in order to improve the ethanol yield from corn by establishing better N management tools for corn fertilization for biofuel production.

Our hypothesis is that N fertilization changes the content and yields of oil, starch and protein in corn grain. The objective of this study was to evaluate the impact of N fertilization on the content and yields of oil, protein, starch in corn grain, the potential ethanol yield, and to determine the relationship between these parameters.

2. Material and Methods

The research was carried out in Southeast Missouri (USA) over a three year period (2007-2009) on a Tiptonville silt loam soil (fine-silty, mixed, superactive, thermic Oxyaquic Argiudolls). The experimental design used was a randomized complete block with four repeats. The nitrogen rates applied were 0, 45, 90, 134, 179, 224, and 269 kg $N \cdot ha^{-1}$. Details on the experimental design, the growth, and the harvest of corn can be found in Holou et al. (submitted to Biomass and Bioenergy Journal).

After harvest, the grain was dried in an oven. Samples from each N rate were analyzed in four replicates. For each plot, seven subsamples were collected and analyzed for their density, moisture content, oil content, protein content, extractable starch content, and total starch content. The grain was analyzed by a Near Infrared (NIR) spectrometer using the Infrared^{TM} Foss 1241 Grain Analyzer (Eden Prairie, MN). The calibration used was that already established in previous work [23-25].

Two kinds of starch content were measured with the NIR: the total starch and the extractable starch. The starch content reported in this paper was normalized to 15% moisture of the grain. The method used to

determine the corn grain yield was explained in previous paper (Holou et al., submitted to Biomass and Bioenergy). Knowing the composition of the grain, the theoretical oil, protein, and starch yield were calculated as follows:

Oil yield ($kg \cdot ha^{-1}$) = [Oil content (%) × Grain yield ($kg \cdot ha^{-1}$)]/100

Total starch yield ($kg \cdot ha^{-1}$) = [Total starch content (%) × Grain yield ($kg \cdot ha^{-1}$)]/100

Extractable starch yield ($kg \cdot ha^{-1}$) = [Extractable starch content (%) × Grain yield ($kg \cdot ha^{-1}$)]/100

The theoretical ethanol yield was calculated as previously described by previous authors [11]. Three different methods were used to extrapolate the ethanol yield from corn: (a) the conventional conversion of grain yield into ethanol, (b) the total starch yield and (c) the extractable starch yield. According to the conventional conversion factor in USA, 0.42 L of ethanol can be made from each kilogram of corn grain [3, 11, 26].

Ethanol yield from total starch = Total starch yield × 1.11 × 0.51

Ethanol yield from extractable starch = Extractable starch yield × 1.11 × 0.51

The data were analyzed using the linear mixed model in SAS 9.2 (SAS Institute Inc., Cary, NC). Significant differences were assumed for $P \leq 0.05$. The year of the study and the N rate were considered the main fixed factors, whereas the block (repeat) was classified as a random variable. To compare the ethanol yields that were obtained from each of the three methods used, a linear mixed model was used in which the method type (conventional conversion factor, total starch method or extractable starch method) was considered as the fixed factor, whereas each block (repeat) was the random factor.

For the Proc Mixed model, the estimation method was the restricted maximum likelihood (REML). When a significant difference was found based on the year of the study, the test was repeated for each year separately. Means were separated and grouped by letter by using the macro developed by Saxton [27]. Significant differences are assumed for $P \leq 0.05$. The data were graphed and fitted into a model using Excel 2007 (Microsoft Corp, Redmond, WA) spreadsheet software. The best regression model was that with the highest R^2. The Pearson coefficient (r) was calculated using the Proc Corr procedure in SAS to determine the linear correlation between variables.

3. Results

3.1 Initial Soil Fertility Summary

The soil characteristics and the weather conditions are summarized in Tables 1 and 2, respectively. The daily precipitation did not depend on the year (P = 0.095). However, the temperature, the vapor pressure, the maximum wind speed, and total solar radiation significantly varied between the years.

3.2 Starch Content and Yield

Starch is the main macromolecule found in corn grain. As expected, the total and the extractable starch content of the grain were statistically different (P < 0.0001). The average total starch content over three years fluctuated between 76.0% and 77.7 %; whereas the extractable starch content varied between 68.0% and 70.4%.

The impact of the N rate on both the total and the extractable starch was significant (P < 0.0001). In addition, the starch content depended on the year (P < 0.0001). In general, N fertilization reduced the total and the extractable starch content of corn grain (Tables 3 and 4). The difference between the total starch yields

Table 1 Initial soil characteristics at Portageville and Hayward, Missouri, in 2008 and 2009.

Variable	2008	2009
pH	6.1	5.5
N.A. (meq/100g)	1.2	2.3
OM (%)	1.4	0.9
CEC (meq/100g)	8.9	10.3
P Bray I ($mg \cdot ha^{-1}$)	37.6	48.6
Ca ($mg \cdot ha^{-1}$)	1,322.3	1,180.9
Mg ($mg \cdot ha^{-1}$)	90.5	226.8
K ($mg \cdot ha^{-1}$)	137.8	78.7

and the extractable starch yield was statistically significant ($P < 0.0001$).

The application of N mostly increased the starch yield from corn grain. The maximum starch yield was obtained with the application of 179 kg N·ha^{-1}. Generally, as the protein yield increased, so did the starch yield in the corn grain (Tables 3 and 4), suggesting an important correlation exists between protein expression and starch yield in corn grain.

3.3 Protein Content and Yield

Proteins are the second major macromolecule found in corn grain. The protein content of the grain oscillated between 6.7% and 8.9%, and averaged 7.8% of the grain weight (Table 3). The impact of the N rate on the protein content of the grain was highly significant in every year ($P < 0.0001$) although the protein yield changed from year to year ($P < 0.0001$). N fertilization improved the protein content of the grain ($r = 0.8$, $P < 0.0001$). The grain yield was positively correlated ($P < 0.0001$) with the protein content ($R^2 = 0.97$) (Tables 3 and 4). However, as the protein content of the grain increased, the starch content decreased ($r = -0.4954$, $P < 0.0001$). The maximum protein yield, like the maximum starch yield, was obtained with the application of 179 kg N·ha^{-1} (Table 3).

Table 2 Weather summary during growing season at Portageville and Hayward, Missouri, in 2008-2009.

Weather	Year	Apr	May	Jun	Jul	Aug	Sep
Total monthly precipitation (mm)	2008	143.8	93.1	35.2	67.1	45	74.1
	2009	139.9	171.2	69.9	106.6	54.9	119.5
Maximum air temperature (℃)	2008	19.1	25.6	32	32.9	30.8	28.2
	2009	20.7	24.8	32.5	30	30	27.6
Minimum air temperature (℃)	2008	8.3	14.1	20.5	21.6	19.8	16.2
	2009	9.3	15.4	20.8	20.1	18.7	17.2
Average air temperature (℃)	2008	13.8	20	26.2	26.9	24.9	21.8
	2009	14.8	20.1	26.5	24.8	24	21.8
Total solar radiation (MJ/M²)	2008	16.5	17.8	21	20.8	18.9	15.1
	2009	16	16.5	21.1	18.8	20.3	13.8
Vapor pressure (KPA)	2008	1.2	1.6	2.1	2.5	2.3	1.9
	2009	1.2	1.8	2.3	2.2	2.3	2.1
Vapor pressure deficit (KPA)	2008	0.5	0.8	1.4	1.2	0.9	0.8
	2009	0.6	0.7	1.3	1	0.8	0.6

Table 3 Impact of N on the composition of corn kernel averaged across all years at Portageville and Clarkton, Missouri, 2007-2009.

Variables†	N rate (kg ha^{-1})							
	0	45	90	134	179	224	269	Average
Grain yield (kg·ha^{-1})	3,636	5,840	8,435	1,0107	1,0200	9,104	9,236	8,080
Total starch content (%)	77.7	77.7	77	76.8	76.7	76	76.6	76.9
Extractable starch content (%)	69.9	70.4	69.7	69.3	69	69	68	69.4
Total starch yield (kg·ha^{-1})	2,836.5	4,560.5	6,514.6	7,790.3	7,845.4	6,850.3	6,947.8	6,174.9
Extractable starch yield (kg·ha^{-1})	2,558.3	4,158.1	5,931.4	7,053.6	7,078.6	6,243.9	6,188.9	5,586.9
Protein content grain (%)	6.7	6.8	7.4	8.2	8.4	8.8	8.9	7.8
Protein yield (kg·ha^{-1})	251	392	633	829	863	788	806	648
Oil content of grain (%)	4.2	4	4.1	4	3.9	4.1	3.8	4
Oil yield (kg·ha^{-1})	151	233	342	402	401	368	343	319
Grain density	1.23	1.24	1.25	1.25	1.26	1.26	1.26	1.25

†: N fertilization changed the composition of corn grain and consequently can affect biofuel production from corn.

3.4 Oil Content and Yield

Corn can be cultivated to produce oil. However, when grown for ethanol production, oil is not of as much interest. The oil content of corn grain ranged from 3.8% to 4.2%. Variation in the oil content was found between years ($P < 0.0001$). No interaction ($P = 0.14$) existed between the effect of the year and that of the N rate. N fertilization did not significantly affect the average oil content of the grain ($P > 0.05$). In contrast, the N rate has a significant impact ($P < 0.0001$) on the oil yield. Indeed, as the N rate went up, the oil yield also increased until it reached its maximum level at 134 N kg·ha^{-1}; from that point, any increase of the N rate decreased the oil yield. The lowest oil yield was recorded in the control plots (Table 3).

3.5 Density and Moisture of Corn Grain

During the three years of the experiment, the density of the corn grain at the time of the NIR measurement was highly affected by the N rate ($P < 0.0001$) and the year ($P < 0.0001$). The grain density increased as the N rate went up ($R^2 = 0.97$) (Tables 3 and 4). Based on the conventional conversion factor that relates grain yield to ethanol yield in USA, only the weight of the grain is accounted for. That may create a bias in the extrapolation of the ethanol yield based on the grain yield only.

The significant impact of the N rate on grain density implies that during the processing of corn in the ethanol plant, the grain weight processed from the same volume of grain will be significantly different based on the year and the N rate. Therefore, the ethanol yield obtained from one bushel of corn will be statistically different depending on the N rate and the year.

3.6 Potential Ethanol Yield

The yield of ethanol from corn is highly dependent on the year ($P < 0.0001$) and the N rate ($P < 0.0001$). In most cases, the maximum ethanol yield was obtained with the application of 179 kg N·ha^{-1}. The highest yield was obtained in 2007, whereas the lowest was in 2009 (Table 5). In 2009, the corn demanded more N (224 kg N·ha^{-1}) before reaching the maximum ethanol yield. Nevertheless, the maximum ethanol yield in 2009 is less than what was produced with the application of less than 45 kg N·ha^{-1} in the other years.

The impact of the method of conversion of the starch into ethanol was statistically significant ($P < 0.0001$); that effect depended on the year and the N rate (Table 5).

Table 4 Summary of the relationship between N fertilization rate, oil, protein, starch, and density of corn grain across all years at Portageville, Missouri.

Dependent variable† (Y)	Independent variable (X)	Equation	R^2
Oil content (%)	N rate (kg·ha^{-1})	y = -0.0009x + 4.1345	0.44
Oil yield	N rate (kg·ha^{-1})	y = -0.0081x^2 + 2.8998x + 141.5	0.98
Total starch content (%)	N rate (kg·ha^{-1})	y = 2E-05x^2-0.0108x + 77.87	0.84
Total starch yield (kg·ha^{-1})	N rate (kg·ha^{-1})	y = -0.1499x^2 + 54.871x + 2727.6	0.96
Extractable starch content (%)	N rate (kg·ha^{-1})	y = -3E-05x^2 - 0.0005x + 70.071	0.88
Extractable starch yield (kg·ha^{-1})	N rate (kg·ha^{-1})	y = -0.1392x^2 + 50.364x + 2463.3	0.97
Density	N rate (kg·ha^{-1})	y = -3E-07x^2 + 0.0002x + 1.2328	0.97
Protein content (%)	N rate (kg·ha^{-1})	y = 0.0094x + 6.609	0.95
Protein yield (kg·ha^{-1})	N rate (kg·ha^{-1})	y = -0.0149x^2 + 6.1584x + 213.73	0.96
Total starch yield (kg·ha^{-1})	Protein yield (kg·ha^{-1})	y = -0.0061x^2 + 14.399x - 294.92	0.97
Extractable starch yield (kg·ha^{-1})	Protein yield (kg·ha^{-1})	y = -0.0062x^2 + 13.71x - 403.91	0.97
Grain yield (kg·ha^{-1})	Protein content (%)	y = -2390.7x^2 + 39286x - 151247	0.97

†: A significant relationship existed between N fertilization rate, oil, protein, starch, and the density of corn grain. This suggested the importance of N management in the sustainability of ethanol production from corn.

Table 5 Mean separation per year and per N rate of the different methods* to calculate the ethanol yield from corn.

Year	Method used to calculate the ethanol yield	Potential ethanol yield (L·ha^{-1}) under different N rate (kg·ha^{-1}):						
		0	45	90	134	179	224	269
2007	Total starch	2,020.0 a	4,676 a	6,002.8 a	6,994.9 a	7,035.1 a	6,240.4 a	6,358.5 a
	Conventional method	1,897.4 b	4,436.3 b	5,782.6 b	6,713.6 b	6,806.7 b	6,035.8 b	6,110.7 b
	Extractable starch	1,854.9 c	4,378.7 c	5,622.6 c	6,521.6 c	6,576.3 c	5,863.5 c	5,867.3 c
2008	Total starch	3,329.0 a	3,364.8 a	4,767.1 a	6,227 a	6,069.5 a	4,903.4 a	5,111.6 a
	Conventional method	3,187.4 b	3,181.2 b	4,517.6 b	5,955.7 b	5,777.4 b	4,728.9 a	4,911.4 b
	Extractable starch	2,979.1 c	2,968.5 c	4,228.4 c	5,462.6 c	5,288.1 c	4,321 b	4,421.5 c
2009	Total starch	693.7 a	1,674.7 a	3,108.6 a	3,374.5 a	3,609.2 a	3,667.2 a	3,645.1 a
	Conventional method	679.6 a	1,639.5 a	3,071.3 b	3,353.2 a	3,585.3 a	3,666.5 a	3,619.4 a
	Extractable starch	616.2 b	1,511.2 b	2,785.3 c	3,042.7 b	3,215.7 b	3,296.1 b	3,221.7 b

* Numbers followed by different letters are significantly different for the same N rate and year; The ethanol yields were calculated based on conversion factor found in the literature. The three methods yield different yield and the gap depended on the N rate. The gap between the three methods used to calculate the ethanol yield depended on the N rate.

Based on the conventional conversion factor, the theoretical ethanol yield from corn grain ranged from 679.6 to 6,806.7 L ethanol·ha^{-1} depending of the N rate and the year (Table 5). The ethanol yield based on the total starch and the extractable starch ranged from 693.7 to 7,035.1 L·ha^{-1} and from 616.2 to 6,576.3 L·ha^{-1} respectively (Table 5). The highest ethanol yield was obtained when the ethanol calculation was based on the total starch yield. In contrast, the lowest ethanol yield was recorded when the extractable starch was used. The conventional conversion factor gave an intermediary yield. In addition, in 2009, the ethanol yield based on the total starch was the same as that based on the conventional conversion factor. With all methods, the N rate has a significant impact on the ethanol yield. During the three years of the experiment, the use of the conventional conversion factor to determine the ethanol yield always overestimated the yield by increasing its value anywhere from 1.3% to 12.0% as compared to the extractable starch method. The gap between the ethanol yields using the conventional factor or the extractable starch linearly increased as the N rate augmented. The highest difference between the two methods was obtained in 2009.

In contrast, the use of total starch to calculate the ethanol yield led to 6.8% and 15.7% more ethanol as compared to the extractable starch method.

4. Discussion

Our results showed that N fertilization changed the composition of corn kernel. As the N rate increased, the starch content of the grain decreased, whereas the protein yield and content, and the starch yield increased until they reached their maximum at a N rate equaling to 179 kg N·ha^{-1}, which we considered as the optimum agronomical N rate in our study area. The oil yield reached the maximum at 134 kg N·ha^{-1}. We showed that the oil content of corn grain ranged from 3.8% to 4.2%, with significant variations found between the years. Those results concurred with data observed in other studies in Missouri where the corn grain oil content ranged from 3.3% to 4.3% [28]. We observed that the N fertilization increased the oil yield of corn grain. With cotton, N fertilization increased the oil yield, due to the increase of the cotton yield [29]. It is possible that N fertilization has the same effect on corn that it does on cotton.

The protein content of the grain obtained in our study oscillated between 6.7% and 8.9%. The impact of the N rate on the protein content of the grain was highly significant in every year. Other authors also observed that the protein content in corn grain ranged from 6% to 9% [28]. Of interest, dried distillers grain (DDGs) is a

coproduct of corn ethanol processing that can be used as fertilizer. The application of DDGs decreased the oil content of corn grain whereas it increased the protein content [28]. Similarly, in the case of cotton, the application of ammonium nitrate significantly reduced the oil content of the grain while the protein content increased [29]. Other scientists also observed an increase in protein content of corn grain as the N fertilization rate increased [30]. With an increase of N rate, corn may be favoring the synthesis of protein while reducing oil biosynthesis. Nitrate favors the expression of genes related to nitrogen metabolism and can change carbon metabolism as well [31]. Therefore, the increase of N fertilization may increase nitrogen metabolism providing a greater nitrogen source for the biosynthesis of amino acids and the expression of proteins. That may explain why a positive correlation was found between the N fertilization rate and the protein content of the grain.

We also found that the total starch content of corn grain fluctuated between 76.0% and 77.7%, whereas the extractable starch content varied between 68.0% and 70.4% of the grain. In Missouri, a previous study recorded slightly lower results with total starch content of grain ranging from 72% to 75%, and the extractable starch varied between 65% and 70% [28]. The difference may be explained by the type of fertilizers and the geographical region. Indeed, Nelson et al. [28] conducted their experiment in Novelty, northeast Missouri, and fertilized their soil with DDGs, whereas we conducted our study in the southeast corner of the state and used ammonium nitrate for fertilizer.

Based on a study in China, corn grain may be richer in starch than sweet sorghum grain which had 39% to 48% starch content [32]. The high starch content of corn grain may be due to the fact that corn does not stock much of its sugar in its stalk like sweet sorghum. In other words, sweet sorghum uses the sugars for juice instead of forming seeds with starch.

Our results showed that N fertilization increased the starch yield until the maximum is reached around 179 kg $N \cdot ha^{-1}$. The total starch yield obtained in our study ranged from 2.8 to 7.8 $mg \cdot ha^{-1}$ whereas the extractable starch varied between 2.6 to 7.1 $mg \cdot ha^{-1}$.

We also observed that N fertilization decreased the grain starch content. Other authors also observed that the grain starch content was reduced by the application of DDGs [28].

Our results proved that the density of corn grain depended on the N fertilization rate. The significant impact of N rate on grain density implies that no clear standard will be possible for the grain weight of one volume of grain. Instead, the year and the N rate must also be considered. This will affect corn processing and the ethanol yield because it will also be impossible to accurately determine the ethanol yield obtained from one volume of corn. Using one conversion factor (0.42 L ethanol per kg corn grain), as is currently done for these calculations, creates a significant bias considering the factors explained above that can change that ratio. Using a different logic, other authors [11] also pointed out that the conversion factor (of corn into ethanol) used in USA industry is "confusing and imprecise, and consequently overstated the ethanol yield". Our data confirmed that hypothesis.

Finally, we showed elsewhere that when farmers add N to their soil to improve grain yield for starch production to be used for biofuel production, they will also be increasing nutrient removal (data not shown). The negative correlation between the N rate and starch content suggested that by adding too much N to soil to increase grain yields, farmers reduce the starch content in those grains. Consequently the quality of the grain will differ based on the agronomical practices used by the farmers. This becomes another source for variation in the biofuel yield. A fair arrangement would be for ethanol plants to pay farmers a premium for corn with high starch content. Lower grain yields from low N fertilizer rates will be unfavorable to farmers, but beneficial to a power plant that will buy the grain because of higher starch content. Therefore, for biofuel production to be beneficial for both farmers and power

plant owners, an agreement may need to be made for the use of fertilizers. We will conduct an economic analysis in the future to determine the most economical and optimum N rate that will yield higher starch content with minimum nutrient removal.

5. Conclusion

Our results showed that N fertilization changed the composition of corn kernel. As the N rate increased, the starch content of the grain decreased. In contrast, as the N fertilization rate increased, the protein yield and content, the starch yield and the oil yield increased. The optimum N rate was considered to be 179 kg $N \cdot ha^{-1}$, which is where most factors involved in this study, reached their maximum. Our results showed that the density of corn grain depended on the N fertilization rate, proving that the conversion factor (0.42 L ethanol per kg corn grain) has a significant bias. Because of the significant impact of N fertilization on the composition of the corn kernel, a fair arrangement would be needed for ethanol plants to pay farmers a premium for corn with high starch content.

Acknowledgments

Funding for this research was covered by a grant from the Missouri Life Science Research Board, and another one from Missouri Fertilizer and Ag. Lime Board. The authors would like to thank these funding agencies. The authors would also like to thank Dr. M. Taylor for reviewing and editing of this manuscript.

References

[1] E. Gnansounou, A. Dauriat, C.E. Wyman, Refining sweet sorghum to ethanol and sugar: Economic trade-offs in the context of North China, Bioresource Technology 96 (2005) 985-1002.

[2] J. Heinimö, M. Junginger, Production and trading of biomass for energy—An overview of the global status, Biomass and Bioenergy 33 (2009) 1310-1320.

[3] R.J. Bothast, M.A. Schlicher, Biotechnological processes for conversion of corn into ethanol, Applied Microbiology and Biotechnology 67 (2005) 19-25.

[4] K.S. Dhugga, Maize biomass yield and composition for biofuels, Crop Science 47 (2007) 2211-2227.

[5] OECD, Economic Assessment of Biofuel Support Policies, Paris, France, 2008.

[6] P. Zuurbier, J. van de Vooren, Sugarcane Ethanol: Contributions to Climate Change Mitigation and the Environment, Wageningen Academic Publishers, The Netherlands, 2008.

[7] M. Dikeman, J. Fritz, E. Wailes, W. Gauther, H. Shapouri, Biomass from crop residues: Cost and supply estimates, in: Paul Gallagher (Ed.), US Department of Agriculture, Office of the Chief Economist, Office of Energy Policy and New Uses. Agricultural Economic Report, No. 819, 2003.

[8] S. Eckhoff, S. Singh, B. Zehr, K. Rausch, E. Fox, A. Mistry, et al., A 100g laboratory corn wet-milling procedure, Cereal Chemistry 73 (1996) 54-57.

[9] G. Ondrey, Chementator: Making bioethanol directly from starch, Chemical Engineering 112 (2005) 19-20.

[10] X. Wu, R. Zhao, L. Liu, S. Bean, P.A. Seib, J. McLaren, et al., Effects of growing location and irrigation on attributes and ethanol yields of selected grain sorghums, Cereal Chemistry 85 (2008) 495-501.

[11] T.W. Patzek, A statistical analysis of the theoretical yield of ethanol from corn starch, Natural Resources Research 15 (2006) 205-212.

[12] S.A. Uhart, F.H. Andrade, Nitrogen deficiency in maize: II. Carbon-nitrogen interaction effects on kernel number and grain yield, Crop Science 35 (1995) 1384-1389.

[13] H.L. Hao, Y.Z. Wei, X.E. Yang, Y. Feng, C.Y. Wu, Effects of different nitrogen fertilizer levels on Fe, Mn, Cu and Zn concentrations in shoot and grain quality in rice (*Oryza sativa*), Rice Science 14 (2007) 289-294.

[14] C. Vojnovich, R. Anderson, E. Griffin Jr, Wet-milling properties of corn after field shelling and artificial drying, Cereal Foods World 20 (1975) 333-335.

[15] A. Gallais, B. Hirel, An approach to the genetics of nitrogen use efficiency in maize, Journal of Experimental Botany 55 (2004) 295-306.

[16] D. Pimentel, Ethanol fuels: Energy security, economics, and the environment, Journal of Agricultural and Environmental Ethics 4 (1991) 1-13.

[17] D. Pimentel, The limits of biomass energy, Encyclopedia of Physical Sciences and Technology (2001) 159-171.

[18] D.R. Keeney, T.H. Deluca, Biomass as an energy source for the Midwestern US, American Journal of Alternative Agriculture 7 (1992) 137-143.

[19] D. Lorenz, D. Morris, How Much Energy Does It Take to Make a Gallon of Ethanol?, Institute for Local Self Reliance (ILSR), Washington DC, August 1995.

[20] H. Shapouri, J. Duffield, M. Graboski, Estimating the net energy balance of corn ethanol, Agricultural Economic Report 721 (1995).

[21] H. Shapouri, J. Duffield, M. Wang, The energy balance of

corn ethanol: an update, Agricultural Economics Reports (2002).

[22] J.R. Heckman, J.T. Sims, D.B. Beegle, F.J. Coale, S.J. Herbert, T.W. Bruulsema, W.J. Bamka, Nutrient removal by corn grain harvest, Agronomy Journal 95 (2003) 587-591.

[23] M.R. Paulsen, L.O. Pordesimo, M. Singh, S.W. Mbuvi, B. Ye, Maize starch yield calibrations with near infrared reflectance, Biosystems Engineering 85 (2003) 455-460.

[24] M. Paulsen, M. Singh, Calibration of a near-infrared transmission grain analyser for extractable starch in maize, Biosystems Engineering 89 (2004) 79-83.

[25] M. Singh, M.R. Paulsen, L. Tian, H. Yao, Site-specific study of corn protein, oil, and extractable starch variability using nit spectroscopy, Applied Engineering in Agriculture 21 (2005) 239-251.

[26] A. McAloon, F. Taylor, W. Yee, K. Ibsen, R. Wooley, Determining the cost of producing ethanol from corn starch and lignocellulosic feedstocks, National Renewable Energy Laboratory Report, NREL/TP-580-28893, 2000.

[27] A. Saxton, A macro for converting mean separation output to letter groupings in Proc Mixed, in: N. Proc. 23rd Annual SAS User Group Int. Conf., TN, March 22-25, SAS Inst., Cary, NC, 1998, pp. 1243-1246.

[28] K. Nelson, P. Motavalli, R. Smoot, Utility of dried distillers grain as a fertilizer source for corn, Journal of Agricultural Science 1 (2009) 3-12.

[29] Z.M. Sawan, A.E.H.A. El-Farra, S.A. El-Latif, Cottonseed, protein and oil yields and oil properties as affected by nitrogen and phosphorus fertilization and growth regulators, Journal of the American Oil Chemists Society 65 (1988) 948-951.

[30] P. Silva, M. Strieder, R. Coser, L. Rambo, L. Sangoi, G. Argenta, et al., Grain yield and kernel crude protein content increases of maize hybrids with late nitrogen side-dressing, Scientia Agricola 62 (2005) 487-492.

[31] M. Stitt, Nitrate regulation of metabolism and growth, Current Opinion in Plant Biology 2 (1999) 178-186.

[32] Y.L. Zhao, A. Dolat, Y. Steinberger, X. Wang, A. Osman, G.H. Xie, Biomass yield and changes in chemical composition of sweet sorghum cultivars grown for biofuel, Field Crops Research 111 (2009) 55-64.

Journal of Life Sciences 5 (2011) 1022-1029

Optimization of Bacterial Doses and Incubation Time on Bio-Ehanol Fermentation of Nipah (*Nypa fruticans*) for Biofuel Energy

Wiludjeng Trisasiwi[1], Ari Asnani[2] and Retna Setyawati[3]

1. Agricultural Engineering, Jenderal Soedirman University, Purwokerto 53123, Indonesia

2. Chemistry, Jenderal Soedirman University, Purwokerto 53123, Indonesia

3. Food Science and Technology, Jenderal Soedirman University, Purwokerto 53123, Indonesia

Received: December 23, 2010 / Accepted: May 26, 2011 / Published: December 30, 2011.

Abstract: Nipah (*Nypa fruticans*) is a species of palm trees that grows in mangroves environment near the sea shore. Nipah is potential to produce biofuel energy. The purposes of this research were 1) to determine the optimum bacterial concentration for fermentation to produce high concentration of bio-ethanol, and 2) to determine the optimum incubation time for fermentation to produce high concentration of bio-ethanol. The research had been conducted from June until November 2009 using nipah sap as the substrate and *Saccharomyces cerevisiae* as a fermentation starter. The experimental design used was a randomized block design (RBD). Factors tested were starter concentration (5%, 7.5%, 10%) and incubation time (2, 4, 6 days). The variables observed were concentration of reducing sugar, total microorganism (CFU/mL), and bio-ethanol production. The results showed that the highest yield of bio-ethanol (8.98%) was produced with 7.5% of starter concentration and 6 days of incubation time.

Key words: Bio-ethanol, bacterial concentration, incubation time, *Nypa fruticans*, *Saccharomyces cerevisiae*.

1. Introduction

In the year of 2007-2010, the Indonesian government targets to replace 1.48 billion liters of gasoline with bio-ethanol in accordance with Government Regulation No.5/2006. It is estimated that bio-ethanol requirements will increase 10% in 2011 to 2015 period, and 15% in 2016-2025 period. In the 3 years of first period (2007-2010), the government plan to replace an average of 30.833 million liters of bio-ethanol per month. Currently, bio-ethanol can only be supplied as much as 137,000 liters per month (0.4%). This means that every month it lacks 30.696 million liters of bio-ethanol as a fuel [1].

Results from research during the last 20 years have found that 60 species of plants can be used as an alternative to produce biofuel energy replacing fossil energy. Until now, alternative biofuels are much studied from maize [2], cassava [3], rice straw [4], and canna starch [5]. So far, research using nipah as raw material for bio-ethanol production is still rare. Smith [6] reported that nipah plants can produce 20 tons/hectare of nipah sap, or 14,300 liters/hectare of bio-ethanol, which is two times greater production than that of sugar cane.

Nipah (*Nypa fruticans*) is a species of palm trees that grows on mangrove forest environment or tidal area near the sea shore. Leaves and flowers grow from a horizontal rhizome that sink in the mud. Actually nipah plants have stems that crept on the ground, forming roots which immerse in mud, only the rosette leaves that emerge above the ground. From the rhizome appears compound pinnate leaves typical of palm, upright or nearly upright, towering up to 9 m above the ground and the stem length between 1-1.5 m. Nipah

Corresponding author: Wiludjeng Trisasiwi, Ph.D., research field: renewable energy. E-mail: wiludjengsiwi@yahoo.com.

flowers appear in auxiliary panicles, the female flowers gathered at the tip to form a ball while male flowers are arranged in panicles similar strands, each strand consisting of 4-5 grains of male flowers with a length of about 5 cm. Bunches of fruit can be tapped approximately four to five months after the flowers grow [7].

Nipah plant is intended to protect land or sea shore from abrasion. Whole nipah plant can be used for various purposes, for example nipah can be tapped to get sweet liquid from young fruit bunches, called nipah sap [7]. Communities in Village Nusadadi, Banyumas Regency, Central Java use nipah sap to make brown sugar [8]. However, the brown sugar obtained has a slightly salty taste and less preferred by consumers. Since nipah sap contains sugar it can be easily converted into bio-ethanol by the aid of microorganism. This condition encourages the utilization of nipah sap to produce bio-ethanol.

In general, bio-ethanol production technologies include 4 (four) series of processes, namely: preparation of raw materials, fermentation, distillation and purification [1]. Fermentation plays an important role in the processing sugar into bio-ethanol. The reaction is $C_6H_{12}O_6 \rightarrow 2C_2H_5OH + 2CO_2$. Microorganisms commonly used in fermentation industry mainly are a class of low levels of bacteria and fungi such as molds and yeasts.

According to Steinkraus [9], microorganisms used for fermentation to produce alcohol are from the groups of bacterial (*Clostridium acetobutylicum*, *Klebsiella pnemoniae*, *Leuconoctoc mesenteroides*, *Sarcina ventriculi*, *Zymomonas mobilis*); the group of mold (*Aspergillus oryzae*, *Endomyces lactis*, *Kloeckera* sp., *Kluyreromyces fragilis*, *Mucor* sp., *Neurospora crassa*, *Rhizopus* sp.); and the group of yeast (*Saccharomyces beticus*, *Saccharomyces cerevisiae*, *Saccharomyces ellipsoideus*, *Saccharomyces oviformis*, *Saccharomyces saki*, and *Torula* sp.). In our previous study, *Saccharomyces cerevisiae* was better than *Zymomonas mobilis* to produce bio-ethanol from nipah sap [10].

Factors that influence the production of bio-ethanol from nipah sap are the concentration of starter and the incubation time of fermentation. Therefore, the aims of this research were: 1) to determine the optimum concentration of starter and 2) to determine the optimum of incubation time on the fermentation to produce bio-ethanol in the high yield.

2. Materials and Methods

2.1 Nipah Sap Collections

Nipah sap was collected from *Nypha fruticans* tree in Nusadadi Village, Sumpiuh District, Banyumas Regency, Central Java, Indonesia. The sap was collected in the morning and directly brought to the laboratory for analysis. Chemical analysis on nipah sap were the percentage of total sugar, percentage of salt, pH, percentage of total protein, and total dissolved solids.

2.2 Saccharomyces cerevisiae Culture

Saccharomyces cerevisiae FNCC 3012 was obtained from the Food and Nutrition of Inter-University Center Gadjah Mada University Yogyakarta. It was cultivated using MEA (Malt Extract Agar) media. Two loops of *Saccharomyces cerevisiae* that had been cultivated was added into 100 mL of starter medium that contains of nipah sap, yeast extract (10 g/L), $MgSO_4 \cdot 7H_2O$ (0.5 g/L), and KH_2PO_4 (1.0 g/L). The mixture was incubated for 24 hours to produce *Saccharomyces cerevisiae*'s culture.

2.3 Fermentation of Nipah Sap

The composition of fermentation medium was a nipah sap, yeast extract (10 g/L), $MgSO_4 \cdot 7H_2O$ (0.5 g/L), and KH_2PO_4 (1.0 g/L). 150 mL of fermentation medium was placed in a 500 mL of Erlenmeyer sealed with a rubber cover. Plastic hoses were placed to remove the CO_2 gas that is formed during the fermentation process. In the end of the system, the plastic hose was dipped into the water to maintain anaerobic condition.

2.4 Determination of Optimum Condition for Fermentation

Saccharomyces cerevisiae's culture with concentration of 5%, 7.5%, or 10% was inoculated into fermentation medium. Incubation was carried out at room temperature for 2, 4, or 6 days. At the end of fermentation, the residual reducing sugar, total microorganism, and bio-ethanol content were analyzed.

The mixture from fermentation system was filtered and the filtrates obtained that contain bio-ethanol were distilled to give purified bio-ethanol. Distillation was carried out using a distillation flask with a temperature 78-80°C. The distillate was collected and measured the volume and the concentration of bio-ethanol. The starter concentration and incubation time which gave the highest yield of bio-ethanol were considered as the optimum conditions for fermentation.

2.5 Statistical Analysis

Experimental design used was a randomized block design (RBD) [11]. Factors tested were starter concentration and incubation time. Factors tested were starter concentration (percent v/v), which were 5%, 7.5%, and 10%; and incubation time, which were 2, 4, and 6 days. The treatment combination obtained was 9 combinations. Each treatment was repeated 2 times, thus the total number of experiment were 18 experimental units.

The variables observed were the determination of bio-ethanol (Conway method), the concentration of reducing sugar (Nelson-Somogyi method), and total microorganism in CFU/mL (pour plate method). The procedure to determine those variables were based on the well known procedures. The best treatment was based on the highest concentration of bio-ethanol.

3. Results

3.1 Analysis of Nipah Sap

The nipah sap was collected from nipah trees in Nusadadi Village, District Sumpiuh, Banyumas Regency. It was located around 3 km from sea shore. The chemical analyses of nipah sap are presented in Table 1.

3.2 Fermentation Process

Fermentation process of nipah sap used *Saccharomyces cerevisiae* with different concentrations of starter and variety of incubation time. The result of fermentation process was analyzed in term of reducing sugar, total microbial, and bio-ethanol yield. The results of chemical analyses are presented in Table 2.

4. Discussion

The total sugar in nipah sap was quite high (13.3%), thereby it was potential as raw material for making bio-ethanol. The concentration of sugar in the raw material will affect bio-ethanol production. If it was too low, then the bio-ethanol yield would be low, too. However, if it was too high it would inhibit microorganism

Table 1 Results of chemical analysis of nipah sap.

Chemical composition	Total
Total solids (Brix)	22.70
pH	6.50
Total sugar content (%)	13.30
Soluble protein content (%)	0.25
Salinity (%)	0.31

Table 2 The chemical analyses of the nipah sap fermentation using *Saccharomyces cerevisiae*.

Treatment	Reducing sugar (%)	Total microbial (CFU/mL)	Bio-ethanol (%)
5% concentration of starter	0.1871	8.35×10^6	3.92
7.5% concentration of starter	0.1535	1.07×10^8	9.55
10% concentration of starter	0.1548	8.27×10^6	8.93
Incubation 2 days	0.2168	1.83×10^6	5.68
Incubation 4 days	0.1454	2.15×10^8	7.73
Incubation 6 days	0.1332	1.88×10^6	8.98

growth due to plasmolysis of the microorganism. The high content of sugar in the fermentation medium cause high osmotic pressure so the cells undergo plasmolysis. According to Fardiaz [12], sugar is a preservative against microorganism damage. In addition, sugar can reduce water activity (Aw) of the substrate, thus the microorganism is inhibited.

The concentration of reducing sugar in the medium at the end of fermentation showed the amount of unconverted sugar. The average value of unconverted reducing sugar in the fermentation medium at different concentration of *Saccharomyces cerevisiae* is presented in Fig. 1, whereas the average value of that with various time of incubation is presented in Fig. 2.

The results of chemical analyses showed that the higher the concentration of starter, the lower the concentration of the remaining reducing sugar in the fermentation medium. These results indicated that sugar as a source of carbon was converted into bio-ethanol by microorganisms *Saccharomyces cerevisiae*. The more starter used would increase microorganism population in the medium which in turned a lot of sugar was consumed by microorganism for its growth and bio-ethanol production. Therefore, the remaining sugar in the fermentation medium decreased. According to Moat and Foster [13], sugar is a source of carbon and energy for microorganism growth and metabolite production.

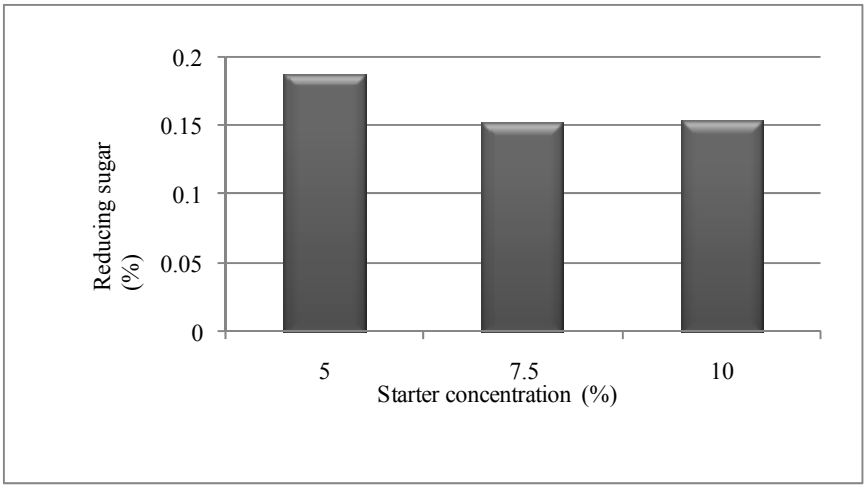

Fig. 1 The average value of reducing sugar concentration in various starter concentrations.

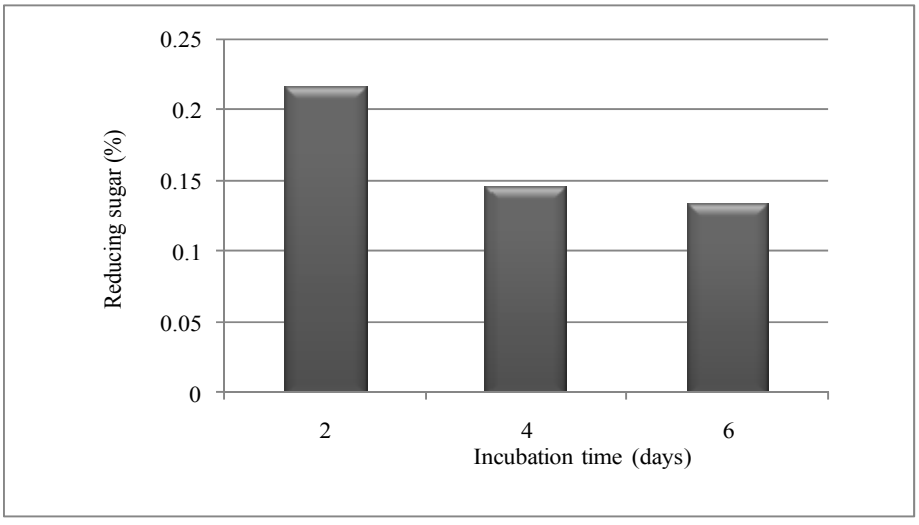

Fig. 2 The average value of reducing sugar content in various incubation times.

The longer the incubation time, the lower the levels of reducing sugar in the fermentation medium. These results indicated that the longer the fermentation time, the sugar was used by microorganisms to grow and to produce metabolites, including bio-ethanol.

The number of microorganisms during the fermentation process could be calculated. The average number of *Saccharomyces cerevisiae* at different concentrations of starter is presented in Fig. 3, and the average number of that at various time of incubation is presented in Fig. 4.

The average number of *Saccharomyces cerevisiae* at a concentration of 5%, 7.5% and 10% were 8.35×10^6 CFU/mL, 1.07×10^8 CFU/mL, and 8.27×10^6 CFU/mL or in log form were 6.9222 CFU/mL, 7.0295 CFU/mL, and 6.9173 CFU/mL, respectively.

Saccharomyces cerevisiae has a specific growth pattern during fermentation process. The increasing number of starter used caused the increasing number of microorganisms until the concentration of starter reached 7.5 percent. Beyond that concentration, the increasing number of starter tended to decrease the number of microorganism. It was assumed that the increasing number of microorganisms in the fermentation medium would lead to microorganism competition for nutrients. Therefore, inhibition of microorganism's growth was observed. According to Fardiaz [14], the pattern of microorganism growth in batch culture will accelerate the competition in obtaining nutrients because in the system during the fermentation process there is no additional nutrient.

The longer the fermentation time, the more average

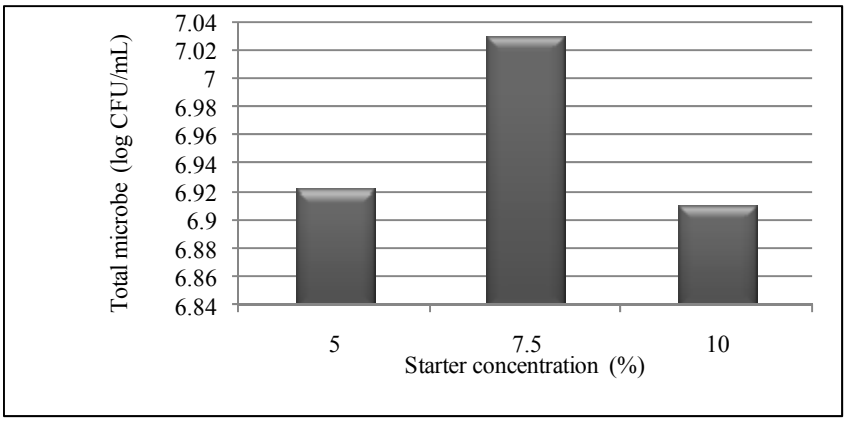

Fig. 3 Average total microbe in various starter concentrations.

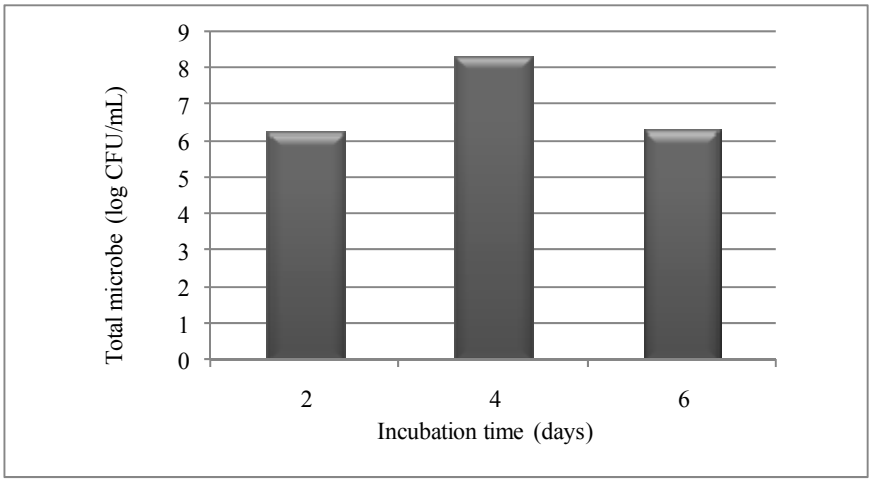

Fig. 4 The average number of microorganism in various incubation times.

number of microorganisms until it reached the optimum incubation time. Beyond that time the average number of microorganism declined, eventually. In this research, the average number of *Saccharomyces cerevisiae* during fermentation process for 2, 4, and 6 days were 1.83×10^6 CFU/mL, 2.15×10^8 CFU/mL, and 1.88×10^6 CFU/mL, respectively, or in log form were 6.2613 CFU/mL, 8.3329 CFU/mL, and 6.2747 CFU/mL, respectively.

The research results indicated that the incubation time of fermentation would affect the growth of microorganisms. The data showed that the number of microorganisms increased until 4 days of fermentation. When the incubation time was continued, it further decreased the number of microorganisms. Probably after 4 days of fermentation, microorganisms entered the stationary growth phase, therefore the number of microorganisms tended to be stationer. This stationary condition occurred due to the decreasing nutrients in the medium and the inhibition of microorganism growth by the presence of bio-ethanol produced.

The average levels of bio-ethanol produced during fermentation by *Saccharomyces cerevisiae* at different concentrations of starter is presented in Fig. 5, and the average level of that at various incubation times is presented in Fig. 6.

The higher starter concentration used in the fermentation process did not necessarily produce high yield of bio-ethanol. The results showed that the highest bio-ethanol was obtained at 7.5% of starter

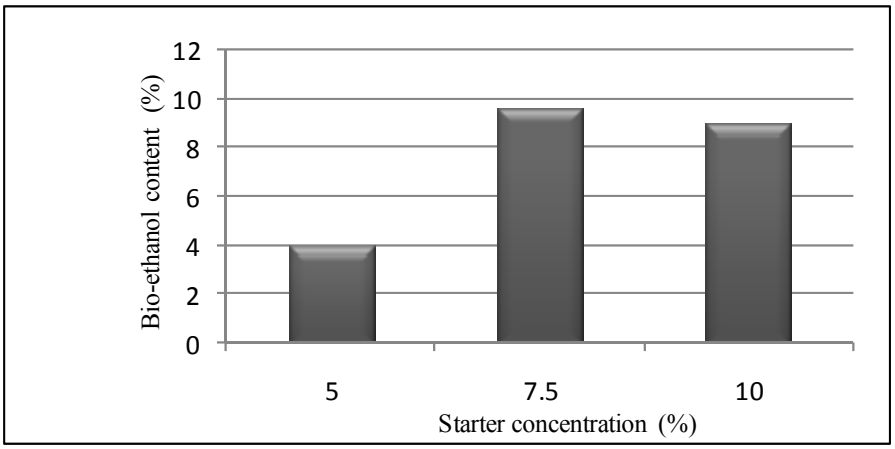

Fig. 5 The average content of bio-ethanol in various starter concentrations.

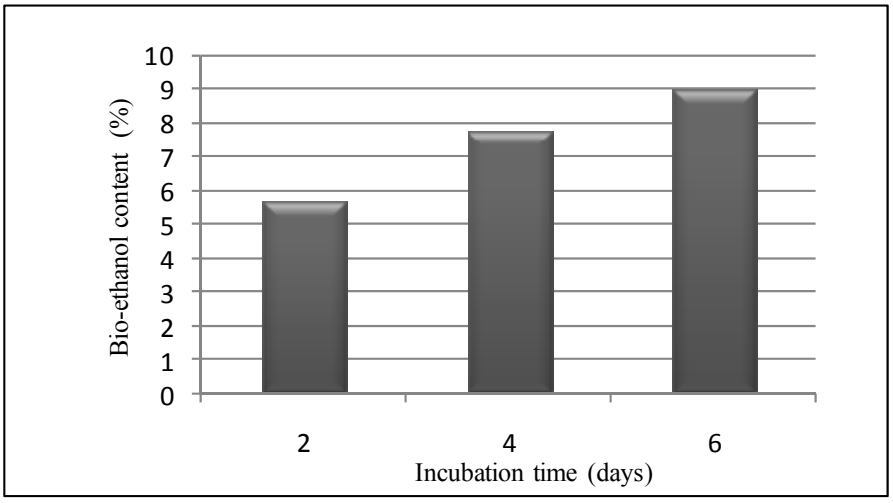

Fig. 6 The average content of bio-ethanol in various incubation times.

concentration using *Saccharomyces cerevisiae*. Using higher concentration of starter concentration tended to decrease bio-ethanol obtained. Probably, the increasing starter concentration raised competition for nutrition's among microorganism, resulting in lower productivity. This assumption was based on the observation that the number of microorganism tended to decrease with the large number of starter.

In the fermentation process of nipah sap, the optimum concentration of starter was 7.5% and bio-ethanol obtained was 8.98%. Fermentation of nipah sap using *Zymomonas mobilis* from our previous study [10] needed 5% of starter concentration to yield 6.22% of bio-ethanol. However, the increasing concentration of starter into 7.5% decrease the bio-ethanol obtained into 5.54%. These results indicated that *Saccharomyces cerevisiae* was a better starter than fermentation of corn meal hydrolyzates, the optimum bio-ethanol production from which *Zymomonas mobilis*. Rakin et al. [15] reported was 10.05% with 5% of starter concentration. Even though the bio-ethanol obtained from nipah sap was relatively lower than that from corn meal hydrolyzates, the nipah sap was more potential to be used as raw material for bio-ethanol production because it did not compete with food-stock availability.

In the fermentation process, the longer the incubation time increased bio-ethanol content. The highest level of bio-ethanol was 8.98%. It was obtained from fermentation with 6 days of incubation time. In the contrary, Putri and Sukandar [5] reported that the optimum bio-ethanol produced from canna starch using *Saccharomyces cerevisiae* was achieved at 24 hours (1 day) of incubation time. It began to decline after 36 hours (1.5 days) of incubation time.

The difference of incubation time indicated that nipah sap was a more suitable substrate for *Saccharomycess cerevisiae* compared to canna starch for the fermentation process. *Saccharomycess cerevisiae* entered stationary phase in 1.5 days if the substrate was canna starch whereas it needed 6 days to reach stationary phase with nipah sap as substrate.

5. Conclusion and Suggestion

5.1 Conclusion

The optimum concentration of starter was 7.5%.

The optimum of incubation time was 6 days.

The bio-ethanol production using 7.5% of starter concentration and 6 days of incubation time was 8.98%.

5.2 Suggestion

Further research using continuous fermentation method and modifying production parameters is necessary to increase bio-ethanol production from nipah sap.

Acknowledgments

This work was funded by the National Strategic Research Scheme 2009, Directorate General of Higher Education, Ministry of National Education, Indonesia. The authors would like to thank N.E. Widyana and S.Z. Sinuraya for laboratory work assistance.

References

[1] S. Bustaman, Strategy of bio-ethanol development base on sago in Moluccas, Perspektif 7 (2) (2008) 65-79. Available online at http://perkebunan.litbang.deptan.go.id. (in Indonesian with English abstract)

[2] D. Trifosa, Corn starch conversion being bio-ethanol, Ph.D. Thesis, Department of Chemistry, Bandung Institute of Technology, 2007. (in Indonesian with English abstract)

[3] Y. Trusmiyadi, Cassava starch being bio-ethanol, Ph.D. Thesis, Department of Chemistry, Bandung Institute of Technology, 2007. (in Indonesian with English abstract)

[4] A. Wulandari, Preliminary study of water juice fermentation of rice straw being bio-ethanol with commercial yeast, Ph.D. Thesis, Department of Chemistry, Bandung Institute of Technology, 2007. (in Indonesian with English abstract)

[5] L.S.E. Putri, D. Sukandar, Starch conversion of ganyong (*Canna edulis* Ker.) to bioethanol using acid hydrolysis and fermentation, Biodiversitas 9 (2) (2008) 112-116. Available online at: http://biodiversitas.mipa.uns.ac.id. (in Indonesian with English abstract)

[6] D. Smith, Nypa palm: Ethanol super-crop? Biofuel

Review, Singapore, 15 June 2006, Download on Sunday, Feb. 15, 2009. Available online at: http://www.mgsm.edu.au.

[7] A.K. Rachman, Y. Sudarto, Nipah Source New Sweetener, Publisher Kanisius, Yogyakarta, 1992. (in Indonesian)

[8] H. Tresnawati, Motivation for women processing of nipah-sugar in improving household income Nusadadi village, District Sumpiuh, Banyumas Regency, Ph.D. Thesis, Faculty of Agriculture, Jenderal Soedirman University, Purwokerto, 2009. (in Indonesian with English abstract)

[9] K.H. Steinkraus, Handbook of Indigenous Fermented Foods, Marcel Dekker Inc., New York, 1983.

[10] W. Trisasiwi, A. Asnani, R. Setyawati, Optimization of kind of bacterial, doses, and incubation time in making bio-ethanol from *Nypha fruticans*, Jenderal Soedirman University, Purwokerto, Indonesia, Research Report, Unpublished, 2009. (in Indonesian with English abstract)

[11] K.A. Gomez, A.A. Gomez, Statistical Procedures for Agricultural Research, 2nd ed., Sjamsuddin, Endang, J.S. Baharsjah (Trans.), University of Indonesia (UI-PRESS), 1995. (in Indonesian)

[12] S. Fardiaz, Food Microbiology, Ministry of Education and Culture Directorate General of Higher Education, Inter-University Center for Food and Nutrition, Bogor Agricultural University, 1989. (in Indonesian)

[13] A.B. Moat, J.W. Foster, Microbial Physiology, 2nd ed., John Wiley & Sons, New York, 1988.

[14] S. Fardiaz, Fermentation Physiology, Inter-University Center for Food and Nutrition, Bogor Agricultural University in collaboration with the Institute of Information Resources, Bogor Agricultural University, 1988. (in Indonesian)

[15] M. Rakin, L. Mojovic, S. Nikolic, M. Vukasinovic, V. Nedovic, Bio-ethanol production by immobilized *Sccharomyces cerevisiae* var. *ellipsoideus* cells, African Journal of Biotechnology 8 (3) (2009) 464-471. Available online at: http://www.academicjournals.org.

Journal of Life Sciences 5 (2011) 1030-1036

Isolation of Marine Actinomycetes from the Mangrove Swamps for Biotechnological Exploration

Rajesh C. Patil[1], Abhishek D. Mule[1], Gajanan V. Mali[2], Rajmahammad R. Tamboli[3], Rahul M. Khobragade[4], Sanjay K. Gaikwad[5], Vasanti I. Katchi[1] and Dhanashree Patil[6]

1. Bhavan's College, Andheri (w), Mumbai 400058, India

2. Department of Microbiology, M.B.S.K. Kanya Mahavidyalay, Kadegaon, Sagli 415304, India

3. Department of Microbiology, M.U. Mahavidyalaya, Udgir, Latur 413512, India

4. Department of Microbiology, Dr. Babasaheb Ambedkar Marathawada University, Sub-campus, Osmanabad 431001, India

5. Department of Cell & Molecular Biology, Rajiv Gandhi Institute of IT and Biotechnology, Bharati Vidyapeeth, Pune 411043, India

6. Gopal Krishna College, Kolhapur 416011, India

Received: June 30, 2011 / Accepted: July 25, 2011 / Published: December 30, 2011.

Abstract: The mangroves are specialized marine environments widely distributed along the coast lines, which support biologically diverse groups of organisms including microbes. The microorganisms present in this ecosystem contribute significantly in the food web of the tropical marine ecosystem. In the present investigation, Actinomycete isolates obtained from mangrove sediments have been studied for diversity as well as for their bioactive potential. Seven different Actinomycete isolates (MS1-MS7) were obtained from the sediments collected from the mangrove swamps. The phylogenetic analysis of these isolates showed that out or seven isolates, 3 isolates belong to *Streptomyces* sp., which has bioactive potential as several bioactive metabolites have been isolated from this group. One bacterium showed genetic similarity with *Corynebacterium* sp.. The microbes from this group are used for very important industrial applications. Three Actinomycete isolates showed very low similarity with the reported strains from the gene bank. In suggests that, these cultures could be novel and further research work is warranted to prove this speculation. In antagonistic studies, three Actinomycete isolates showed promising results. This investigation highlights the importance of mangrove ecosystem as a rich source of diverse Actinomycete strains for biotechnological applications.

Key words: Actinomycetes, mangrove swamps, phylogenetic analysis, bioactivity.

1. Introduction

Actinomycetes are best known for their ability to produce antibiotics and are gram positive bacteria which comprise a group of branching unicellular microorganisms. They are predominant in dry alkaline soil. Studies on actinomycetes are very limited and the actinomycetes have been mentioned incidentally, on the microbial community of marine habitats. Further, only little information is available on the actinomycetes of the mangrove environment (which is one among the most productive coastal ecosystems) with regard to their occurrence and distribution [1].

Identification of actinomycetes using only microscopic and cultural biochemical techniques is not enough to ascertain the organism. Genetic methods are the best in class methods to identify the organisms; primers had been developed by researchers to target specifically the 16S rRNA sequence of the Actinomycetes [2, 3]. Identification of actionmycetes to genus level was made possible in a fast and accurate manner. This has been a great advancement in the area of identification as that the ability to obtain the genus of the actinomycetes in just a few hours is now possible.

Corresponding author: Rajesh C. Patil, Ph.D., Prof., research field: environmental microbiology. E-mail: rcpatil68@rediffmail.com.

The phylogenetic analysis of microbes further helps in selecting potential candidates for biotechnological applications.

Mangrove forests are the only forests situated at the sea-land interface in tropical and subtropical latitudes. They are often called as "marine tidal forests", "coastal woodlands" or "oceanic rainforests". The Mangrove forest ecosystem supports biologically diverse groups of organisms. Mangroves are specialized marine environments widely distributed along the cost lines and microorganisms present in them are connected with degradation and mineralization of mangrove leaves, wood, sea grasses and other lignocellulosic materials those are significant primary sources in the food web of the tropical marine ecosystem [4]. Those microbes survive on sediments as well as in the intertidal region of mangrove stands.

Actinomycetes are best known for their ability to therapeutic molecules with special emphasis on antibiotics. They produce branching mycelium which may be of two kinds *viz*., substrate mycelium and aerial mycelium. Among actinomycetes, the streptomycetes are the dominant. The non-streptomycetes are called rare actinomycetes, comprising approximately 100 genera. Members of the actinomycetes, which live in marine environment, are poorly understood and only few reports are available pertaining to actinomycetes from mangroves swamps [1].

Interestingly, considerable new marine diversity is also being discovered within the genus *Streptomyces*, a taxonomically complex group of actinomycetes that commonly occur in soils and account for the vast majority of antibiotics discovered so far [5]. These marine actinomycetes include alkaliphilic *Streptomyces* spp., the marine clade MAR4, and what seems to be a new genus within the family Streptomycetaceae for which the name "*Marinispora*" has been proposed. Chemical studies of these actinomycetes are proving to be particularly interesting, and they provide added perspective on the correlations between phylogenetic diversity and secondary-metabolite production.

Actinomycete isolates obtained from mangrove sediments have been studied for diversity as well as bioactivity purpose. Recently Crude bioactive compounds of actinomycetes isolated from manakkudy (India) mangrove sediment have been studied for antibacterial activity against human and fish pathogens [6]. In other investigation it was found that actinomycetes isolated from mangrove habitats are a potentially rich source for the discovery of anti-infection and anti-tumor compounds, and of agents for treating neurodegenerative diseases and diabetes [7]. Phylogenetic analysis and antimicrobial activities of *Streptomyces* isolates from mangrove sediment of Manakudi estuary near the Arabian Sea, India, was analyzed recently [8].

2. Materials and Methods

2.1 Collection of Sediment Samples

The sediment sample (10 g) was collected from the mangrove swamps of Achara, Malvan (16°03'N, 73°30' E), Maharashtra, India. The sample was labeled and brought back to the laboratory in sterile plastic bags. The sediment sample (0.1 g) was dried at 50°C for 5 hours and used further for microbial isolation.

2.2 Isolation of Actinomycete Cultures

Three different culture media such as Glycerol Yeast Extract Agar (Glycerol 0.5 mL, Yeast extract 0.2 g, K_2HPO_4 0.01 g, Peptone 2.5 g, Agar 1.5 g, Filtered Sea water 50% and Distilled water 50%), ISP2 Medium (Malt extract 1 g, Yeast extract 0.4 g, Glucose 0.4 g, Agar 1.5 g, Distilled water 100 mL) and Actinomycete Isolation Agar (Himedia # M490-500G) were prepared for Actinomycete isolation. The dried sediment sample was dispensed in 1 mL sterile distilled water, diluted (up to 10^{-3} dilutions) and spread plated on each of above media. The plates were incubated at 37°C for 48 hours. The isolated colonies were preserved on ISP2 agar slants. The colony characteristics were observed and reported in Table 1.

Table 1 Morphological characteristics of Actinomycete isolates obtained from mangrove swamps.

Isolate code	Pigment	Diffusible pigment	Consistency of pellet	Penetration	Sporulation	Colony surface	Media
MS1	Yellow	-	soft	Poor	-	rough	ISP2
MS2	Cream	-	soft	-	-	buds	GYEA
MS3	Yellow	-	hard	Moderate	Scarce orange	rough	ISP2
MS4	Off white	-	soft	Poor	Dense grey	rough	AIA
MS5	Brown	-	soft	Poor	Dense grey	rough	GYEA
MS6	Dark brown	Dark brown	soft, flat	Poor	Dense grayish brown	Rough	ISP2
MS7	Off white	-	soft	Deep	White peripheral	Smooth	AIA

2.3 Microscopic Studies

The smears of all isolated Actinomycete cultures were prepared and heat fixed. Gram's staining was carried out using Himedia Gram's staining kit (Cat No K001-1KT). The cultures were observed under oil immersion and microscopic characteristics were recorded. The sample Actinomycete isolate (MS4) cultured from the mangrove swamps is shown in Fig. 1.

Fig. 1 Sample Actinomycete isolate (MS4) cultured from the mangrove swamps.

2.4 Phylogenetic Analysis of Actinomycetes

Phylogenetic analysis of Actinomycete isolates obtained from mangrove sediments was carried out by using following steps.

2.4.1 DNA Extraction

DNA Extraction from 7 actinomycetes isolated from marine soil was carried out using SDS-Ammonium acetate method. A small piece of mycelia was picked up with a sterile loop and ground in 0.5 mL extraction buffer (50 mM Tris-HCl, 50 mM EDTA, 250 mM NaCl, 1.5% Sucrose). 80 μL of SDS (20%) was added to it. The solution was vortexed for few seconds and incubated for 30 min at 65°C, 150 μL of 7.5 M Ammonium acetate was then added to the above solution and mixed by inverting. The tubes were incubated at 4°C for 15 min. DNA was extracted using 0.5 mL of chloroform: isoamyl alcohol mixture (24:1) and centrifuging at 10,000 rpm for 5 min. Double volume of ethanol (96%-100%) was added to the aqueous phase in a new tube, inverted twice and allowed to stand at 4°C for 30 min. The mixture was then centrifuged at 10,000 rpm for 15 min. After air drying for few seconds pellet was dissolved in 50 μL elution buffer (10 mM Tris-HCl, 1 mM EDTA). The DNA was stored at 4°C for further use. Agarose gel electrophoresis was performed to check the presence of DNA using 0.8% Agarose.

2.4.2 DNA Quantification

DNA concentration was determined using Quant-iT^{TM} dsDNA BR Assay Kit of invitrogen. Quant-iT^{TM} working solution was prepared for Z1 sample and 2 standards by diluting the Quant-iT^{TM} dsDNA BR reagent 1:200 in Quant-iT^{TM} dsDNA BR buffer in a plastic container. 190 μL of working solution was dispensed in 2 Qubit assay tubes for standards and 198 μL was dispensed in each sample tube. 10 μL of each of the two standards were added to the respective standard tubes and 2 μL of each of the sample was added to the respective sample tubes. The tubes were vortexed and incubated at room temperature for 2 min. The Quant-iT^{TM} dsDNA BR was chosen on Qubit^{TM} fluorometer and calibration done using the

two standards. Sample reading was taken and calculated for 2 µL. The result was obtained in µg/mL.

Concentration of DNA for the samples was found to be in a range of 80-100 µg/mL.

2.4.3 Gel Electrophoresis

Agarose powder was mixed with 1 × TAE buffer (Fermentas, #B49) to prepare 0.8% solution. 1 × TAE buffer was prepared by diluting 50 × TAE buffer of Fermentas (Composition: 43.12 g Tris, 22 g Acetic acid, 2.96 g EDTA in 1,000 mL distilled water). The solution was heated to dissolve agarose. GelRed stain (10,000 × Biotium-41003) was added (0.3 µL in 30 mL). The hot, clear agarose solution was poured into the tray and was allowed to cool. After cooling the gel tray was placed in an electrophoresis chamber, which was filled with 1 × TAE buffer, covering the gel. This allows electrical current from poles at either end of the gel to flow through the gel. Finally, DNA samples were loaded on the gel. Tracking dye was not required as it was already presented in PCR master mix. Electrophoresis was performed and Gel was observed through UV transilluminator to detect presence of DNA.

2.4.4 PCR Amplification

PCR amplification was carried out, following the method of Thakur et al. [9]. PCR amplification was performed in a total volume of 50 µL containing the appropriate reaction mixture. For first culture MS1 bacteria specific universal primers 27f (5' AGA GTT TGA TCC TGG CTC AG 3') and 1385r (5' CGG TGT GTA CAA GGC CC 3'), corresponding to *Escherichia coli* 16S rDNA numbering were used. However for remaining Actinomycete cultures specific universal primers S-C-Act-235-a-S-20 (5'-CGC GGC CTA TCA GCT TGT TG-3') and S-C-Act-878-a-A-19 (5'-CCG TAC TCC CCA GGC GGGG-3') were used. For PCR 2 × Jumpstart REDTaq Readymix PCR Reaction Mix from Sigma (P 0982) was used. The amplification was carried out at annealing temperature 52°C for first pair of primer and 60°C for second set of primer by using Biometra (T-personal) thermo-cycler. Agarose gel electrophoresis was performed using 1.2% gel to detect PCR product. The obtained PCR product was further purified by using PCR product purification kit (Quiagen QIAquick 96 PCR purification kit, Catalogue No. 28180).

2.4.5 Sequencing and BLAST Analysis

The purified PCR products were sequenced on Applied biosystems machine using BigDye® Terminator v3.1 Cycle Sequencing Kit. The sequences were recorded for further analysis. The sequences of PCR products were analyzed by using Basic Local Alignment Search Tool (BLAST). Nucleotide-nucleotide BLAST was carried by using three databases like NCBI, EMBL and DDBJ. The sequences of for potential Actinomycetes strains (MS4–MS7) were deposited in NCBI gene bank and the accession numbers were obtained. The phylogenetic tree was constructed by using software program Archaeopteryx0.957b. The phylogenetic tree is presented in Fig. 2.

2.5 Antagonistic Studies

All the seven Actinomycete isolated obtained from mangrove were studied for their antagonistic properties against each other by Agar Plug method. One day prior to the assay bacterial lawns were spread on agar plates and incubated overnight at 37°C. These lawns were used to pick agar plugs for the assay. On the next day bacteria were spread plated in triplicates on respective agar plates. Agar plugs were picked from the master plate and placed carefully on the assay plates. These were again incubated at 37°C overnight. The results (inhibitive, supportive or auto toxicity) obtained were recorded. The diameter of agar plug was 10 mm. The inhibition zones were calculated as diameter of total inhibition zone minus diameter of agar plug.

3. Results and Discussion

Altogether seven Actinomycete isolates (MS1-MS7) were obtained from the sediments collected from the mangrove swamps. Out of 7 isolates, 3 were isolated

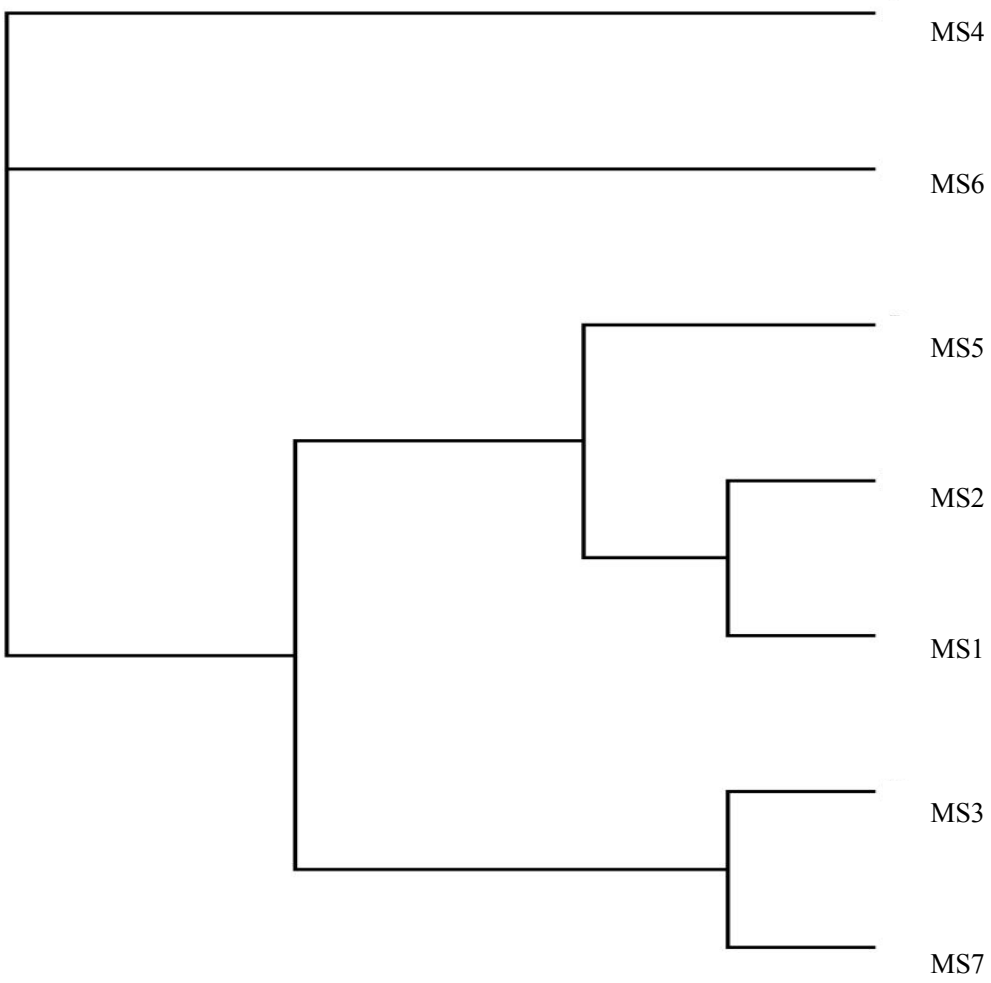

Fig. 2 Phylogenetic tree constructed by using sequences of all 7 Actinomycete isolates obtained from the mangrove sediments.

on ISP2 agar, 2 were isolated on GYEA agar and 2 were isolated on AIA agar. All these isolates were obtained from 10^{-2} and 10^{-3} dilutions. All these 7 Actinomycete isolates were purified and preserved on ISP2 agar slants. The morphological characterics of these Actinomycete isolates are recorded in Table 1. Interestingly all these isolates were found to be differed in their pigmentation and sprorulation pattern.

It was observed that the ISP2 agar used for isolation in this study proved to be better than even readymade Actinomycete isolation agar from the company. Initially diverse colonies were appeared on ISP2 agar plate as compared to other media. In previous studies, ISP2 agar with malt extract has also been recommended for the isolation of unique groups of Actinonycetes from environmental samples (unpublished work).

The 16S rRNA gene was amplified by using specific primers. The amplification of MS1 culture by using 27F and 1385R primers gave a PCR product of size 1,331 bp. However, the amplification of MS2-MS7 isolates by using Actinomycete specific primers gave a PCR product of size 643 bp.

The obtained sequences were BLAST by using three important gene databases like NCBI, EMBL and DDBJ. After comparing the BLAST results of three databases, it was observed that there are slight differences in the phylogenetic neighbors of these Actinomycete isolates. The results are shown in Table 2.

After comparing the BLAST results from three different databases, closest phylogenetic neighbour

Table 2 Phylogenetic analysis of Actinomycete isolates.

Isolate No.	NCBI database		EMBL database		DDBJ database	
	Phylogenetic neighbor	% similarity	Phylogenetic neighbor	% similarity	Phylogenetic neighbor	% similarity
MS1	*Beutenbergia cavernae* DSM 12333	86	*Cellulomonas* sp. CG-311	93	*Promicromonospora sukumoe* gene	91
MS2	*Corynebacterium amycolatum* SK46 contig00010	99	*Corynebacterium hansenii* partial 16S rRNA gene	98	*Corynebacterium xerosis* partial 16S rRNA gene	100
MS3	*Streptomyces coelicolor* A3(2)	91	*Streptomyces olivoverticillatus* strain JS-2	85	*Streptomyces* sp. CNQ-301_SD01	95
MS4	*Streptomyces coelicolor* A3(2)	100	*Streptomyces* sp. 1A01559	98	*Streptomyces* sp. 'ST-1 Sivasamy BU'	100
MS5	*Streptomyces coelicolor* A3(2)	99	*Streptomyces scabies*	98	*Streptomyces* sp. 'ST-1 *Sivasamy* BU'	100
MS6	*Micrococcus luteus* NCTC 2665	99	*Streptomyces* sp. CNR940 PL04	98	*Streptomyces niger* strain AS 4.1244	100
MS7	*Kytococcus sedentarius* DSM 20547	95	*Curtobacterium* sp. EPI-B9	77	*Streptomyces* sp. LK2231.1	96

was selected based on the percentage similarity. The isolate MS1 showed 93% similarity with *Cellulomonas* sp.. This perticular genus belongs to the Actinobacterial family. The isolate No. 2 MS2 showed 100% similarity with *Corynebacterium xerosis*. This particular Actinomycete strain is considered as a commensal microorganism of human skin and mucous membranes. The isolate MS3 showed 95% similarity with *Streptomyces* sp., where as isolate MS4 was showing 100% similarity with *Streptomyces coelicolor*. The isolate MS5 showed 100% similarity with *Streptomyces* sp. and the isolate MS6 showed 100% similarity with *Streptomyces niger*. The last isolate MS7 showed 96% similarity with *Streptomyces* sp. in DDBJ database but the same isolate showed 95% similarity with *Kytococcus sedentarius* in NCBI database.

In this investigation sequence similarity results were obtained by using three interlinked databases. Surprisingly all the seven isolates showed different results in different databases. In this case nearest phylogenetic neighbor was selected based on the highest sequence similarity.

The phylogenetic tree shows that isolate MS1 and MS2 are related species, and shared ancestors with MS5. Similarly MS7 and MS3 are analogous, whereas MS4 and MS6 are independent and evolved separately during the course of evolution (Fig. 2).

The results of antagonistic activity are presented in Table 3. The results of inhibition zones are given in mm. In this assay, four Actinomycete isolates showed antibacterial activity. These isolates were MS4 (*Streptomyces* sp.), MS5 (*Streptomyces* sp.), MS6 (*Streptomyces niger*) and MS7 (*Streptomyces* sp.). All four cultures showed prominent inhibitory activity against MS3 (*Streptomyces* sp.) and MS6 (*Streptomyces niger*) isolates. Interestingly MS5 isolate showed autotoxicity.

The antagonistic activity is considered to be the rapid and feasible method for the prediction of bioactive potential of environmental microbes. This technique was used earlier by various researchers [10].

Table 3 Antagonistic activity of Actinomycete isolated cultured from mangrove sediments.

Test actino cultures	MS1	MS2	MS3	MS4	MS5	MS6	MS7
MS1				3	-	-	-
MS2				1	2	2	3
MS3				4	3	1	4
MS4				-	1	1	-
MS5				1	2	1	1
MS6				5	3	-	2
MS7				1	2	2	-

Values show diameter of zone of inhibition in mm.

In this investigation, one bacterium showed genetic similarity with genus *Corynebacterium.* Non-pathogenic species of *Corynebacterium* are used for very important industrial applications, such as the production of amino acids, nucleotides, enzymes and secondary metabolites like antibiotics [11].

In this study, three Actinomycete strains showed very low sequence similarity with the reported strains from the gene bank. Out of these three, one strain showed potential antagonistic activity. This is an important finding, which suggests the possibility of getting novel strains from this environment for industrial applications. The sequences of all four potential Actinomycete isolates were deposited in NCBI gene bank with accession number JF935147 (MS4), JF935148 (MS5), JF935149 (MS6) and JF935150 (MS7).

4. Conclusion

Marine microorganisms are known to be rich sources of novel compounds. However, only a very small proportion of microbial organisms living in this environment have been isolated and even fewer successfully grown in the laboratory. To facilitate this avenue of research, there is a need for new methods to collect, isolate and identify marine microorganisms as well as new source for the isolation. The present study was an attempt to isolate marine Actinomycete cultures from mangrove swamps for biotechnological applications. Interestingly, diverse Actinomycete cutlers were obtained from this ecosystem. Some of the cultures showed significant Antagonistic activity which suggests their bioactive potential. This investigation highlights the importance of mangrove swamp area for the isolation of unique groups of microorganism for biotechnological applications.

References

[1] K. Siva Kumar, Actinomycetes of an Indian mangrove (Pichavaram) environment: An Inventory, Ph.D. Thesis, Annamalai University, India, 2001.

[2] F. Schwieger, C.C. Tebbe, A new approach to utilize PCR-Single Strand-Conformation Polymorphism for 16S rRNA gene-based microbial community analysis, Appl. Environ. Microbiol. 64 (1998) 4870-4876.

[3] Y. Wang, Z. Zhang, S.J.S. Ruan, Y.M. Wang, S.M. Ali, Investigation of actinomycete diversity in the tropical rainforests of Singapore, J. Ind. Microbiol. Biotechnol. 23 (1999) 178-187.

[4] P. Prema, Mangrove actinomycetes as sources of biocatalysts and bioactive compounds, in: India 7th Asia Pacific Marine Biotechnology Conference, Kerala, India, 2006.

[5] J. Berdy, Bioactive microbial metabolites, J. Antibiot. (Tokyo) 58 (2005) 1-26.

[6] S. Ravikumar, P. Suganthi, F. Moses, Crude bioactive compounds of actinomycetes from manakkudy mangrove sediment, J. of Pharm. Res. 4 (2011) 877-879.

[7] K. Hong, A. Gao, Q. Xie, H. Gao, L. Zhuang, H. Lin, et al., Actinomycetes for marine drug discovery isolated from mangrove soils and plants in China, Mar Drugs. 7 (2009) 24-44.

[8] S.V. Satheeja, R.D. Solomon, Jebakumar phylogenetic analysis and antimicrobial activities of *Streptomyces* isolates from mangrove sediment, J. of Basic Microbiol. 51 (2011) 71-79.

[9] N.L. Thakur, A.C. Anil, W.E.G. Müller, Culturable epibacteria of the marine sponge *Ircinia fusca*: Temporal variations and their possible role in the epibacterial defense of the host, Aquat. Microb. Ecol. 37 (2004) 295-304.

[10] K. Sivasubramanian, S. Ravichandran, M. Vijayapriya, Antagonistic activity of marine bacteria *Pseudoalteromonas tunicata* against microbial pathogens, African Journal of Microbiology Research 5 (2011) 562-567.

[11] Available online at: http://en.wikipedia.org/wiki/ Corynebacterium.

Journal of Life Sciences 5 (2011) 1037-1041

Evaluation of Three Sunflower (*Helianthus annuus* L.) Hybrids for Salt Tolerance *in Vitro*

Abedaljasim M. Jasim Al-Jibouri[1], Samar F. Altahan[2] and Tarek A. Al-Anii[2]

1. Plant Biotec. Dept., Biotechnology Research Center, Al-Nahrain University, Baghdad 10072, Iraq

2. Biology Sci. Dept., College of Science for Women, Baghdad University, Baghdad 10071, Iraq

Received: April 29, 2011 / Accepted: June 10, 2011 / Published: December 30, 2011.

Abstract: This study aimed to induce callus from three sunflower (*Helianthus annuus* L.) hybrids, namely Anna, Alhaja and Kuds, and to evaluate their callus for salt stress tolerance. Cotyledons and hypocotyl were taken from seedling of these hybrids and cultured on MS media contained 2,4-D (0.0, 0.5, 1.0, 1.5 and 2.0 mg/L) and kinetin (0.0, 0.5, and 1.0 mg/L). The cultures incubated at 25 ± 1°C under light condition (1,000 Lux) for 16 h/day. After 6 weeks observations were taken on the response of cotyledons and hypocotyl to callus induction. The induced callus were cultured on the same MS media that contained appropriate concentrations of 2,4-D and kinetin for callus induction as well as contained various concentration of sodium chloride NaCl (0.0, 0.05, 0.1, 0.15 and 0.2%). After six weeks callus fresh and dry weights, proline and total carbohydrates concentrations were measured. The results showed significant differences among the hybrids, explants, 2,4-D and kinetin concentration and significant interaction between them in their percentage response for callus induction. The results also revealed that fresh and dry weights were significantly reduced with increased NaCl concentration in the medium, hybrids showed significant differences in their response to salt stress. Proline and total carbohydrate concentration increased in callus as NaCl increased in the media. Significant interaction was showed between hybrids and NaCl concentration in these parameters.

Key words: Sunflower hybrids, *Helianthus annuus* L., callus, salt stress, cotyledons, hypocotyls, proline, carbohydrate.

1. Introduction

Salinity is considered as the main constraint to plant production. According to Mass and Hoffman [1], nearly one third of the world irrigated lands are salt-affected. In Iraq, percent of salt-affected soils is 75% of middle and southern lands due to saline groundwater and the absence or poor drainage systems [2]. In addition, the mismanagement of irrigation projects elevated the problems. Sun flower is moderately salinity crop and grow well in soils with salinity less than 6 ds/m. Increased salinity above this level required high energy for tolerating salinity stress and the grown in high salinity stress environment. High salinity is decreasing the quantity and quality of crops per unit area. In addition, its effect extends to the surrounding environment through desertification, reduction in plant cover, and environmental pollution. To overcome this problem, plant breeders initiated research programs and induced salt-tolerant genotypes. Further more, they screened the introduced genotypes for salinity and then cultivated these genotypes in saline environment using classical methods as well as new techniques [3]. Research findings indicated the importance of using tissue culture in parallel with classical methods by growing cells on media of high salinity and select salinity tolerant cells capable of regenerate plants that tolerate salinity stress [4]. The introduced hybrids can be evaluated by using tissue culture technique for selection the salt-tolerant genotypes [5, 6]. The aim of this investigation is studying the effect of sodium chloride on cellular

Corresponding author: Abedaljasim M. Jasim Al-Jibouri, Ph.D., Assist. Prof., research field: plant biotechnology. E-mail: dr_aljibouri@yahoo.com.

content of three sunflower hybrid calluses.

2. Materials and Methods

Seeds of three sunflower hybrids, namely: Anna, Alhaja, and Kuds (taken from Ministry of Agriculture of Iraq), have been treated with 4% sodium hypochloride (NaClO) for 10 min [7]. Murashige and Skoog [8] medium (MS) were prepared (Table 1) and sterilized by autoclaving under 1.04 kg/cm^2 pressure and 121°C for 15 min. Seeds were cultured on MS medium and incubated on 25 ± 1°C and 1,000 Lux for 16 h/day. After two weeks, the explants cotyledons and hypocotyls were taken from the seedlings and cultured on the same MS medium with 2,4-D (0, 0.5, 1.0, 1.5 and 2.0 mg/L) and kinetin (0, 0.5, and 1.0 mg/L). The cultures were incubated under the same conditions to induce the callus. After six weeks, observations on percentage of callus induction were taken. Basing on results of callus induction, callus of hypocotyls were cultured on MS supplemented with 1.0 mg/L of 2.4-D and kinetin for the hybrids Anna and Alhaja; for the Kuds hybrid, we used 0.5 mg/L of 2,4-D and kinetin. After 4 weeks we recaptured the callus on the same media to obtain sufficient quantity of callus. We took 30 mg from callus of each hybrid and cultured on the same media supplemented with NaCl (0, 0.05, 0.1, 0.15, and 0.2%) and incubated on the same condition. After six weeks, fresh and dry weigh of callus were taken, protein and carbohydrate in the callus were measured using HPLC. All experiments were carried out by using complete randomized design (CRD) with 10 replicates for each hybrid and each concentration and results were analyzed statistically according to LSD in probability level of 0.05 [9].

Table 1 Component of media used for seeds germination of sunflower hybrids.

Medium components	Concentration (mg/L)
MS	Full strength
Prodoxine-HCl	0.5
Glycine	2.0
Nicotinic acid	0.5
Thiamine-HCl	0.1
Myo-inositol	100
Sucrose	30,000
Agar	8,000

3. Result and Discussion

Result indicated to the presence of significant difference between the hybrids in the percentages of callus induction (Table 2).

The two hybrids Anna and Alhaja gave 46.7% and 45.3% callus induction, respectively, and differed significantly from 5.7% callus induction for the Kuds hybrid. Also, the hypocotyls surpass significantly the cotyledons in the callus induction percent and reached 43.7% and 21.0%, respectively. There was significant effect for the growth regulator 2,4-D and kinetin in the callus induction. The concentration 1.0 mg/L of 2,4-D gave a high value of 39.2% and differed significantly from the control 17.5%. On the other hand, the concentration 1.0 mg/L kinetin with 37.3% callus induction surpasses the concentration 0.5 mg/L of 27.8% callus induction. Also, there were interaction among the treatments in the percent of callus induction; the highest induction was 85% and the lowest was 5.5%. We conclude that the callus induction is affected by many factors included composition of media, type and concentration of growth regulator, source of plant tissue cultured, and hybrid [10-12] in their test on callus induction of sunflower and wheat confirmed that the genotype and media composition have the main role in *in vitro* callus induction. Fresh weight of callus decreased with the increased salt concentration of media. It was 36.6 mg under salt concentration 0.20% and differed significant from all treatments except salt level 0.10% which gave mean weight 40.3 mg (Table 3). The hybrid Alhaja gave mean 45.6 mg and differed significant from the hybrids Anna and Kuds which gave mean weights of 38.8 and 39.5 mg, respectively. Also it is noticed the presence of significant interaction among hybrids and the levels of salinity. The mean fresh weight of callus was 52.0 mg under salinity level 0.05% and differed significantly from most of the interactions, whereas the lowest callus mean weight was 30.0 mg for the hybrid Anna and salt concentration 0.20%.

Table 2 Effect of explants and growth regulators (2,4-D and kinetin) concentrations of three sunflower hybrids on the percentage of callus induction.

		Kinetin concentration mg/L	2,4-D concentration, mg/L					Mean (% of callus induction)
			0.0	0.5	1.0	1.5	2.0	
Anno	Cotyledons	0.0	0	0	20	85	50	46.67
		0.5	0	0	0	50	0	
		1.0	20	50	50	20	50	
	Hypocotyls	0.0	0	50	85	85	85	
		0.5	85	20	85	85	0	
		1.0	85	85	85	85	85	
Alhaja	Cotyledons	0.0	0	50	50	20	50	45.33
		0.5	0	85	20	20	20	
		1.0	20	85	50	20	20	
	Hypocotyls	0.0	0	85	50	85	85	
		0.5	20	50	85	50	50	
		1.0	85	50	85	50	20	
Kuds	Cotyledons	0.0	0	0	20	0	0	5.67
		0.5	0	0	0	0	20	
		1.0	0	0	0	0	0	
	Hypocotyls	0.0	0	0	0	0	0	
		0.5	0	50	20	0	20	
		1.0	0	20	0	0	0	
Mean of 2,4-D			17.50	37.77	39.16	36.50	30.83	
Mean of explants			Cotyledons = 20.98, Hypocotyls = 43.60					
Mean of kinetin			0.0 = 32.50, 0.5 = 27.83, 1.0 = 37.33					
L.S.D 0.05			Hybrids = 9.45, 2,4-D concentration = 16.07 Explants = 10.16, Kinetin concentration = 9.45 Interaction = 34.98					

Table 3 Effect of salt concentration and hybrids on callus fresh weight after 6 weeks of incubation (mg).

NaCl %	Hybrids			Mean
	Anna	Alhaja	Kuds	
0.0	44.00	46.33	38.00	42.78
0.05	35.33	52.00	40.66	42.66
0.10	35.86	47.00	38.33	40.33
0.15	48.66	40.33	43.00	44.00
0.2	30.00	42.33	37.33	36.55
Mean	38.77	45.59	39.46	
L.S.D. 0.05	NaCl % = 4.13, Hybrids = 5.33, Interaction = 9.23; NaCl % × Hybrids = 9.23			

Callus dry weight of hybrids significantly decreased with the increased salinity level of the media and approached 3.0 mg under 0.20% salt concentration and differed from all treatments with the exception 0.10% salt concentration which gave mean weight 3.4 mg (Table 4). The Alhaja hybrids surpass in this character and the dry weigh was 3.86 mg as compared with the lowest mean weigh 2.9 mg for Anna hybrid. There were significant interaction among hybrids and salinity levels in callus dry weight where the Alhaja hybrid surpass other hybrids and the callus dry weight for its control was 5.80 mg. The lowest callus dry weight was 2.1 mg for Anne under 0.20% salt concentration.

The decrease in callus means fresh and dry weight for sunflower hybrids under 0.20% salt concentration is attributed to the variation in cell water relationship. This necessitates regulate cells osmotic stress for adjustment to the new salinity conditions. Al-Jibouri et al. [13] indicated that salinity condition would lower availability of water and nutrients which have negative

effect on growth and division callus cells of four cultivar of bread wheat. In their study on the effect of salinity stress on the growth of four wheat genotype, Alhabaidy et al. [14] found similar results in callus growth of two genotypes of Soya beans with the increased salinity of media.

Results indicated that salinity has an effect on proline content of callus (Table 5). This content increased with the increased salinity level. It was 12.7 mg/g under 0.15% salinity level and significantly differed from the remaining treatments, whereas the lowest proline concentration of 1.2 mg/g was observed for the control. Also, the callus of Kuds significantly differed in its content of proline from other two hybrids and gave the highest concentration 10.5 mg/g. The lowest concentration of proline (4.3 mg/g) was observed in callus of Alhaja hybrid. Significant interactions were observed among salinity levels and hybrids in the concentration of the amino acid proline in callus tissue. The hybrid Kuds surpassed other hybrids under salinity level 0.15% for all interactions and approached 23.6 mg/g of callus tissue. The lowest praline concentration 0.11 mg/g was observed for the control of Alhaja hybrid in all interactions.

The increase in proline of callus tissue subjected to salinity stress is attributed to the adjustment inside cells to the imbalance between gap space and cytoplasm on one side and environment on the other side [15]. It may act as protective factor for enzymes in cell cytoplasm [16]. Therefore, the increase of proline concentration in cell tissue may be considered as indicator for plant salt. Tolerance Regeneration of callus sunflower hybrid in proline can be observed from genetic variation between hybrids. This finding was confirmed by Barakat and Abdul-latif [17] and Al-jibouri et al. [7] for wheat genotypes subjected to salinity stress.

For callus content of carbohydrate, results indicated the increase in carbohydrate of callus tissue with the increased salinity level of media (Table 6). The highest level of carbohydrate 61.8 mg/g was observed at the salinity level 0.20% and differed significantly from most of salinity levels; the control gave 39.2 mg/g of carbohydrate. The hybrids differed in carbohydrate content where Kuds gave 55.8 mg/g and differed significantly from Alhaja with 44.8 mg/g carbohydrate in callus. There were significant interactions among hybrids and NaCl levels in callus carbohydrate concentration. The carbohydrate for the Anna was 65.1 mg/g at the 0.15% salinity level and differed significantly from most of interactions. The lowest concentration was 35.5 mg/g in callus of Anna control.

Table 4 Effect of NaCl concentration and hybrids on callus dry weight after 6 weeks (mg).

NaCl %	Hybrids			Mean
	Anna	Alhaja	Kuds	
0.0	3.7	5.80	2.73	4.07
0.05	2.83	3.43	2.53	2.93
0.10	2.50	3.60	4.00	3.36
0.15	3.63	3.06	4.63	3.77
0.2	2.06	3.43	3.40	2.96
Mean	2.94	3.86	3.46	
L.S.D. 0.05	NaCl % = 0.49, Hybrids = 0.64, Interaction = 1.10; NaCl % × Hybrids = 1.10			

Table 5 Effect of NaCl concentration and hybrids on proline concentration (mg/g) in the callus tissue of sunflower hybrids.

NaCl %	Hybrids			Mean
	Anna	Alhaja	Kuds	
0.0	3.09	0.11	0.36	1.18
0.05	3.74	3.04	17.26	8.01
0.10	7.67	3.92	4.04	5.21
0.15	10.04	4.52	23.61	12.72
0.2	13.09	1012	7.31	10.17
Mean	7.52	4.34	10.51	
L.S.D. 0.05	NaCl % = 2.01, Hybrids = 1.08, Interaction = 3.18 NaCl % × Hybrids = 31.88			

Table 6 Effect of NaCl concentration and hybrids on carbohydrate concentration (mg/g) in the callus tissue of sunflower hybrids.

NaCl %	Hybrids			Mean
	Anna	Alhaja	Kuds	
0.0	35.49	38.60	43.64	39.25
0.05	38.83	39.17	54.36	44.12
0.10	63.38	41.48	58.35	54.40
0.15	65.06	45.09	61.33	57.16
0.2	63.92	59.92	61.53	61.79
Mean	53.34	44.85	55.84	
L.S.D. 0.05	NaCl % = 7.42 , Hybrids = 5.42,Interaction = 9.45 NaCl % × Hybrids = 9.46			

Results obtained were different from many researches which indicated that the carbohydrate of callus tissue decreased with the increasing of salinity stress. For instance, Al-jibouri et al. [5] found this decrease of carbohydrate for some wheat hybrids and Reddy and Vaidyanath [18] for rice hybrids. The reason for this increase was the low concentration of NaCl added to the media which decreased the energy required for water and nutrients.

4. Conclusions

Using of tissue culture is a successful technique for evaluation of genotypes and hybrids introduced to the country for salt tolerance, recommendations can be given on the salt-tolerant hybrids for cultivation in salt-affected land of middle and southern of Iraq.

References

[1] E. Mass, G. Hoffman, Crop salt tolerance-current assessment, ASCE, J. Irrig. and Drainage Div. 103 (1977) 115-134.

[2] P. Buringh, Soil and Soil Conditions in Iraq, in: H. Veenman, N.Z. Zonen (Eds.), Waseningen, Netherlands, 1960.

[3] S.A. Yousif, I.S. Al-Saadawy, A.Y.N. Alla, The effect of salt and radiation on rice growth amber Baghdad and amber furat callus and plant regeneration, Iraqi J. Agric. 12 (2007) 13-21.

[4] S. Basu, G. Gangopadhyay, B. Mukherjee, S. Gupta, Plant regeneration of salt adapted callus of indica rice (Var. Basmati 370) in saline conditions, Plant cell Tiss. Org. Cult. 50 (1997) 153-159.

[5] A.A.M. Al-Jibouri, A.A. Sulaiman, R.A. Dallul, Tissue culture technique and gamma irradiation used in evaluation of five genotypes of bread wheat to salinity tolerance, Iraq J. Sci. Tech. 2 (2005) 24-35.

Q. Zheng, Y. Zhu, W. Chen, X. Tang, Selection of salt tolerant variant of wheat *in vitro*, Tsukuba Japan 6 (1986) 619-622.

[6] A.A.M. Al-Jibouri, A. Al-Salihy, K.M. Zamil, Effect of gamma radiation and salinity on some cellular content of callus of six bread wheat genotypes (*Triticum aestivium* L.), Sci. J. Iraq-Atomic Commission 3 (2001) 137-148.

[7] T. Murashige, F. Skoog, A revised for rapid growth and bioassays with tobacco tissue cultures, Physiol. Plant (1962) 473-497.

[8] R.G.D. Steel, J.H. Torrie, Principle and Procedure of Statistics, 2nd ed., McGraw-Hill, New York, 1980.

[9] G.I. Franklin, R.A. Dixon, Initiation and maintenance of callus and cell suspension cultures, in: R.A. Dixon, R.A. Gonzales (Eds.), Plant Cell Culture Practical Approach, 2nd ed., Oxford Univ. Press, 1996, pp. 1-83.

[10] A.M.S. Mohammad, I.Y. Roof, Initiation and growth of sunflower (*Heliathus annuus* L.) callus, Raf. J. Sci. 4 (1981) 54-67.

[11] A.S. Mohamand, M.W. Nabors, Comparison of two methods callus culture and plant regeneration in wheat (*Triticum aestivium* L.), Plant Cell Tiss. Org. Cult. 26 (1991) 185-187.

[12] A.A.M. Al-Jibouri, A.A. Al-Taie, R.A.A. Al-Roomi, Effect of salinity stress on callus growth and plants, regeneration of four bread wheat cultivars (*Triticum aestivium* L.), Iraqi J. Agric. 8 (2003) 146-156.

[13] H.K. Alhabaidy, S.H. Mahmod, K.M. Irahim, A.A.M. Aljibouri, Effect of salinity stress on callus growth of two soybean genotypes (*Glycine max* L.) *in vitro*, Almustanseria J. Sci. 19 (2008) 47-62.

[14] A. Delauney, D. Verma, Proline biosynthesis and osmo-regulation in plants, Plant J. 4 (1993) 215-223.

[15] A. Solomen, S. Beer, Y. Waisel, G. Jones, G. Paleg, Effects on NaCl on the carboxylating activity of Rubisco from *Tamarix Jordanis* in the presence and absence of proline-related compatible solutes, Physiol. Plant 90 (1994) 198-204.

[16] M.N. Barakat, T.H. Abdel-latif, *In vitro* selection of wheat callus tolerant to high levels of salt and plant regeneration, Euphytica 91 (1996) 127-140.

[17] J.P. Reddy, K. Vaidyanath, In vitro characterization of salt stress effects on the selection of salt tolerance in rice, Theor. Appl. Gnet. 71 (1986) 757-760.

Journal of Life Sciences 5 (2011) 1042-1045

Comparison of Wheat Planting Methods and Residue Incorporation Under Saline-Sodic Soil

Muhammad Arshadullah, Massomma Hassan, Arshad Ali and Syed Ishtiaq Hyder

Land Resources Research Institute, National Agricultural Research Center, Islamabad 45500, Pakistan

Received: June 22, 2011 / Accepted: July 21, 2011 / Published: December 30, 2011.

Abstract: The present research was conducted to monitor the wheat productivity along with residue incorporation under saline-sodic soils by examining different planting methods at Zaidi Farm, Kakar Gill, Sheikhupura District, Punjab Province in 2007-2008. Randomized Complete Block Design (RCBD) with three replications was used having treatments: control (broadcast), zero till wheat plantation, wheat plantation using happy seeder and wheat plantation on raised beds. It was observed that tillering was pretty higher (141 and 139 m^{-2}) under raised bed as well as happy seeder plantation as compared to zero tilled wheat and broadcast technique. A significant relation was detected among maximum straw and grain yield (4,898 and 1,752 $kg \cdot ha^{-1}$) in raised bed followed by happy seeder planting method. The lowest grain yield was recorded in the broadcast method. Maximum net revenue earned by raised bed planting method (39,908 PKR) followed by happy seeder methodology (37,533 PKR). The overall study suggests that raised bed and happy seeder wheat plantation are the superior planting methods.

Key words: Wheat, planting methods, crop residue, saline-sodic.

1. Introduction

Rice-wheat is among the major cropping systems of Pakistan that is extensively cultivated on about 12 million hectares of land [1]. Wheat is a Rabi crop, planted over 9.05 million hectares every year as compared to 2.96 million hectares of rice plantation. However, there is a substantial gap between actual and potential wheat yields [2, 3]. The major responsible factors are delayed wheat sowing and high costs of seedbed preparation following rice. Thus, there is a need for adoption of new resource conservation techniques to enhance productivity along with reduction in the production cost [4-6]. Rice is grown on 2.96 mha land with annual straw production of about 4 million tons [1]. A large amount of loose cut straw is left behind in the field after combine harvest of rice. Although crop residues retain 25% nitrogen and phosphorus, 50% sulphur and 75% potassium uptake by cereal crops [7], but rice straw is not preferred as fodder due to its low digestibility, low protein, and high lignin and silica contents.

This leftover rice residue hinders farm operations by blocking/choking of tillage machinery and thus delays seed bed preparation for wheat on 40% of area. Consequently, this delay after optimal sowing time results in 1-1.5 percent yield reduction per day. Farmers prefer to burn it to save time and energy for land preparation for wheat [8]. Burning loses the soil organic matter, plant nutrient, particularly, N and S and a major cause of environmental pollution in the grown area. Straw recycling in the soil can improve soil organic matter with N-immobilization of the soil in the initial years but reduce the negative effect with continuous incorporation [9].

Different wheat planting methods are being practiced to save resources like water, labor, time and fertilizers. In this study, different planting methods like broadcasting, zero tilled wheat, use of happy seeder for wheat plantation and raised bed Methods were compared along

Corresponding author: Muhammad Arshadullah, Ph.D., senior scientific officer, research field: agronomy. E-mail: arshad_pak786@yahoo.com.

with residue to explore how this precious resource can be utilized and managed for improving soil physico-chemical and biological health for enhancing and sustaining productivity. The suitable planting method, especially bed planting has been shown to improve water distribution and efficiency, fertilizer use efficiency, reduced weed infestation and lodging and it also reduces seed rate without sacrificing yield [10]. Raised bed plantation is extensively used in obtaining high yield of wheat growing areas in Mexico [11]. Therefore an experiment was designed to assess the impact of planting methods and residue incorporation on the productivity of wheat under saline sodic soil.

2. Materials and Methods

The impact of different planting methods with paddy straw management on growth, yield and salt dynamics of wheat (Var. Bakkar 2000) under salt affected soil (Table 1) was studied during Rabi season 2007-2008 at Zaidi farm, Kakar Gill, Sheikhupura. The treatments were: Control (Broadcast), Zero-till plantation, Happy-Seeder plantation and Raised bed plantation. Randomized complete block design (RCBD) with three replications was followed. The basal recommended doses of N (two equal split doses at sowing and tillering stage), P, K (full dose at sowing time) at the rate of 100, 80, 50 kg·ha^{-1} was applied with 5 tons·ha^{-1} chopped rice straw addition. Crop was harvested at maturity, the straw and grain yield were determined on the dry weight basis. Ground plant samples were digested in perchloric-nitric acid in 2:1 N mixture [12] to estimate Na^+, K^+ and Mg^{2+} concentration by atomic absorption spectrophotometer. The data thus obtained were subjected to statistical analysis using MSTATC statistical package. Treatment means were separated using Duncan's Multiple Range (DMR) test.

Table 1 Physico-chemical analysis of the soils.

Parameters	Soil	Water
pH	8.22	8.31
EC_e (dS·m^{-1})	4.92	1.62
SAR (mmol$_{(c)}$·L^{-1})$^{1/2}$	14.15	-
OM (%)	1.3	-
$CaCO_3$ (%)	16.80	-
Sand (%)	39	-
Silt (%)	30	-
Clay (%)	31	-
Soil	Clay loam	-
RSC (mmol$_{(c)}$·L^{-1})$^{1/2}$	-	14.71
HCO^{-3} (Meq·L^{-1})	-	16.32

EC: electrical conductivity; SAR: sodium adsorption ratio; OM: organic matter; RSC: residual sodium carbonate.

3. Results and Discussion

3.1 Growth and Yield

Residual incorporation positively influenced wheat growth and yield planted under different sowing methods. Tillering was much higher (141 and 139 m^{-2}) for raised bed and happy seeder plantations respectively (Table 2). However, maximum plant heights (105.67 cm and 103.33 cm) were observed for the control (broadcast) followed by the zero-tillage. Among various sowing methods, the maximum straw and grain yields (4,898 and 1,752 kg·ha^{-1} respectively) were harvested from raised bed plantations (Table 2). The lowest grain yield was attained in case of control. Grain yield also showed highest in bed planting due to higher yield attributes. Similar trend was followed in case of straw yield. Meisner et al. [13] reported that the growth and grain yield of wheat were significantly influenced by planting methods. Sayre and Romos [14] had the similar observation when they worked with different planting methods. These results are in agreement with the findings of Ref. [10]. The maximum grain yield was obtained from bed planting [15].

3.2 Ionic Concentration

A non-significant difference of Na^+, Ca^{2+}, K^+ and Mg^{2+} concentrations in straw indicates planting methods do not make significant change in salt accumulation. However, high yield producing planting methods (Raised bed and happy seeder) showed significant increase in Na uptake by wheat straw, followed by other methods of plantation i.e. Zero tillage and Broad casting (Table 3).

Table 2 Effect of different planting methods on wheat growth and yield planted at Zaidi Farm, Kakargill, Sheikhupura.

Treatments	No. of tillers (m^{-2})	Plant height (cm)	Straw yield ($kg \cdot ha^{-1}$)	Grain yield ($kg \cdot ha^{-1}$)
Control (broadcasting)	87 b	105.67 a	3,344 b	1,239 c
Zero tillage	108 b	103.33 a	3,407 b	1,461 b
Happy seeder	139 a	99.67 ab	4,153 ab	1,580 b
Raised beds	141 a	92.00 b	4,898 a	1,752 a
LSD	4.95	3.44	678.7	101.1

LSD: least significant difference; The same letters show there is statistically no significant ($P < 5$) difference.

Table 3 Effect of different planting methods on Na, Ca, K and Mg concentration and uptake by straw at Zaidi Farm, Kakargill, Sheikhupura.

Treatments	Na	Ca	K	Mg	Na	Ca	Mg
	Concentration ($mg \cdot kg^{-1}$)				Uptake ($kg \cdot ha^{-1}$)		
T1 = Control (broadcasting)	814.33	1,027.66	1,710.00	315.00	2.28 b	3.59	0.88
T2 = Zero tillage	786.66	1,330.00	2,059.33	276.66	2.22 b	3.98	0.80
T3 = Happy seeder	787.33	1,296.00	1,926.33	298.00	3.05 ab	4.55	1.16
T4 = Raised beds	738.33	1,489.00	1,828.00	306.66	3.39 a	3.60	0.98
LSD	NS	NS	NS	NS	0.892	NS	NS

Table 4 Economic analysis, partial budget analysis of different planting methods, Zaidi Farm, Kakar Gill, Sheikhupura.

	T1 Control (Broadcasting)	T2 Zero tillage	T3 Happy seeder	T4 Raised beds
Plantation cost, (Rs.)	2,000	1,000	2,500	2,000
Application cost, (Rs.)	0	0	0	0
Total cost that vary	2,000	1,000	2,500	2,000
Yield grain, ($kg \cdot ha^{-1}$)	1,825	1,991	2,172	2,218
Yield adjusted, (10% Low)	1,642	1,791	1,954	1,996
Output price, (Rs./kg)	16	16	16	16
Yield straw	2,796	2,875	3,894	4,431
Yield adjusted	2,516	2,587	3,504	3,987
Output price, (Rs./Kg)	2.5	2.5	2.5	2.5
Gross field benefits	32,571	35,139	40,038	41,908
Net benefits	30,571	34,139	37,533	39,908

3.3 Economic Analysis

Cost benefit analysis is core and crux of an intervention. This appeals farmers to adopt the new technology and innovation to better off their economic conditions. Therefore, economic analysis has been conducted to evaluate the cost benefit summary. Economic viability of any intervention is must for adoption in field and is the basic theme of the research. All the agronomic practices and plant protection measures were the same. Only sowing methods were different. Cost of plantation varied with the planting methods. Raised bed and broadcasting cost Rs. 2,000/ha, happy seeder Rs. 2,500/ha and zero tilled wheat Rs. 1,000/ha (Table 4).

Net benefits attained by broadcasting, zero tilled, happy seeder and raised bed plantation were Rs. 30,571, 34,139, 37,533 and 39,908, respectively. Raised bed and happy seeder wheat plantation proved to be better planting methods in terms of benefits.

4. Conclusion

Raised bed planting technique proved to be the

superior in a way which not only saves resources but also enhances growth and yield of wheat but more investigation is needed to carry out depending upon the ecologies.

References

[1] Government of Pakistan, Agricultural Statistics of Pakistan, Ministry of Food, Agriculture and Livestock Economic, Trade and Investment Wing, Islamabad, 2009, p. 289.

[2] D. Byerlee, A.D. Sheikh, M. Aslam, P.R. Hobbs, Wheat in the rice-based farming system of the Punjab: Implications for research and extension, in: NARC/CIMMYT Reports Series No. 4, Islamabad, 1984.

[3] A.D. Sheikh, M. Zubair, M. Asif, Barriers in enhancing the productivity of the rice-wheat farming system of the Punjab, in: AERU, NARC, Technical Report, 2000, p. 75.

[4] P.R. Hobbs, R.K. Gupta, Rice-wheat cropping systems in the indo-gangetic plains: Issues of water productivity in relation to new resource-conserving technologies, in: J.W. Kijne, R. Barker, D. Molden (Eds.), Water Productivity in Agriculture: Limits and Opportunities for Improvement, CABI Publication, Wallingford, UK, 2003, pp. 239-253.

[5] J.K. Ladha, J.E. Hill, J.M. Duxbury, R.K. Gupta, R.J. Buresh, Improving the productivity and sustainability of rice-wheat systems: Issues and impacts, in: American Society of Agronomy, Crop Science Society of America, Soil Science Society of America (Eds.), ASA Special Publication Number 65, Madison, Wisconsin, USA, 2003.

[6] A.S. Qureshi, T. Shah, M. Akhtar, The groundwater economy of Pakistan, in: International Water Management Institute, IWMI Working Paper 64, Pakistan Country Series No. 19, Lahore, Pakistan, 2003.

[7] E.W. Byous, E. Williams, G.E. Jonesa, W.R. Horwath, C. Kessel, Nutrient requirement of rice with alternative straw management, Better Crops 36 (2004) 6-11.

[8] R.K. Gupta, R.K. Naresh, P.R. Hobbs, Z. Jiaguo, J.K. Ladha, Sustainability of post green revolution agriculture: The rice-wheat cropping systems of the Indo-Gangetic Planes and China, Improving the productivity and sustainability of rice-wheat systems: Issues and impacts, in: ASA Special Publication 65, Wisconsin, USA, 2003, pp. 1-26.

[9] T.S. Verma, R.M. Bhaga, Impact of rice straw management practices on yield, N uptake and soil properties in a wheat-rice rotation in Northern India, Fertilizer Research 33 (1992) 97-106.

[10] P.R. Hobbs, Y. Sing, G.S. Giri, J.G. Lauren, J.M. Dusbury, Direct seeding and reduced tillage options in the rice wheat systems of the Indo-Gangetic plain of South Asia, in: IR Workshop, Bankok, Thailand, Jan. 25-28, 2000.

[11] O.A.L. Limon, K.D. Sayre, C.A. Francis, Wheat nitrogen use efficiency in a bed planting system in Northwest Mexico, Agron. J. 92 (2000) 303-308.

[12] J.D. Rhoades, Cation exchanges capacity, in: A.L. Page (Ed.), Methods of Soil Analysis, Part 2. Chemical and Microbiological Properties, Amer. Soc. Agron., Madison, Wisconsin, USA, 1982, pp. 149-158.

[13] C.A. Meisner, E. Acervedo, D. Flores, K. Sayre, L. Ortizmonasterio, D. Byerlee, Wheat production and grower practices in the Yaqui Valley, in: CIMMYT, Wheat Special Report, No. 6, Sonora, Mexico, 1992.

[14] K.D. Sayre, O.H. Morens Romos, Application of raised bed planting system to wheat, in: Wheat Program Special Res. 31, CIMMYT, Mexico, 1997, pp. 14-22.

[15] I. Hossain, Khair-ul-Islam, A. Sufian, C.A. Meisner, Sayeed-ul-Islam, Effect of planting method and nitrogen levels on the yield and yield attributes of wheat, J. Bio-Sci. 14 (2006) 127-130.

Journal of Life Sciences 5 (2011) 1046-1057

Edible Wild Fruit Highly Consumed during Food Shortage Period in Togo: State of Knowledge and Conservation Status

Abalo Atato[1], Kpérkouma Wala[1], Komlan Batawila[1], Niéyidouba Lamien[2] and Koffi Akpagana[1]

1. Laboratoire de Botanique et Ecologie Végétale, Faculté des Sciences, Université de Lomé, Lomé B.P. 1515, Togo

2. Centre Régional de Recherches Environnementales et Agricoles (CRREA) du Centre, Koudougou B.P. 10, Burkina Faso

Received: March 08, 2011 / Accepted: May 31, 2011 / Published: December 30, 2011.

Abstract: The aim of this work is to inventory Edible Wild Fruit Species (EWFS) highly consumed by local people during food shortage periods in Togo. Ethnobotanical surveys were carried out in four ecological zones (I, II, III & IV) involving a sample of 433 persons from 29 ethnic groups. Semi-structured interview, field observation, group discussions were used to collect data. Food shortage periods were defined using the agricultural calendar of main crops in three ecological zones (I, II, & III). One hundred and one EWFS belonging to 84 genera and 39 families were inventoried. The three main types of use of the EWFS were direct consumption, condiments and medicines. Twenty among the 101 EWFS recorded were highly consumed during food shortage periods with respectively 15 EWFS in ecological I, 14 in zone II and 12 in ecological zone III. All edible fruits consumed during food shortage periods were fresh fruits with abundant pulp. Six fruit species were sold to bring income to local households. These species were those which benefit from conservation measures through their husbandry in agroforestry systems.

Key words: Ethnic group, ethnobotany, food crisis, household, uses, Togo.

1. Introduction

Food shortage period generally lasts from crops planting to harvest [1]. It coincides with staple foods, notably cereals stocks depletion when new cropping activities are starting. It also induces changes to food consumption patterns. Nowadays, the period of food shortage is equivalent to an increase of main crops prices.

From the past time to now, local populations have developed various strategies of survival to cope with food shortage. Many studies in Africa [1-8] reveal the role of non timber forest products in food security and income generation. These studies have also showed that the gathering and consumption of wild food are regular with higher intake during staple food shortage.

Edible fruits are the most important among wild food species consumed in normal and food shortage conditions [1, 8]. In Togo, ethnobotanical survey on wild food and particularly wild fruits species are at the beginning. Diversity of EWFS and diversity of their use according to different ethnic communities are now documented.

Togo's local people know and use many wild fruit species both in normal and food shortage conditions for a long period. The objective of this study is to document indigenous knowledge on EWFS and particularly those highly consumed during food shortage period and assess their current conservation status.

2. Materials and Methods

2.1 Study Area

The study was conducted in Togo (6° and 11° N and

Corresponding author: Abalo Atato, Ph.D., research fields: ethnobotany, ecology and participatory domestication of indigenous fruit trees. E-mail: atatoa@yahoo.fr, atato@live.fr.

0°15' and 2° E), West Africa. Climate is sub-equatorial in the southern and tropical in the northern. Average annual precipitation varies between 800 and 1,500 mm with an average annual temperature of approximately 27°C. Togo is mainly covered by savannas with a few clumps and patches of semi-deciduous forest occurring in mountain of southwest [9]. Togo is divided into five eco-floristic zones [10] (Fig. 1).

2.2 Ethnobotanic Surveys

Surveys were conducted in seventy-nine villages selected from four ecological zones where twenty-nine ethnic groups are living. Focus groups discussions with 3 to 7 persons (Table 1 and Fig. 1) were undertaken regardless sex and age. Semi-structured interviews according to Refs [2, 11-13], were carried out. Some lists of vernaculars names of EWFS were established with different ethnic groups. In addition different uses and optimal period of fruit harvesting were documented.

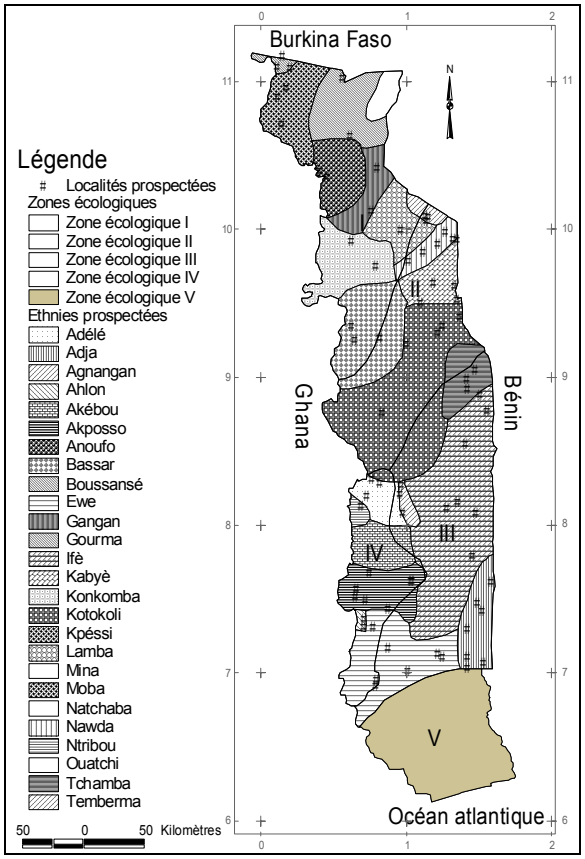

Fig. 1 Ecological zones, ethnic communities and spatial distribution of the prospected villages.

Data analysis included establishment of the list of fruit species by ecological zone, ethnic groups and ecosystems. For classification of wild fruits, extrinsic criteria (knowledge, use) and intrinsic like types of fruit according to Ref. [14] were used. Shortage periods were determined by analyzing the agricultural calendar of main crops and the comparison with optimal period of fruit harvesting allowed identifying fruit species consumed in shortage period.

3. Results

3.1 Taxonomy Diversity

Ethnobotanical survey had permitted to record 101 EWFS distributed in 84 genera and 39 families (Appendix A). Most of the species inventoried were Anacardiaceae, Annonaceae, Rubiaceae, Apoynaceae, Moraceae, Sapindaceae, Sapotaceae, Sterculiaceae, Tiliaceae, Caesalpiniaceae, and Chrysobalanaceae.

The number of species with edible fruits varied from an ecological zone to another. Within the same ecological zone, this number varied from an ethnic group to another and within the same ethnic group from a village to another. The predominant families in savanna zone (ecological zones I, II, and III) were Anacardiaceae, Annonaceae, Rubiaceae, Caesalpiniaceae and Chrysobalanceae. In forest zone (ecological zone IV), Annonaceae Apocynaceae and Moraceae were the most important. Annonaceae family was the only one which is found in the two main ecosystems described in Togo (savanna, semi-deciduous forest). Most of EWFS are microphanerophyts (35%), mesophanerophyts (25%) and lianas (18%). In term of the phytogeographic distribution of the EWFS, taxa from the Guineo-Congolian zone (GC) dominate with 33%. They were followed by taxa from soudano-zambezian zone with 18%.

3.2 Fruit Parts Consumed and Types of Fruit

There is a diversity of parts used by local populations of Togo (Fig. 2). More than 75% of the

Table 1 Number of villages, ethnic groups and people, surveyed in four ecological zones.

Ecological zone	Ethnic groups	Villages	Focus groups	Number of persons surveyed	Total
Zone I	Anoufo	2	2	10	115
	Bissa	1	1	8	
	Gangan	1	1	10	
	Gourmantché	2	2	15	
	Konkomba	2	2	10	
	Lamba	3	3	15	
	Moba	4	4	35	
	Tamberma	2	2	7	
	Yenga	1	1	5	
Zone II	Bassar	3	3	12	87
	Kabyè	5	6	35	
	Nawdm	2	3	13	
	Sola	1	2	7	
	Tem	5	5	20	
Zone III	Adja	5	5	15	128
	Agnagan	4	3	12	
	Agounagbé	1	1	15	
	Ani	1	1	8	
	Bago	1	1	3	
	Ewé	4	4	25	
	Ifè	5	5	30	
	Kpessi	1	1	5	
	Koussountou	1	1	5	
	Tchamana	2	2	10	
Zone IV	Adélé	3	3	10	103
	Akébou	3	2	11	
	Akposso	5	5	35	
	Ewé	5	5	25	
	Igo	2	2	12	
	Ntribou	2	1	10	
Total		29	79	433	433

fruits consumed were collected for their pulp. Fig. 3 showed that berries (42%) and drupaceous fruits (34%) are most important whereas indehiscent fruits, follicles, pods with 20% are less important. Fig and capsular fruit are seldom collected for consumption.

3.3 Periods of Fruit Availability

EWFS bore fruits throughout the whole year (Appendix B). However, the importance of fructification varies from one season to another (Fig. 4). In all the ecological zones, the period from October to March shows a low number of species fruiting. In the first half of this season 15% of species bear fruits (October and December) and 20% from January to March. The best fruiting period in all ecological zones goes from April to September. This period coincides with the rainy season. The optimal period for fruit harvesting is from April to June in all the ecological zones with 59%-81% of species bearing fruits (Fig. 4).

3.4 Food Shortage Period and Local Fruit Use

The analysis of the agricultural calendar of the main crops allowed determining food shortage periods in each ecological zone (Table 2). In the ecological zones I, II and the northern region of the ecological zone III, food shortage period begun from the last ten days of

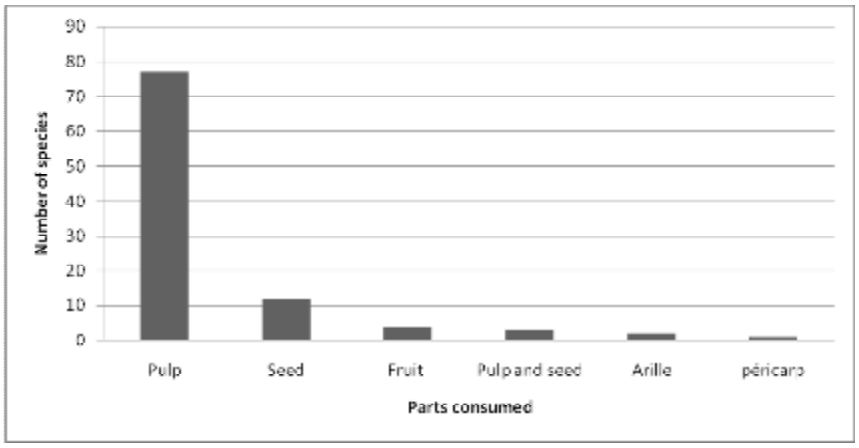

Fig. 2 Proportion of fruit parts consumed.

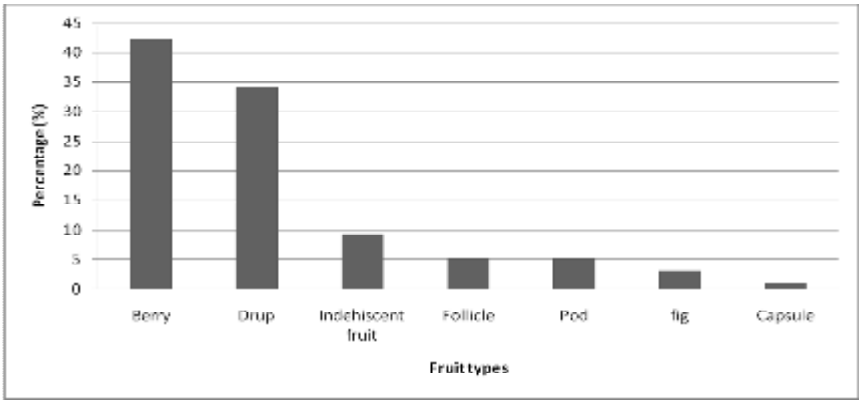

Fig. 3 Proportion of fruit categories.

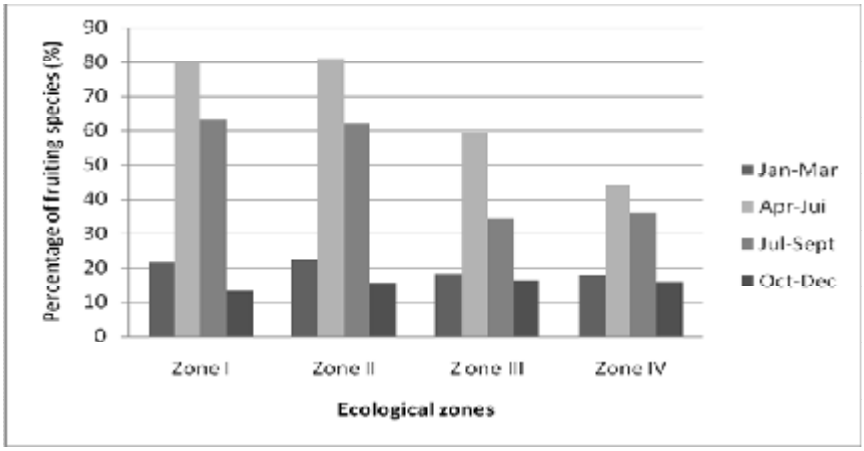

Fig. 4 Optimal period of harvest according to ecological zones.

May to the last ten days of September. This period lasts from crops sowing to harvesting and is about 110 to 130 days of duration (Appendix C). In the ecological zone IV and the southern region of the ecological zone III, the existence of two rainy seasons allows permanent availability of food.

Based on the agricultural calendar of the main crops (Appendix C) and optimal fruit harvesting periods (Appendix B) a total of 20 EWFS belonging to 19 genera and 13 families was recorded as fruit species consumed during food shortage periods (Table 2). These species bore generally fresh fruits whose pulp is

Table 2 Species whose fruits are available during food shortage periods.

Species	Family	Zone I	Zone II	Zone III	Consumed parts	Use
Haematostaphis barteri	Anacardiaceae	+	-	+	pulp	Fresh fruit
Lannea microcarpa	Anacardiaceae	+	-	-	pulp	Fresh fruit
Sclerocarya birrea	Anacardiaceae	+	-	-	pulp	Fresh fruit
Spondias mombin	Anacardiaceae	-	+	+	pulp	Fresh fruit
Annona glauca	Annonaceae	+	+	-	pulp	Fresh fruit
Annona senegalensis	Annonaceae	+	+	+	pulp	Fresh fruit
Hexalobus monopetalus	Annonaceae	-	+	-	pulp	Fresh fruit
Uvaria chamae	Annonaceae	-	+	+	pulp	Fresh fruit
Saba comorensis	Apocynaceae	+	+	+	pulp	Fresh fruit
Parinari curatellifolia	Chrysobalanaceae	-	+	+	pulp	Fresh fruit
Flacourtia flavescens	Flacourtiaceae	-	+	+	pulp	Fresh fruit
Strychnos spinosa	Loganiaceae	+	+	+	pulp	Fresh fruit
Parkia biglobosa	Mimosaceae	+	+	+	pulp	Fresh fruit
Syzygium guineense	Myrtaceae	+	-	-	pulp	Fresh fruit
Ximenia americana	Olacaceae	+	-	-	pulp	Fresh fruit
Gardenia erubescens	Rubiaceae	+	+	-	pulp	Fresh fruit
Sarcocephalus latifolius	Rubiaceae	+	+	+	pulp	Fresh fruit
Vitellaria paradoxa	Sapotaceae	+	+	+	pulp	Fresh fruit
Vitex doniana	Verbenaceae	+	+	+	pulp	Fresh fruit
Balanites aegyptiaca	Zygophylaceae	+	-	-	pulp	Fresh fruit

well appreciated and consumed immediately by people when gathering or as dietary supplements. *Parkia biglobosa* and *Vitellaria paradoxa* are high value species because of their by-products which were sold to bring incomes for rural households during food shortage periods. The seeds of *P. biglobosa* were used to produce a fermented paste used as sauces ingredients. The crush pulp is mixed to the flour of maize or sorghum to make a sort of paste consumed in poor households during these food shortage periods. Oil is extracted from the nuts of *V. paradoxa* to be used in culinary. The fruits of *Gardenia erubescens* is crushed and mixed to flour of millet (*Pennisetum* sp.) by Gourmantché ethnic community to make a local meal. Ripe fruits of *Lannea microcarpa*, *Vitex doniana*, *Saba comorensis*, *Spondias mombin* were sold in local markets.

3.5 Conservation Status of Fruit Species Consumed during Food Shortage Periods

EWFS are facing threats in their natural habitats from various human activities. Most of them were harvested in savanna and fallows areas. During the extension of cropping areas, farmers removed all fruit species with low value. The efforts of conservation concerned only fruit species with high value such as *P. biglobosa*, *V. paradoxa* and *V. doniana* and *S mombin, L. microcarpa*, *S. birrea.* The integration of the species in cropping areas is the unique farmers' practice of conservation identified in this study.

4. Discussion

This survey revealed that the flora of Togo had a significant diversity in terms of EWFS. It also appears that there is a high level of knowledge of EWFS fruit species among rural populations. These edible fruits had a real potential of food and income generation for rural populations.

Most of the recorded fruit species are reported in other countries of Africa like Burkina Faso [1, 15, 16], Cameroon [17, 18], Côte d'Ivoire [19], DR Congo [20],

Ethiopia [2, 4, 8], and Senegal [21].

Many of reported edible fruits are fleshy and sought for their pulp. Studies undertaken in Southern-Shaba (DR Congo) [20] and in Côte d'Ivoire [19] also pointed out the importance of fleshy fruits from edible fruits quoted by Bemba and Malinké people.

The interest for the fruits species varies according to the period of the year. Fruits which are available in period of food abundance (November-March) are often seldom exploited whereas those which ripe in food shortage period (April-September), when reserves of staple food are exhausted, are very coveted. In Togo, food shortage period coincided with the period of abundance of fruits and they were much consumed by the children to complete their daily diet. Their ability to cater for their own energy sources relieves the parents. In Zimbabwe [22] also showed that the wild fruit gathering and consumption decrease during the principal season of the fruits, but reach their maximum when the food from crop plants has suddenly missed. In Ethiopia, children consume the fruits in normal times, but when food is short; adults as an additional consumer category collect and consume fruits from wild trees [8].

From one hundred-one (101) edible fruits species reported from local populations, twenty (20) are fruiting during food shortage period and represent for rural populations a source of food and energy. In Burkina Faso, one hundred fifty-seven (157) species highly consumed during food crisis (food shortage and famine) were recorded [1]. Thirty-five (35) of 157 species are edible fruit species and fourteen from thirty-five fruit species have been quoted by local people in Togo as fruit species consumed in food shortage period. In Ethiopia thirty-eight (38) of eighty (80) identified and listed as wild-food species are edible fruits consumed in food shortage period [8].

All EWFS recorded in this study are fresh fruits and are consumed raw without further processing. But some authors reported that the fruits of some species such as *Syzygium guineense*, and *Ximenia americana* are used to make juice in Ethiopia [4]. The fact, all edible fruits are fleshy is an advantage to be exploited. These fruits can be used to make jams. This processing could add value to them and make their consumption a non backward behavior.

But their current status i.e. wild species is a significant factor of their threat. Despite their role in food security and income generation, most of EWFS are removed during areas clearing for farms. In Ethiopia, the Derashe and Gamo populations rated agricultural expansion as the principal threat to wild edible plant species [4]. People collecting and using wild food have to travel ever further from their villages because more and more bush land is being destroyed and turned into arable land for cultivation [8]. This reduces gradually the contact with the bush and increase the loss of indigenous knowledge related to EWFS and their use among particularly children and young people [2, 20].

5. Conclusion

This study which is a contribution to the valorization of EWFS revealed a high level of knowledge among local populations on one hand and on the other hand, their high potential as sources of food and energy in normal times and especially in food shortage periods. The fruits used in food shortage periods are generally fresh fruits. That explains their significant consumption during this period by children and adults.

The high number of EWFS used in food shortage period (20) is an indication that local communities can utilize wild flora as one coping strategy to bridge periods of food scarcity. In order to optimize benefit from wild flora, it would be valuable to select and domesticate EWFS with high value. At the same time, scientifically investigate on their nutritional composition and toxicology is needed. Moreover, ethnobotanical and ecological studies on edible wild plant species at the national level will probably contribute to a sustainable food supply and conserve the dwindling biological resources of the country.

Acknowledgments

The authors are grateful to IFS (International Foundation for Science), UNESCO (United Nations for Education, Science and Culture) and INIA-BIOVERSITY whose financial support permit the achievement of this work.

References

[1] Milogo-Rasolodimby, L'homme, le climat et les ressources alimentaires végétales en période de crises de subsistance au cours du 20è siècle au Burkina Faso Thèse de Doctorat, Université de Ouagadougou, Burkina Faso, 2001. (in French)

[2] G. Addis, K. Urga, D. Dikasso, Ethnobotanical study of edible wild plants in some selected districts of Ethiopia, Humanity Ecology 33 (1) (2005) 83-118.

[3] F.K. Akinnifesi, F.R. Kwesiga, J. Mhango, A. Mkonda, T. Chilanga, et al., Towards the development of miombo fruit trees as commercial tree crops in southern Africa, Forests, Trees and Livelihoods 16 (2006) 103-121.

[4] K. Balemie, F. Kebebew, Ethnobotanical study of wild edible plants in Derashe and Kucha Districts, South Ethiopia, Journal of Ethnobiology and Ethnomedicine 2 (53) (2006) 1-9.

[5] D. Mithöfer, H. Waibel, F.K. Akinnifesi, The role of food from natural resources in reducing vulnerability to poverty from Zimbabwe, in: the 26th Conference of International Association of Agricultural Economists (IAAE), Queensland, Australia, Aug. 12-18, 2006.

[6] F.K. Akinnifesi, F.R. Kwesiga, J. Mhango, A. Mkonda, T. Chilanga, R. Swai, Domesticating priority miombo indigenous fruits as a promising livelihood option for smallholder farmers in southern Africa, Acta Horticulturae 632 (2004) 15-30.

[7] D. Mithöfer, H. Waibel, Income and labour productivity of collection and use of indigenous fruit tree products in Zimbabwe, Agroforesty Systems 59 (2003) 295-305.

[8] Y. Guinand, D. Lemessa, Wild-food plants in Southern Ethiopia: Reflections on the role of "famine-foods" at a time of drought, UN-Emergencies Unit for Ethiopia, Report, 2000.

[9] K. Adjossou, K. Kokou, Flore forestière de la zone montagneuse sub-humide du Togo (Afrique de l'Ouest), in: X. van der Burgt, J. van der Maesen, J.M. Onana (Eds), Systématique et Conservation des Plantes Africaines, Royal Botanic Gardens, Kew, 2009, pp. 615-624.

[10] K. Kokou, K. Adjossou, A.D. Kokoutse, Considering sacred and riverside forests in criteria and indicators of forest management in low wood producing countries: The case of Togo, Ecological Indicators 8 (2) (2007) 158-169.

[11] P.A. Twamassi, Social Research in Rural Communities, 2nd ed., Ghana Universities Press, Accra, 2001.

[12] K.B. Tom Kumekpor, Research Methods and Techniques of Social Research, SonLife Press and Services, Accra, 2002.

[13] H. Castadena, J.R. Stepp, Ethnoecological importance value (EIV) methodology: Assessing the cultural importance of ecosystems as sources of useful plants for the Guaymi people of Costa Rica, Ethnobotany Research & Application 5 (2007) 249-257.

[14] B.K. Kunz, K.E. Linsenmair, Fruit Traits in Baboon Diet: A comparison with plant species characteristics in west Africa, Biotropica 42 (3) (2010) 363-371.

[15] P. Ouôba, J. Boussim, S. Guinko, Le potentiel fruitier de la forêt classée de Niangoloko au Burkina Faso, Fruits 61 (1) (2006) 1-11.

[16] M. Belem-Ouédraogo, J. Yaméogo, S. Guinko, Les Ligneux alimentaires des galeries forestières de la réserve de biosphère de la mare aux hippopotames, Burkina Faso, Sub-Saharan African Fruits, Fruit, Vegetable and Cereal Science and Biotechnology 4 (Special Issue 1) (2009) 10-17.

[17] J. Vivien, J.J. Faure, Fruitiers sauvages d'Afrique-Espèces du Cameroun, Editions Nguila-Kerou, France, 1996.

[18] O. Eyog Matig, O. Ndoye, J. Kengue, A. Awono, Les Fruitiers Forestiers Comestibles du Cameroun, IPGRI, 2006.

[19] G.A. Ambe, Les fruits sauvages comestibles des savanes guinéennes de Côte-d'Ivoire: État de la connaissance par une population locale, les Malinké, Biotechnology Agronomy Society and Environment 5 (1) (2001) 43-58. (in French)

[20] F. Malaisse, Se nourrir en forêt claire africaine, Approche écologique et nutritionnelle, Presses agronomiques de Gembloux, Wageningen, Pays Bas: CTA, Gembloux, Belgique, 1997. (in French)

[21] M. Guèye, M. Diouf, C.O. Ba, O. Dieme, C. Lo, L.E. Akpo, Les Espèces négligées au Sahel et en zone Soudano Sahélienne: cas des Légumes-Feuilles Traditionnels et des fruitiers sauvages au Sénégal, Article présenté à la Xème Animation Scientifique Régionale sur les Biotechnologies et la valorisation du patrimoine végétal sous-exploité en zone sahélienne et soudano-sahélienne, Dakar, Sénégal, Nov. 10-13, 2009. (in French)

[22] A. Campbell, The use of wild food droughts in Botswana, Journal of Arid Environment 1 (1986) 81-91.

Appendix A: Edible wild fruit bearing-species recorded.

Family	Species	Life form	Phytogeographic distribution	Consumed parts
Anacardiaceae	*Haematostaphis barteri* Hook. f.	mp	S	pulp
Anacardiaceae	*Lannea acida* A. Rich.	mP	PRA	pulp
Anacardiaceae	*Lannea kerstingii* Engl. & K. Krausse	mP	PRA	pulp
Anacardiaceae	*Lannea microcarpa* Engl. & K. Krausse	mP	SZ	pulp
Anacardiaceae	*Sclerocarya birrea* (A. Rich.) Hochst.	mp	AT	pulp
Anacardiaceae	*Spondias mombin* L.	mp	AT	pulp
Annonaceae	*Annona glauca* Schum. & Thonn.	np	S	pulp
Annonaceae	*Annona senegalensis* Pers.	mp	PRA	pulp
Annonaceae	*Hexalobus monopetalus* (A. Rich.) Engl. & Diels var. monopetalus	mp	SZ	pulp
Annonaceae	*Monodora myristica* (Gaertn.) Dunal	mP	GC	pulp
Annonaceae	*Uvaria chamae* P. Beauv.	Lmp	PRA	pulp
Annonaceae	*Xylopia aethiopica* (Dunal) A. Rich.	mP	GC	fruit
Apocynaceae	*Ancylobotrys amoena* Hua	LmP	GC	pulp
Apocynaceae	*Carissa edulis* Vahl	mp	Aaas	pulp
Apocynaceae	*Landolphia owariensis* P. Beauv.	LmP	SZ	pulp
Apocynaceae	*Picralima nitida* (Stapf) Th. & H. Dur.	mP	GC	seed
Apocynaceae	*Saba comorensis* (Bojer) Pichon	Lmp	PRA	pulp
Bombacaceae	*Adansonia digitata* L.	MP	SZ	pulp and seed
Caesalpiniaceae	*Detarium microcarpum* Guill. & Perr.	mp	SZ	pulp
Caesalpiniaceae	*Detarium senegalense* J. F. Gmel.	mP	GC	pulp
Caesalpiniaceae	*Dialium guineense* Willd.	mP	GC	pulp
Caesalpiniaceae	*Tamarindus indica* L.	mp	Pan	pulp
Chrysobalanaceae	*Maranthes polyandra* (Benth.) Prance	mp	SG	pulp
Chrysobalanaceae	*Parinari congensis* F. Didr.	mP	GC	pulp
Chrysobalanaceae	*Parinari curatellifolia* Planch. ex Benth.	mp	SZ	pulp
Chrysobalanaceae	*Parinari glabra* Oliv.	MP	GC	pulp
Chrysobalanaceae	*Parinari exelsa* sabine	MP	GC	pulp
Connaraceae	*Santaloides afzelii* (R. Br. ex Planch.) Schellenb.	Lmp	SG	pulp
Cucurbitaceae	*Momordica charantia* Linn.	Lnp	Pan	pulp
Ebenaceae	*Diospyros elliotii* (Hiern.) F. White	mp	GC	pulp
Ebenaceae	*Diospyros mespiliformis* Hochtst. Ex A. DC.	mP	SZ	pulp
Euphorbiaceae	*Bridelia ferruginea* Benth.	mp	PRA	pulp
Euphorbiaceae	*Flueggea virosa* (Roxb. ex Willd.) Voigt.	Ch	Pal	pulp
Euphorbiaceae	*Phyllanthus muellerianus* (O. Ktze.) Exell.	Lmp	AT	pulp
Fabaceae	*Pterocarpus santalinoides* L'Hérit. Ex DC.	mp	PRA	seed
Flacourtiaceae	*Flacourtia flavescens* Willd.	mp	PRA	pulp
Flacourtiaceae	*Oncoba spinosa* Forsk.	mp	SZ	pulp
Guttiferae	*Garcinia afzelii* Engl.	mP	GC	pulp
Guttiferae	*Garcinia kola* Heckel	mP	GC	seed
Guttiferae	*Pentadesma butyracea* Sabine	mP	GC	seed
Icacinaceae	*Icacina senegalensis* A. Juss.	Lmp	SG	pulp
Irvingiaceae	*Irvingia gabonensis* (Aubry-Lecomte ex O' Rorke) Baill.	mP	GC	pulp

(to be continued)

Lecythidaceae	*Napoleonaea vogelii* Hook. & Planch.	mp	GC	pulp
Loganiaceae	*Strychnos spinosa* Lam.	mp	AM	pulp
Menispermaceae	*Discoreophyllum cumminsii* (Stapf) Diels	Lnp	GC	pulp
Mimosaceae	*Acacia nilotica* (L.) Willd. ex Del.	mp	S	fruit
Mimosaceae	*Parkia biglobosa* (Jacq.) Benth.	mP	Pal	pulp and seed
Mimosaceae	*Parkia filicoidea* Welw. ex Oliv.	MP	GC	pulp
Mimosaceae	*Prosopis africana* (Guill. & Perr.) Taub.	mP	SZ	seed
Moraceae	*Ficus gnaphalocarpa* (Miq) A. Rich.	mP	SZ	fruit
Moraceae	*Ficus vallis-choudae* Delile	mP	AT	fruit
Moraceae	*Myrianthus arboreus* P. Beauv.	mp	GC	pulp
Moraceae	*Treculia africana* Decne	MP	GC	seed
Moraceae	*Trilepisium madagascariense* DC.	mP	GC	seed
Myrtaceae	*Eugenia togoensis* Engl.	mp	GC	seed
Myrtaceae	*Sizygium guineense* (Willd.) DC.	mP	AT	pulp
Olacaceae	*Ximenia americana* L.	np	Pan	pulp
Opiliaceae	*Opilia amentacea* (Guill. & Perr.) Endl. Ex walp.	Lmp	SZ	pulp
Palmae	*Borassus aethiopum* Mart.	MP	SZ	pulp
Palmae	*Hyphaene thebaica* (L.) Mart.	mp	SZ	pulp
Palmae	*Phoenix reclinata* Jacq.	mP	GC	pulp
Passifloraceae	*Passiflora foetida* L.	Lnp		pulp
Passifloraceae	*Piper guineense* Shum. & Thonn.	Lnp	GC	fruit
Rhamnaceae	*Ziziphus abyssinica*.	mp		pulp
Rhamnaceae	*Ziziphus mucronata* Willd.	mp	PRA	pulp
Rubiaceae	*Fadogia agrestis* Schweinf. ex Hiern.	np	s	pulp
Rubiaceae	*Gardenia erubescens* Stapf	np	S	pulp
Rubiaceae	*Macrosphyra longistyla* (DC.) Hiern	np	SG	pulp
Rubiaceae	*Sabicea brevipes* Wernham	Ge	SG	pulp
Rubiaceae	*Mussaenda elegans* Schum. & Thonn.	Lmp	GC	pulp
Rubiaceae	*Sarcocephalus latifolius* (Smith) Bruce.	mp	AT	pulp
Sapindaceae	*Blighia sapida* Konig	mP	Pan	pulp
Sapindaceae	*Deinbollia pinnata* Schum. & Thonn.	mp	GC	pulp
Sapindaceae	*Lecaniodiscus cupanioides* Planch. ex Benth.	mp	GC	pulp
Sapindaceae	*Paullinia pinnata* L.	Lmp	AA	pulp
Sapindaceae	*Zanha golungensis* Hiern.	mp	SG	pulp
Sapotaceae	*Bequaertiodendron oblanceolatum* (S. Moore) Heine & J. H. Hemsley	mp	GC	pulp
Sapotaceae	*Mimusops kummel* Bruce ex A. DC.	mp	SZ	pulp
Sapotaceae	*Pachystella brevipes* (Bak.) Baill.ex Engl.	mp	GC	pulp
Sapotaceae	*Synsepalum dulcificum* (Schum. & Thonn.) Daniell	mp	GC	pulp
Sapotaceae	*Vitellaria paradoxa* C.F. Gaertner	mp	S	pulp and seed
Sterculiaceae	*Cola gigantea* Brenan & Keay	mP	GC	seed
Sterculiaceae	*Cola millenii* K. Schum.	mP	GC	pulp
Sterculiaceae	*Cola nitida* (Vent.) Schott & Endl.	mP	GC	seed
Sterculiaceae	*Hildegardia barteri* (Mast.) Kosterm.	mP	GC	seed
Sterculiaceae	*Sterculia setigera* Del.	mp	SZ	seed

(to be continued)

Thymelaeaceae	*Synaptolepis retusa* H. H. W. Pearson	He	SZ	pulp
Tiliaceae	*Grewia carpinifolia* Juss.	Lmp		pulp
Tiliaceae	*Grewia cissoides* Hutch. & Dalz.	np	S	pulp
Tiliaceae	*Grewia lasiodiscus* K. Schum.	np	S	pulp
Tiliaceae	*Grewia venusta* Fresen.	np	S	pulp
verbenaceae	*Lantana rhodesiensis* L.	np	Pan	pulp
verbenaceae	*Vitex doniana* Sweet	mp	AT	pulp
verbenaceae	*Vitex simplicifolia* Oliv.	np	SZ	pulp
Vitaceae	*Cissus populnea* Guill. & Perr.	Lmp	PRA	pericarp
Vitaceae	*Cyphostemma flavicans* (Bak.) Descoings	He	SG	pulp
Zingiberaceae	*Aframomum alboviolaceum* (Ridley) K. Schum.	np	SZ	pulp
Zingiberaceae	*Aframomum sceptrum* (Oliv. & Hanb.) K. Schum.	np	GC	pulp
Zygophyllaceae	*Balanites aegyptiaca* (L.) Del.	mp	SZ	pulp

Appendix B: Optimal period of harvest of edible wild fruits recorded.

Species	Month											
	J	F	M	A	M	J	J	A	S	O	N	D
Haematostaphis barteri Hook. f.												
Lannea acida A. Rich.												
Lannea kerstingii Engl. & K. Krausse												
Lannea microcarpa Engl. & K. Krausse												
Sclerocarya birrea (A. Rich.) Hochst.												
Spondias mombin L.												
Annona glauca Schum. & Thonn.												
Annona senegalensis Pers.												
Hexalobus monopetalus (A. Rich.) Engl. & Diels var. monopetalus												
Monodora myristica (Gaertn.) Dunal												
Uvaria chamae P. Beauv.												
Xylopia aethiopica (Dunal) A. Rich.												
Ancylobotrys amoena Hua												
Landolphia owariensis P. Beauv.												
Picralima nitida (Stapf) Th. & H. Dur.												
Saba comorensis (Bojer) Pichon												
Adansonia digitata L.												
Detarium microcarpum Guill. & Perr.												
Detarium senegalense J. F. Gmel.												
Dialium guineense Willd.												
Tamarindus indica L.												
Maranthes polyandra (Benth.) Prance												
Parinari congensis F. Didr.												
Parinari curatellifolia Planch. ex Benth.												
Parinari glabra Oliv.												
Santaloides afzelii (R. Br. ex Planch.) Schellenb.												
Diospyros mespiliformis Hochtst. Ex A. DC.												

(to be continued)

Bridelia ferruginea Benth.
Phyllanthus muellerianus (O. Ktze.) Exell.
Pterocarpus santalinoides L'Hérit. Ex DC.
Flacourtia flavescens Willd.
Oncoba spinosa Forsk.
Garcinia kola Heckel
Pentadesma butyracea Sabine
Icacina senegalensis A. Juss.
Irvingia gabonensis (Aubry-Lecomte ex O' Rorke) Baill.
Strychnos spinosa Lam.
Discoreophyllum cumminsii (Stapf) Diels
Parkia biglobosa (Jacq.) Benth.
Ficus vallis-choudae Delile
Treculia africana Decne
Sizygium guineense (Willd.) DC.
Ximenia americana L.
Opilia amentacea (Guill. & Perr.) Endl. Ex walp.
Borassus aethiopum Mart.
Hyphaene thebaica (L.) Mart.
Ziziphus mucronata Willd.
Gardenia erubescens Stapf
Mussaenda elegans Schum. & Thonn.
*Sarcocephalus latifolius (*Smith) Bruce.
Sabicea brevipes Wernham
Blighia sapida Konig
Paullinia pinnata L.
Zanha golungensis Hiern.
Mimusops kummel Bruce ex A. DC.
Pachystella brevipes (Bak.) Baill.ex Engl.
Vitellaria paradoxa C.F. Gaertner
Cola gigantea Brenan & Keay
Cola millenii K. Schum.
Cola nitida (Vent.) Schott & Endl.
Sterculia setigera Del.
Grewia carpinifolia Juss.
Grewia cissoides Hutch. & Dalz.
Grewia lasiodiscus K. Schum.
Grewia venusta Fresen.
Vitex doniana Sweet
Vitex simplicifolia Oliv.
Cissus populnea Guill. & Perr.
Balanites aegyptiaca (L.) Del.

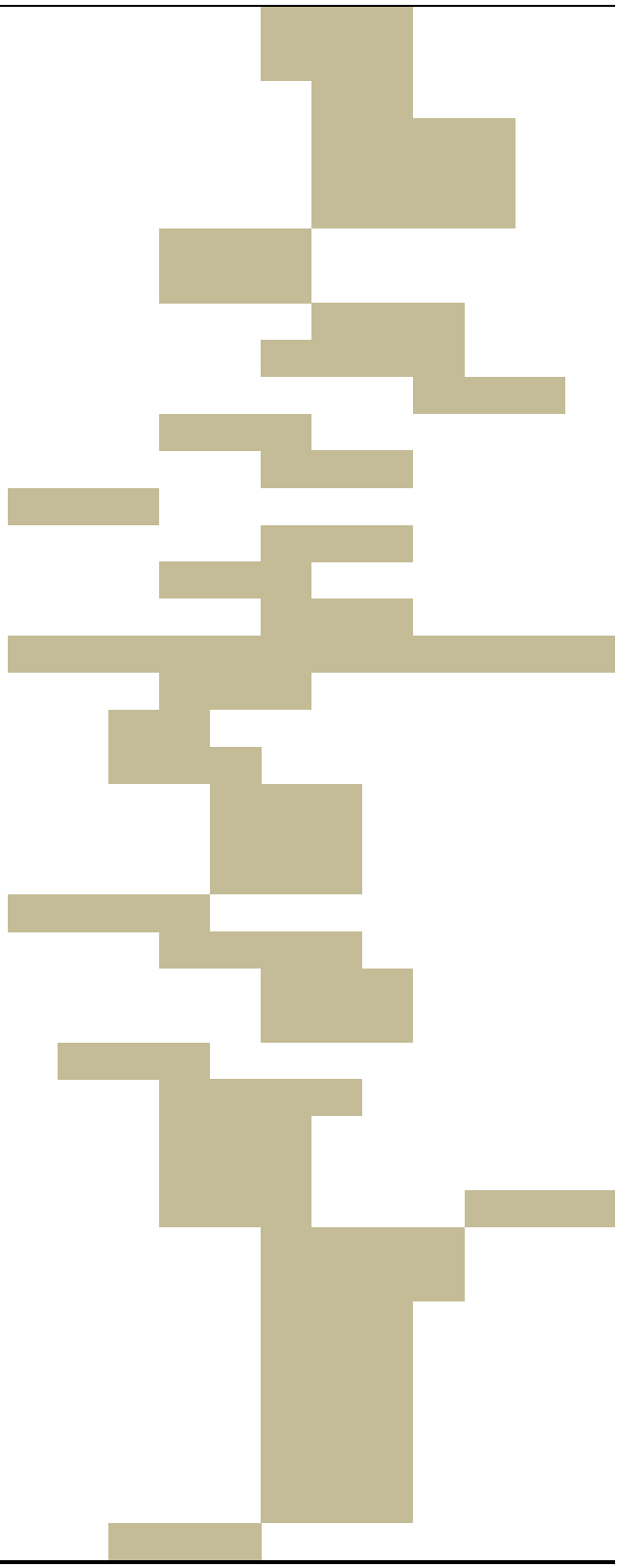

Appendix C: Agricultural calendar of the main crops in Togo.

Crops	Ecological zones	Month											
		Jan	Feb	Mar	Apr	May	June	July	Aug	Sept	Oct	Nov	Dec
Maize	Zone IV												
	Zone III												
	Zone II												
	Zone I												
Sorghum	Zone IV												
	Zone III												
	Zone II												
	Zone I												
Peanut	Zone IV												
	Zone III												
	Zone II												
	Zone I												
Bean	Zone IV												
	Zone III												
	Zone II												
	Zone I												
Rice	Zone IV												
	Zone III												
	Zone II												
	Zone I												

: Sowing : Harvest : Shortage period; Source: Direction des Statistiques, de l'informatique et de la Documentation (DSID).

Journal of Life Sciences 5 (2011) 1058-1071

Morphometric, Reproductive Parameters and Seasonal Variations in Fatty Acid Composition of the Mantis Shrimp *Squilla mantis* (Crustacea: Stomatopoda) in the Gulf of Gabes (Tunisia)

Sami Mili[1, 2], Nawzet Bouriga[3, 4], Hechmi Missaoui[5] and Othman Jarboui[2]

1. Institut Supérieur de Pêche et d'Aquaculture de Bizerte, BP 15, Menzel Jemil 7080, Tunisie

2. Institut National des Sciences et Technologies de la Mer, 28. Rue 2 Mars 1934, Salammbô 2025, Tunisie

3. Unité de Biologie Marine, Faculté des Sciences de Tunis, Campus Universitaire, Tunis 2092, Tunisie

4. LATP, CNRS-UMR 6632, Evolution Biologique et Modélisation, Case 5, Université de Provence, Place Victor Hugo, Marseille Cedex 3 13331, France

5. Direction Générale de la Pêche et de l'Aquaculture, 32 Rue Alain Savary, Tunis 1002, Tunisie

Received: July 25, 2011 / Accepted: August 22, 2011 / Published: December 30, 2011.

Abstract: The growth, reproductive properties and the variations in total lipids and fatty acids in the gonads and muscle tissue of the mantis shrimp *Squilla mantis* (Crustacea: Stomatopoda) caught from the gulf of Gabes in Tunisia were studied by sampling carried out between Jan. 2005 and Dec. 2006 to elucidate the importance of these components during sexual maturation. A total of 16,569 specimens were examined. The sex of this species was determined macroscopically and the proportion of females (47.07%) was significantly lower than that of males (52.93%) with a ratio of 1:1.12 (male/female). The mean total lengths (TL) of the male and female individuals were 142.02 ± 22.76 mm and 141.45 ± 24.37 mm, respectively. Length-weight (TL-W) relationship was estimated as $W = 7 \times 10^{-6} TL^{3.0644}$ for females and $W = 4 \times 10^{-6} TL^{3.2097}$ for males, being allometrically positive for both sexes. The reproductive season, evaluated from the gonado-somatic index (GSI), extended from Dec. to July, with a peak in Feb.. The smallest mature female was 93 mm total length. Fifty percent of the females were mature at 147.19 mm total length. The levels of lipid displayed pronounced seasonal fluctuations with the highest value in Feb. and the lowest value in Oct.. Major fatty acids in both gonads and muscle tissue (female and male) were C14:0, C16:0, C18:0, C18:1n-9, C18:2n-6, C18:3n-3, C20:4n-6, C20:5n-3 and C22:6n-3. Significant increases in the levels of saturated and poly-unsaturated fatty acids were observed in gonads. The levels of *n*-3 poly-unsaturated fatty acids (PUFA), particularly C20:5n-3, decreased in gonads as ovarian development proceeded. Docosahexaenoic acid (DHA), linoleic acid (LA) and eicosapentaenoic acid (EPA) were the most abundant polyunsaturated fatty acids (PUFAs) in the muscle tissue for both male and female. The highest percentages for EPA and DHA were found in winter and summer season for *Squilla mantis* in the Gulf of Gabes. The *n*-3/*n*-6 ratio fatty acids ratio in *Squilla mantis* can be significantly influenced by spawning and season. It was concluded that the mantis shrimp is a healthy item in the human diet during the winter and summer period when balanced *n*-3/*n*-6 ratios and EPA and DHA levels are considered.

Key words: *Squilla mantis*, mantis shrimp, growth, reproduction, fatty acid, Gulf of Gabes.

1. Introduction

The spot-tail mantis shrimp *Squilla mantis* L. (1758) (Crustacea: Stomatopoda) is found in Mediterranean waters and in the adjacent Atlantic, where it has been reported from the Gulf of Cadiz and from the Canary Islands and Madeira, its southernmost distribution being Angola [1]. This species of Stomatopods is very

Corresponding author: Sami Mili, Ph.D., Ass. Prof., research fields: marine biology and fisheries. E-mail: sami_mili@yahoo.fr.

abundant in the Tunisian coasts especially on muddy bottoms in the Gulf of Gabes [2]. *Squilla mantis* is a species which has little economic importance in the Tunisian markets, but its abundance in the gulfs of Tunis, Hammamet and Gabes make it a relatively important for fisheries. *S. mantis* is one of the most dominant species in the demersal crustacean's fauna of the Gulf of Gabes (Fig. 1), south western Tunisian water and is captured mainly by bottom trawls although catches with trammel nets, grill nets, and baited traps [2].

Many studies of this species have been conducted in north of Mediterranean Sea, such as age, growth, mortality, reproductive and feeding biology and the life cycle of this species of Stomatopodos is well known in this area [3]. In spite of the importance of *S. mantis* fisheries, no investigation has focused on the biology of this species in the Tunisian coast.

Crustaceans are an important part of the Mediterranean diet. The beneficial effect of crustacean consumption on human health has been related, among other factors to the high content of *n*-3 or ω 3 fatty acids, especially eicosapentaenoic acid (C20:5n-3) and docosahexaenoic acid (C22:6n-3). Today it is known that *n*-3 fatty acids in the diet are essential for normal growth and development and may play an important role in the prevention and treatment of coronary artery disease, diabetes, hypertension and cancer. They also affect neurodevelopment in infants, fat glycemic control, learning ability and visual function [4]. It is thus important, for human health, to increase the consumption of marine products, which are rich in polyunsaturated fatty acids of the *n*-3 family and poor in polyunsaturated fatty acids of the *n*-6 family [5].

Despite the numerous cited studies on molecular and

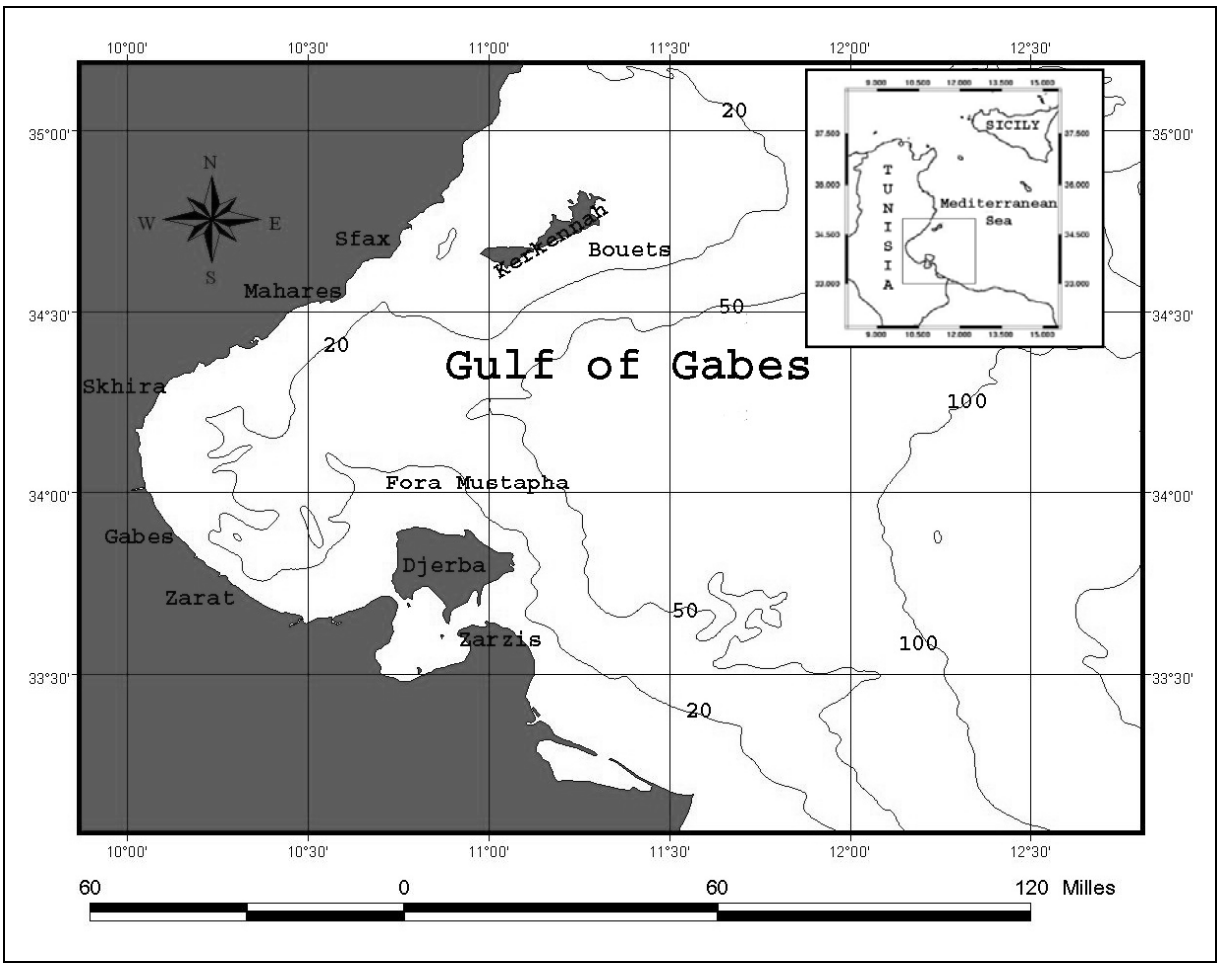

Fig. 1 Study area: The Gulf of Gabes (Southeastern Tunisia).

biological analysis of *S. mantis*, no detailed biochemical studies of the lipid and fatty acids involved this crustacean in Tunisia.

The aim of this study was to describe the growth, reproduction and the fatty acid profile of the spot-tail mantis shrimp, *Squilla mantis* in the gulf of Gabes, which has not been studied in this area before.

2. Material and Methods

2.1 Samples

Samples of *S. mantis* were collected monthly from Jan. 2005 to Dec. 2006 during which 430 trawls were made in Golf of Gabes, Tunisia [2]. Sampling surveys were conducted during the daytime and nighttime by a commercial bottom-trawl. A beam trawl with a cod end mesh size of 20 mm was used for the sampling. The mouth of the trawl was 7 m wide and 1 m high [6]. A total of 16,569 spot-tail mantis shrimps of various sizes were caught in the sampling. All fresh specimens captured were transported to the laboratory where total (TL) and cephalotorax length (Lc) were measured to the nearest 0.1 mm. Total weight (Wt), and weight of gonads (Wg) recorded with an electronic analytical balance to the nearest 0.01 g. The sex of this species was determined macroscopically (8,770 males and 7,799 females). Samples for biochemical analysis were kept in ice, transported immediately to the laboratory where they were rapidly weighted, measured, frozen in liquid nitrogen and stored at -40°C until analysis.

2.2 Sex Ratio (SR)

Sex of *S. mantis* is easily identified by the presence in the male of a pair of copulatory organs arising from the base of the third pair of pereiopods corresponding to the 8th thoracic segment and in the female, by the presence of the genital plate on the 6th thoracic segment sternite. The sex-ratio was estimated monthly during the study period, being expressed as the percentage of females in the various size classes [7].

The overall sex ratio was assessed using Chi square test (χ^2) [8];

Where: f_{iobs}: Observed proportion; f_{th}: Theoretical proportion.

Statistical analyses were performed with SPSS 11.5 software package and a significant level of 0.05 was accepted.

$$x^2 = \sum_{i=1}^{r} \frac{(f_{iobs} - f_{th})^2}{f_{th}}$$

$$SR = \frac{N_f}{N_m} \times 100$$

2.3 Size at the First Sexual Maturity

In this study, size at the first sexual maturity (Lm50) was defined as the size class at which 50% of individuals are mature. Specimens were grouped in 10 mm size classes and the proportion of mature and immature individuals was recorded. The percentage of mature individuals in each size class was calculated by fixing the threshold of maturity starting from the maturation stage II, which corresponds to the phase of ovary development [9]. The total length at which 50% of the specimens were mature was estimated by a method based on a logistic non-linear least-squares regression [10]:

$$\Pr = \frac{1}{1 + \exp\left[-a(L - Lm\,50)\right]}$$

Where, (Pr) is the proportion of mature individuals at length (TL); a is a parameter determining the slope of the maturity curve; and $Lm50$ is the total length at which 50% of the shrimps are mature.

2.4 Sexual Cycle and Period of Spawning

The spawning period of the Spot-tail mantis shrimp was determined by analyzing the evolution of the gonado-somatic index (GSI). The GSI was calculated as: GSI = Gonads weight (Wg) × 100/Total weight (Wt) [9]. The GSI was computed for each month for females.

2.5 Length-Weight Relationship

The relationship between the total length and total weight were determined by fitting the data to a

potential relationship in the form of:

$W = aL^b$ [11].

Where W is the weight in grams; L: the total length in millimetres; a and b are the parameters to be estimated, with b being the coefficient of allometry.

The degree of association between the variables was computed by the determination coefficient, R^2. Student's *t*-test was used to determine if the coefficient b was significantly different from 3 [12].

2.6 Fatty Acid Profile

For this analysis samples were collected bimonthly. Total lipids were extracted according to the method of Folch [13], using chloroform/methanol (2/1). Aliquots of the chloroform layer extracts were evaporated to dryness under nitrogen and the lipids were quantified gravimetrically.

Fatty acids methyl esters (FAMEs) were obtained by the method described in Ref. [14]. A fraction of the lipid extract was saponified with 0.5 N NaOH in methanol followed by methylation in 14% boron trifluoride in methanol (BF3/MeOH). The methylated sample was then extracted with 8 mL *n*-hexane. All of these reactions were performed in quadruplet for each sample. The resulting methyl esters were analysed using an Agilent Gaz chromatograph system 6890N equipped with a flame ionization detector (FID), a splitless injector and a polar INNOWAX fused silica capillary column (30 m × 0.25 mm i.d. × 0.25 μm film thickness). The temperature of the injector and the detector were 250°C and 275°C respectively. Helium was used as a carrier gas with a flow rate of 1.5 mL/min. Peaks were identified by comparison of their retention times with PUFA 3 FAMEs standards (SUPELCO).

2.7 Statistical Analysis

Statistical analysis was performed using SPSS software, version 10.0. The comparison of different biochemical parameters were tested using Duncan's test (95% confidence interval) with one-way ANOVA.

3. Results and Discussions

3.1 Sexual Cycle and Spawning Period

The gonado-somatic index (GSI) was used to determine the reproductive period, which was calculated from samples taken monthly from females (Fig. 2).

The average GSI during the 24-month period was 2.28% for females. The GSI began to rise in Dec. (2.75%), peaked in Feb. (6.38%), and dropped between Apr. (6.07%) and June (2.18%). In July, the GSI value decreased because all samples had presumably dispensed of their eggs. After Oct., the gonads began to develop and the values of GSI again started to gradually increase until Feb..

This study showed that the highest average values of GSI were observed in Feb. for the females of *Squilla mantis*. The monthly evolution of gonadosomatic index (GSI) of the spot-tail mantis shrimp in the gulf of Gabes indicated an extended spawning period, from Dec. to June, with a peak in Feb. when GSI is considerably higher.

According to Do Chi [15], the mating season occurs from winter to spring (Jan. to June), when females have a maximal gonad development and cement glands active, although the activity of these glands may start as early as Oct.. Eggs are shed from Apr. to June [15]. In spring and early summer, females incubate the eggs in their burrows. During incubation, females do not leave their burrows [16, 17]. Larvae hatch between late spring and late summer [16, 17]. In the eastern Ligurian Sea, females with mature gonads were found from Jan. to June, with a clear peak in Apr.; this trend was also confirmed by the monthly development of the maturity stages (and further confirmed by the gonadosomatic index), that reached maximum values in Mar.-Apr. [3]. In the central Adriatic, the peak of ovarian maturity was reported in Feb. and Mar., when up to 80% of the females had ripe ovaries from Apr. to Sep.; mainly spent females were observed [18]. Ovarian maturation starts in larger individuals in Oct., and thereafter involves individuals of progressively smaller size; the insemination

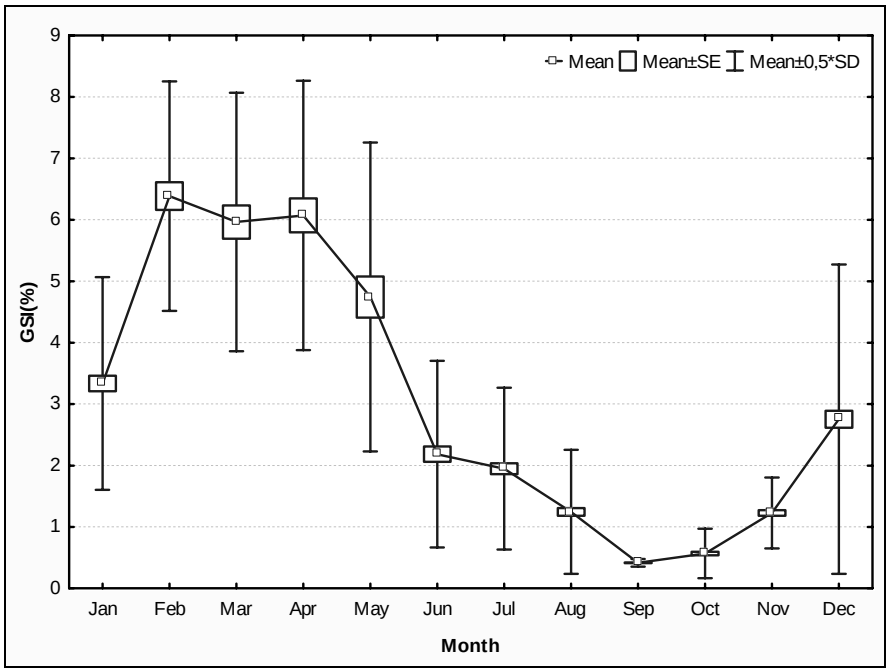

Fig. 2 Monthly changes in the gonadosomatic index (GSI) of *Squilla mantis* (female).

occurs in early winter and egg-laying in Mar. for *S. mantis* in the Gulf of Triest [19].

3.2 Sex-Ratio

All individuals were sexed, the proportion of females was significantly lower than that of males, with reference to the distribution of males and females in the Spot-tail mantis shrimp of the gulf of Gabes samples, the males predominate in 5 months especially in spring and early summer, when females incubate theirs eggs and do not leave their burrows (Fig. 3).

The overall sex-ratio value estimated as 52.93% in favour to males. Chi-square test showed a significant difference (χ^2 obs = 56.9 >> χ^2 th = 3.84; $P < 0.05$). Further, an unequal sex ratio was observed, males were dominant in all size classes with equilibrium only in 14 size classes (Fig. 4).

The sex ratio for the whole sample was 1:1.124 (female/male). The overall sex ratio in *Squilla mantis* was significantly different from the ratio 1:1 ($P < 0.05$), which indicated a dominance of males in the gulf of Gabes. Males and females do not differ significantly in size, as reported for the Catalan Sea, the Adriatic, and the eastern Ligurian Sea [3]. Abelló and Martìn [7] pointed out that the sex-ratio within each size class oscillated between 0.4 and 0.6 and did not indicate any tendency towards a significant dominance of either sex. Moreover, size distribution patterns are also similar for both sexes in the Ebro Delta. The sex-ratio in the Adriatic Sea is very variable with time and area [18]. During the spawning season, the females hide in the galleries and are therefore less vulnerable than males; in this case sex-ratio (M/F) is relatively high [20]. Seasonal variations in catchability result from reduced out-of-burrow activity, because females rarely exit their burrow when they are incubating their egg mass (decreasing their catchability) in spring and early summer [18]. Additionally, catches of females also diminish in spring and summer because the adults disappear from the population after spawning [7].

3.3 Length-Weight Relationship

Of the 16,569 specimens ranged in size and weight from 61-211 mm TL and 1.5-97.02 g W, respectively, 7,799 were females and 8,770 were males. Females measured 61 to 211 mm TL ($\vec{x}$ = 141.45 ± 24.37 mm TL), males 61 to 204 cm TL ($\vec{x}$ = 142.02 ± 22.76 mm TL). Moreover, weight distribution was found to range from

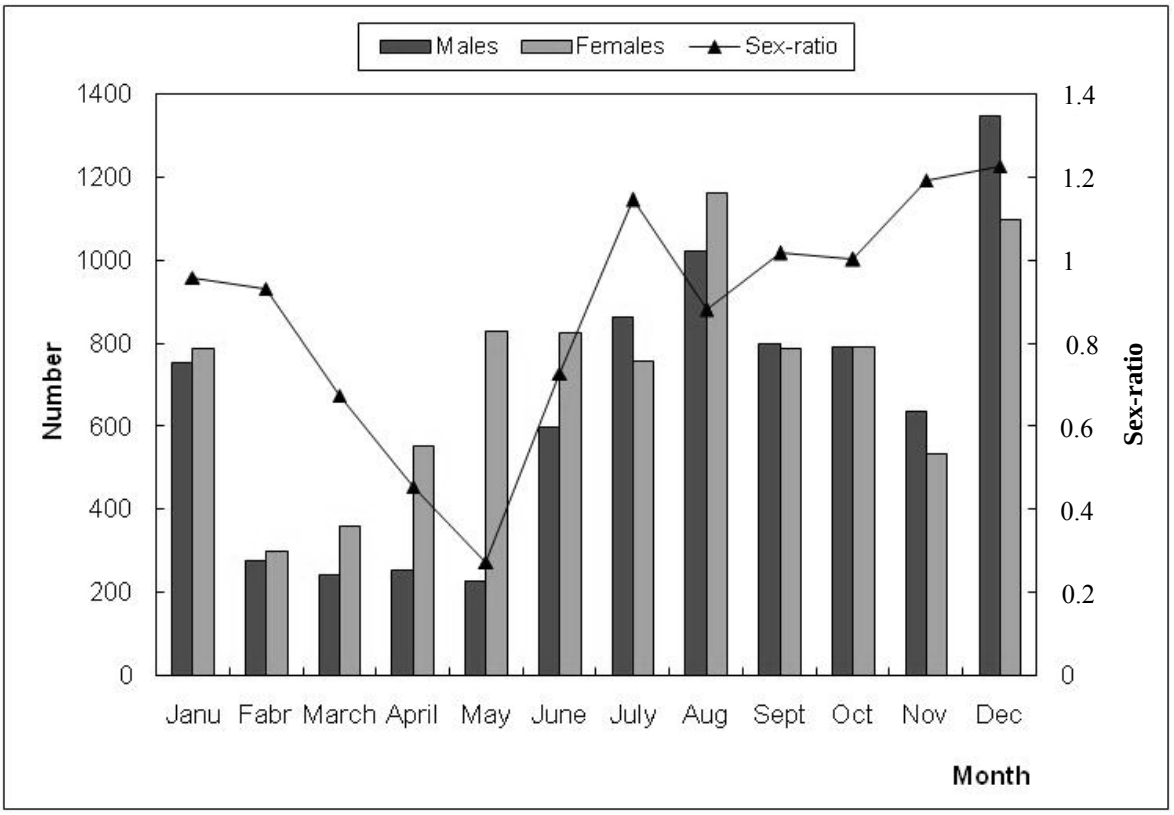

Fig. 3 Sex ratio monthly evolution for *Squilla mantis* (female and male).

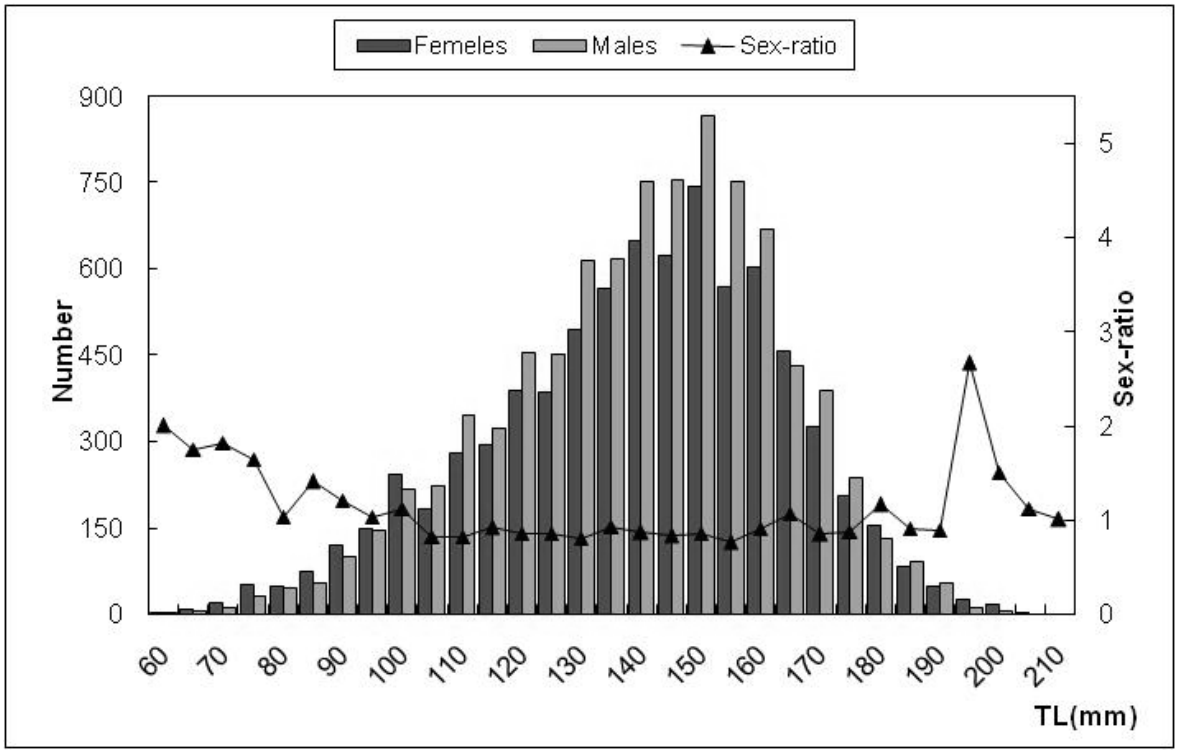

Fig. 4 Sex ratio evolution by size class in *Squilla mantis* (female and male).

1.86-97.02 g for females and 1.5-93.02 g for males.

The length-weight relationship of spot-tail mantis shrimp of the gulf of Gabes indicated a positive allometry (Fig. 5) and was described by the following equation: $W = 5 \times 10^{-6} TL^{3.1375}$.

The analysis by sex (males: $W = 4 \times 10^{-6} TL^{3.2097}$; females: $W = 7 \times 10^{-6} TL^{3.0644}$) showed a significant difference in the b coefficient (Table 1).

The results of statistical analyses showed significant differences between males and females. The value b for males (3.2097), for females (3.0644) and both sexes (3.1375) displayed a positive allometric growth.

The experimental relationship between total length and weight indicated a negative allometric growth (*b* < 3). The *b* value estimated by many others [11, 15, 20, 21] of the Mediterranean. *Squilla mantis* population showed a negative allometric growth except the male in the Adriatic Sea, while Froglia [18] reported a positive allometric growth in the central Adriatic Sea. Maynou [3] mentioned that the variation "*b*" values between populations can be affected differently, because of the geographic location and environmental conditions.

3.4 Size at First Sexual Maturity

The smallest mature female observed during the present study was 93 mm total length. The estimated mean size at which 50% of females were mature was 147.19 mm, using the gonad maturity stages. The interval of maturation estimated wish range between 25% and 75% of females was 130 mm and 164.7 mm, respectively (Fig. 6).

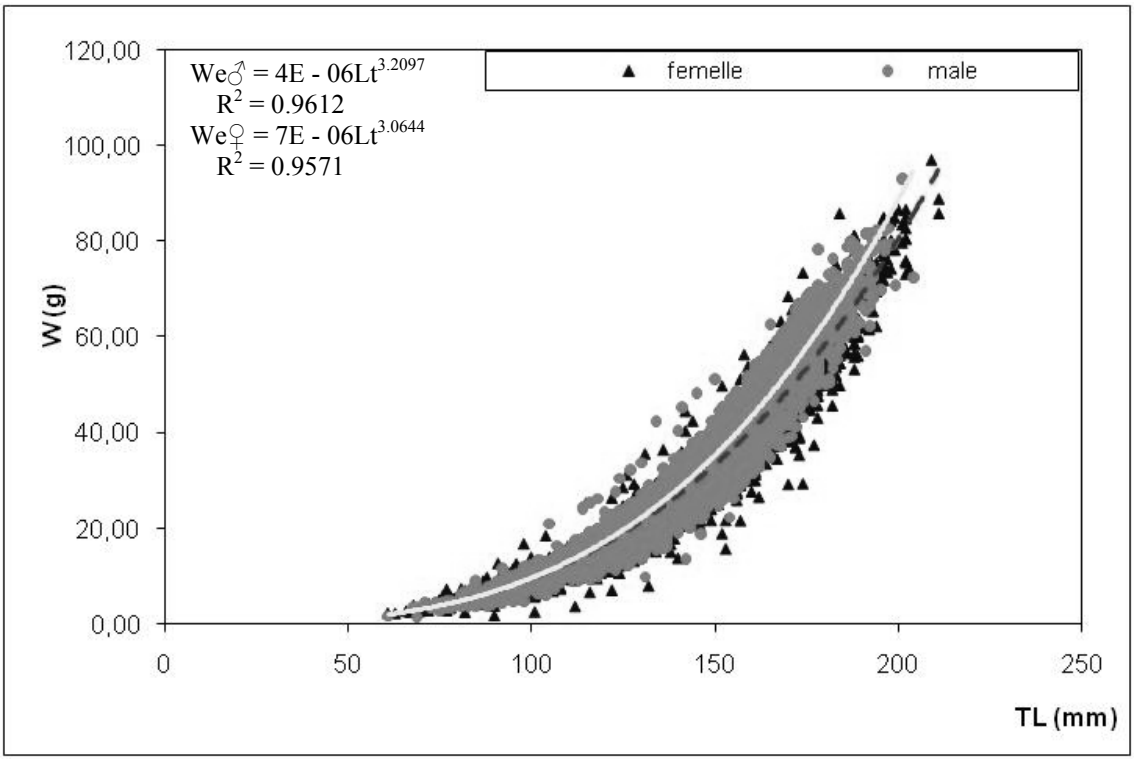

Fig. 5 Relationship between total length (TL) and total weight (W) in *Squilla mantis* (sexes separated).

Table 1 Values of the regression parameters (a, b, R^2) of the length-weight relationship.

Equations	Sex	a	b	R^2	t obs	Significance	Allometry
$W = aTL^b$	♀	7×10^{-6}	3.0644	0.96	8.76	+	Positive
	♂	4×10^{-6}	3.2097	0.96	30.45	+	Positive
	♀+♂	5×10^{-6}	3.1375	0.96	26.76	+	Positive

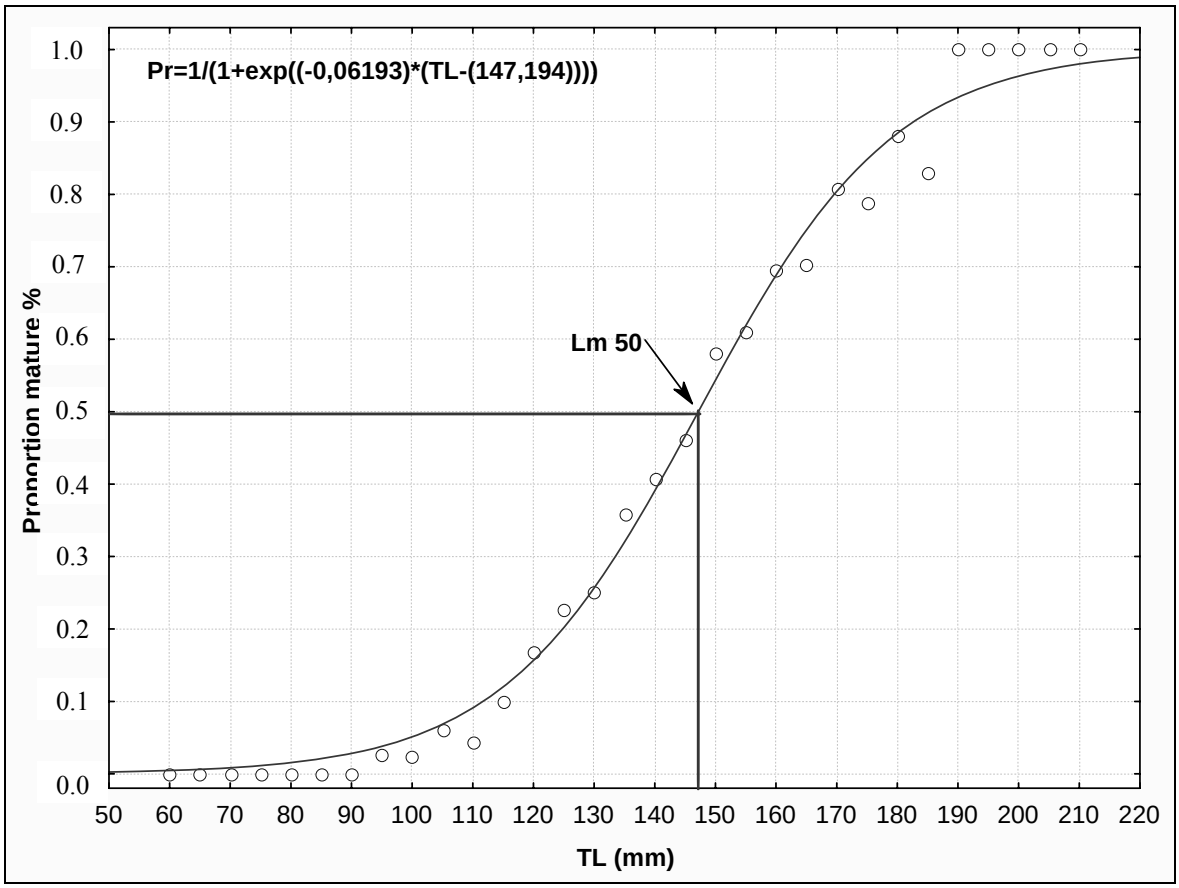

Fig. 6 Size at first sexual maturity of *Squilla mantis* (Female).

Sizes at maturity for females is 20-24 mm CL, when considering maturity by the gonads and cement glands development [11, 15, 16, 18], i.e., female *Squilla mantis* mature within 1 year of settlement to the bottom and spawn within their second year of life [20]. The onset of sexual maturity is at 20-24 mm CL for females, starting with the development of cement glands [11, 15, 16]. Ben Mariem [12] attributed differences in sizes at first sexual maturity for crustaceans to the geographic location of the studied areas and consequently to the different environmental conditions.

3.5 Total Lipids

The lipid content of edible and non edible parts (gonads of female, muscle tissue of male and female) is shown in Table 2. The lipid content of gonads varied between 32. 40 g/100 g fresh weight and 48.06 g/100 g fresh weight and was significantly affected by seasons.

The female had higher levels of lipids of muscle tissue (12.31 g/100 g fresh weight) than male (8.11 g/100 g fresh weight). Gonads contained the highest lipid especially in Dec.-Feb. (Maturation period of gonads). The lowest levels were in Aug. (End of spawning period). The fat content of Muscle tissue for both male and female was also maximal at the end of winter and minimal at the beginning of summer. A high fat content in the winter has also been reported for *Penaeus semisulcatus* and *Metapenaeus monoceros* [22]. Researching the effect of climate on lipid content variation, Krzynowek [23] reported that the fat content of some fish and crustacean species might vary by approximately 10% according to the season. The percentage of body fat is known to depend on the life cycle stage and energy intake of the animal [24] and higher temperature periods are characterised by faster growth rates and large intakes [25]. Our studies about sexual cycle and spawning period indicated that the

Table 2 Lipids composition of *Squilla mantis* in different seasons (g/100g fresh weight).

	Oct.	Dec.	Feb.	Apr.	June	Aug.	AV
Gonads %	34.82 ± 0.42 a	44.12 ± 1.44 a	48.06 ± 1.63 a	39.16 ± 0.12a	36.72 ± 0.22 b	32.40 ± 0.13 b	***
Flesh male %	7.22 ± 0.02 b	8.11 ± 0.1 b	7.98 ± 0.54 a	6.95 ± 0.01 b	6.15 ± 1.14 a	6.72 ± 0.08 a	*
Flesh female %	11.28 ± 0.01 b	12.31 ± 0.12 a	11.67 ± 0.46 a	10.57 ± 0.09 b	9.78 ± 0.03 b	10.03 ± 0.11 a	**

Means (n = 6) with the same letter within rows are not significantly different ($P > 0.05$); AV: Analysis of variance; NS: no significant; * Significance at 0.05; ** Significance at 0.01; *** Significance at 0.001.

reproductive season of the specie is between Dec.-Jun. and eggs are shed from Apr. to June. In this period, sexual maturation has been found to reduce lipid body stores in *Squilla mantis* because lipid stores are directed to gonad lipids or used for energy.

In spring and early summer, females incubate the eggs in their burrows [3]. During incubation, females do not leave their burrows. In this period and during sexual maturation, *Squilla mantis* as many crustacean species tend to stop or reduce their food intake, essential fatty acids and other nutrients needed for ovarian growth are taken from the reserves in their bodies. Low levels of lipid were observed in the spawning and eggs incubation periods.

3.6 Fatty Acid Profile

The fatty acid composition of Gonads, throughout the maturation period is presented in Table 3. During one year period, polyunsaturated fatty acids PUFA of Gonads lipid of *Squilla mantis* extracts constitute the majority of the fatty acids pool, followed by Saturated fatty acids SFA and monounsaturated MUFA, especially during Aug. and Oct., saturated fatty acids SFA constitute the majority of the fatty acids pool, followed by polyunsaturated fatty acids PUFA and monounsaturated MUFA.

The predominant fatty acids were myristic (C14:0), palmitic (C16:0), stearic (C18:0), oleic (C18:1n-9) and linoleic (C18:2n-6) acids, whereas linolenic (C18:3n-3), arachidonic (C20:4n-6; ARA), eicosapentaenoic (C20:5n-3; EPA) and docosahexaenoic (C22:6n-3; DHA) acids were present at intermediate levels. Saturated and poly-unsaturated fatty acids in the gonads increased significantly as ovarian development proceeded (Oct.-Feb.). In contrast, mono-unsaturated fatty acids (MUFA) decreased. No significant variation in the relative amount of n-6 polyunsaturated fatty acids (PUFA) was detected.

From Oct. to June, the higher contents of poly-unsaturated fatty acids in the gonads were 46.55%. Among poly-unsaturated fatty acids (PUFA), the levels of C18:2n-6, C18:3n-3 and C20:4n-6 significantly increased from Oct. to Feb. (Maturation period). Significant increases in the content of saturated and poly-unsaturated fatty acids in the gonads were evident throughout ovarian development. Saturated fatty acids may also have been catabolised for the production of energy while n-6 PUFA and n-3 PUFA were conserved. Saturated and poly-unsaturated fatty acids are the major sources of energy during embryonic [26] and early larval development of *M. rosenbergii* [27].

In our study, the gonads concentration of C18:2n-6 increased significantly during maturation, suggesting some important metabolic function or response. Relative to this apparent need, C18:2n-6 has been shown to affect positively the fecundity of *M. rosenbergii* [28].

PUFA, especially the n-3 series, have been found to be important for the maturation and reproduction of penaeid shrimp [29-33]. ARA and EPA are important as structural components of cell membranes and as precursor of prostaglandins [34], while DHA may play an important role in the development of the central nervous system of crustaceans [35]. In the present study, lipids of gonads contained higher proportions of ARA, EPA and DHA than those found in the muscle tissue of female and male. EPA was present in higher

Table 3 Seasonal fatty acid composition of Gonads of *Squilla mantis* (% of total lipid).

FA	Oct.	Dec.	Feb.	Apr.	June	Aug.	AV
C14:0	11.70 ± 0.34 b	6.30 ± 0.09 c	3.38 ± 0.16 a	1.53 ± 0.24 a	9.22 ± 0.01 a	10.80 ± 0.09 c	***
C16:0	23.52 ± 0.10 a	18.43 ± 0.10 a	20.79 ± 0.10 a	21.61 ± 0.42 a	21.17 ± 0.34 b	27.03 ± 0.10 b	*
C18:0	10.84 ± 0.28 a	9.73 ± 0.05 a	6.24 ± 0.07 a	7.14 ± 0.04 a	10.62 ± 0.01 a	9.95 ± 0.30 c	**
C16:1n-7	4.58 ± 1.93 c	2.37 ± 0.31 c	2.85 ± 0.09 a	9.20 ± 0.28 a	3.02 ± 0.03 b	4.62 ± 0.00 a	***
C18:1n-9	16.84 ± 0.04 b	13.69 ± 0.18 b	10.23 ± 0.12 b	8.50 ± 0.15 a	15.73 ± 0.41 b	9.44 ± 0.10 a	**
C18:1n-7	1.79 ± 0.17 b	2.35 ± 0.01 a	2.14 ± 0.17 b	2.54 ± 0.02 a	1.83 ± 0.06 a	2.49 ± 0.03 b	*
C20:1n-9	1.57 ± 0.05 c	2.43 ± 0.11 a	1.54 ± 0.01 c	2.35 ± 0.12 a	1.71 ± 0.02 b	1.11 ± 0.01 a	**
C16:2n-4	1.44 ± 0.10 a	1.86 ± 0.04 b	1.26 ± 0.10 a	1.09 ± 0.01 a	2.03 ± 0.01 a	1.13 ± 0.54 b	*
C18:2n-6	13.00 ± 0.17 b	14.36 ± 0.05 b	14.42 ± 1.93 c	10.87 ± 0.02 a	13.54 ± 0.04 b	13.54 ± 0.80 a	**
C18:3n-3	5.70 ± 0.01 c	6.10 ± 0.06 b	7.60 ± 0.05 c	4.20 ± 0.04 a	5.80 ± 0.01 a	4.80 ± 0.01 a	*
C20:4n-6	3.42 ± 0.02 b	4.37 ± 0.12 a	6.78 ± 0.01 c	7.31 ± 0.11 a	3.06 ± 0.08 a	5.41 ± 1.80 a	*
C20:4n-3	0.46 ± 0.04 b	0.84 ± 0.04 b	0.91 ± 0.10 a	0.61 ± 0.02 a	0.63 ± 0.01 b	0.34 ± 0.05 b	*
C20:5n-3	3.34 ± 0.11 b	9.48 ± 0.07 b	9.27 ± 1.64 a	12.92 ± 0.12 a	7.52 ± 0.12 a	7.21 ± 0.03 a	***
C22:5n-3	1.33 ± 0.17 b	1.94 ± 0.01 a	1.56 ± 0.01 a	1.31 ± 0.03 a	0.94 ± 0.07 b	1.86 ± 0.01 b	**
C22:6n-3	4.89 ± 0.02 a	4.32 ± 0.17 b	4.75 ± 0.02 a	2.93 ± 0.37 a	5.24 ± 0.11 a	4.16 ± 0.01 a	**
SFA	46.06 ± 0.19 b	34.46 ± 0.41 a	30.41 ± 0.92 a	30.28 ± 0.68 a	41.01 ± 0.59 b	47.78 ± 0.40 b	**
MUFA	24.78 ± 1.72 b	20.84 ± 0.37 b	16.76 ± 0.59 a	21.59 ± 0.41 a	22.29 ± 1.64 a	17.66 ± 1.80 a	**
PUFA	33.40 ± 0.57 a	43.27 ± 0.59 a	46.55 ± 0.54 a	41.24 ± 0.68 a	38.76 ± 0.92 b	28.45 ± 0.92 b	***
∑ n-3	15.72 b	22.68 a	28.87 a	21.97 a	20.13 b	16.37 a	**
∑ n-6	16.42 b	18.73 a	19.20 a	18.18 a	16.60 a	20.90 a	**

Means (n = 6) with the same letter within rows are not significantly different ($P > 0.05$); AV: Analysis of variance; NS: no significant; * Significance at 0.05; ** Significance at 0.01; *** Significance at 0.001.

levels than DHA in all tissues examined. The concentration of EPA dropped significantly in the tissues, but remained constant in the gonads lipids during maturation. The experimental results of Xu [35] indicate that dietary levels of EPA and DHA positively affected the fecundity and egg hatchability of *P. chinensis*, respectively. Similarly, high levels of n-3 PUFA in the eggs of *M. rosenbergii* improved not only hatchability but also quality of the larvae [28].

Muscle tissue, for both male and female, contained levels of fatty acids that were lower than those of the gonads examined (Tables 4 and 5). In all tissues examined in our study the proportion of saturated and mono-unsaturated fatty acids was greater than that of PUFA. The results show remarkable changes in the individual fatty acids during the one-year period.

The fatty acid profile in muscle tissue of *Squilla mantis* was typical of marine animals with the dominance of the palmitic acid (C16:0) for saturated fatty acids (SFA), contributing approximately 19.45%-24.8% for female and 17.43%-22.52% for male to the total SFA content of the lipids for *Squilla mantis*. Ackman [36] pointed out that palmitic acid was a key metabolite in fish and its level was not influenced by diet. Also, the Oleic acid (C18:1) was identified as the major monounsaturated fatty acids MUFA in the spot-tail mantis shrimp.

According to the season, DHA (C22:6n-3), LA (C18:2n-6), and EPA (C20:5n-3) were the predominant PUFAs for muscle tissue for both male and female. The same data were found by Pirini [37] and Surh [38].

An increase in the lipid level resulted in an increase also in the fatty acid levels, except for n-3. The maximum level of n-3 was found in August. From these results, it could be speculated that *Squilla mantis* in Gulf of Gabes uses the n-3 series as an energy source.

In the present study, the percentages (in total lipid) of EPA and DHA which have a vital role in human nutrition was between 3.21%-6.48% (female), 4.03%-7.25% (male) and 5.16%-9.32% (female), 5.76%-8.82% (male), respectively. The highest percentages

Table 4 Seasonal fatty acid composition of female flesh (% of total lipid).

FA	Oct.	Dec.	Feb.	Apr.	June	Aug.	AV
C14:0	4.28 ± 0.01 b	4.51 ± 0.10 c	4.48 ± 0.02 b	3.12 ± 0.03 a	5.20 ± 0.54 a	3.96 ± 0.20 a	**
C16:0	23.12 ± 0.46 a	24.80 ± 0.01 b	20.15 ± 0.10 c	22.40 ± 0.01 b	23.50 ± 1.44 a	19.45 ± 0.40 a	**
C18:0	4.89 ± 0.50 b	5.74 ± 0.03 a	6.04 ± 0.01 c	4.420 ± 0.04 b	6.52 ± 0.46 a	5.53 ± 0.04 a	*
C16:1n-7	10.54 ± 0.02 a	10.78 ± 0.44 b	8.48 ± 0.03 c	11.34 ± 0.01 b	9.74 ± 0.11 a	8.32 ± 0.28 a	**
C18:1n-9	19.64 ± 0.03 c	17.80 ± 0.02 a	16.53 ± 0.20 c	19.37 ± 0.50 b	17.30 ± 0.10 b	16.20 ± 0.15 a	***
C18:1n-7	2.52 ± 0.01 a	1.78 ± 0.50 b	2.82 ± 0.03 c	2.75 ± 0.44 b	1.93 ± 1.63 a	2.35 ± 0.02 a	*
C20:1n-9	1.01 ± 0.11 a	1.67 ± 0.08 a	1.52 ± 0.01 b	2.65 ± 0.01 a	1.78 ± 0.12 a	2.44 ± 0.12 a	**
C16:2n-4	1.12 ± 0.02 b	1.46 ± 0.05 b	2.12 ± 0.08 a	1.19 ± 0.02 b	2.02 ± 0.08 a	1.86 ± 0.01 a	**
C18:2n-6	11.28 ± 0.01 a	8.73 ± 0.07 b	7.51 ± 0.05 b	11.43 ± 0.01 b	8.50 ± 0.22 b	8.26 ± 0.02 a	***
C20:4n-6	2.21 ± 0.01 b	1.09 ± 0.02 c	2.76 ± 0.02 c	2.22 ± 0.08 b	2.06 ± 1.14 a	3.27 ± 0.04 a	**
C20:4n-3	0.34 ± 0.01 b	0.46 ± 0.02 b	0.91 ± 0.01 b	0.61 ± 0.07 b	0.60 ± 0.03 b	0.84 ± 0.11 a	**
C20:5n-3	3.21 ± 0.02 a	5.34 ± 0.01 b	5.87 ± 0.01 c	4.82 ± 0.01 b	4.52 ± 0.13 b	6.48 ± 0.02 a	**
C22:5n-3	0.86 ± 0.01 a	1.33 ± 0.01 b	1.56 ± 0.01 b	1.31 ± 0.02 b	0.94 ± 0.20 c	1.94 ± 0.12 a	**
C22:6n-3	5.16 ± 0.01 b	6.89 ± 0.03 a	7.75 ± 0.03 a	6.53 ± 0.01 a	7.24 ± 0.08 b	9.32 ± 0.03 a	***
SFA	32.29 ± 0.01 b	35.05 ± 0.01 a	30.67 ± 0.00 c	29.94 ± 0.10 b	35.22 ± 0.02 a	28.94 ± 0.37 a	***
MUFA	33.71 ± 0.44 b	32.03 ± 0.07 b	29.35 ± 0.10 c	36.11 ± 0.01 b	30.75 ± 0.01 a	29.31 ± 0.68 a	***
PUFA	24.18 ± 0.01 a	25.30 ± 0.01 a	28.48 ± 0.20 c	28.11 ± 0.01 b	25.88 ± 0.07 b	31.97 ± 0.41 a	***
∑ n-3	9.57 b	14.02 a	16.09 a	13.27 b	13.30 a	18.58 a	***
∑ n-6	13.49 b	9.82 a	10.27 a	13.65 a	10.56 b	11.53 a	**
∑ n-3/n-6	0.70 b	1.42 a	1.56 a	0.97 a	1.25 c	1.61 b	**

Means (n = 6) with the same letter within rows are not significantly different ($P > 0.05$); AV: Analysis of variance; NS: no significant; * Significance at 0.05; ** Significance at 0.01; *** Significance at 0.001.

Table 5 Seasonal fatty acid composition of male flesh (% of total lipid).

FA	Oct.	Dec.	Feb.	Apr.	June	Aug.	AV
C14:0	5.38 ± 0.02 b	5.61 ± 0.09 b	5.38 ± 0.02 b	4.53 ± 0.05 a	6.12 ± 0.04 b	4.36 ± 0.07 b	**
C16:0	21.03 ± 0.01 b	22.52 ± 0.59 b	18.79 ± 0.10 c	20.10 ± 0.01 b	21.17 ± 0.08 a	17.43 ± 0.68 a	**
C18:0	5.95 ± 0.04 b	6.84 ± 0.01 b	7.24 ± 0.01 c	5.54 ± 0.04 b	7.62 ± 0.09 b	6.73 ± 0.02 a	*
C16:1n-7	9.62 ± 0.59 b	9.58 ± 0.01 a	7.85 ± 0.03 c	10.26 ± 0.09 b	8.02 ± 0.01 b	7.37 ± 0.01 a	**
C18:1n-9	19.44 ± 1.63 a	17.94 ± 0.27 c	16.23 ± 0.27 c	19.40 ± 0.59 b	17.73 ± 1.63 a	16.69 ± 0.37 a	***
C18:1n-7	2.49 ± 0.05 a	1.89 ± 0.05 a	2.14 ± 0.03 c	2.54 ± 0.44 b	1.82 ± 0.01 c	2.15 ± 0.01 b	*
C20:1n-9	2.11 ± 0.01 b	2.57 ± 0.01 b	2.54 ± 0.01 b	3.35 ± 0.01 a	2.71 ± 0.04 b	3.43 ± 0.01 b	**
C16:2n-4	1.13 ± 0.05 a	1.44 ± 0.08 a	2.26 ± 0.08 a	1.07 ± 0.02 b	2.03 ± 0.02 b	1.42 ± 0.02 a	**
C18:2n-6	10.54 ± 0.44 b	7.73 ± 0.02 c	6.42 ± 0.05 b	10.37 ± 0.03 b	7.54 ± 0.08 a	7.36 ± 0.44 b	***
C20:4n-6	2.61 ± 0.08 a	1.22 ± 0.03 b	2.98 ± 0.02 c	2.41 ± 0.08 b	2.26 ± 0.03 a	3.57 ± 0.08 a	**
C20:4n-3	0.28 ± 0.59 b	0.52 ± 0.08 a	0.83 ± 0.01 b	0.72 ± 0.07 a	0.63 ± 0.01 b	0.76 ± 0.09 b	**
C20:5n-3	4.03 ± 0.05 b	6.44 ± 0.01 b	6.89 ± 0.01 c	5.83 ± 0.01 b	5.49 ± 0.01 b	7.25 ± 0.11 c	**
C22:5n-3	1.06 ± 0.02 b	1.63 ± 0.01 a	1.86 ± 0.01 b	1.61 ± 0.02 b	1.04 ± 0.01 b	2.04 ± 0.05 b	**
C22:6n-3	5.76 ± 0.09 b	6.39 ± 0.68 a	7.25 ± 0.03 a	6.03 ± 0.01 a	7.84 ± 0.03 a	8.82 ± 0.44 b	***
SFA	32.36 ± 0.08 a	34.97 ± 0.44 b	31.41 ± 0.08 c	30.17 ± 0.14 b	34.91 ± 0.14 b	28.52 ± 1.63 a	***
MUFA	33.66 ± 0.01 b	31.98 ± 0.27 c	28.76 ± 0.11 c	35.55 ± 0.09 b	30.28 ± 0.28 c	31.22 ± 0.37 b	***
PUFA	25.41 ± 1.44 a	25.37 ± 0.09 b	28.49 ± 0.28 c	28.04 ± 0.07 b	26.83 ± 0.44 b	31.97 ± 0.59 b	***
∑ n-3	11.13 a	14.98 b	16.83 a	14.19 b	15.00 a	18.87 a	***
∑ n-6	13.15 b	8.95 a	9.40 a	12.78 b	9.80 b	10.93 a	**
∑ n-3/n-6	0.84 a	1.67 b	1.79 a	1.11 b	1.53 a	1.72 a	**

Means (n = 6) with the same letter within rows are not significantly different ($P > 0.05$); AV: Analysis of variance; NS: no significant; * Significance at 0.05; ** Significance at 0.01; *** Significance at 0.001.

for EPA and DHA were found in summer season. Thus, among the n-3 series, the spot-tail mantis shrimp are good sources of EPA and DHA. Sargent [39] reported that n-3 PUFA, principally DHA, has a role in maintaining the structure and functional integrity of marine organism cells. In addition, DHA has a specific and important role in neural cell membranes, the brain and eyes. Moreover, it is considered a desirable property in fish and crustacean for human nutrition and health.

The results obtained in this study show shorter (C:18) chain n-3 acids in the food to be elongated and desaturated in the shrimp body, where longer-chain PUFAs, mainly DHA, are formed.

The fatty acid profile in the lipid composition of muscle tissue (male and female) observed in our investigation may have been caused by foods and/or composition at the sampling stations.

The results demonstrate that *Squilla mantis* is highly capable of transforming native forms of C18:n-3 into long-chain acids, as a result of which the shrimp has a high DHA content. Similar results were obtained by Xu et al. [35] who analyzed dietary effects on fatty acid composition in muscles of *Perca fluviatilis*; they found high DHA contents. There are close relationships between the crustacean lipid composition and the diets [40]. The most common prey of *Squilla mantis* was benthic Crustaceans and fish. The shrimp due to their consumption of preys in which chain elongation and desaturation is completed were rich in long chain n-3 PUFAs [41].

The n-3/n-6 ratio is a good index for comparing relative nutritional value of marine organisms [42]. It is important for human health to increase the consumption of fish and crustacean, which are rich in PUFAs of the n-3 family and poorer in PUFAs of the n-6 family [43]. However, there is no recommended intake in terms of n-3/n-6 ratios but evidence in wild animals and estimated nutrient intake during human evolution suggest a diet ratio of 1:1 [44]. The present data show that the n-3/n-6 ratio for female and male, respectively was (1.61, 1.72) in Aug., (1.42, 1.67) in Dec., (1.56, 1.79) in Feb., (0.97, 1.65) in April, (1.25, 1.11) in June and that the lowest value (0.70, 0.84) was in Oct.. A high level of n-6 lowered the n-3/n-6 ratio in Oct..

An increase in the human dietary n-3/n-6 fatty acid ratio is essential in the diet to help coronary heart disease by reducing plasma lipids and to reduce cancer risk [45]. It is thus important for human health to increase the consumption of n-3 fatty acids [46, 47].

This study has shown that *Squilla mantis* is a suitable item in the human diet during the winter and the summer season when the levels of EPA, DHA and n-3/n-6 ratio are considered. This condition can be regarded as an explanation for the fact that the *Squilla mantis* in Gulf of Gabes are richer in n-3 fatty acids, taking into consideration with the fatty acid profile of the shrimp. As a consequence, when human health is taken into account, *Squilla mantis* appears to be quite nutritious in terms of fatty acid composition and ratio.

4. Conclusion

The Eco-biology of *Squilla mantis* is affected by seasonal fluctuations, by meteorological factors and trophic factors; wish may influence in the biochemical composition of this species. Autumn represents the season of transition between one maturative cycle and the next, when energy investment is devoted instead to molting processes, which take place more frequently in this period.

The Spot-tail mantis shrimp *Squilla mantis*, caught from the Gulf of Gabes shows a great similarity in growth and reproduction proprieties with many other Mediterranean populations.

In the present study, lipids of gonads contained higher proportions of ARA, EPA and DHA than those found in the muscle tissue of female and male. EPA was present in higher levels than DHA in all tissues examined. The concentration of EPA dropped significantly in the tissues, but remained constant in the gonads lipids during maturation.

This study has shown that the Spot-tail mantis

shrimp is a desirable item in the human diet when the levels of EPA and DHA are considered. This condition can be regarded as an explanation for the fact that *S. mantis* in the Gulf of Gabes is richer in n-3 fatty acids in winter and summer, taking into consideration with the fatty acid profile of this shrimp. As a consequence, when human health is taken into account, the Spot-tail mantis shrimp from the Gulf of Gabes appears to be quite nutritious in terms of fatty acid composition and ratio. Revealed the biology and the ecology of *S. mantis* shrimp population in Tunisia are very important to plan the fishery strategy.

Acknowledgments

The authors would like to thank Mr. Ahmed Hammami and Taieb Sp for their great help on the biochemical analyses as well as Dr. Anissa Chouikha. We also thank Tarek Zrelli for her assistance in the beginning of this research.

References

[1] P. Abelló, A. Carbonell, P. Torres, Biogeography of epibenthic crustaceans on the shelf and upper slope off the Iberian Peninsula Mediterranean coasts: Implications for the establishment of natural management areas, Scientia Marina 66 (2002) 183-198.

[2] S. Mili, O. Jarboui, H. Missaoui, Caractères biométriques de la squille *Squilla mantis* dans les eaux tunisiennes, Bulletin de l'Institut National des Sciences et Technologies de la Mer de Salammbô 3 (2008) 1-14. (in French)

[3] F. Maynou, P. Abelló, P. Sartor, A review of the fisheries biology of the mantis shrimp, *Squilla mantis* L. (1758) (Stomatopoda, Squillidae) in the Mediterranean, Crustaceana 77 (2005) 1081-1099.

[4] S.L. Goodstine, T.R. Zheng, T. Holford, B.A. Ward, D. Carter, P.H. Owens, et al., Dietary (n-3)/(n-6) fatty acid ratio: Possible relationship to premenopausal but not postmenopausal breast cancer risk in US women, The American Society for Nutritional Sciences, Journal of Nutrition 133 (2003) 1409-1414.

[5] M.L. Burr, Fish and the cardiovascular system, Program of Food Nutrition Science 13 (1989) 291-316.

[6] R. M'rabet, Les engins de pêche les plus utilisés dans les eaux tunisiennes et les effets néfastes causés par certains engins sur les ressources halieutiques, Rapports et Documents de l'INSTOP 1 (1995) 1-13. (in French)

[7] P. Abelló, P. Martín, Fishery dynamics of the mantis shrimp *Squilla mantis* (Crustacea: Decapoda) population off the Ebro Delta (northwestern Mediterranean), Fishery Research 16 (1993) 131-145.

[8] R. Sokal, F. Rohlf, Introduction to Biostatistics, Freeman and Company, 1987, p. 365.

[9] K. Kodama, T. Shimizu, T. Yamakawa, I. Aoki, Reproductive biology of the female Japanese mantis shrimp *Oratosquilla oratoria* (Stomatopoda) in relation to changes in the seasonal pattern of larval occurrence in Tokyo Bay, Japan, Fisheries Science 70 (2004) 734-745.

[10] M. King, Fisheries Biology: Assessment and Management, Fishing New Books, Osney Mead, Oxford Ox 2 OEL, England, 1995, p. 341.

[11] P. Abelló, F. Sardá, Some observations on the biology and fishery of *Squilla mantis* L. in the Catalan area (NW Mediterranean), in: E.A. Ferrero (Ed.), Biology of Stomatopods, 1989, pp. 229-239.

[12] S. Ben Mariem, Taille de première maturité et période de ponte de *Penaeus kerathurus* dans le golfe de Gabès, Tunisie (Decapoda, Penaeidae), Crustaceana 65 (1993) 82-96. (in French)

[13] J. Folch, M. Lees, G. Stanley, A simple method for the isolation and purification of total lipids from animal tissue, Journal of Biological Chemistry 226 (1957) 497-509.

[14] L. Metcalfe, A. Schimitz, J. Pelka, Rapid preparation of fatty acids esters from lipids for gas chromatographic analysis, Annexe of Chemistry 38 (1966) 524-535.

[15] T. Do Chi, Biométrie de la reproduction de *Squilla mantis* (L.) (Crustacé Stomatopode) dans le golfe d'Aigues-Mortes (Méditerranée noroccidentale), Pubbl. Staz. Zool. Napoli 39 (1975) 114-139. (in French)

[16] C. Piccinetti, G. Piccinetti-Manfrin, Osservazioni su alcuni aspetti della biologia di *Squilla mantis* L., Pubbl. Staz. zool. Napoli 38 (1970) 119-124. (in Italian)

[17] T. Do Chi, Modèles cinétiques et structuraux en dynamique des populations exploitées, Application aux squilles, *Squilla mantis* (L.) (Crustacé Stomatopode) du Golfe du Lion., Thèse de l'Université de Montpellier, 1978, p. 272. (in French)

[18] C. Froglia, Growth and behaviour of *Squilla mantis* (mantis shrimp) in the Adriatic Sea, Final Report, EU Study DG XIV/MED/93/016, 1996.

[19] Ea. Ferrero, R. Marzari, A. Mosco, D. Riggio, Dynamics of morphometric and biochemical parameters of the reproductive condition of *Squilla mantis* fished by creels in the Gulf of Trieste, Use of the VTGs as biochemical markers, Boll. Soc. Adriatica Sci., 70 (1988) 47-59.

[20] C. Giovanardi, G. Piccinetti-Manfrin, Summary of biological parameters of *Squilla mantis* L. in the Adriatic Sea, FAO Fish Report 290 (1984) 131-134.

[21] P. Righini, R. Baino, Parametri popolazionistici della pannocchia (*Squilla mantis*, Crustacea: Stomatopoda), Biol. Mar. Mediterranea 3 (1996) 565-566.

[22] Y. Yanar, M. Celik, Seasonal variations of fatty acid composition in wild marine shrimps (*Penaeus*

semisulcatus De Haan, 1844 and *Metapenaeus monoceros* Fabricus, 1789) from the Eastern Mediterranean Sea, Food Science and Technology International 11 (5) (2005) 391-395.

[23] J. Krzynowek, D. Peton, K. Wiggin, Proximate composition, cholesterol, and calcium content in mechanically separated fish flesh from three species of the Gadidae family, Journal of Food Science 49 (1984) 1182-1185.

[24] M. Jobling, Fish Bioenergetics, Chapmen & Hall, London, 1994, p. 309.

[25] B. García García, F.M. Rueda, M.D. Hernández, F. Aguado, M.A. Egea, F. Faraco, Crecimiento e índice de conversión del sargo picudo (*Puntazzo puntazzo* Gmelin, 1789) en engorde intensivo en tanques, in: H. Fernández-Palacios, M. Izquierdo (Eds.), Convergencia entre Investigación y Empresa: Un reto para el siglo XXI, Monografías del ICCM 4 (2001) 385-390.

[26] A. Clarke, J.H. Brown, L.J. Holmes, The biochemical composition of eggs from *Macrobrachium rosenbergii* in relation to embryonic development, Comp. Biochem. Physiol. B: Comparative Biochemistry 96 (1990) 505-511.

[27] P. Roustaian, M.S. Kamarudin, H. Omar, C.R. Saad, M.H. Ahmad, Changes in fatty acid profile during larval development of freshwater prawn *Macrobrachium rosenbergii* (de Man), Aquacult. Res. 30 (1999) 815-824.

[28] R.O. Cavalli, T. Montakan, P. Lavens, P. Sorgeloos, Variations in lipid classes and fatty acid content in tissues of wild *Macrobrachium rosenbergii* (de Man) females during maturation, Aquaculture 193 (3-4) (2000) 387-402.

[29] B.S. Middleditch, S.R. Missler, H.B. Hines, J.P. Mcvey, A. Brown, D.J. Ward, et al., Metabolic profiles of penaeid shrimp: dietary lipids and ovarian maturation, J. Chromatogr 195 (1980) 359-368.

[30] S. Teshima, A. Kanazawa, S. Koshio, K. Horinouchi, Lipid metabolism of the prawn *Penaeus japonicas* during maturation: variation in lipid profiles of the ovary and hepatopancreas, Comp. Biochem. Physiol. B: Comparative Biochemistry 92 (1989) 45-49.

[31] O.M. Millamena, F.P. Pascual, Tissue lipid content and fatty acid composition of *Penaeusmonodon* Fabricius broodstock from the wild, J. World Aquacult. Soc. 21 (1990) 116-121.

[32] V.R. Alava, A. Kanazawa, S. Teshima, S. Sakamoto, Effect of dietary phospholipids and n-3 highly unsaturated fatty acids on ovarian development of kuruma prawn, Nippon Suisan Gakkaishi 59 (1993) 345-351.

[33] C. Cahu, J.C. Guillaume, J. Stéphan, L. Chim, Influence of phospholipid and highly unsaturated fatty acids on spawning rate and egg and tissue composition in *Penaeus vannamei* fed semi-purified diets, Aquaculture 126 (1994) 159-170.

[34] M.L. Lilly, N.R. Bottino, Identification of arachidonic acid in Gulf of Mexico shrimp and degree of biosynthesis in *Penaeus setiferus*, Lipids 16 (1981) 871-875.

[35] X.L. Xu, W.J. Ji, J.D. Castell, R.K. O'dor, Influence of dietary lipid sources on fecundity, egg hatchability and fatty acid composition of Chinese prawn (*Penaeus chinensis*) broodstock, Aquaculture119 (1994) 359-370.

[36] R.G. Ackman, Composition and nutritive value of fish and shellfish lipids, fish and fisheries products, composition, nutritive properties and stability, in: A. Ruiter (Ed.), CAB International, 1995, pp. 117-156.

[37] M. Pirini, P.P. Gatta, S. Testi, G. Trigari, P.G. Monetti, Effect of refrigerated storage on muscle lipid quality of sea bass (*Dicentrarchus labrax*) fed on diets containing different levels of vitamin E, Food Chemestry 68 (2000) 289-293.

[38] J. Surh, J.S. Ryu, H. Kwon, Seasonal variations of fatty acid compositions in various Korean shellfish, Journal of Agriculture and Food Chemestry 51 (2003) 1617-1622.

[39] J.R. Sargent, Origins and functions of egg lipid, in: N.R. Bromage, R.J. Roberts (Eds.), Broodstock Management and Egg and Larval Quality, Blackwell, Oxford, 1996, pp. 353-372.

[40] D.J. Mckenzie, G. Piraccini, M. Piccolella, J.F. Steffensen, C.L. Bolis, E.W. Taylor, Effects of dietary fatty acid composition on metabolic rate and responses to hypoxia in the European eel (*Anguilla anguilla*), Fish Physiology and Biochemistry 22 (2000) 281-296.

[41] V. Bartulovie, D. Lueie, A. Conides, B. Glamuzina, J. Duleie, D. Hawner, et al., Food of sand smelt, *Atherina boyeri* Risso, 1810 (Pisces: Atherinidae) in the estuary of the Mala Neretva River (middle-eastern Adriatic, Croatia), Scientia Marina 68 (2004) 597-603.

[42] G.M. Piggott, B.W. Tucker, Effects of technology on nutrition, Liver in Japanese catfish (*Silurus asotus*), New York: Marcel Dekker, Comp. Biochem. Physiol. B: Comparative Biochemistry 129 (1990) 185-195.

[43] M. Buzzi, R.J. Henderson, J.R. Sargent, Biosynthesis of DHA acid in trout hepatocytes proceeds via 24 carbon intermediates, Comp. Biochem. Physiol. B: Biochem. Mol. Biol. 116 (2) (1997) 263-267.

[44] Ap. Simopoulos, Summary of NATO advanced research workshop on dietery n-3 and n-6 fatty acids: Biological effects nutritional essentiality, Journal of Nutrition 199 (1989) 512-528.

[45] J.E. Kinsella, B. Lokesh, R.A. Stone, Dietary n-3 polyunsaturated fatty acids and amelioration of cardiovascular disease: Possible mechanism, American Journal of Clinical Nutrition 52 (1990) 1-28.

[46] G.J.M. Coetzee, L.C. Hoffman, Effects of various dietary n-3/n-6 fatty acid ratios on the performance and body composition of broilers, South African Journals of Animal Sciences 32 (2002) 175-184.

[47] A.P. Simopoulos, Omega-3 fatty acids in health and disease and in growth and development, American Journal of Clinical Nutrition 54 (1991) 463-483.

Journal of Life Sciences 5 (2011) 1072-1077

New Silver Nanosensor for Nickel Traces: Synthesis, Characterization and Analytical Parameters

María Carolina Talio[1], Marta O. Luconi[2] and Liliana P. Fernández[1, 2]

1. Chemical Institute of San Luis (INQUISAL-CONICET), Chacabuco y Pedernera, San Luis 5700, Argentina

2. Area of Analytical Chemistry, Faculty of Chemistry, Biochemistry and Pharmacy, Nacional University of San Luis, San Luis 5700, Argentina

"In memoriam" of Dr. Adriana Masi, prominent researcher, dear colleague and friend, who passed away prematurely, as a consequence of public insecurity, killed by a shot in the head at the door of her house.

Received: June 14, 2011 / Accepted: July 22, 2011 / Published: December 30, 2011.

Abstract: A new fluorescence silver nanosensor assisted by surfactant has been synthesized and applied to ultra trace nickel determination. Operational variables which influence nanomaterial synthesis have been studied and optimized. Synthesis was very fast and simple using non polluting solvents; silver chemical reduction was carried out at room temperature. Spectroscopic studies were carried out in order to assure the uniformed of nanomaterial obtained. Fluorescent signal of silver nanoparticles resulted enhanced in presence of Ni(II). At optimal experimental conditions, a detection limit of 0.036 $pg \cdot L^{-1}$ and quantification limit 0.12 $pg \cdot L^{-1}$ were obtained. The calibration sensitivity was 2×10^{14} $L \cdot pg^{-1} \cdot cm^{-1}$ for the new methodology, with a range of linearity of six orders of magnitude between 0.12 and 2.93×10^5 $pg \cdot L^{-1}$. The tolerance levels for potential interferent ions were studied with good results. The proposed methodology represents a promising approach for Ni(II) traces quantification due to its low operation cost, simplicity of instrumentation, high sampling speed and non-polluting solvents.

Key words: Fluorescence nanosensor, micellar silver nanoparticles, nickel traces.

1. Introduction

Silver nanoparticles (AgNPs) have acquired importance due to their unusual optical, electronic and chemical properties [1-3]. The spectral characteristics of silver nanoparticles are strongly dependent on their size, shape, interparticle spacing and environment [4]; therefore, the geometry of noble metal nanoparticles may provide important control on optical properties [5-7]. The characteristics of nanomaterials depend on the method employed in the synthesis [8-10]. A common difficulty of nanomaterials is related to the aggregation of colloids, which causes modifications in their optical properties [11]. Many efforts have been done to stabilize nanoparticles in solution and improve the reproducibility and performance of the synthesis step. The most common strategy for the formation of stable nanoparticles is the use of a protective agent, which prevents their aggregation through functionalization reactions [12]. In this respect, surfactants have been used with success [13-16].

It has been observed that the size distribution and stability of nanoparticles depend critically on the properties of the surfactant employed [17]. Sodium dodecyl sulphate (SDS), an anionic surfactant, has been shown to be a very appropriate capping agent [18].

In this work, a fluorescence sensitive nanosensor is presented as an advantageous alternative to traditional instrumental methods. AgNPs are synthezised in SDS medium (SDS-AgNPs) and the obtained nanomaterials are applied to trace nickel quantification.

Correponding author: Liliana P. Fernández, chemical doctor, research fields: luminescent methods and supramolecular systems. E-mail: lfernand@unsl.edu.ar.

2. Experimental

2.1 Reagents

Ni(II) stock solutions 1×10^{-9} mol·L^{-1} were prepared by dilution of 1,000 μg·mL^{-1} standard solution plasma-pure (Leeman Labs, Inc.). Tris (Mallinckrodt Chemical Works, NY, USA) solution 1×10^{-2} mol·L^{-1} was prepared by weighting and subsequent dilution with ultrapure water and adjusted to the desired pH, with aqueous $HClO_4$ (Merck, Darmstadt, Germany) or NaOH (Mallinckrodt Chemical Works, NY, USA). $AgNO_3$ (Sigma-Aldrich, St. Louis, USA) 1×10^{-3} mol·L^{-1} was prepared by dilution of 17 mg in 100 mL ultrapure water. Citric acid (Hopkin and Williams, England), hexadecyltrimethylammonium bromide (J.T. Baker, Mallinckrodt Baker, Inc., NJ, USA) and sodium dodecylsulfate (J.T. Baker, Mallinckrodt Baker, Inc., NJ, USA) were used without further purification. All used reagents were of analytical grade.

2.2 Apparatus

Fluorescence measurements were made using a Shimadzu RF-5301 PC spectrofluorometer equipped with a 150 W Xenon lamp and 1.00 cm quartz cells. A combined glass electrode and a pH meter (Orion Expandable Ion Analyzer, Orion Research, Cambridge, MA, USA) Model EA 940 were used for pH adjustments. A centrifuge was used in AgNPs purification. All used glass materials were previously washed with a 10% v/v HNO_3 water solution and then with ultrapure water.

2.3 Micellar AgNPs Synthesis and Purification

0.5 g SDS were dissolved in 4 mL $AgNO_3$ 1×10^{-3} mol·L^{-1}. Immediately, 0.5 g citric acid was added. The reacting mixture was vigorously stirred for 1 min at room temperature and then put into 15 mL centrifuge tube and centrifuged for 10 min at approximately 1,000 g. The rinsing step was repeated three times to remove excess of reagents. Sediments containing SDS-AgNPs were redissolved in 5 mL absolute ethanol.

2.4 Proposed Methodology

Appropriate aliquots of standard solution Ni(II) (1.2×10^{-4}-2.93×10^{2} ng·L^{-1}), 100 μL buffer Tris solution 1×10^{-2} mol·L^{-1} (pH = 6.3) and 500 μL of synthesized SDS-AgNPs, were placed in a 10 mL graduated centrifuge tube. The whole mixture was diluted to 3 mL with ultrapure water. Fluorescent emission was measured at λ_{em} = 348 nm using λ_{exc} = 240 nm.

2.5 Interferences Study

Different amounts of common ions were added to the test solution containing 5.81 ng·L^{-1} of Ni(II) and the proposed methodology was applied.

3. Results and Discussion

3.1 Spectral Study of Synthesized Micellar Ni(II) Nanosensor

Optical absorption spectrum of silver nanoparticles is a good indicator of their size and shape. The plasmon absorption of synthesized nanoparticles in the visible region presented an absorption maximum in the 440 nm region (Fig. 1), in agreement with other studies [19-21]. Spectral studies of the synthesized nanomaterial were performed by fluorescent spectroscopy. The nanosized colloids presented an excitation and emission maximum at 240 and 348 nm, respectively (Figs. 2a and 2b). In presence of nickel traces, the AgNPs fluorescent signal showed a notable increase (Figs. 2c-2e), which was validated scanning blank solutions (SDS solution; citric acid solution; Ni(II) + SDS solution; Ni(II) + citric acid solution). For consigned systems, there were no fluorescent signals.

This spectral behavior could be justified by the postulation of an association between the SDS-AgNPs (negatively charged) and nickel ions by electrostatic interaction. The association thus formed presents a more rigid configuration, minimizing the nonradiative deactivation phenomena and promoting the fluorescent emission.

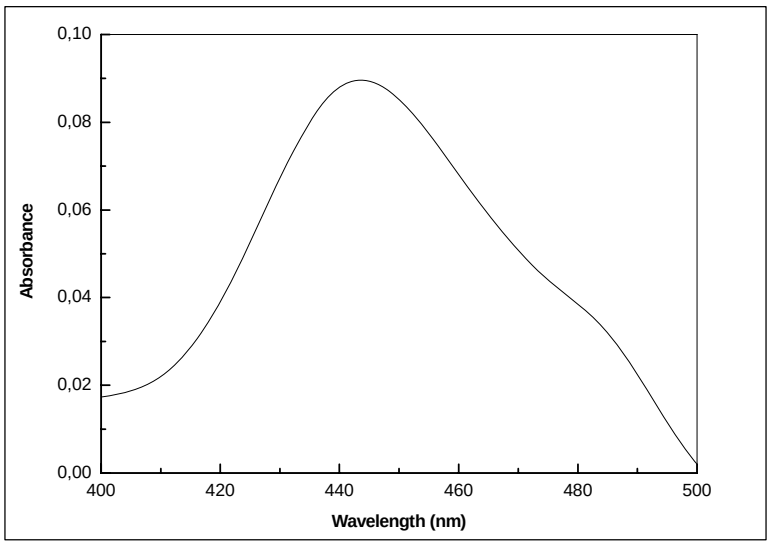

Fig. 1 Absorption spectrum of synthesized SDS-AgNPs.

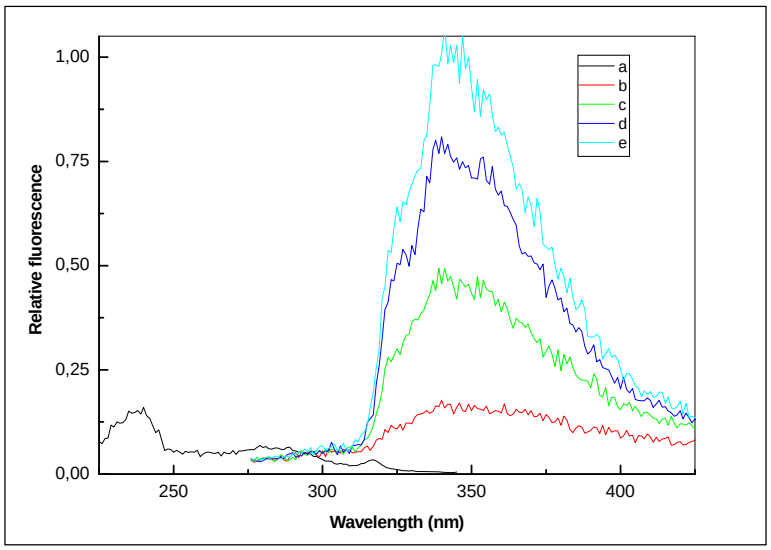

Fig. 2 Excitation and fluorescent emission spectra of SDS-AgNPs and Ni(II)-SDS-AgNPs systems.
a: Excitation spectrum of SDS-AgNPs (λ_{em} = 348 nm); b: Emission spectrum of SDS-AgNPs (λ_{exc} = 240 nm); c: Idem b with Ni(II) 2.60 ng·L^{-1} (λ_{exc} = 240 nm); d: Idem b with Ni(II) 4.73 ng·L^{-1} (λ_{exc} = 240 nm); e: Idem b with Ni(II) 5.81 ng·L^{-1} (λ_{exc} = 240 nm).

In order to find the optimum experimental conditions for trace nickel determination, parameters affecting the synthesis and association reaction between Ni(II) and AgNPs were investigated.

3.2 AgNPs Synthesis Optimization and Its Luminescent Response in Presence of Ni(II)

Table 1 shows fluorescent intensity of synthesized AgNPs in presence of SDS (anionic surfactant) and CTAB (cationic surfactant), at three different reaction times. The results indicated that the fluorescent characteristics of AgNPs were not influenced by this parameter. However, there were well marked differences between the fluorescence intensities of the AgNPs assisted by different surfactants, being the highest that obtained in presence of SDS.

In order to optimize the fluorescent signal of obtained AgNPs, synthesis reactions were carried out

Table 1 Surfactant assisted AgNPs, time of reaction and fluorescent response without and with Ni(II).

Parameter	Fluorescence intensity	
	SDS	CTAB
Reaction time (min)		
1.0	47.21	22.01
2.5	47.52	20.10
5.0	48.01	21.80
Surfactant concentration		
250 CMC	20.74	12.77
500 CMC	47.65	18.55
1,000 CMC	18.85	11.68
With Ni(II)		
250 CMC + 77 ng·L^{-1}	20.56	13.21
250 CMC + 102 ng·L^{-1}	21.44	12.04
500 CMC + 77 ng·L^{-1}	190.33	15.44
500 CMC + 102 ng·L^{-1}	236.84	18.95
1,000 CMC + 77 ng·L^{-1}	20.9	12.03
1,000 CMC + 102 ng·L^{-1}	17.65	10.57

at different surfactant concentration levels. Best results were obtained when using 500 × critical micellar concentration (CMC) for surfactant SDS, in agreement with previous reports [18].

The AgNPs resulting from synthesis in the different surfactant media were explored in presence of increasing Ni(II) concentrations. Luminescent responses indicated that SDS-AgNPs are adequate for trace Ni(II) detection.

In order to establish the adequate SDS-AgNPs volume for Ni(II) determination, experiments were carried out keeping other variables constant. Results are shown in Fig. 3. A volume of SDS-AgNPs of 500 μL was chosen for the following assays.

3.3 Influence of pH on Ni(II) Nanosensor Fluorescent Response

Taking into account that pH plays a important role on the formation of metallic associations, the luminescent response of the Ni(II)-SDS-AgNPs system was evaluated at different pH values (Fig. 4). A plateau was obtained at pH between 6.0 and 7.0. Due to this behavior, pH 6.3 was selected as the working value for the following experiments.

In acidic medium, protons compete effectively with Ni(II) for bonding sites of SDS-AgNPs. On the other hand, in alkaline medium, the interaction between Ni(II) and SDS-AgNPs is hindered by the presence of hydroxile ions.

3.4 Order of Reagents Addition

The best order of reagent addition proved to be SDS-AgNPs, buffer Tris and Ni(II). The complex was stable for at least 12 h.

3.5 Influence of Nature and Concentration of Buffer

Effects of different buffers on the fluorescent Ni(II)-SDS-AgNPs system were tested. The most enhanced fluorescent emission was obtained for buffer Tris. The system was studied within a Tris concentration range from 5×10^{-3} to 4×10^{-2} mol·L^{-1}. Best stability and sensitivity were achieved for a Tris concentration of 1.1×10^{-2} mol·L^{-1}.

3.6 Interferences Study

The effect of foreign ions on Ni(II) determination was tested. An ion was considered as interferent when it caused a variation in the fluorescent signal of the analyte greater than ± 5%. At optimal conditions, Na^+, K^+ can be present at 1,000:1 excess to Ni(II) without interfering; Fig. 5 and Table 2 show the obtained tolerance results for a group of regular ions. Considering these results, it can be concluded that the proposed methodology exhibits an adequate tolerance.

Table 2 Study of anions interferences.

Anion	Tolerated interferent/Ni(II) ratio	Fluorescent emission	% RE[a]
CO_3^{2-}	1,000/1	41.52	0.09
SO_4^{2-}	1,000/1	41.48	0.01
NO_3^-	1,000/1	42.21	1.76
$CH3COO^-$	1,000/1	41.35	0.30
Cl^-	1,000/1	42.03	1.33
Br^-	1,000/1	40.59	- 2.15
F^-	100/1	43.05	3.77

[a]: 100 × relative error; Ni (II): 5.81 ng·L^{-1}; other experimental conditions are described in the manuscript.

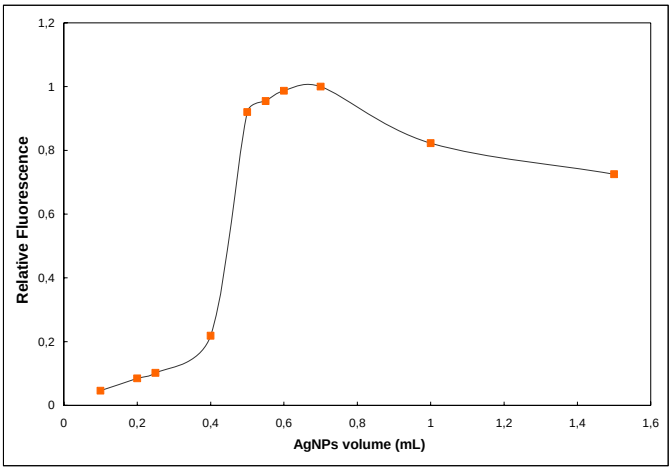

Fig. 3 Optimization of volume of SDS-AgNPs.

Experimental conditions: Ni (II) 5.81 ng·L^{-1}; pH = 6.3 buffer Tris; λ_{em} = 348 nm and λ_{exc} = 240 nm.

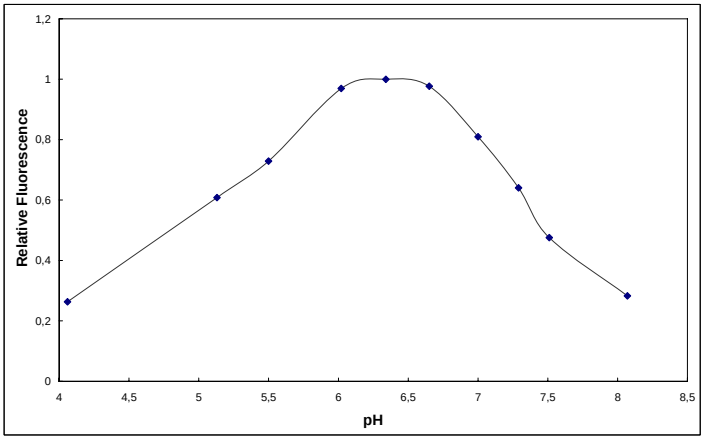

Fig. 4 Influence of pH on fluorescent emission of Ni(II)-SDS-AgNPs.

Experimental conditions: Ni(II) 5.81 ng·L^{-1}; SDS-AgNPs volume 0.5 mL; λ_{em} = 348 nm and λ_{exc} = 240 nm.

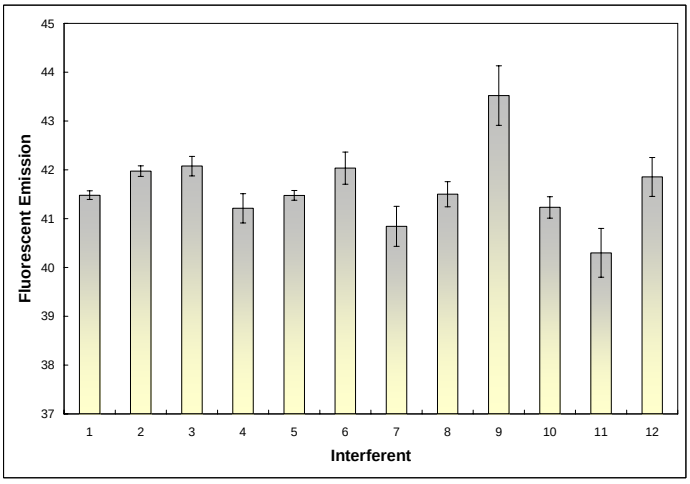

Fig. 5 Tolerances of cations in (interferent/Ni(II)) ratio for Ni(II)-SDS-AgNPs system, for each interferent, %SD has been included.

Fluorescence signal ± SD. 1: Ni(II) 5.81 ng·L^{-1}; 2: Ni(II) in presence of K(I); interferent/Ni(II) ratio 1,000/1; 3: Idem 2 for Na(I); 4: Ni(II) in presence of Cu(II); interferent/Ni(II) ratio 100/1; 5: Idem 4 for Pb(II); 6: Idem 4 for Zn(II); 7: Idem 4 for Mg(II); 8: Idem 4 for Mn(II); 9: Idem 4 for Co(II); 10: Idem 4 for Cd(II); 11: Idem 4 for Ca(II); 12: Idem 4 for Fe(III).

4. Conclusion

In the present work a surfactant assisted fluorescent nanosensor has been synthesized. The enhancement of AgNPs fluorescent signal in presence of Ni (II) has been proposed for ultra trace nickel quantification. The method showed good sensitivity and adequate tolerance to foreign constituents. The proposed methodology may constitute a promising approach in the area of metal monitoring with low operation costs, simplicity of instrumentation, high sampling speed and non-polluting solvents.

Acknowledgments

The authors wish to thank to Instituto de Química San Luis-Consejo Nacional de Investigaciones Científicas y Tecnológicas (INQUISAL-CONICET), National University of San Luis (Proyect 22/Q828) for the financial support.

References

[1] S. Schultz, D. Smith, J. Mock, D. Schultz, Single-target molecule detection with nonbleaching multicolor optical immunolabels, Proc. Natl. Acad. Sci. U.S.A. 97 (2000) 996-1001.

[2] T. Taton, C. Mirkin, R. Letsinger, Scanometric DNA array detection with nanoparticle probes, Science 289 (2000) 1757-1760.

[3] S. Kalele, A.C. Deshpande, S.B. Singh, S.K. Kulkarni, Tuning luminescence intensity of RHO6G dye using silver nanoparticles, Bull. Mater. Sci. 31 (2008) 541-544.

[4] C. Rao, G. Kulkarni, P. Thomas, P. Edwards, Size-dependent chemistry: Properties of nanocrystals, Chem. Eur. J. 8 (2002) 28-35.

[5] C.J. Espinoza González, Propiedades físicas y químicas de partículas metálicas de tamaño nanométrico, Nanopartículas de Plata (Physical and chemical properties of nanometric metalic particles, silver nanoparticles,), Diseño de Materiales Poliméricos Avanzados (Design of Advanced Polymeric Materials) 6 (2007) 23-27. (in Spanish with English abstract)

[6] Z. Jiang, W. Yuan, H. Pan, Luminescence effect of silver nanoparticle in water phase, Spectrochim. Acta Part A 61 (2005) 2488-2494.

[7] S. Pramanik, S.C. Bhattacharya, T. Imae, Fluorescence quenching of 3,7-diamino-2,8-dimethyl-5-phenyl phenazinium chloride by AgCl and Ag nanoparticles, J. Lumin. 126 (2007) 155-159.

[8] L. Balan, J. Malval, R. Schneider, D. Burget, Silver nanoparticles: New synthesis, characterization and photophysical properties, Mat. Chem. Phys. 104 (2007) 417-421.

[9] A. Pyatenko, M. Yamaguchi, M. Suzuki, Laser photolysis of silver colloid prepared by citric acid reduction method, J. Phys. Chem. B 109 (2005) 21608-21611.

[10] Y. Luo, X. Sun, Rapid, single-step preparation of dendrimer-protected silver nanoparticles through a microwave-based thermal process, Mater. Lett. 61 (2007) 1622-1624.

[11] M. Treguer, F. Rocco, G. Lelong, A.L. Nestour, T. Cardinal, A. Maali, et al., Fluorescent silver oligomeric clusters and colloidal particles, Solid State Sci. 7 (2005) 812-818.

[12] C. Rao, G. Kulkarni, P. Thomas, P. Edwards, Metal nanoparticles and their assemblies, Chem. Soc. Rev. 29 (2000) 7-35.

[13] X. Xingwei, Y. Ruqiang, L. Honglai, Synthesis of silver nanoparticles in reverse micelles stabilized by natural biosurfactant, Colloids and Surfaces A: Physicochem. Eng. Aspects 279 (2006) 175-178.

[14] D. Sik Bae, E. Jung Kim, J. Hee Bang, S. Woo Kim, K. Sop Han, J. Kyu Lee, et al., Synthesis and characterization of silver nanoparticles by a reverse micelle process, Met. Mater. Int. 11 (2005) 291-294.

[15] N. Wang , H.F. Yang , X. Zhu, R. Zhang, Y. Wang, G.F. Huang, et al., Synthesis of anti-aggregation silver nanoparticles based on inositol hexakisphosphoric micelles for a stable surface enhanced Raman scattering substrate, Nanotechnology 20 (2009) doi: 10.1088/0957-4484/20/31/315603.

[16] S.A. Al-Thabaiti, F.M. Al-Nowaiser, A.Y. Obaid, A.O. Al-Youbi, Z. Khan, Formation and characterization of surfactant stabilized silver nanoparticles: A kinetic study, Colloids. Surfaces B: Biointerfaces 67 (2008) 230-237.

[17] F. Mafune, J. Kohno, Y. Takeda, T. Kondow, H. Sawabe, Structure and stability of silver nanoparticles in aqueous solution produced by laser ablation, J. Phys. Chem. B 104 (2000) 8332-8337.

[18] Z. Li, A. Gu, Q. Zhou, Growth of spindle-shaped silver nanoparticles in SDS solutions, Cryst. Res. Technol. 44 (2009) 841-844.

[19] T. Itakura, K. Torigoe, K. Esumi, Preparation and characterization of ultrafine metal particles in ethanol by UV irradiation using a photoinitiator, Langmuir 11 (1995) 4129-4134.

[20] P.K. Khanna, N. Singh, D. Kulkarni, S. Deshmukh, S. Charan, P.V. Adhyapak, Water based simple synthesis of re-dispersible silver nano-particles, Mater. Lett. 61 (2007) 3366-3370.

[21] C.C. Wang, M.O. Luconi, A.N. Masi, L.P. Fernández, Derivatized silver nanoparticles as sensor for ultra-trace nitrate determination based on light scattering phenomenon, Talanta 77 (2009) 1238-1243.

Journal of Life Sciences 5 (2011) 1078-1084

Advance of Study on SSR Molecular Marker in *Citrus* and Its Close Relatives

Xue-Fei Wang, Zhi-Hui Wang, Xi-Rui Xiong, Qiao-Qiao Yan and Xue-Li Pu

College of Horticulture, Sichuan Agricultural University, Xinkang Road No. 46, Ya'an City, Sichuan 625014, China

Received: July 09, 2011 / Accepted: September 14, 2011 / Published: December 30, 2011.

Abstract: Simple sequences repeat (SSR) molecular maker, as a new type of DNA molecular marker, the second generation based on the polymerase chain reaction (PCR), is valuable and of great potential as genetic markers for its characteristics of abundant quantity, high polymorphic, reproducibility, specific site amplification, high occurring frequency, and co-dominant inheritance etc. This paper outlined its principles and characteristics, and introduced its application to variety identification, phylogenetic relationship analysis, genetic diversity analysis, DNA fingerprinting and linkage map constructing etc. in recent years in *Citrus* and its close relatives.

Key words: *Citrus*, SSR, variety identification, phylogenetic relationship analysis, genetic diversity analysis, DNA fingerprinting, linkage map constructing.

1. Introduction

Simple sequences repeat (SSR), which were discovered by Hamad in cardiac muscle action gene in human [1], are short (1-6 bp) tandem DNA sequences repeat [2]. It has been demonstrated that SSR are ubiquitously and randomly distributed in eukaryote genome but can also be found to a lesser extent in prokaryote genome [3]. SSR molecular marker, also known as microsatellites, was found by Moore in 1991 [4]. At present, it has been widely applied to variety identification [5], phylogenetic relationship analysis [6], genetic diversity analysis [7], DNA fingerprinting constructing [8, 9], linkage map constructing [10] and gene locating [11] etc in fruit trees.

Citrus and its close relatives are represented by 28 genera in the tribe Citreae of the subfamily Aurantioideae in the family Rutaceae [12]. Before the advent of molecular data, *Citrus* was classified based on morphology or biochemical techniques such as isozymes. Currently, there are two commonly used classifications of *Citrus*: Swingle et al. [12] and Tanaka [13]. The Swingle system recognizes 16 species in the genus *Citrus*, whereas the Tanaka system recognizes 162 species in the genus *Citrus*. Scora [14] and Barrett & Rhodes [15] suggests that there are only three "basic" true species of *Citrus* within the subgenus *Citrus* as defined by Swingle: citron (*C. medica* L.), mandarin (*C. reticulata* Blanco), and pummelo (*C. maxima* L. Osbeck). Other cultivated *Citrus* species within the subgenus *Citrus* are believed to be hybrids derived from these true species, species of the subgenus *Papeda*, or closely related genera. This idea has gained support in recent years from data derived from molecular markers [16, 17].

2. The Principles and Characteristics of SSR Molecular Marker

2.1 The Principles of SSR Molecular Marker

There are relatively conservative sequences at two poles of SSR, which are single-copy. For this we can design a pair of specific primers to use SSR-PCR to

Corresponding author: Zhi-Hui Wang, Ph.D., associate professor, research fields: plant physiology and molecular biology technology. E-mail: wangzhihui318@126.com.

amplify tandem sequences repeat, and amplify fragment polymorphism via electrophoresis. Then according to the number of tandem repeat, we analyze their corresponding genetic characteristics, and reveal the length polymorphism of microsatellites DNA [18], the number of SSR, the repetitions and basic units of SSR, and the copy number of variation as well as their distribution in chromosomal vary species [19].

2.2 The Characteristics of SSR Molecular Marker

SSR usually inspect a single locus. The amount of SSR, covering the whole genome, is in abundance and evenly distributes. Most of them are non-functional and polymorphic, and have a wide variation of loci among variety. Both two sides of them are conservative sequences and nearly the same in the same species and among different genetic types. SSR molecular marker abides by co-dominant inheritance, and accords with Mendel inheritance. It directly represents in the form of DNA, and is limited little. Its loci are specific and easy to be analyze based on PCR. It demands low quantity and purity of DNA. It has good reproducibility, reliability, and neutral performs, and does not affect the expression of target traits, besides, it not necessarily links with the bad traits [20].

And SSR molecular marker has more advantages, compared to other frequently used DNA molecular markers, which is shown in Table 1.

3. The Application of SSR in *Citrus*

3.1 Variety Identification

Formerly, identifying *Citrus* and its close relatives was based on plant morphology and fruit shape features, sometimes combined with cytological or physiological or biochemical characteristics. These approaches had limitation and were difficult to accurately identify *Citru*s and its close relatives or sort out. However, the DNA molecular markers came forth and could provide a lot of genetic information in the DNA level, which were effective to identify *Citrus* and its close relatives. And because of its high degree of polymorphism and reproducibility, SSR molecular marker was one of important molecular markers used for identifying plant and animal genotypes, including *Citrus* and its close relatives. Recently, Ruiz et al. [22] distinguished between zygotic and nucellar seedlings using SSR molecular marker and isozymic marker and compared them. They considered, in most cases, SSR molecular marker was more efficient than isozymic marker to identify the sexual origin of *Citrus* seedlings, given their higher level of polymorphism and the scarce number of polymorphic isozymes in some populations. Oliveira et al. [23] described the combined use of visual selection based on the leaf apex morphology and SSR molecular marker to differentiate hybrid from nucellar seedlings derived from the cross between the “Murcott” tangor [*Citrus reticulata* Blanco × *Citrus sinensis* (L.) Osb.] and “Pêra” sweet orange [*Citrus sinensis* (L.) Osb.]. Putative hybrid seedlings were confirmed through the analysis of SSR molecular marker. They considered that the combination of visual selection and SSR molecular marker for the identification of hybrids derived from the cross of polyembryonic *Citrus* cultivars could improve the accuracy of the selection, save time, and reduce the costs involved in the use of molecular markers alone in *Citrus* breeding programs. Li et al. [24] clarified the possible parentage of Zigui Tangor via ploidy analysis morphological markers and molecular markers including amplified fragment length polymorphism (AFLP) molecular marker, chloroplast simple sequence repeat (cpSSR) molecular marker, and SSR molecular marker. cpSSR and SSR molecular marker clearly showed that its female parentage was the sweet orange [*Citrus sinensis* (L.) Osb.] and its male parentage was the tangerine (*Citrus reticulata* Blanco). Han et al. [25] identified the hybrid nature of 159 offsprings from the two cross combinations of Shatian pummelo, and analyzed the genetic relationship between parents and offsprings with UPGMA. One hundred and three hybrids was identified from 104 F_1 seedlings of “Shatianyou” ×

Table 1 The trait of SSR and compared to other frequently used DNA molecular markers [21].

Trait	RFLP	RAPD	SSR	ISSR	ARLP
Heredity patten	Co-dominance	Dominance	Co-dominance	Dominance	Dominance
Polymorphic	Low	Mean	High	High	High
Position spot for analyzing	1-4	1-10	1	40-100	20-150
Repeat	High	Low	High	Mean	High
DNA quality request	High	Low	Low	Low	High
DNA dosage	5-10 μg	< 50 ng	50 ng	< 50 ng	250 ng-5 μg
Technology request	High	Low	High	Low	High
Time	Long	Short	Short	Short	Mean
Cost	High	Low	High	Mean	High

"Chandler" pummelo by 4 pairs SSR primers, and 70 progenies had non-parent markers in primer AGC9. All offsprings from "Shatianyou" × "Hongjiangcheng" were proved to be hybrids with 5 pairs SSR primers, one homozygous maker AAT 12 was obtained, and some markers were absent in 55 F_1 seedlings in primer GA18 and AGC9. The cluster analysis of SSR data indicated that the genetic variation of hybrids from the two cross combinations was obviously, and the genetic diversity between the two combinations of crosses was obviously different.

3.2 Phylogenetic Relationship Analysis in Citrus

Before, phylogenetic relationship analysis, which was not accurate, was mostly based on plant morphology, cytologic，physiological or biochemical (such as isozymic marker) characteristics. For now, molecular markers were widely used for analyzing phylogenetic relationship, including SSR molecular marker. Pang et al. [26] investigated phylogenetic relationship among 29 accessions belonging to *Citrus*, *Poncirus*, *Fortunella*, *Microcitrus*, *Eremocitrus*, *Atlantia* and *Severinia* by 7 primer pairs of SSR molecular marker. Cluster analysis via neighbor-joining method showed that *Microcitrus* was close to *Citrus*; *Poncirus* was distant from *Citrus*, which suggested that *Poncirus* could not be derived from *Citrus*. High frequency of the homozygous SSR locus supported the species status of Fumin trifoliate orange. Seperation of neither *Papeda* and *Citrus* nor *Archicitrus* and *Metacitrus* was well resolved. The present work confirmed citron, pummelo and mandarin as basic species of cultivated *Citrus* since they could be placed into three distinct clusters. Noelle et al. [27] utilized 24 primer pairs of SSR molecular marker to detect molecular polymorphisms among 370 mostly sexually derived *Citrus* accessions from the collection of *Citrus* germplasm maintained at the University of California, Riverside. Phylogenetic relationship among all *Citrus* accessions and putative non-hybrid *Citrus* accessions were determined by constructing neighbor-joining trees. There was strong support for morphology at the species level when hybrid taxa were removed from the data set. Both of these trees indicated that *Fortunella* clustered within the genus *Citrus* but *Poncirus* was a sister genus to *Citrus*. Zhang et al. [28] investigated phylogenetic relationship among 18 accessions belonging to *Fortunella* and *Citrus* by using SSR molecular marker. 14 pairs were selected from 22 primer pairs of SSR molecular marker, which were used in *Citrus* before. Cluster analysis via NTSYS-PC software showed that *Citrus* was close to *Fortunella*. The results of SSR molecular marker supported that the species status of Changshou kumquat; the Ningbo kumquat, Rong' an kumquat and Lanshan kumquat were the same species of *Fortunella*; some of *Citrus* primer pairs of SSR molecular marker could be used in *Fortunella*. It can be used for preservation, breeding and classification in *Fortunella*.

Accordingly, SSR molecular marker has been successful in phylogenetic relationship analysis in *Citrus* and its close relatives.

3.3 Genetic Diversity Analysis in Citrus and Its Close Relatives

The genetic diversity is mainly the genetic variation summation of the same species but different populations or of the same population but different individuals. For the most importance, we should select the appropriate genetic markers to analyze genetic diversity. There are many natural hybrid types in *citrus*, and the new varieties of *Citrus* were breeding mainly via seedling selection, mutant selection or intercrossing pollen. So it was difficult to judge their parents. Therefore understanding the genetic background of *Citrus* was awfully helpful to select targeted parents to cultivate new varieties of *Citrus*, whose character are better. However, SSR molecular markers, who is polymorphic, widely used for genetic diversity analysis in fruit trees [29], including *Citrus* and its close relatives in recent years. Liu et al. [30] analyzed the genetic diversities of 110 accessions pummelo germplasms and 12 of their relatives by SSR and AFLP molecular marker. They showed that 122 accessions pummelo genotypes and their relatives could be divided into eight groups, and the pummelo genotypes composed mainly of Shatian pummelo varieties group, Wendan pummelo varieties group and a huge hybrid pummelo varieties group. The classification result was expected to widen the genetic background of pummelos using various target varieties. Cao et al. [31] assessed genetic diversity of 43 accessions of male sterile, low fertile, containing sterile cytoplasm and 13 fertile ones in *Citrus* by SSR molecular marker. Cluster analysis showed that three groups could be obtained from those accessions. The cultivars of mandarin were classified into group 1; those of sweet orange, grapefruit, ponkan or tangor into group 2; *Microcitrus* with male sterile cytoplasm into group 3. Cluster analysis also revealed that satsuma mandarin had closer relatedness with Bendiguangju mandarin than with Zaoju, Manju, Bendizao tangerine. Noelle et al. [27] utilized twenty-four primer pairs pf SSR molecular marker to detect molecular polymorphisms among 370 mostly sexually derived *Citrus* accessions from the collection of *Citrus* germplasm maintained at the University of California, Riverside. Genetic diversity statistics were calculated for each individual SSR molecular marker, the entire population, and for specified *Citrus* groups. Gong et al. [32] analyzed the genetic diversity and phylogenetic relationship of 28 accessions of trifoliate orange (*Poncirus trifoliata* Raf.), hybrids and seven accessions of its relatives by SSR molecular marker and cpSSR molecular marker. The SSR molecular marker result showed a rich genetic diversity of China trifoliate orange germplasm. Fumin trifoliate orange was genetically distant from common trifoliate orange, from its hybrids as well as relatives. Therefore it could be regarded as a true species. Jannati et al [33] estimated the level of polymorphism among 23 *Citrus* genotypes and 4 natural hybrids or bud mutation selected from Kotra Germplasm Bank (IRAN) by fifteen primer pairs of SSR molecular marker. All fifteen loci assayed in *Citrus* plant possessed a high level of polymorphism. Cluster analysis with SSR molecular marker resulted in 2 cluster groups: Group A: Yuzo and *Poncirus*. Group B: There were three separate subgroups within Group B; (i) genus *Fortunella* sp. (ii) Mandarin subgroup: *Citrus reticulate (Citrus clemantin)*, *Citrus sinensis* (Pineapple, Washington Navel), Natural types (Siahvaraz, Shalmahaleh, Moallemkoh and Kotra 4 hybrids) and (iii) *Citrus Limon* (Amol lemon-pear, Eureka, Rough Lemon), *Citrus aurantifolia*, *Citrus aurantium*, *Citrus medica* and *Citrus grandis*. SSR molecular marker clustered citron and sour orange cv cluster but these taxa were quiet distant from *Fortunella* sp.. Xiang et al. [34] studied genetic diversity of 7 induced or natural polyploid samples of Shatianyou pomelo (*Citrus grandis* var. Shatianyou

Osbeck.) by using SSR molecular marker with 21 pairs of primers. SSR molecular marker Cluster analysis showed that they were partitioned with 3 types. Type Ⅰ: natural tetraploids; type Ⅱ: induced tetraploids and natural triploid; type Ⅲ: the diploid. The genetic similarity between natural triploid and the diploid was higher than that between tetraploid especially natural autotetraploid and the diploid. Natural and artificial tetraploids could be distinguished by 4 pairs of primers (CAT01, TAA33, AG14 and TC26). According to the results of SSR bands there was DNA variation of natural triploid natural and induced tetraploids of Shatianyou that had new bands and bands deleted with corresponding diploid.

Consequently, SSR molecular marker has been successful in genetic diversity analysis in *Citrus* and its close relatives.

3.4 DNA Fingerprinting and Linkage Map Constructing in Citrus and Its Close Relatives

Constructing a DNA fingerprinting database of major *Citrus* cultivars could provide a possibility of establishment of a technical standard system for purity and authenticity identification of *Citrus* nursery trees. Lei et al. [35] used SSR molecular marker and ISSR molecular marker to analyze the DNA fingerprinting of 102 accessions *Citrus* cultivars (lines) and then to choose suitable primers for the construction of DNA fingerprinting database of *Citrus* cultivars (lines). 12 primer pairs of SSR molecular marker, with high polymorphisms and good repeatability, regarded as specific primers, which could identify 42 accessions cultivars (lines), were selected from 200 primer pairs of SSR molecular marker. A total of 70 accessions *Citrus* cultivars (lines) could be identified by 12 SSR and 2 ISSR primer pairs of SSR molecular marker. Finally, a DNA fingerprinting database containing 70 accessions major *Citrus* cultivars (lines) was constructed by those 12 SSR and 2 ISSR primer pairs. The results indicated that SSR and ISSR molecular marker were suitable for the construction of DNA fingerprinting database of *Citrus* cultivars (lines).

For a long time, most of genetic linkage maps constructing were based on their morphology, physiological or biochemical indicators. Most of them were still low resolution, large figure distance, and low saturation, which limited their application. In recent years, genetic linkage maps of the species were higher and higher density, which were constructed by DNA molecular markers and sometimes combined with a number of isozyme markers or morphological markers. So SSR molecular marker was very useful for building high-density genetic linkage maps. Gulsen et al. [36] used a population of 164 F_1 individuals derived between “Clementine” mandarin (*Citrus reticulata* Blanco “Clementine”) and “Orlando’ tangelo” (*C. paradisi* Macf. “Duncan” 9 × *C. reticulate* Blanco “Dancy”) to establish genetic linkage map of *Citrus*. A total of 609 markers, including 385 Sequence-related amplified polymorphism (SRAP), 97 randomly amplified polymorphic DNA (RAPD), 95 simple sequence repeats (SSR), 18 inter-simple sequence repeats (ISSR), 12 peroxidase gene polymorphism (POGP), and 2 resistant gene analog (RGA) markers were used in linkage analysis. The “Clementine” linkage map has 215 markers, comprising 144 testcross and 71 intercross markers placed in nine linkage groups. The “Clementine” linkage map covered 858 cM with and average map distance of 3.5 cM between adjacent markers. The “Orlando” linkage map has 189 markers, comprising 126 testcross and 61 intercross markers placed in nine linkage groups. The “Orlando” linkage map covered 886 cM with an average map distance of 3.9 cM between adjacent markers.

4. Conclusion

In summary, though its application in genetic research of *Citrus* and its close relatives is still in its infancy at present，SSR molecular marker has a promising prospect, which was considered the best

way to study the variation of population. However, any molecular markers can not solve all the problems in genetic research. Sometimes we should use at least two or more markers to study molecular polymorphic markers. With a comparative result, the reliability of the results can be increased. And it is difficult to develop the primers of SSR molecular marker, which has hindered the development of its application in *Citrus* and its close relatives or other fruit trees. If we could speed up the development of its primers, we will promote the innovation of *Citrus* and its close relatives germplasm and breeding new *Citrus* and its close relatives.

References

[1] H. Hamada, T. Kakunaga, Potential Z-DNA forming sequences are highly dispersed in the human genome, Nature 298 (1982) 396-398.

[2] D. Tautz, Hypervariability of simple sequence as a general source of polymorphic DNA markers, Nucleic Acids Research 17 (1989) 6463-6471.

[3] W. Powell, G.C. Machray, Polymorphism revealed by simple sequence repeats, Provan J. Source: Trends in Plant Science 1 (1996) 215-222.

[4] S.S. Moore, L.L. Sargeant, J.T. King, S.J. Mattick, M. Georges, D.J.S. Hetzel, The conservation of dinucleotide microsatellites amongmammalian genomes allows the use of heterologus PCR primer pairs in closely related species, Genomics 10 (1991) 654-660.

[5] J.I. Horamza, Molecular characterization and similarity relationships among apricot (*Prunus armeniaca* L.) genotypes using simple sequence repeats, Appl. Gente. 104 (2002) 321-328.

[6] M.A. Viruel, J.I. Hormaza, Development, characterization and variability analysis of microsatellites in lychee (*Litchi chinensis* Sonn., Sapindaceae), Theor. Appl. Genet. 108 (2004) 896-902.

[7] Y.F. Cao, F.Z. Liu, Y. Gao, L.J. Jiang, K. Wang, Z.Y. Ma, et al., SSR analysis of genetic diversity of pear cultivars, Acta Horticulturae Sinica 34 (2) (2007) 305-310.

[8] H. Akagi, Highly polymorphic microsatellites of rice consist of AT repeats and a classification of closely related cultivars with these microsatellite loci, Theor. Appl. Genet. 94 (1) (1997) 61-67.

[9] G.Y. Li, S. Dreisigacker, M.L. Warburton, X.C. Xia, Z.H. He, Q.X. Sun, Development of a fingerprinting database and assembling an SSR reference kit for genetic diversity analysis of wheat, Acta Agronomica Sinica 32 (12) (2006) 1771-1778.

[10] P. Lambert, L.S. Hangen, P. Arus, J.M. Audergon, Genetic linkage maps of two apriot cultivars (*Prunnus armeniaca* L.) compared with the almond Texas × peach Earlygold reference map for *Prunnus*, Theor. Appl. Genet. 108 (2004) 1120-1130.

[11] K. Rassmann, C. Schlotterer, D. Tautz, Isolation of simple sequence loci for use in polymerase chain reaction-based DNA fingerprinting, Electrophoresis 12 (1991) 113-118.

[12] W.T. Swingle, P.C. Reece, The botany of *Citrus* and its wild relatives, in: W. Reuther, H.J. Webber, L.D. Batchelor (Eds.), The *Citrus* Industry, University of California Press, Berkeley, 1967, pp. 190-430.

[13] T. Tanaka, Fundamental discussion of *Citrus* classification, Stud. Citrologia. 14 (1977) 1-6.

[14] R.W. Scora, On the history and origin of *Citrus*, Bull. Torr. Bot. Club 102 (1975) 369-375.

[15] H.C. Barrett, A.M. Rhodes, A numerical taxonomic study of affinity relationships in cultivated *Citrus* and its close relatives, Syst. Bot. 1 (1976) 105-136.

[16] C.T. Federici, D.Q. Fang, R.W. Scora, M.L. Roose, Phylogenetic relationships within the genus *Citrus* (Rutaceae) and related genera as revealed by RFLP and RAPD analysis, Theor. Appl. Genet. 94 (1998) 812-822.

[17] E. Nicolosi, Z.N. Deng, A. Gentile, S. La Malfa, G. Continella, E. Tribulato, *Citrus* phylogeny and genetic origin of important species as investigated by molecular markers, Theor. Appl. Genet. 100 (2000) 1155-1166.

[18] Z. Zhen, Q.Q. Cao, Y.Y. Shen, L. Qin, SSR technique and application in fruit tree research, Chinese Agricultural Science Bulletin 23 (6) (2007) 145-148.

[19] H.B. Zhu, X.J. Fang, R.C. Yang, Developing SSR markers using punlic rice genome sequence data, Molecular Plant Breeding 1 (2) (2003) 273-276.

[20] S.F. Yuan, Q.D. Shen, Z.H. Huang, P. Xu, Application of study on SSR and ISSR molecular markers in genetic polymorphism, Joural of Aquaculture 2 (26) (2005)10-13.

[21] X.M. Pang, Studies on Phylogeny of *Citrus* and Its Relatives and on Genetic Diversity of Ponicrus Using Molecular Markers, Huazhong Agricultural University, China, 2002.

[22] M. Carlos Ruiz, P, Breto, M.J. Asins, A quick methodology to identify sexual seedlings in *Citrus* breeding programs using SSR markers, Euphytica 112 (2000) 89-94.

[23] A.C. de Oliveira, A.N. Garcia, M. Cristofani, M.A. Machado, Identification of *Citrus* hybrids through the combination of leaf apex morphology and SSR markers, Euphytica 128 (2002) 397-403.

[24] J.F. Li, C.H. Xiang, X.X. Deng, Exploring the origin of natural *Citrus* hybrid Zigui Tangor, Journal of Fruit Science 26 (4) (2009) 425-430.

[25] G.H. Han, S.Q. Xiang, W.X. Wang, X. Wei, B. He, X.L. Li, et al., Identification and genetic diversity of hybrid progenies from shatian pummelo by SSR, Scientia Agricultura Sinica 43 (22) (2010) 4678-4686. (in Chinese)

[26] X.M. Pang, C.G. Hu, X.X. Deng, Phylogenetic relationships among *Citrus* and its relatives as revealed by SSR markers, Acta Genetica Sinica 30 (1) (2003) 81-87.

[27] A. Noelle Barkley, L. Mikeal Roose, R. Robert Krueger, T. Claire Federici, Assessing genetic diversity and population structure in a *Citrus* germplasm collection utilizing simple sequence repeat markers (SSRs), Theor. Appl. Genet. 112 (2006) 1519-1531.

[28] L.F. Zhang, J. He, Y. Feng, L. Liu, Q.G. Guo, G.L. Liang, Phylogenetic relationships among *Fortunella* and its relatives as revealed by SSR markers, Journal of Fruit Science 23 (3) (2006) 335-338.

[29] L.X. Ou, X. Xiang, F.X. Di, L.J. Bai, J.Z. Chen, Q.M. Sun, Advances of studies on SSR markers in Litchi, Biotechnology Bulletin (supplement) (2009) 83-87. (in Chinese)

[30] Y. Liu, Z.H. Sun, D.C. Liu, B. WU, J.J. Tao, Assessment of the genetic diversity of pummelo germplasms using AFLP and SSR markers, Agricultural Sciences 4 (10) (2005) 733-740.

[31] Q.Q. Cao, H.J. Meng, X.P. Wen, H.L. Xiao, H.L. Yi, X.X. Deng, Genetic diversity of male sterile and low fertile germplasm of citrus reealed using SSR markers, Journal of Agricultrual Biotechnology 14 (6) (2006) 937-941.

[32] G.Z. Gong, Q.B. Hong, Z.C. Peng, Genetic diversity of *Poncirus* and its phylogenetic relationships with relatives as revealed by nuclear and chloroplast SSR, Acta Horticulturae Siniea 35 (12) (2008) 1742-1750.

[33] M. Jannati, R. Fotouhi, A. Pourjan Abad, Z. Salehi, Genetic diversity analysis of Iranian *Citrus* varieties using micro satellite (SSR) based markers, Journal of Horticulture and Forestry 1 (7) (2009) 120-125.

[34] S.Q. Xiang, J. He, B. He, W.X. Wang, X.L. Li, Q.G. Guo, Genetic diversity of polyploids of shtianyou pommelo by SSR markers, Journal of Fruit Science 26 (3) (2009) 382-385.

[35] T.G. Lei, Y.R. He, X. Wu, L.X. Yao, A.H. Peng, L.Z. Xu, et al., Construction of DNA fingerprinting database of *Citrus* cultivars (Lines), Scientia Agricultura Sinica 42 (8) (2009) 2852-2861.

[36] O. Gulsen, A. Uzun, I. Canan, U. Seday, E. Canihos, A new *Citrus* linkage map based on SRAP, SSR, ISSR, POGP, RGA and RAPD markers, Euphytica 173 (2010) 265-277.